ERGENICS, INC.
681 Lawlins Road
Wyckoff, NJ 07481

DESIGN AND FABRICATE A METALLIC HYDRIDE HEAT PUMP WITH A COOLING CAPACITY OF 9000 BTU/H

Contract No. DAAK70-86-C-0123

FINAL REPORT

7 February 1989

by
P.M. Golben
and
E. Lee Huston

Prepared for:

US ARMY TROSCOM
Belvoir R, D, & E Center
Fort Belvoir, VA 22060-5606

CONTENTS

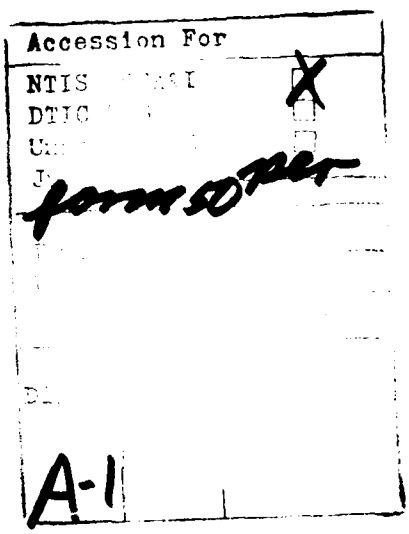

CHAPTER 1

EXECUTIVE SUMMARY

SUMMARY

This report summarizes development work performed by Ergenics, Inc for Belvoir R,D & E Center under Contract No. DAAK70-86-C-0123. The contract originated from a Small Business Innovation Research (SBIR) proposal submitted by Ergenics on 28 January 1986 in response to solicitation A86-100 (Cooling Tactical Shelters with Waste Heat). Contract award date was 29 September 1986. The original scope of work called for the design, fabrication and testing of a 9000 BTU/H air conditioning unit employing a metal hydride heat pump and a silicone heat transfer fluid. The contract was subsequently modified on 29 September 1987 to include life testing of the metal hydride and a design study for an air-to-air hydride heat exchanger to eliminate the silicone interface. Mr. Robert Rhodes and Mr. Terry Dubois were the Contracting Officer's Representatives.

Existing environmental control equipment (ECE) for truck mounted electronic communication shelters are powered by Army generator sets. Fully 50% of the generated power is consumed by the ECE and innovative [illegible]echnology was sought to reduce this electrical load. The heat content of the [illegible]sel generator exhaust gas was viewed as a potential "waste heat" source for thermally driven ECE systems. Metal hydride heat pumps were proposed as for this application. However, only laboratory bench experiments have been reported to confirm theoretical expectations. The purpose of this contract was to produce a prototype metal hydride air conditioner of 9000 BTU/H capacity and compare system size, weight, electric power requirements and performance with a Standard Army Air Conditioner of the same capacity.

A waste heat driven prototype air conditioner for Army shelter cooling based on metal hydride technology was designed, fabricated and successfully tested. The measured cooling capacity of 7869 BTU/hr (with a thermodynamic COP of 0.33) came very near the design point of 9000 BTU/hr, thus confirming that the assumptions and techniques used on the design were correct and appropriate.

A single heat transfer fluid, Slytherm 800®, was used to extract heat from a simulated exhaust gas source and provide heating and cooling for the four metal hydride coils. The hydride coils contained a total of 35.6 lbm of reversible metal hydriding alloy and weighed 126 lbms. The prototype hydride air conditioning system occupied a volume of 9.7 Ft^3 and weighed 365 lbm. These values exceeded those of the comparable standard military freon based air conditioner unit by 67% and 83% respectively. The actual electrical power consumption of the prototype air conditioner (1500 watts) was almost half of that consumed by the conventional freon based units (2950 watts). The excess weight arises from the components needed to contain, circulate and heat exchange the silicone fluid.

Accelerated life testing of the hydriding alloy used in the high temperature (220°C) coils, $LaNi_{4.5}Al_{.5}$, indicated that only 15% of the hydriding capacity would be lost by disproportionation over a 6 month operating life. Further, the capacity could be restored by simple vacuum-thermal treatments.

A comprehensive design of an air-to-air metal hydride air conditioner was also completed. In this unique design, the hydride heat exchangers are alternately heated and/or cooled by exhaust gas, ambient air or shelter air. The silicone heat transfer interface was eliminated. The heat exchangers are compact coils of tubing containing the metal hydride. For a 9000 BTU/H design, 70.5 lbm of

metal hydride is required (approximately twice that used in the liquid design). However the system is estimated to weigh 165 lbm and require only 387 watts of electrical power. The air-to-air design is thus 17% lighter and uses only 13% of the power of the Standard Army air conditioner. This design uses proven Ergenics hydride coil technology and components already evaluated in the silicone system prototype.

No further work is recommended on the metal hydride air conditioner using a silicone heat transfer fluid. Future efforts should be directed to the fabrication and testing of the designed air-to-air system prototype (Chapter 5). Experimental tests would quickly verify the design calculations for the cycle time of the compact hydride heat exchanger. Ergenics would welcome the opportunity to do this work for Belvoir R,D & E Center.

CHAPTER 2

BACKGROUND REVIEW OF METAL HYDRIDE AND CONVENTIONAL FREON REFRIGERATION SYSTEMS

TABLE OF CONTENTS

2.1 INTRODUCTION

This chapter covers the background information on metal hydride and freon based refrigeration systems. Section 2.3 reviews the theory of metal hydride refrigeration/heat pump concepts. Appendix 3.2 provides a more detailed review of the actual hardware used in the construction and operation of metal hydride/hydrogen compressors which operate very similarly to the metal hydride air conditioner. Lastly, Section 2.4 contains a detailed description of the freon based air conditioner which is the military standard.

2.2 BACKGROUND INFORMATION - GENERAL

The United States Army currently uses electrically powered, freon based, air conditioners for the cooling and heating of field portable environmental shelters. These shelters contain electronic equipment that receive their electrical power from a large diesel motor generator set. More than one half of the electric power produced by these generators is consumed by the freon air conditioner while an additional 600% more thermal energy is lost via high temperature heat (i.e., the hot exhaust gas from the engine). This results in actual chemical to electrical energy conversion of only about 15%. This is not only wasteful, but also generates a large infrared thermal signal.

What is needed is a metal hydride air conditioner that will use the high temperature exhaust gas heat to produce the desired cooling. The metal hydride heat exchanger would greatly decrease the electrical power consumption required for cooling, as well as decrease the high temperature infrared thermal signal.

Ergenics, Inc. was, therefore, awarded a Phase I Small Business Innovative Research Program as contract DAAK70-86-C-0123 on 29 Sept., 1986. This contract was issued by US ARMY TROSCOM Belvoir R, D & E Center for the design and fabrication of a prototype metallic hydride heat pump with a cooling capacity of 9000 BTUH.

This Phase I SBIR was an ambitious undertaking in that the deliverable is a prototype system based on the novel metal hydride cooling technology, packaged for direct comparison (eg, weight, volume, power, operating points, etc.) with the standard horizontal compact, 9000 BTUH air conditioner, Model MC11HAL6-115, military specification #MIL-527.

2.2.1 Military Significance

Transformation of the hot exhaust gas of a diesel electric generator into cooling air for tactical communication shelters will eliminate the need for mechanical air conditioning equipment and free additional electrical power for communication functions. The tests indicate that metal hydrides produced cooling air can be provided at system weights and volumes comparable to or less than existing system values. In addition the Metal Hydride Air conditioner...

* can be operated under NBC conditions
* has no major rotating parts and few moving parts for improved reliability and maintenance
* does not contain any freon type refrigerants, which have recently been found to have very detrimental effects on the earths' ozone layer

Lastly, the great reduction in the amount and quality of the hot exhaust gas coming from the diesel generator (due to the operation of the metal hydride air conditioner) will greatly reduce the detectible infrared signal from the diesel generator. This has obvious military importance.

2.3 TECHNICAL BACKGROUND

The novel air conditioning system under development in this program consists of a chemical heat pump utilizing reversible metal hydride beds and non-condensable hydrogen gas as the working fluid. Important properties of hydride materials and the operating principles of the hydride heat pump are given in section 2.3.1.

2.3.1 Hydride Technology

A tutorial for reversible metal hydrides and hydride heat pumps is provided as a ready reference for those readers not familiar with the technology.

2.3.1.1 Reversible Metal Hydride Technology There are a number of metals, Me, (elements, alloys and intermetallic compounds) that will react directly with gaseous H_2 to form a metal hydride, MeHx. Often such reactions are reversible at convenient temperatures and pressures, according to the general chemical equation:

$$(2/x)Me + H_2 \rightleftharpoons (2/x)MeH_x \qquad \text{(EQ.2.1)}$$

The forward reaction consumes H_2 gas and is termed absorption, while the reverse reaction, termed desorption, produces H_2 gas. MeHx is called a "rechargeable metal hydride" and Me a "hydrogen storage metal or alloy". Thus, we can think of reversibly storing gaseous hydrogen in the form of a solid metal compound (hydride). For most practical hydrides $1 \leq x \leq 2$.

Eq.2.1 provides strong cooling on desorption and heating on absorption. These effects will be discussed subsequently.

Hydrides offer very favorable volumetric hydrogen packing densities, a consequence of the H atoms being very efficiently packed in the ordered sites of the metal crystal lattice. Volumetric packing densities of H in typical metal hydrides are many times that of high pressure (2000 psig) gas and even significantly greater than that of liquid H_2 !.

The absorption and desorption properties of metal hydrides are determined experimentally in the form of pressure-composition (P-C) isotherms, examples of which are shown in Fig. 2.1 for a $LaNi_{4.7}Al_{0.3}$ alloy. To do this one loads a granular sample of a hydrogen storage metal into a container, evacuates the residual air, and then slowly adds gaseous H_2 to the container while holding the container and specimen at constant temperature, say 25 C. As the H_2 pressure is increased, a small amount of H_2 is absorbed by the metal in solid solution (to point A of Fig. 2.1). The specimen will then begin to absorb substantial quantities of H_2 at nearly constant pressure (called the plateau pressure,Pp). This corresponds to the formation of a discrete MeHx hydride phase according to Eq.2.1. The plateau represents a two-phase mixture of hydrogen saturated metal, Me, and hydride, MeHx. When the sample has been completely converted to the hydride phase (to point B), a further increase in applied H_2 pressure results in the saturation of the hydride phase MeHx, and a direct increase in system pressure.

If the pressure of hydrogen in the container is reduced by venting some of the gaseous H_2 in contact with the hydride, the equilibrium dictated by the 25 C isotherm in Fig. 2.1 is disturbed and the hydrogen will tend to

"outgas", releasing the chemically bound hydrogen and producing a cooling of the hydride bed. The small difference between the absorption and desorption isotherms at 25 C in Fig. 2.1 is real and is referred to as hysteresis. Throughout the hydride literature, hydrogen composition is usually expressed as the ratio of hydrogen atoms to metals atoms (H/M). Ergenics, Inc. manufactures and markets hydriding alloys under the HY-STOR® trademark.

Increasing the temperature of the P-C isotherm (Fig. 2.1) increases the plateau pressure. The pressure increase is exponential with temperature and is given by the van't Hoff relation:

$$\ln Pp = \Delta H/RT - \Delta S/R = A/T + B. \qquad \text{(Eq. 2.2)}$$

Pp is in atmospheres, ΔH is the heat enthalpy of the reaction per mole of hydrogen gas, T is temperature in K, R is the gas constant in units consistent with Pp and ΔH) and ΔS is the entropy change of the reaction. The constants A and B are tabulated for many rechargeable metal hydrides in (Reference 2.1).

The absorption of hydrogen gas by the metallic alloy is exothermic - - heat (ΔH) is given off. On the other hand, gaseous hydrogen desorption from the hydride is endothermic - - heat (ΔH) is required. The magnitude of (ΔH) is usually determined by plotting lnPp versus reciprocal T (the van't Hoff plot, Fig. 2.2). The slope of the straight lines thus obtained is $-\Delta H/R$. For $LaNi_{4.7}Al_{0.3}$ the heat of reaction is 8100 cal/mole of hydrogen absorbed. This value is approximately 15% of the lower heating value for hydrogen/oxygen combustion. Van't Hoff curves for many other hydride formers are also shown in Fig. 2.2.

2.3.1.2 Reversible Metal Hydride Heat Pump The reversibility of the metal-hydrogen reaction (Eq.2.1) and the heat of chemical reaction (Eq.2.2) provide the basis for hydride heat pumps. These devices are closed units in which hydrogen serves as an energy carrier ("vector") between two or more hydride beds. By selecting appropriate hydriding alloys, heat sources, and heat sinks, heat can be pumped over wide temperature differentials with no moving parts except possibly heat exchanger fluid control valves.

Elements of the process are illustrated in the accompanying diagrams. A container of hydride forming alloy A is exposed to H_2 gas at pressure P_2. The hydriding reaction (forward reaction of Eq.2.1) proceeds spontaneously producing a temperature T_2 (determined by Eq.2.2) in the container, and gives off heat, Q_A, in proportion to the quantity of H_2 consumed and the heat of reaction, ΔH. This hydriding reaction proceeds until all of the metal has been consumed. If hydrogen is now released from the container at a lower pressure, P_1, the dehydriding reaction (reverse reaction of Eq.2.1) proceeds spontaneously. The hydride bed will cool to a temperature T_1 (set by Eq.2.2) absorbing heat, Q_A, until all of the metal hydride is exhausted.

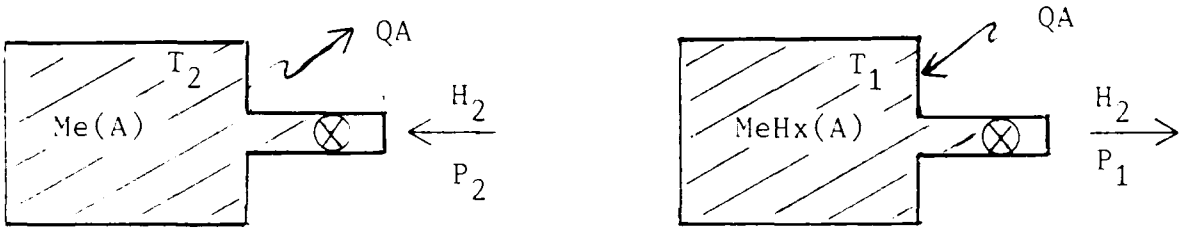

A cyclic process results, the bed is alternatively charged and discharged. The temperatures at which heat is removed or added depends upon the particular metal hydride former, Me, and the pressure of the hydrogen gas.

The system gas pressure can be controlled by a second bed of metal hydride former of different composition, Me(B), coupled to the first bed. By maintaining these beds at different temperatures hydrogen gas is recycled and heat transformed.

There are two basic cycles for heat pump operation: refrigeration (Reference 2.2) and temperature-upgrading (Reference 2.2 & 2.3). It is convenient to visualize the operation of these cycles by following the changes in pressure and temperature of each alloy on a van't Hoff plot. For ease of narration, these curves are idealized. Many engineering properties of metal hydrides must be considered in a detailed explanation (e.g., hysteresis, plateau slope, cyclic stability, etc.). The two cycles are shown in Fig. 2.3.

In the refrigeration cycle, hydride B at, say 40 C (T_2), is heated to about 90 C (T_3). Heat is absorbed (Q_B) from the high temperature heat source to dissociate hydrogen. The quantity of heat is related to the heat of reaction, ΔH_B, and the number of moles of hydrogen transferred. This hydrogen in turn reacts with hydride former A, releasing heat (Q_A) at the intermediate temperature heat sink. Hydride A desorbs hydrogen and cools, thereby absorbing heat (Q_A, refrigeration) at a low temperature, (T_1). The hydrogen reacts with alloy B releasing additional heat (Q_B) at the intermediate temperature and completes the cycle. The net result is heat Q_A + Q_B delivered to the intermediate temperature with Q_B taken from a high temperature source and Q_A from a low temperature source (the refrigeration load). The cycle operates continuously requiring only switching of heat transfer fluids from heat sinks and sources.

The temperature upgrading cycle, Fig. 2.3, has the hydrogen flow in the

opposite direction. This results in the removal of heat from the intermediate temperature bed and delivery to higher (T_3) and lower (T_1) temperature sinks. The temperature range (0-100 C) in Figure 2.2 through 2.4 illustrates that hydride heat pumps can operate with low-grade heat. Much larger temperature ranges can be achieved by selecting different alloy pairs (e.g., Mg_2Ni-$LaNi_5$).

Estimates of the theoretical performance (Coefficient of Performance, COP) of hydride heat pumps can be obtained directly by inspection of Figure 2.3. These estimates (upper bounds) neglect the heat capacity of the alloys, hydrides, and containers as well as effects of the material properties mentioned earlier. The sensible heat of the heat pump components can be largely recovered each cycle by proper thermal management of the heat transfer media. The coefficient of performance in the heat pumping mode is

$$COP \leq (Q_A+Q_B)/Q_B \leq 2.$$

The refrigeration mode is

$$COP \leq Q_A/Q_B \leq 1;$$

or if both heat pumping and refrigeration are obtained,

$$COP \leq (2Q_A+Q_B)/Q_B \leq 3.$$

While the temperature upgrading cycle is

$$COP \leq Q_B/(Q_A+Q_B) \leq 0.5.$$

2.4 DESIGN CONSIDERATIONS

The basic goal of this project was not only to develop a heat driven metal hydride air conditioner, but to do so in such a way as to be competitive in weight, size and cost with that of the currently used (freon) electrically driven air conditioners. The next section outlines the design goals by presenting the specifications of the freon based, electrically powered air

conditioner that is currently used in Army shelter cooling.

2.4.1 Contractual Specifications

The following are the basic contractual requirements and specifications as presented to Ergenics from the Army.

SBIR No. A86-100; Section C

1. The work and services to be performed under Section B shall be subject to the following requirements.

2. The United States Army uses many electronic systems consisting of truck mounted shelters containing varieties of electronic assemblages supported by shelter mounted Army environmental control (air conditioning and heating) equipment (ECE), powered by an Army generator set. More than 50% of the electrical power is consumed by the environmental control equipment. The army is searching for environmental control technology to reduce this electric power burden without significantly increasing the ECE weight, volume, cost and without reducing reliability.

3. The purpose of this effort and the desired result, is to produce a metallic hydride air conditioner with the potential for superiority when compared on a cost-effectiveness basis, with a standard Army air conditioner (ECE) of equal cooling capacity. Evaluation of the metallic hydride air conditioner resulting from this exploratory development effort, will be made considering its weight, volume and the electrical energy it consumes. Additional evaluation will consider projected values of noise, cost, reliability and its ability to withstand the

rigors imposed by military use and exposure to worldwide environments and transportation as given in MIL-STD-810.

4. The concept of producing a cooling effect using heat operated hardware fabricated of metallic hydrides with gaseous hydrogen as the refrigerant is demonstrated technology. This task is to design and fabricate the first iteration of a metallic hydride air conditioner, using engine exhaust energy as the main source of power. Small fans, controls and pumps may be electrically powered.

5. Cooling capacity of the hydride air conditioner shall be approximately 9000 BTUH when cooling a conditioned space at 90°F air temperature and when the ambient air (sink) temperature is 120°F. For design purposes, consider adequate engine exhaust energy available at an exhaust manifold temperature of 800°F. The temperature exiting the exhaust gas heat exchanger shall be above the dew point (about 350°F) of the products of combustion.

6. The metallic hydride air conditioner components shall be installed within an aluminum housing with operating controls on the same vertical face as the conditioned air supply and return. The hydride air conditioner shall have a horizontal configuration with openings similar to that shown on enclosure 1. Electricity required shall be from a 120V, 60 Hertz, single phase source.

7. The assembled waste heat air conditioning unit will be hydrogen activated and tested by Ergenics, Inc. personnel. Operational tests will include a measurement of the system COP (coefficient-of-

performance) (delivered cooling BTU's divided by the waste heat input, plus electrical power required) and verification of the design parameters. Adequate state point data shall be taken to determine the thermodynamics of each component and each fluid systems including the "sink" air flow.

8. The final report shall be written in accordance with item A0^3 of the DD 1423 attachment A, but shall contain all hardware design, thermodynamic analysis, fluid flow analysis, cycle COP (coefficient-of-performance) heat transfer considerations, problems and choices, including rationale. In addition the report shall include a section describing the test philosophy, procedure and methods and shall contain the raw data taken for each state point in the cycle.

8.1 The contractor shall, in the report, evaluate the test results and describe the accomplishment in terms of the present state of the technologies incorporated within the scope of this effort. He shall also estimate, in technical terms, with rationale, the effectiveness of this technology for military use, considering worldwide thermal and atmospheric environments, and the physical abuse common to military equipment.

2.4.2 Current Technology: Freon Based, Air Conditioner Specifications

The 9,000 BTU/hr, compact, horizontal, air conditioning unit (Figs. 2.4 and 2.5 and Reference 2.4) is 23-3/4 inches wide, 26-3/8 inches deep, and 16-1/16 inches high. The maximum weight of the unit, charged and ready to operate, is 200 pounds. The unit is an integral package divided into sections. The condenser is at the rear, and the control panel, electrical

controls, and evaporator compartments are at the front. Sealing and thermal insulation are provided as required to minimize heat transfer and air leakage between the sections. The condenser section contains a hermetically sealed motor-compressor with integral suction line filter and intercooler, a condenser with an integral subcooling coil, a condenser air-discharge opening with refrigerant pressure-controlled louver, a shrouded condenser (Centrax) fan with a propeller fan wheel driven by a dual-speed motor, a quench valve (thermal expansion), a receiver, a suction pressure-regulating valve or a hot-gas bypass valve, fresh-air or CB-air opening, electrical power receptacles, refrigerant piping, a sight glass, a filter-drier, a heat-pressure control actuator, service valves, solenoid valves (liquid line and equalization), a high-pressure relief valve, and high-pressure and low-pressure safety cutout devices. The evaporator compartment contains an evaporator coil, a shrouded evaporator fan wheel (double forward curved centrifugal) driven by a dual-speed motor, a discharge-air grille, a return-air grille, an air filter, a condensate drain pan assembly, refrigerant piping, a main thermostatic expansion valve, electrical heaters, a heater high-temperature cutout, and a fresh-air opening and filter. The fresh-air filter, which is held in place by a wire-formed retainer, is located at the lower right rear corner of the evaporator section.* For fresh-air filter service, the return-air grille-filter assembly must be removed, the fresh-air filter retainer screw released, and the retainer pulled free. The fresh-air filter can then be removed.

A separate compartment on the evaporator side of the unit contains the control module, time delay relay, transformer, rectifier, control circuit

* The final design is to have the filter on the rear of the unit in an integral frame behind the ventilation air inlet screen. The filter will be accessible for servicing by removal of the inlet screen.

breaker, contactors, high-and low-pressure cutouts, terminal strips, phase sensing relay, and the main power receptacle. The control module, which can be remote mounted, contains the mode selector switch, the evaporator fan speed selector switch, the thermostat, and the compressor circuit breaker. The external casing is a structurally rigid, block-shaped aluminum shell with suitable openings, panels, recessed handles, and rounded corners. Internal panels, separators, supports, and brackets are also aluminum, and their arrangement provides for maximum increased strength when components such as heat exchanger coils are installed. The motors and compressor are provided with suitable elastomer mounts to minimize shock, vibration and noise. The top is a three-piece cover. The center cover is approximately 3 inches wide (to accommodate the wall thickness of a standard shelter). The purpose of strip is to allow the front (evaporator) cover, the rear (condenser) cover, or both to be removed while the unit remains mounted in the wall of a shelter. Access for inspection and service is thus provided. The return-air grille and filter are at the front. These can be removed simultaneously and the filter can be separated for servicing.

The evaporator fan motor and the condenser fan motor are identical. The evaporator air impeller is a double forward curved centrifugal wheel mounted on the motor shaft and inclosed in a fiberglass-lined shroud. The return airflow is controlled by thumb latches on the return-air grilles, and the ventilation air damper is controlled by a thumb knob to the right of the discharge-air opening. The evaporator fan motor speed (high or low) is controlled by a toggle switch on the control panel. The fan pulls air through the return-air grille-filter combination, the fresh air filter, or both and pushes this air over the heaters, through the evaporator coil, and from the unit through the discharge-air grille. The filters are a permanent

type which can be cleaned with hot water or steam. Application of a filter fluid after each cleaning is indicated.

Condenser airflow is controlled by a louver which, in turn, is controlled by the head-pressure controller in the high-pressure refrigerant line. A link-cable mechanism between the controller and the louver causes increased louver opening as pressure rises, and decreases louver opening as pressure falls. The head-pressure controller is fully extended (louvers full open) at head pressures at or above 250 psig and is completely retracted (louvers closed) at pressures at or below 165 psig. Varying the air delivery controls the output of the condenser heat exchanger which, in turn, controls the head pressure. An outdoor thermostat supplements this control by automatically choosing the condenser fan motor speed. This motor is in high speed at ambients above 100°F and is at low speed at ambients below 100°F. The condenser fan pulls air through the rear guard and condenser coil, and then pushes this air through the shroud and louvers and from the unit. The fan motors have single shafts, two speeds, sealed bearings, and require no lubrication.

A transformer and rectifier provide for the electrical control components of the unit to operate on 24-volt direct current. The direct-current control system is used for either the 60-cycle or the 400-cycle unit. Major portions of the control components are interchangeable among units of different electrical characteristics as well as other units of the compact, horizontal family. The electrical controls consist of the following components: Wiring, selector switch, thermostat, electric heat contactor, compressor contactor, condenser fan motor contactors, compressor circuit breaker, control circuit breaker, transformer, rectifier, time delay relay,

temperature protectors, pressure protectors, a phase sequence protector, and an evaporator fan motor speed selector switch. Each wire is number coded and can be traced by reference to the wiring diagram. The selector switch, located in the control panel with a knob extending through the front access panel, has five modes or positions: HI-HEAT, LO-HEAT, OFF, VENTILATE or VENT, and COOL. The OFF mode electrically disconnects all power from the control circuit. The LO-HEAT mode provides thermostatic operation of one-half the heaters and continuous evaporator fan operation. The HI-HEAT mode provides constant operation of the remaining heaters in addition to the LO-HEAT functions. The VENT mode provides continuous evaporator fan operation without any cooling or heating. The COOL mode provides continuous compressor, evaporator fan, and condenser fan operation. The cooling function of the unit is controlled by the adjustable thermostat, located in the control panel next to the selector switch. The thermostat controls the refrigerant liquid line solenoid valve in response to the return-air temperature. This causes the refrigerant system to be either in the cooling cycle or in the bypass cycle of operation. When the compressor stops operating (for any reason), a normally open solenoid valve allows the suction and head pressures to equalize.

The thermostat, which has an adjustment range of 60°F to 90°F, has a remote sensing bulb located in the evaporator return-air plenum. In the COOL mode, higher return-air temperatures than the thermostat setting will cause the unit to cool the air by the normal cooling cycle. Lower return-air temperatures than the thermostat setting will cause the unit to be in the bypass cycle and therefore not perform any cooling function.

The refrigerant cycle of the unit employs the vapor cycle principle which uses monochlorodifluoromethane refrigerant (R-22). The refrigerant system consists of the following components: Piping, a hermetically sealed compressor with an integral suction line filter and intercooler, condenser coil with integral subcooler, filter-drier, suction-line service valve, discharge-line service valve, pressure-relief valve, liquid-line solenoid valve, liquid sight glass, main thermal expansion valve (TEV), evaporator coil, pressure-regulating (hot-gas bypass) valve, liquid quench expansion valve, high-pressure safety cutout, low-pressure cutout, receiver, head-pressure control actuator, and equalization solenoid valve. During the normal cooling cycle of operation, the liquid solenoid valve and evaporator TEV are open, and the quench expansion valve and pressure-regulating valve are closed. The compressor pumps the refrigerant through the condenser coil, receiver, subcooler, sight glass, filter-drier, liquid solenoid valve, TEV, and evaporator coil to the suction side of the compressor. During the bypass cycle of operation, the liquid solenoid valve is closed and the pressure-regulating valve and quench valve are open as the pressure and superheat of the suction gas reaches 58 psig and 25°F, respectively. During the bypass mode of operation, the refrigerant is pumped by the compressor and is split into two piping circuits. Most of the refrigerant is forced through the pressure-regulating valve, mixed with the liquid from the quench valve, and drawn into the suction side of the compressor. The remaining refrigerant, the quantity depending upon the liquid quench expansion valve, is forced through the condenser coil, receiver, sub cooler, sight glass, filter-drier and liquid quench expansion valve; mixed with the hot gas; and drawn into the suction side of the compressor. The pressure-regulating valve is preset to maintain a sufficiently high suction pressure (55 to 58 psig) to prevent evaporator coil freeze up. Suction pressure is inherently

low under low cooling load conditions and at low ambient temperatures. The quench expansion valve feeler bulb (located just before the suction line filter) senses refrigerant temperature and the pressure-regulating condenser head-pressure controls to assure sufficient head pressure under low ambient temperatures. After shutdown of the compressor, the equalization solenoid valve opens and the system pressure equalizes. This permits the compressor to start under unloaded conditions, which reduces the starting current.

Table No. 2.1 lists the relevant operating characteristics for this air conditioner such as its electrical power draw of 2.95 KW.

Concluding then, the basic design specifications that will influence the design of the 9000 BTU/Hr metal hydride air conditioner are listed below:

Electrical power draw = 2.95 KW

Size: 23.75" wide, 26.375" deep, 16" high

Weight: 200 Lbm

2.5 LIST OF REFERENCES

2.1 Huston, E.L. and Sandrock, G.D., Engineering Properties of Metal Hydrides, J. Less-Common Metals, 74 (1980) 435-443.

2.2 Terry, L.E., Hydrogen/Hydride Absorption Systems and Methods for Refrigeration and Heat Pump Cycles. U.S. Patent 4,055,962, November 1, 1972. (Owned by Ergenics, Inc.)

2.3 Sirovich, B.E., Hydride Heat Pump. U.S. Patent 4,200,144, April 29, 1980.

2.4 Report 1903, "Nominal 9,000 BTU/Hr, Compact, Horizontal Air Conditioning Units". Task #1M643303D54503 July 1967, pages 5-12.

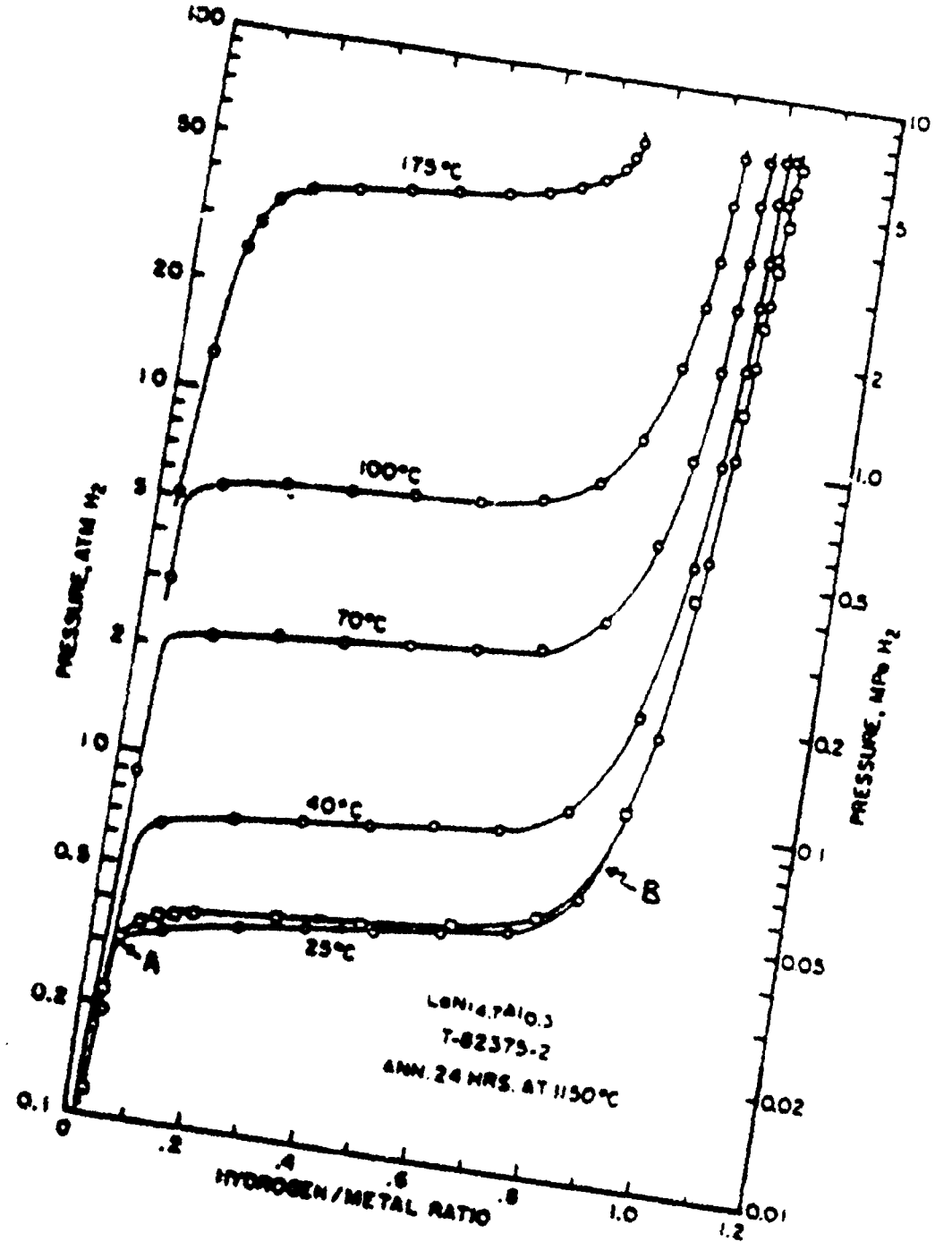

Figure 2.1 - Pressure-Composition Isotherms (PCT curve) for the Metal Hydride Alloy $LaNi_{4.7}Al_{0.3}$

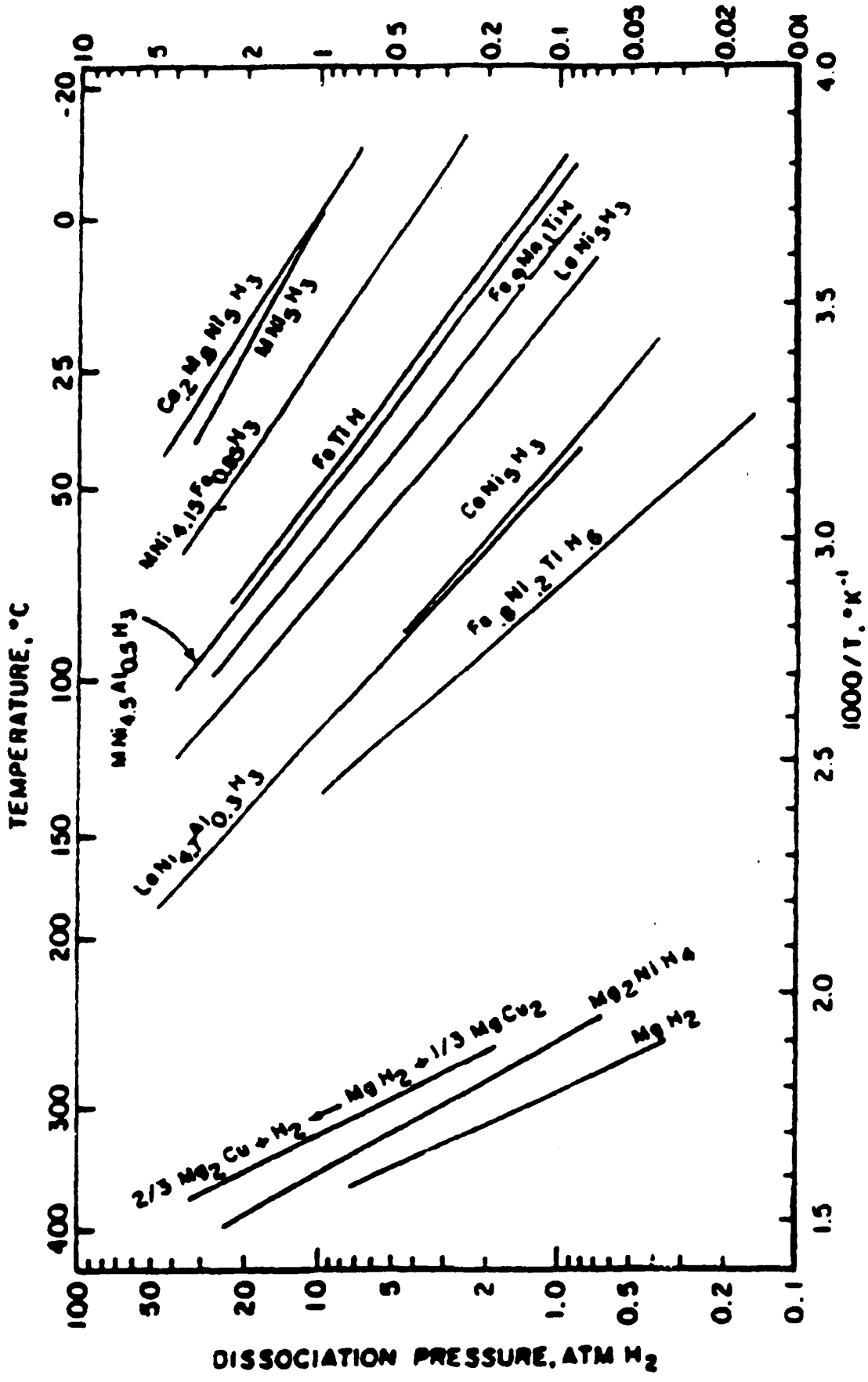

Figure 2.2 - Van't Hoff Plots (Desorption) for Various Hydrides

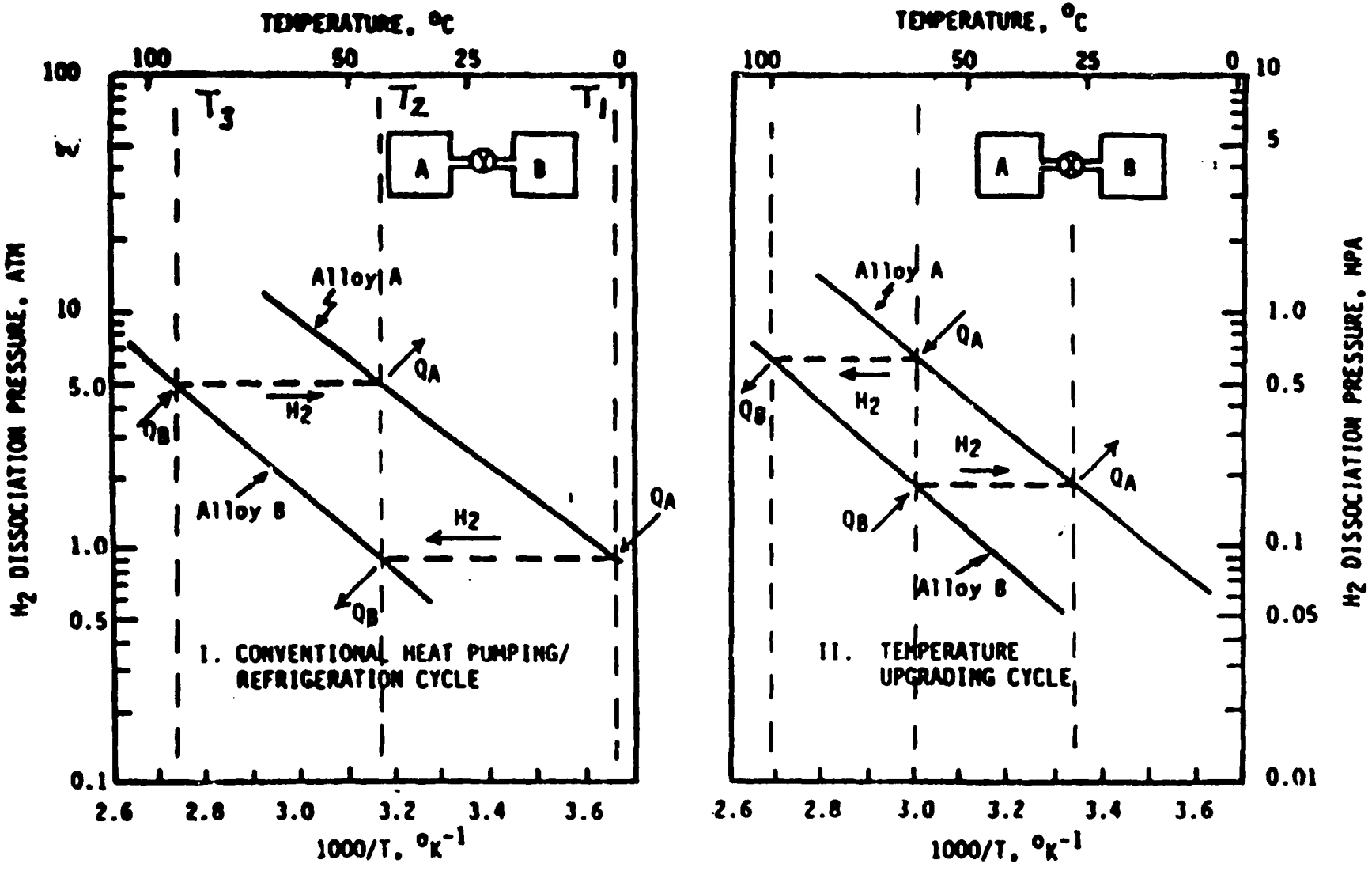

Figure 2.3 - Metal Hydride Refrigeration and Temperature Upgrading "Heat Pump" Cycles

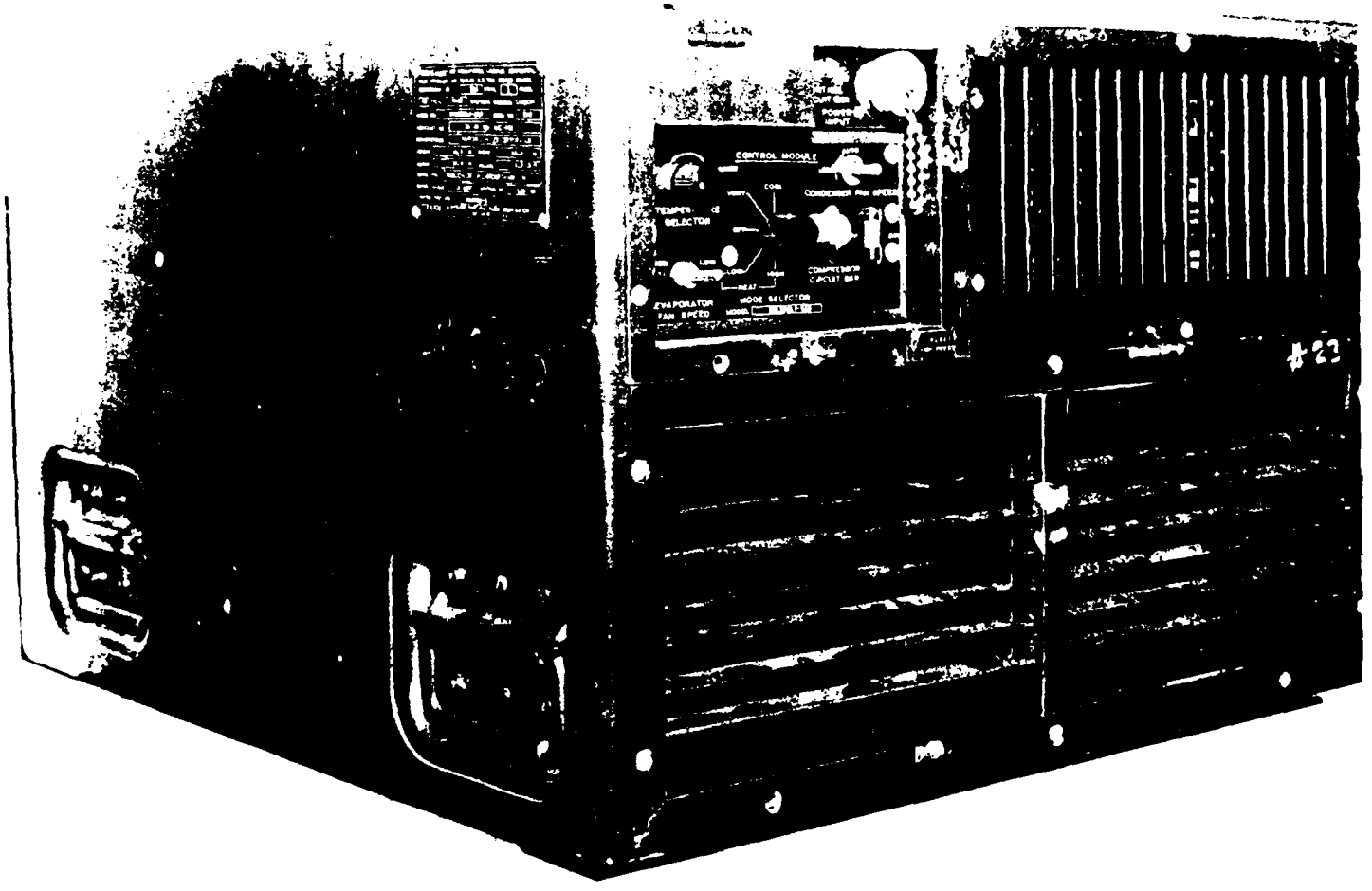

Figure 2.4 - Front and left side of 9,000 BTU/hr, compact, horizontal, air-conditioning unit, Model MC11HA L6-115

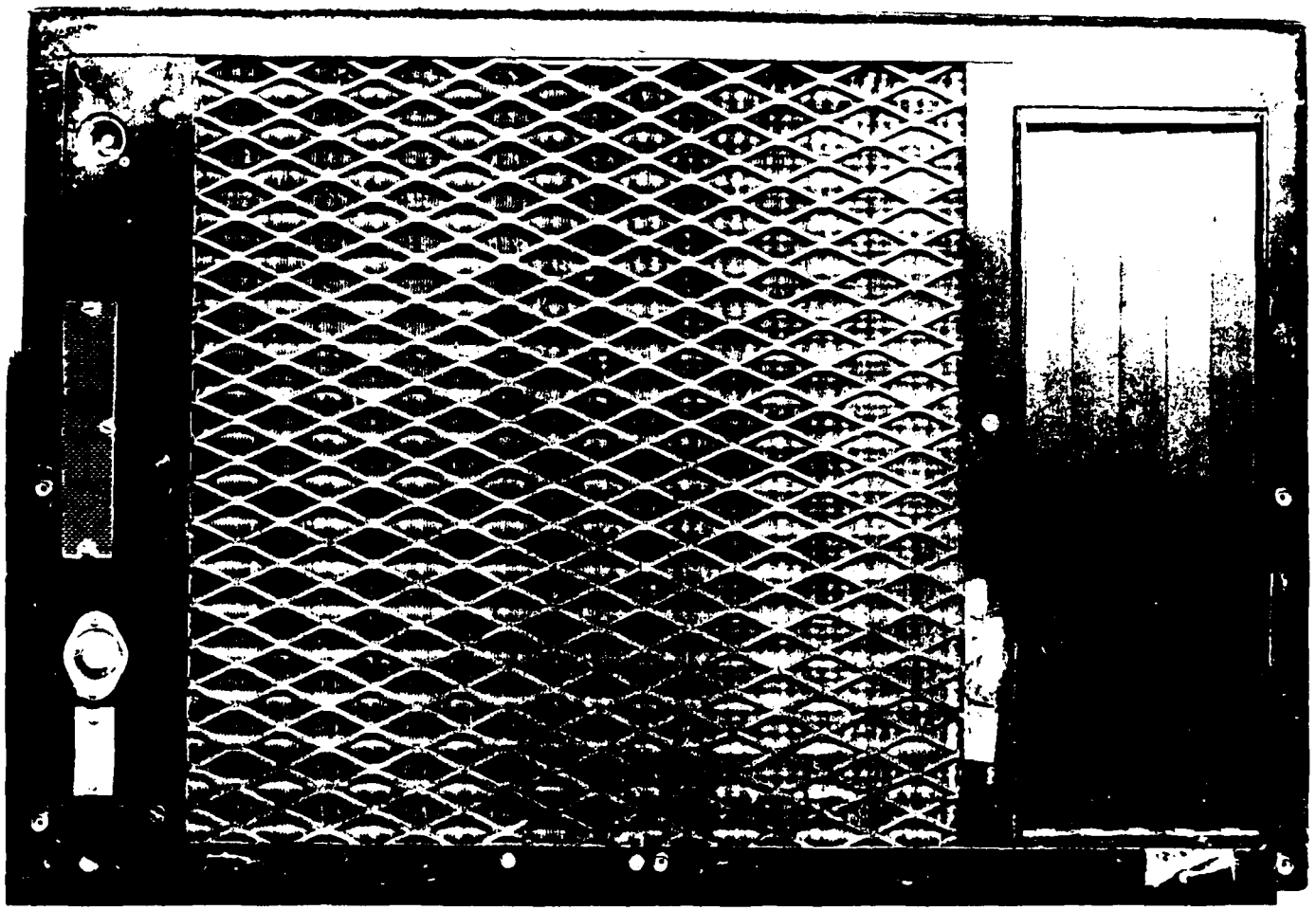

Figure 2.5 - Rear of 9,000 BTU/hr, compact, horizontal, air-conditioning unit, Model MC11HA L6-115

Results of Cooling Capacity Test,
Model MC11HAL6-115

Measurement	Test Condition			
	1	4	7	10
	120/80-75	120/80 dry		
Capacities (Btu/hr)				
Total	10,220	9,881	8,950	8,450
Latent	3,070	0	1,850	0
Sensible	7,150	9,881	7,100	8,450
Sensible Heat Factor (%)	70.0	100	79.0	100
Coefficient of Performance (Btu/hr/watt)	3.46	3.79	3.51	3.40
Air Temperatures (°F)				
Entering Evaporator, Dry Bulb	90.3	90.3	79.9	79.8
Entering Evaporator, Wet Bulb	75.1	66.0	66.9	53.5
Leaving Evaporator, Dry Bulb	70.2	-	61.2	60.4
Outside Room Temperature (°F)	120.1	120.0	95.1	95.2
Airflow (scfm/ton), Evaporator	348	-	353	378
Refrigerant Temperatures (°F)				
Superheat at Bulb	2.0	9.4	1.0	1.0
Subcooling at Condenser	5.0	12.1	11.0	10.0
Discharge Pressure (psig)	378	382	350	340
Suction Pressure (psig)	90	85	76	74
Electrical Characteristics				
Voltage	115	115	115	115
Amperage	26.5	23.8	23.0	22.5
Power (kw)	2.95	2.61	2.55	2.50
Power Factor (%)	96.7	95.3	93.0	96.6

Notes: Test conducted with an external static pressure of 0.125 in. of water on the evaporator.

Hyphens signify that these data were not taken.

Table 2.1 - Results of Cooling Capacity Tests on the Conventional Freon Based Air Conditioner Model MC11HAL6-115 (from Reference 4)

CHAPTER 3

METAL HYDRIDE AIR CONDITIONER

LIQUID SYSTEM

TABLE OF CONTENTS

3.14 LIST OF TABLES

3.15 APPENDICES

3.1 SUMMARY

A waste heat driven prototype air conditioner for Army shelter cooling based on metal hydride technology was designed, fabricated and successfully tested. The measured cooling capacity of 7869 BTU/hr (with a thermodynamic COP of 0.33) came very near the design point of 9000 BTU/hr, thus confirming that the assumptions and techniques used on the design were correct and appropriate.

The prototype metal hydride air conditioner used silicone fluid as a heat transfer media which resulted in a prototype whose size, 9.7 Ft^3, and weight, 365 lbm, exceeded that of the comparable standard military freon based air conditioner unit by 67% and 83% respectively.

The actual electrical power consumption of the prototype air conditioner (1500 watts) was almost half of that consumed by the conventional freon based units (2950 watts).

In order to meet the size and weight targets for the waste heat driven metal hydride air conditioner, it is recommended that future work be devoted to the design and fabrication of an air-to-air heat exchanged system. Such a system will eliminate the components associated with the liquid heat transfer media and result in a lighter less bulky unit with even further reductions in power requirements. An "air system" design study is presented in Chapter 5.

3.2 BASIC METAL HYDRIDE AIR CONDITIONER DESIGN ASSUMPTIONS

Thermal energy contained in the hot exhaust gas of a diesel generator set is to be utilized to provide conditioned air for Army shelter use. Energy conversion is by a chemical heat pump employing coupled reversible metal hydride beds. The principal design problem is to size the hydride beds and provide adequate energy transfer between the source gas, the hydride beds and the shelter air.

At the start of this project, it was decided to rely on Ergenics' metal hydride, fast heat transfer technology consisting of metal h 'ride alloy contained in long lengths of small diameter tubing that receive and reject heat to a liquid heat transfer media such as water. Several hydride tubes are placed inside a larger tube jacket and the assembly coiled yielding a "compact" system. Appendix 3.2 is a detailed review of Ergenics' metal hydride compressor technology which is the basis for this refrigeration work. Since the scope of this first phase work was to design, build and test a heat driven metal hydride air conditioner, it was decided to rely on this proven technology employing a liquid heat transfer media and not attempt an air-to-air heat transfer design which, for hydirde heat pumps, is less well advanced. It was recognized that this decision would result in a metal hydride air conditioner of greater mass and power requirements than that of an air system design, but the high degree of operational confidence that the liquid system offered outweighed this concern.

This decision set the metal hydride air conditioner operational process. A liquid media is used to transfer heat from the tubes containing the metal hydride to the high efficiency fluid-to-air heat exchangers as shown in

Figure 3.1. Thus, the basic design of the air conditioner would focus on these three main topics:

1) Liquid Heat Transfer Media Selection
2) Metal Hydride Containment Design Selection
3) Liquid to Air Heat Exchanger Selection.

Each of these main design topics will be examined in detail in the following sections.

The selection of a liquid fluid as the heat transfer media also quickly set the component needs of the air conditioner :

1) Two "pairs" of metal hydride heat exchangers
2) A "cold side" liquid to air heat exchanger
3) A "cold side" liquid pump
4) A "cold side" fan(s).
5) An "ambient side" liquid to air heat exchanger
6) An "ambient side" liquid pump
7) An "ambient side" fan(s).
8) A "hot side" liquid pump.
9) A "hot side" heat exchanger
10) Liquid control valves to direct the liquid fluid to and from the appropriate metal hydride heat exchangers.

These decisions yielded the basic operational flow schematic for the metal hydride air conditioner shown in Figure 3.2. The actual size and weight of these components were set after individual component tests and design iteration.

Figure 3.2 is the operational schematic for the metal hydride air conditioner. Here it is shown that the air conditioner operates by the

continuous cycling of "paired" metal hydride heat exchanger coils. Each hydride pair consists of a low temperature hydride coil ("B" coil) that is coupled to a high temperature hydride coil ("A" coil). The object in the air conditioner's operation is to "charge up" the low temperature coil with hydrogen gas that has been released from the coupled high temperature coil. This is done by heating up the high temperature coil with a high temperature (200°C) silicone fluid. This raises the hydrogen desorption pressure in the "A" coil to a high enough pressure that it can flow into the "B" coil. The formation heat that is generated by the absorption of this hydrogen by the "B" coil is rejected to the ambient environment through the use of a fluid-to-air heat exchanger. Once this process is complete, the silicone fluid flow will switch and the cooling aspect of the hydride coils will start. Then, hydrogen that is now stored in the hydride "B" coil flows back into the "A" coil that now has ambient temperature fluid flowing through it, releasing this heat to the fluid-to-air ambient heat exchanger. As hydrogen gas leaves the "B" coil, this "B" coil gets cold. Silicone fluid flowing through the shelter's cold side heat exchanger, picks up this "cooth", cooling down the shelter. The air conditioner incorporates 2 complete sets of these hydride pairs, so that while one pair is recharging, the other pair is producing cooling.

A single heat transfer fluid, a silicone, is used throughout. Figures 3.2A through 3.2D show the separate silicone fluid paths (cold, ambient and hot) as the air conditioner cycles through the various heat transfer conditions.

3.3 HEAT TRANSFER FLUID SELECTION

Since the design of the metal hydride heat exchangers and the liquid to air radiators depend on the heat transfer fluid used, then the selection of this fluid will be discussed here first.

Several important factors in the selection of the heat transfer fluid are listed below in the order of their importance.

1) A low vapor pressure at the hot exhaust gas operating temperature (220°C).
2) Chemical stability of the liquid at the heat source temperature of the metal hydride air conditioner (~ 220°C).
3) Toxic qualities of the liquid
4) The viscosity/temperature profile of the liquid [ie: we want to make sure that the viscosity is low enough (20 cP) at colder temperatures (5°C)].
5) Thermalconductivity of the liquid
6) Safety aspects - ie: flammability of the liquid
7) The sensible heat of the liquid
8) The density of the liquid
9) Price and availability of liquid

Of overriding concern in the selection of this fluid was the requirement that the vapor pressure of the liquid be near or below atmospheric pressure at the high temperature to which it will be exposed. This high temperature heat is used to heat up the "A" type coils (see the operational schematic in figure 3.2) to a temperature high enough to drive the hydrogen back into its paired "B" type hydride coil. This high temperature will be around 220°C (~ 430°F) and low fluid pressure at this temperature greatly reduces the safety hazard in the event of a fluid leak. It was for this reason that water or ethylene

glycol were not considered as candidates for this heat transfer liquid (the vapor pressure of water at 220°C is 330 psig). Many different fluids and oils were examined. Table 3.1 is a summary of these fluids and their relevant characteristics. Of the fluids examined, two were selected for further testing. These fluids were Dow Corning's Syltherm 800® and Dow Chemical LF® Heat transfer fluid due primarily to their very low vapor pressure at 220°C. The Dow Chemical LF® Fluid, however, was soon rejected due to its very disagreeable odor and its tendency to chemically attack the polysulfone fluid flow meters. The Dow Corning Syltherm 800®, however, performed very satisfactorily in all aspects of our operation and testing.

3.4 METAL HYDRIDE HEAT EXCHANGER DESIGN

Typical Ergenics' hydride heat exchangers consist of small diameter (3/8" OD) metal tubes that are about 20 ft. long. Inside of the metal tube is the Ergenics' gas distribution system. Metal hydride alloy is packed in the remaining tube void volume. This system acts as a hydrogen conduit and allows hydrogen gas to travel down the entire length of the tube.

The object of Ergenics' heat exchanger design for this project was to identify the optimum combination of metal tube diameter, tube material and hydride alloy bed thickness that produced the best hydride heat exchanger for this application.

The approach that was taken to determine the best hydride "coil" design was to build several different "test reactors" and test each reactor for its heat transfer properties.

The results of these heat transfer tests indicated the best design to which the metal hydride heat exchanger should be constructed. The determination of the "best" heat exchanger design involved the examination of many factors; such as the reactor's rate of heat transfer, material compatible to the surrounding environment, ease of fabrication and its overall reliability and longevity.

3.4.1 Metal Hydride Test Reactor Fabrication

Essentially, these test reactors possess identical heat transfer characteristics and are representative of the full scale system. The only difference is one of size, but since normalized heat transfer rate performance is not size dependent, (see Reference 3.2) these test reactors provide an excellent means of quickly determining the full scale system performance.

Several of the test reactors were designed, built and tested and their specifications are given below. All reactors used $LaNi_5$ from Heat T-1111A. Mass Ratio refers to the total heat exchanger mass divided by the metal hydride mass. Construction details are summarized below.

Reactor ID	11-13-86	11-24-86	12-3-86	12-16-86	1-6-87
Tube Matl.	Al	304	304	Al	304
Tube OD, inch	.375	.375	.375	.375	.281
Tube Wall, inch	.035	.020	.035	.049	.010
Tube Length, inch	35	35	35	35	54
Alloy Wt., gms	91	151.4	98.3	46.8	60.4
Mass Ratio	1.90	1.82	3.00	2.73	2.56
Alloy/ft, g/ft	31.2	51.9	33.7	16.0	13.4

Reactor 1-6-87 was built to test a small-diameter thin-wall tube. It was done to determine whether the very thin walled tubing (.010") could be bent (coil Φ = 10") without structural damage. The reactor was constructed and successfully bent to a 10" coil diameter without damage, however, time did not permit heat

transfer testing.

3.4.2 Metal Hydride Test Reactor Heat Transfer Test Setup

After a metal hydride test reactor was constructed, it was tested to determine its heat transfer characteristics. In general, this is a test that will tell us how "fast" the hydrogen gas that is stored in the metal hydride alloy can be absorbed and/or desorbed. Basic parameters such as time, incoming fluid temperature, pressure and hydrogen flow rate are simultaneously recorded and the results are normalized to present a time comparison of the reactors heat transfer rates. Reference 3.2 is a detailed report on this heat transfer test technique, and is presented in this report in Appendix 3.1.

Figure 3.3 shows the heat transfer test setup as practiced for this project. Here the heat transfer fluid (with water or silicone fluid) is made to flow past the test reactor at a known rate and temperature. At the start of an absorption test, the valve to the reactor is opened and hydrogen gas (at a known pressure) is allowed to enter the reactor. The rate of flow of hydrogen gas is automatically recorded on a strip chart recorder (Soltec #3616). This flow rate of hydrogen gas is a direct indicator of the rate of heat transfer for the reactor.

3.4.3 Metal Hydride Test Reactor Heat Transfer Test Results

Results of these heat transfer tests are presented as "time to 90% Hydrogen transferred vs. temperature plots". These are plots of the time it takes to transfer 90% of the total transferred hydrogen as a function of the absolute temperature difference between the metal hydride in the reactor and the temperature of the heat transfer fluid flowing past the reactor. As described in Appendix 3.1, the temperature of the metal hydride is determined from the

measured hydrogen gas pressure. Figures 3.4 through 3.7 show the results of the heat transfer tests for each reactor. Figure 3.8 shows the result of all of the tests on a single graph.The following discussion illustrates how the curves on Figure 3.8 are to be interpreted and used for design purposes.

Previous Ergenics experience has found that optimal heat transfer performance occurs when the absolute temperature between the metal hydride and the heat transferred fluid is about 12°C. If we draw a vertical line on Figure 3.8 at 12°C, this line intersects the reactor heat transfer curves at points A, B, C & D. These points are the "90% times" for each reactor, and thus provide the basic 1/2 cycle time information needed to design the hydride air conditioner using any of these reactor designs. In the example of our 12°C temperature, we find that reactor #11-24-86 (which had the lowest metal hydride mass ratio of 1.89) would require a 1/2 cycle time of 2.75 minutes. Reactor #12-3-86 (hydride mass ratio of 3.00) results in a 1/2 cycle time of 2.2 minutes, and reactor #12-16-86 (MR=2.73) had a 1/2 cycle time of 1.06 minutes.

It should be noted that due to silicone fluid's lower thermoconductivity (1/2 that of water), heat transfer times using silicone fluid will be slower, but the general curve relationship will be the same.

3.4.4 Metal Hydride Full Scale Heat Exchanger Design

With the determination of both the required 1/2 cycle time for a given temperature difference (between the metal hydride and the fluid) and a given reactor design, it is now possible to construct a metal hydride heat exchanger "mass map" that graphically illustrates the total mass of the full scale hydride heat exchanger. The procedure for determining the full scale heat exchanger's "mass map" is shown below:

1) Knowing the required 1/2 cycle time and the amount of cooling we desire per hour (9000 BTU/hr), we now can determine how much cooling must be generated during the 1/2 cycle time of the heat exchanger. For example, if we have a 1/2 cycle time of 3 minutes (1/20th of an hour), then we must produce 1/20th of 9000 BTU or 450 BTUs during this 1/2 cycle time.

2) Knowing how much cooling per 1/2 cycle time is required, we now can calculate how much metal hydride alloy will be required. For example, for our 3 minute, 1/2 cycle time requirement, we need to produce 450 BTUs. The amount of heat (or cooling) that is produced when 1 mole of hydrogen gas leaves the metal hydride alloy is about 27 BTUs. This value does not consider the sensible heat of the system (metal and fluid). Sensible heat is largely recoverable by appropriate direction of the fluid flows. An additional safety factor is obtained by cycling the system faster than the design cycle time. Therefore, in order to produce the 450 BTU we need to transfer about 450/27 = 16.7 moles of hydrogen gas. Now 16.7 moles of hydrogen gas has a mass of 33.6 grams (2.016 grams per mole H_2), and if we assume the typical hydrogen mass storage density for the metal hydride of 1%, then the required mass of metal hydride is 100 x 33.6 or 3360 grams of metal hydride.

3) Now that we know how much metal hydride alloy is required in the heat exchanger, we now can calculate how many feet of hydride tubing is required. This is done by simply dividing the total hydride mass (3360 grams) by the mass of metal hydride contained in the tube per foot. So that in the example we have been looking at if we assume that the full scale hydride heat exchanger to the design used in test reactor #11-24-86, then we will need 3360/51.9 = 64.7 -t. of tubing.

4) From the information available from the construction of the test reactor in question, we can now calculate the mass of the other non-hydride components of the reactor. In the case of test reactor #11-24-86 :

mass of metal hydride alloy	51.92 grams/ft
mass of non hydride material	42.62 grams/ft
therefore, the total mass of the metal hydride heat exchanger per foot is	94.54 grams/ft

5) Concluding then, the total mass of the hydride heat exchanger will now be the mass of the heat exchanger tube per foot times the number of feet required or... 94.54 x 64.7 = 6,120 grams

= 13.5 lbms

This total mass now becomes the mass number that corresponds to the 1/2 cycle time determined earlier. It is this calculation process that produces the "hydride mass map" shown in Figure 3.9 for various test reactors.

The final step in the design of the full scale heat exchanger is to determine of what the length of each hydride tube should be. This length, of course, will be determined by the number of tubes that are placed inside the tube's "water" jacket.

Figure 3.10 illustrates a typical Ergenics' hydride heat exchanger configuration. This usually consists of 4 - 3/8" OD metal hydride containing tubes placed side by side in a larger 1-1/8" OD copper water jacket. The length of this water jacket (and each hydride tube) is Side" Air Fans:about 20 ft. After the hydride tubes have been placed inside the water jacket, the tube is slowly "coiled" or wrapped into the spiral type configuration shown in Figure 3.11. This process results in a flat heat exchanger that is torous

shaped (ID = 18", OD = 30") and presents a much more convenient and manageable package.

For this project, it was desired to obtain as small a torous shaped package as possible, therefore, it was decided to use a 7 hydride tube bundle instead of the usual 4. This would result in a water jacket length of less than 10 ft., and yet the water jacket diameter would still be a managable 1-3/8". The final result of this design is a torous shaped package with a 12" ID, and a 24" OD (see Figure 3.12).

3.5 LIQUID-TO-AIR HEAT EXCHANGER PRELIMINARY DESIGN ANALYSIS

The final major selection process was that for the fluid-to-air heat exchangers. These heat exchangers are used in two key processes in the air conditioner; the absorption of heat from the shelter room air into the silicon fluid, and the rejection of heat from the silicone fluid to the outside ambient air (see Figure 3.2). Slytherm 800® silicone fluid is the fluid of choice.

From the contractural specifications given in Chapter 2 of this report, it was determined that the "cold side" fluid to air heat exchanger should be designed to transfer at least 9000 BTU per hour from the air inside of the shelter to the liquid heat transfer fluid, where a temperature gradient of 20°C (36°F) exist between these two medias. Concurrently, the "ambient side" fluid to air heat exchanger should be designed to reject 28,000 BTU per hour from the liquid heat transfer fluid to the ambient air with this same temperature gradient of 20°C (36°F). This 28,000 BTU per hour represents the two 9,000 BTU per min. heat loads that are present when hydrogen is being absorbed by the metal hydride, plus an extra 9,000 BTU per min. added as a safety factor.

Initially it was decided to examine high pressure tube and fin heat exchangers like those already used in conventional freon type air conditioners. They are used to reject heat from the hot (and high pressure) freon to the ambient air. However, this type of fluid-to-air heat exchanger turned out to be very inefficient due to the process of press fitting the fins onto the high pressure tubing. When a high pressure tube fin manufacturer was found that soldered or brazed the fin to tubes of the heat exchanger they were highly priced due to the small quantities involved (e.g. Vapor Manuf., Model Q860231). These units were deemed unacceptable due to the attempt to utilize low cost, mass produced components in the design. This dilemma was finally resolved when it was realized that we did not need the high pressure capability offered by the pressed fin and tube heat exchangers since the pressure of the silicon heat transfer fluid was always near ambient. The use of a much lower pressure fluid to air heat exchanger was possible. This permitted the consideration of car water and/or oil radiators. Since the car radiator's fins are soldered onto flat tubes and it is mass produced, it offered the perfect choice for our design.

3.5.1 Liquid to Air Heat Exchanger - Candidate Selections

A literature search and expert survey were conducted to identify candidate car radiators that could be purchased and performance tested. This search resulted in the selection of 5 types of radiators that warranted further experimental examination. These were...

1) Valley Plate Type Oil Cooler :

This is a plate type fluid to air heat exchanger (5.6 x9.5 x 1.5 inches) that was selected for further study primarily because of the lack of published engineering performance data. It consists of thin plates through which the heat transfer fluid circulates with the air cooling stream flowing on the other side of the plates.

2) Corvette "Heater Core" Car Radiator, Model #4R702262 :

This is the heater core used in the interior heater of a car. It was picked due to its exceptionally deep air travel dimension of 2 1/2 inches. Its overall dimensions are 7 3/16x6 1/4x2 1/2 inches, and utilized copper fins soldered to copper plates.

3) Audi 5000 Car Radiator :

This radiator was chosen because car radiator experts consider it one of the best radiators in its weight and size class. Its overall dimensions of 22 1/4x12x1 3/4 inches, and mass of 18.75 lbs presented a nice package that fit well with the projected size of our hydride air conditioner design. Heat transfer to the air is via copper fins soldered to thin and flat copper tubes. In addition, this radiator is unusual in that it incorporates lightweight plastic fluid headers.

4) Modine 2-1/4" Core, Aluminum Brazed Oil Radiator, Model 1E2930 :
This radiator consists of an all aluminum design that utilizes thin aluminum fins that are aluminum brazed to flat aluminum tubing (see Figure 3.13). Of special consideration is the fact that this type of radiator was specially built for using an oil based heat transfer fluid and used a special internal aluminum extended surface matrix inside of the flat aluminum tubes to facilitate heat transfer from the oil based fluid to the aluminum wall.

5) Modine 1-1/16" Core, Aluminum Brazed Oil Radiator, Model #2978
This heat exchanger has similar construction to that of the Modine 2-1/4" core radiator except for its 1-1/16" core. Its low air pressure vs air flow rate data (Figure 3.14) suggested that it would be a good heat exchanger for the cold side process. The construction dimensions for this unit are shown in Figure 3.15.

3.5.2 Liquid to Air Heat Exchangers Test Set Up and Results

The general experimental setup used for the performance testing of the candidate radiators is shown in Figure 3.16. Test data such as inlet and outlet fluid temperatures and fluid velocity were recorded in order to determine the radiators' relative heat transfer effectiveness.

The results of these tests are presented in Tables 3.2.A through 3.2.F. The test results have been normalized by the weight and face area of the heat exchanger required to reject 28,000 BTU/Hr. From Table 3.2.C we see that the Modine #2930 aluminum radiator performed the best at 37.5 BTU/Hr/Ft^2/15°C/100 ft/min/lbm. What is of added importance is that this heat exchanger requires the least driving pressure differential to produce the necessary fluid flow rates (see Figure 3.17).

From this information, the Modine #2930 aluminum radiator was selected as the ambient side fluid-to-air heat exchanger. By a similar analysis, the Modine #2978 aluminum radiator was selected as the cold side fluid-to-air heat exchanger.

3.6 ANCILLARY EQUIPMENT DESIGN AND SELECTION

The basic operational schematic of the metal hydride waste heat air conditioner shown in Figure 3.2 requires equipment for the pumping and control of the silicon heat transfer fluid. Due to the low specific heat of the silicone fluid (about 1/3 of that of water) a much higher mass flow rate (than that of water) is required to transfer the heat from the metal hydride coils to the liquid-to-air heat exchangers. An estimate of the required silicon fluid flow rate was made by assuming a 15°C temperature change for the silicone fluid whose specific heat is approximately 0.35 BTU/lbm°F. For a 28,000 BTU/Hr heat load, a fluid flow rate of 10 GPM is required. It will, therefore, be necessary to flow 5 gal/min of silicon fluid through each of the metal hydride heat exchangers. The circulating pumps and the fluid control valves must also be able to produce and control this fluid flow rate. (Please note here that the ambient pump must actually be able to pump 10 gal/min since its output flow is divided into two equal flow patterns of 5 gal/min each). Similar estimates were also made to arive at air flow rates of 500 to 700 CFM.

Estimates of the pressure differential that would be required to move the silicone fluid through the system path were made. Correspondingly the size of tubing needed to provide the low pressure flow path for this fluid was determined to be 1-1/8" OD. This large size is primarily due to the many elbows and unions that would be employed in the unit and, therefore, a large size was needed to keep these pressure drops small.

Of primary concern in the selection of these components was their impact on volume, mass and electrical power requirements, since it was desired that the total system mass and volume be kept as low as possible. Literally hundreds of candidate pumps and valves were looked at before selecting the equipment used.

A list of the ancillary equipment, the estimate of the fluid flow requirement and the make and model number of the selected pumps, valves and fans are shown below.

1) The silicone fluid ambient temperature pump:

Requirements: Must pump 10 GPM at 24 ft. of water of head pressure.

Best Choice: March Mfg. Magnetically coupled centrifugal pump.

Model #AC-5,5C-MD

Pumps 10 gpm at 31 ft. head

Envelope size: 6 7/16"Φ, 11 5/8" long

Weight: 15 1/2 lbms

Electrical power consumption: 290 watts

2) The silicone fluid cold system pump:

Requirements: Must pump 5 gpm at 24 ft. of head pressure

Best Choice: March Mfg. Magnetically coupled centrifugal pump.

Model #AC-5C-MD

Pumps 5 gpm at 25.5 ft. head

Envelope size: 5 13/16" Φ, 9 1/8" long

Weight: 9 1/2 lbms

Electrical power consumption: 227 watts

3) The silicone fluid "hot system" pump:

Requirements: Must pump 5 gpm at 24 ft. head pressure positive displacement pump. Must be able to pump 430°F (220°C) Hot Oil Fluid.

Best Choice : Hypro Series 500 Roller Pump

Model #505C

Pumps 5 gpm at 50 ft. head

Envelope size: 6"Φ, 14" long (with Bodine 1/6 Hp electric motor)

Weight: 19 lbms

Electrical power consumption: 375 watts

4) Silicone Fluid Control Valves:

Requirements: Must handle 5 gpm with a pressure loss of only 6 ft. of head. Must be able to handle 430°F silicone fluid. Must have a small envelope. Low energy consumption.

Best Choice: Humphrey 3-way diaphragm valve Model #590A (aluminum housing with a Viton diaphragm).

At a flow of 5 gpm the pressure loss is 4.5 ft. of head*

Has a very small envelope size of 4"x3 1/2"x3".

Weighs only 1 1/2 lbms.

Uses air pressure, therefore, does not consume very much power.

* Valve was operated in reverse to yield the desired flow pattern. A brass "diaphram support" ring was removed from the valve in order to obtain this low pressure drop.

5) A small air compressor to produce the control air pressure needed to actuate the Humphrey diaphragm valves.

Requirements: Small size must compress .002 CFM of air up to 40 psig.

Best Choice : Thomas Air Compressor

Model #004CA33

Compressor 0.25 CFM air up to 40 psig.

Envelope size: 4.34"x3.62"x5.37"

Weight: 3.5 lbm

Energy consumption: 187.5 watts, but since this motor runs only a few seccnds every few minutes, the actual average energy consumption is only about 20 watts.

6) "Cold Side" Air Fans:

Requirements: Must be lightweight and be able to displace 750 CFM of air under a static pressure loss of 0.3 inches of water.

Best Choice : Two (2) 8" EBM fans

Model #SZE200-BA19

Each fan...

will displace 375 CFM at 0.325" H_2O

has an envelope size of 8" Φx2.83" thick, weights 4 lbms

and consumes 82 watts of power.

7) "Ambient Side" Air Fans:

Requirements: Must be lightweight, efficient and displace 800 CFM of air under a static pressure of 0.4 inches of water.

"Best Pick": 2 - 12" EBM Fans

Model #SZE 300-BA05

Each fan...

will displace 800 CFM at 0.41" H_2O

and will have an envelope size of 12" Φx3.7" thick

weighs 6.5 lbms.

and consumes 230 watts of power

3.7 METAL HYDRIDE ALLOY SELECTION

The selection of the metal hydride heat exchangers and the liquid to air radiators determine the temperature gradients necessary to provide the heat transfer required for a desired cycle time. This information along with the temperature specifications of the waste heat air conditioner (90°F max shelter temperature, 120°F max ambient) set the bounds for alloy selection. Additional constraints are also imposed by the hydrogen pressure drops present in the coupled system and the maximum working pressure desired in the system.

Candidate alloy pairs were plotted on a van't Hoff plot and compared with the constraints. For this design a maximum hydrogen pressure of 1000 psia was adopted. Similarly, a minimum hydrogen pressure of 30 psia was selected to assure that internal pressure drops would not hinder hydrogen transfer.

3.7.1 Metal Hydride Alloys Selected

Four 50 lbm heats of alloy were melted for this program. Heats 1317-V and 1320-V had nominal compositions of $LaNi_{4.5}Al_{.5}$ and $LaNi_{4.475}Al_{.525}$ respectively and were intended for the high temperature "A" coil. Heats 1318-V and 1319-V had nominal compositions $MmNi_{4.52}Al_{.48}$ and $MmNi_{4.54}Al_{.46}$ respectively (Mm = mischmetal, a natural mixture of rare earth metals). Hydrogen desorption isotherms were measured at 25° and 85° C in order to obtain pressure points for the van't Hoff plots.

Heat 1317-V was selected as the high temperature alloy. Both of the low temperature candidates were too stable (i.e. the plateau pressure was too low) for the design conditions. An alternate, Heat 1163-V was selected from the Ergenics stock. Heat 1163-V is $CFMNi_5$, where CFM is Cerium-free mischmetal.

Figure 3.18 shows the actual van't Hoff plots for the metal hydrides used in this liquid prototype air conditioner. For this alloy pair, silicone fluid exceeding 215°C (419°F) is required when the ambient air is 49°C (120° F). Below is a list of the pertinent properties of each of the metal hydride alloys selected.

<u>High Temperature Alloy (Type A):</u>

Formula: $LaNi_{4.5}Al_{0.5}$

Ergenics Melt No. T-1317-V-2

Heat of formation: -9083 cal/gram mole H_2

Reversible hydrogen capacity = 0.587 H/M

The pressure/composition/isotherm for this alloy are shown in Figure 3.19.

<u>Low Temperature Alloy (Type B):</u>

Formula: $(CFM)Ni_5$

Ergenics Melt No. T-1163-V

Heat of formation: -6500 cal/gram mole H_2

Reversible hydrogen capacity = 0.683 H/M

The pressure/composition/isotherm for this alloy is shown in Figure 3.20.

3.8 METAL HYDRIDE AIR CONDITIONER - FABRICATION

After the selection of all of the major components, fabrication of the liquid prototype proceeded in two major avenues; that of metal hydride heat exchangers and the box enclosure. The driving consideration in this process was the conservation of space, since it was desired to make this first prototype as small as possible and thus be identical to the conventional freon type air conditioners in size (see Chapter 2).

This approach, though ambitious, did present major problems in fabrication, such as difficulty in sealing and tightening couplings. This became especially aggravating when silicone oil leaks started after the unit had been started up and then shut down (due to the expansion and then contraction of the coupling). It is strongly recommended that in any future work with liquid systems VCO* (registered trademark of Cajon Co.) type unions be utilized. They have been found to be leakfree, even in high vibration conditions.

3.8.1 Metal Hydride Heat Exchanger Assembly

As determined in Section 3.4.4, the design selected for the metal hydride containment was that of a 3/8" OD, 0.020" wall 304 stainless steel tube which was modeled after test reactor #11-24-86. This design is covered by an existing U.S. Patent assigned to Ergenics (Reference 3.3) The full scale hydride heat exchanger consists of seven 3/8" OD hydride tubes encased in a 1-3/8" OD, 0.035" wall, copper water jacket. The length of this water jacket (and thus the lengths of each 3/8" OD hydride tube) was determined by calculating the amount of metal hydride needed to produce the required cooling (see section 3.4.4), and dividing this number by the amount of metal hydride contained in a one foot length of 3/8" OD tube. Due to the smaller hydrogen storage capacity of the type A alloy, ($LaNi_{4.5}\ Al_{0.5}$) than that of the type B

alloy ($CFMNi_5$), a longer length of tubing for the type A alloy was used. The actual hydride coil lengths on each hydride heat exchanger are listed below.

Metal Hydride Coils A1 and A2

Metal hydride used: $LaNi_{4.5}Al_{0.5}$

Heat Number: T-1317-V-2

Mass Used: 4410 grams

Metal hydride alloy is contained in 7 - 3/8" OD stainless steel tubes (0.020" wall). Each tube is 15 ft. long. The 7 tube bundle is enclosed in a 1-3/8" OD (0.035" wall) water jacket.

Metal Hydride Coils B3 and B4

Metal hydride used: $(CFM)Ni_5$

Heat number: T-1163-V

Mass used: 3675 grams

Metal hydride alloy is contained in 7 3/8" OD stainless steel tubes (0.020" wall). Each tube is 12.5 ft. long. The 7 tube bundle is encased in a 1 3/8" OD (0.035"wall) water jacket.

Figures 3.21 through 3.24 detail the construction of these heat exchangers. It should be noted that before each 7 tube bundle was inserted into the water jacket, a small steel wire (dia = 0.0348") was carefully wrapped around each tube (see Figure 3.23). This wire served as both a tube separator to assure adequate fluid flow to the innermost hydride tube, and as a fluid agitator to disturb the fluid boundary layer, creating turbulence and thus improving heat transfer.

3.8.2 Hydride Air Conditioner Enclosure Assembly

Fabrication of the prototype air conditioner started with the selection of the various components required for operation (see Section 3.6). With these components selected, an overall view of their placement inside the "box" could begin. This was done through the construction of a styrofoam mockup (see Figures 3.25 and 3.26) that allowed quick and easy changes in the component positions and preliminary layout of piping. This technique yielded a very compact unit which contained all of the components in a 30"x26"x21 1/2" box. Figures 3.27 and 3.28 are structural drawings of the final version, while Figure 3.29 and 330 are photographs showing the compactness of the unit.

Figure 3.28A shows the air flow pattern through the enclosure. Here, shelter air that is to be cooled is pulled through the Modine 2978 heat exchanger, passing up through the plenum space, and then discharged out of the 8"Φ EBM SZE-200 fans. The ambient cooling air was of similar technique with the ambient air being pulled through the Modine 2930 and exiting through the 12" EBM SZE-300 fans that were placed on the top of the unit.

A primary concern in this compact placement was whether the close proximity of the metal hydride heat exchangers to the Modine 2930 ambient heat exchanger, would impede air flow through the Modine 2930. In order to determine this, efficiency tests on the Modine 2930 were conducted to determine how the heat rejection capabilities of the Modine 2930 were effected as the hydride coils were placed closer and closer to the Modine 2930. Figure 3.31 shows the result of these tests and clearly indicated that the Modine 2930's performance was not severely affected even at the very close placement of 1/2 inch.

Figures 3.32 through 3.35 delineates the construction of the prototype. While the size of the unit was kept at the 30"x26"x21 1/2" limit, the weight of the

unit climbed to 365 lbms. The following is a list of each component used in the prototype and its corresponding weight.

Aluminum box frame, 1/8" thick, 1" angle	=	8.9	lbms
Aluminum sides, 0.032" thick	=	12.7	lbms
Metal hydride heat exchangers, 2 at 35 lbm each 2 at 28 lbm each	=	126.0	lbms (total)
Modine 2978 cold side radiator	=	9.0	lbms
Modine 2930 ambient side radiator	=	25.0	lbms
8"Φ EBM SZE200 fans, 2 at 4.0 lbms each	=	8.0	lbms
12"Φ EBM SZE 300 fans, 2 at 6.5 lbms each	=	13.0	lbms
March #AI-5C-MD cold side pump	=	9.5	lbms
March #AC-5.5C-MD ambient side pump	=	15.5	lbms
Hypro #505C hot side pump and motor	=	19.0	lbms
Humphrey #590A 3-way diaphragm valves, 8 at 1.5	=	12.0	lbms
Nupro #SS-HBVVC04-0 air actuated hydrogen valves, 2 at 1.5 lbms each	=	3.0	lbms
Assorted unions at 1.0 lbms each	=	20.0	lbms
40 ft of 1 3/8" OD Copper tubing	=	26.0	lbms
Slytherm 800 silicon fluid 5.26 gal. at lbm/gal	=	42.0	lbms
Thomas #004CA-33 air compressor	=	3.5	lbms
Humphrey minimizer air valves, 5 at 0.15 lbm/ea	=	0.8	lbms
Air reservoir and associated fittings	=	3.0	lbms
Miscellaneous Wiring, Timers & Insulation	=	8.0	lbms
TOTAL	=	365	lbms

Although 365 lbm is 83% greater than the 200 lbm mass of the conventional freon based air conditioner, this is not deemed excessive when one considers that this was the first prototype of its kind. Much greater weight savings can be utilized with future designs incorporating faster heat transfer techniques. Much of this heat transfer is achieved by using metal hydride containment tubes that are much smaller in diameter than the 3/8" OD tubes used in this design. The air/air system design proposed in Part III of this report suggests a weight savings of 200 lbms due to the elimination of the heat transfer liquid and pumps and valves needed for its movement and control.

3.8.3 High Temperature Heat Exchanger Assembly

Heating of the silicone fluid in this first prototype was accomplished with the fabrication of a simple tube heat exchanger. Heating was supplied via the combustion of hydrogen gas which was later changed to propane due to the ease of fuel supply handling, i.e., one propane tank would replace 10 hydrogen gas

cylinders.

This heater was sized to provide about 30,000 BTU/hr of simulated diesel exhaust heat (220°C) to the metal hydride air conditioner. During the initial test of the prototype, it became evident that this was not enough heat for full system output operation, therefore, a second high temperature heat exchanger was made that utilized a different design.

The second high temperature heat exchanger (see figure 3.36) consisted of about 100 ft. of 1-1/8"OD copper tubing that was coiled into a spiral type formation. Propane burners were installed under this copper coil. The air conditioner's silicone fluid flows through the inside of the copper tubing and is heated by the propane gas that is burning on the outside of the copper tube. This heat exchanger was designed to produce 48,000 BTU/hr of heat at the required temperature of 220°C. A thermocouple placed inside of the copper tube constantly monitored the temperature of the silicone fluid exiting the high temperature heater. This thermocouple was also connected to a temperature controller that controlled the operation of a solenoid valve through which the propane gas flowed.

3.9 METAL HYDRIDE AIR CONDITIONER - TESTING

After assembly of metal hydride air conditioner was completed, some initial "debugging" was performed. While these tests did produce some cooling (about 4500 BTU/hr), it soon became clear that meaningful results could not be achieved unless key test data such as the actual silicone fluid flow through the metal hydride heat exchangers could be monitored at all times.

Therefore, for the next phase of the prototype's testing fluid flow, meters and

temperature thermocouples were procured. The silicone fluid flow meters were placed on the inlets of each metal hydride heat exchanger. The immersion type thermocouples were placed on both the inlet and outlet of each metal hydride heat exchanger. With this new test data in hand, the exact amount of cooling produced by the metal hydride air conditioner could be calculated for any operating point.

3.9.1 Instrumentation Setup - Fluid Flow Meters

At the beginning of the bridge contract, a search was initiated to find a robust fluid flow meter that would provide quick and easy determination of the silicone fluid flow and also be able to handle the high temperature of the silicone fluid which was at 220°C (440°F). The fluid flow meter selected was a Sentinel/Rhodes Model number 904, which is actually a fluid flow indicator that visually shows the fluid flow. These flow indicators were an excellent choice due to their compact size and high pressure and temperature capabilities (150 psig at 400°F).

Four Rhodes 904 fluid flow indicators were purchased. They were calibrated against a standard in-line flow meter to ensure that their indication was accurate. Figure 3.37 is the calibration curve for these flow meters. After the calibration of the Rhodes flow meters was completed, the metal hydride air conditioner was disassembled and a flow meter was assembled onto the inlet of each hydride heat exchanger. Figure 3.38 shows the air conditioner with the flow indicators in place after reassembly.

3.9.2 Instrumentation Setup - Thermocouples

After the prototype air conditioner was disassembled, a 0.040"Φ type K subminiature thermocouple (Omega #KMTSS-040G) was placed on the inlet and

outlet of each metal hydride heat exchanger. In the placement of these thermocouples, the tip of each thermocouple is inserted directly into the silicone fluid. By the use of this technique, a near instantaneous (time constant < 2 sec) measurement of the true fluid temperature was obtained. Output from these thermocouples was recorded on a Soltec #3616 strip chart recorder which employed two, thermocouple recorders.

In order to present the temperature data in the most comprehensive and understandable form, a bread board "switching station" was made (Figure 3.39). The switching station consisted of a solid state repeat timer and multiple toggle switches that enabled the output from any of the thermocouples to be recorded by either of the Soltec strip chart pens almost instantaneously. This technique generated a unique temperature output that recorded both the inlet temperature (to the metal hydride heat exchanger) and the outlet temperature (from the metal hydride heat exchanger) alternately on the same strip chart pen. This generated the "shaded" recording as shown in Figure 3.40, whose boundaries represent either the inlet or outlet temperature data. Therefore, heat load calculations can now be performed if one knows the fluid flow through the metal hydride heat exchanger that is being analyzed. The silicone oil fluid flow is, of course, known by the indication on the Rhodes 904 flow meters that were placed on each heat exchanger.

3.9.3 Test Procedures and Variables

Of prime importance in the testing of any metal hydride related equipment is the effect of "cycle time" on the equipment's operation. The 1/2 cycle time is the length of time allowed for absorption or desorption of the hydrogen gas into or out of the metal hydride heat exchangers. Other variables such as the heat source temperature and the sensible heat delay temperature also effect

device performance. A minimum cycle time consistent with full hydrogen transfer is desired. The heat source temperature should be kept as high as possible--but not to exceed 235°C, the temperature at which the equilibrium hydrogen pressure equals 1000 psia. The sensible heat delay temperature is usually set at the average value between the temperatures of the fluid sources in question. (A detailed explanation of this metal hydride technology is given in Appendix 3.2 and explains, at length, concepts such as sensible heat delay.)

Another variable of interest is the hydrogen valve delay timer. This is the delay timer that controls the hydrogen valves that separate the paired metal hydride heat exchangers. These normally open valves are closed just after the fluid switching of the hydride coils. The closing of these hydrogen valves at the start of the cycle keeps hydrogen gas from flowing prematurely from one of the hydride heat exchangers to the other. This keeps the thermal energy from the hydrogen/hydride reaction from occurring until the temperature of the heat transfer fluid has changed to the new process temperature (see Figure 3.2).

As described in sections 3.9.1 and 3.9.2, the test data collected consisted of strip chart thermocouple output and silicone fluid flow rate data that was obtained visually from the inline fluid flow meters. The test procedure consisted of recording both the inlet and outlet fluid temperatures (of a hydride heat exchanger such as the B type coil B4) on the same strip chart pen. This was done by setting the repeat timer on the thermocouple "switching board" to a 3 second cycle. This means that once every 3 seconds, the repeat timer would connect the strip chart pen alternately to the fluid inlet and outlet thermocouple. This produced the "shaded" graph type output shown in Figure 3.40. Simultaneously the silicon fluid flow rate through the relevant hydride heat exchanger in question was recorded manually in the margin of the "shaded

curve" shown in Figure 3.40.

The data were recorded in steady state conditions after the air conditioner had completed a few cycles at a given 1/2 cycle time and heat source temperature. This technique eliminated any misleading data that could be generated by abrupt changes in operating conditions. Once the data had been recorded, the test parameter would be changed (such as changing the 1/2 cycle time from 3 minutes to 3.5 minutes). In this way, an operation map could be quickly generated.

Appendix 3.3 at the end of this chapter is a short explanation of the general operating instruction for this prototype.

3.9.4 Test Data Analysis

Of critical interest in the operation of the hydride air conditioner is the amount of cooling produced by the B type hydride coils, therefore, this section will "walk through" the actual analysis procedure that was used to determine the true amount of cooling generated by the hydride heat exchanger.

The following discussion describes the analysis of one test #5/26/88/31. The test analysis procedure shown here was used to determine all of the test results shown in section 3.9.5.

Analysis of Hydride Air Conditioner Test Point #5/26/88/31

Test Conditions

1/2 cycle repeat time = 3.5 minutes

Temperature of the hot silicone fluid = 220°C (428°F).

Temperature of ambient air = 24.7°C

Average flow rate of silicone fluid through hydride heat exchangers #A1 = 5.45 gpm

Average flow rate of silicone fluid through hydride heat exchanger #A2 = 4.40 gpm

Average flow rate of silicone fluid through hydride heat exchanger #B3 = 5.30 gpm

Time delay of the hydrogen valves = 1 sec.

Hot side sensible heat temperature delay setting = 120°C (248°F)

Cold side sensible heat temperature delay setting = 30°C (86°F)

Air flow rate of the air passing through the Modine #2978 cold side radiator = 700 ft/sec

Air flow rate of the air passing through the Modine #2930 cold side radiator = 700 ft/sec

In this test, the metal hydride heat exchanger that is producing the "cooling" is hydride bed B4. The actual data generated is shown in the lower curve of Figure 3.41.

The first step in analyzing this data is to redraw the temperature profile shown in Figure 3.41 to a new graph which will expand the time frame involved. This was done for this test and the new graph is shown in Figures 3.42A and 3.42B.

The second step is to draw above the new temperature profile curve (Figures 3.42A and 3.42B) the true flow rate curve of the silicone fluid flowing through the B4 heat exchanger. The flow rate data for this curve is obtained by taking the flow meters indicating number (which was recorded during the test) and finding the true calibrated flow rate valve from the flow meter calibration curve shown in Figure 3.37. A correction to the indicated flow rate of 0.8 is also included to account for a slight tilting of the Rhodes flow meter when it

was placed on the air conditioner. The new true flow rate curve is shown above the temperature profile curve shown in Figure 3.42A and 3.42B.

The next test reduction step done was to break out the temperature profile curve and the flow rate curve shown in Figures 3.42A and 3.42B into discreet time intervals of 0.1 minute duration.

Now the exact amount of cooling produced during each time interval can be determined by the basic sensible heat equation,

$$Q = M * C_p * \Delta T$$

where,

Q = the amount of heat generated (or lost) during the time interval in BTU

M = the mass of silicone fluid that flowed during the interval in lbms.

C_p = the heat capacity of the silicone fluid in BTU/(Lbm°F)

ΔT = the difference in the temperature of the inlet and outlet silicone fluid flow in °F. Please note that if the outlet temperature is less than the inlet temperature, the metal hydride extracted heat out of the silicone fluid and thus produced "cooling" during this time interval.

Since the mass flow data on the silicone fluid is actually obtained as volumetric flow (v, gal/min), the sensible heat equation can be changed to

$$Q = v * \rho * \Delta t * C_p * \Delta T$$

where ρ is the fluid density in lbm/gal. A curve showing how the density and heat capacity of the silicone fluid varies with temperature is given in Figure 3.43.

When this sensible heat calculation is performed on each time interval, the total cooling load can be "integrated" and thus determined. Tables 3.3A through 3.3C shows the results of each sensible heat calculation for the test data shown in Figures 3.42A and 3.42B.

From Table 3.3A and 3.3B one can see that if each integration interval is added together, a total value of 483 BTU of cooling was generated by the hydride coil. This, however, is not totally correct since additional cooling was used to cool down the metal hydride heat exchanger from the warm ambient temperature to the cooler shelter air temperature. Most of this sensible heat is recovered in each cycle by delaying output fluid switchover (by 0.3 min in this example). Only when the hydride heat exchanger is producing cooling below the shelter air temperature can it be considered to be producing net shelter air cooling. Therefore, any cooling produced on the fluid that has a temperature above the ambient temperature (24°C) must be subtracted from the gross cooling value of 483 BTU (see the ambient temperature line in Figure 3.42A and 3.42B. When this is done we find that about 24 BTU must be subtracted from the total cooling value of 483 BTUs to obtain the true net cooling value of 459 BTU. And since this amount of cooling was produced in a 3.5 min. time frame, then the cooling rate of the hydride air conditioner becomes 459 BTU/3.5 min. = 131 BTU per minute, or 7869 BTU per hour.

The above analysis determines the quantity of cooling imparted by the hydride coil (B-coil) to the silicone fluid. This cooling is transformed to conditioned air via the cold-side fluid-to-air heat exchanger. Response time is rapid since the volume of silicone fluid in this portion of the system (about 1 Gal.) is small relative to the quantity of fluid circulated through

the heat exchangers during the cooling cycle (about 12 Gal.).

3.9.5 Test Results

The test analysis described above in 3.9.4 was performed on each desired test point. The results of these calculations on these test points are shown on Table 3.4.

Figure 3.44 is a plot of the net cooling produced by the metal hydride air conditioner versus the 1/2 cycle time. This curve reveals a definite peaking of the cooling output from the air conditioner of about 7900 BTU/hr at a 1/2 cycle time of 4 minutes. This 7900 BTU/hr is about 14% lower than the design point of 9000 BTU/hr.

The slightly lower than design point cooling achieved is thought to be caused by the low silicone fluid flow rates during the operation of the "cold side" hydride heat exchanger. Flow rates of only 3.3 GPM were obtained (see Figure 3.42). Faster flow rates would shift the peak in Figure 3.44 to shorter times and increase the cooling output. The cause of this reduced fluid flow is due to the higher viscosity of the silicone fluid as it cools down. This fluid viscosity change (from 10 cst at 25°C to 25 cst at 5°C) has a very detrimental effect on the operation of the cold side fluid pump, which is of the centrifugal type. However, the viscosity change of the silicone fluid does not fully account for the low fluid flow reading of 3.7 gpm when the fluid is at the "warm" temperature of 25°C. The cold side fluid flow in this condition should be closer to the design point of 5 gpm, which means one can only conclude that higher than expected pressure drops are also being experienced in the system piping.

Of equal importance in the analysis of this test data is the determination of the air conditioner's thermodynamic coefficient of performance (COP). This is done by determining the amount of heat that was used to run the air conditioner. Figure 3.41 also shows the temperature data on the A type hydride heat exchanger that is being heated by the hot silicone oil. Determination of the amount of heat used by the "A" type coils is done just like the approach that was used to determine the amount of cooling that was generated by the B type hydride heat exchanger; with temperature changes and silicone fluid flow rates being used to determine the sensible heat changes of the silicone fluid. When this was done for the test point of 5/26/88/5 (at a 1/2 cycle time of 4.5 minutes, and a hot silicone fluid temperature of 220°C) we find that 23,880 BTU/hr of heat was used to run the unit. From Figure 3.44, the net cooling at a 4.5 min cycle is approximately 7800 BTU/Hr. Therefore, the thermodynamic COP of the metal hydride air conditioner at this point was 7800/23,880 = 0.33.

Another important result found from the test data is the very small effect of the hydrogen valve delay time on the cooling output of the air conditioner. Comparison of test points 5/26/88/31 and 5/26/88/29 which were conducted with the same 1/2 cycle times but different H_2 valve delay times illustrates this result. The data shows that even though the amount of H_2 delay time differed greatly in the two tests (1 sec for test #-31 and 32 sec for test #-29). The actual effect on the cooling produced by the air conditioner is negligible with 7869 BTU/hr being produced in test #-31 (1 sec H_2 time delay) and 7571 BTU/hr being produced in test #-29 (32 sec H_2 time delay).

3.10 CONCLUSIONS

The successful operation and testing of the waste heat driven metal hydride air conditioner shows that viable air conditioning can indeed be generated via metal hydride technology.

At peak operating performance, the hydride air conditioner produced 7868 BTU/hr of cooling (see Figure 3.44) with a thermodynamic COP of 0.33. Electrical power consumption at this point was 1500 watts, which is about 1/2 of the electrical power required to run a comparably sized freon based conventional air conditioner.

It was further demonstrated that the use of hydrogen valves to control the movement of hydrogen gas between the metal hydride heat exchanging is unnecessary since their delayed operation seemed to have little or no effect in the overall performance of the air conditioner.

The final metal hydride package size of 30"x26"x21 1/2" is 67% larger than the conventional freon size of 23 3/4"x26 3/8"x16 1/16". The weight of 365 lbms is 83% heavier than the 200 lbm weight of the conventional freon air conditioner. This is extremely encouraging for a first-of-a-kind prototype.

Lastly, the metal hydride's electrical power consumption of 1500 watts is much less than that required for the freon unit of 2950 watts.

These results on the performance of the first prototype waste heat driven metal hydride air conditioner are extremely encouraging. Future improvements can be expected from more advanced metal hydride units. This is confirmed in Chapter

5 of this report which details the design of an air to air type metal hydride air conditioner that does not require the use of an intermediate fluid such as silicone oil (nor the fluids' pumps and valves). The results of this study suggest a much lighter hydride air conditioner of 165 lbms with an electrical power consumption of only about 365 watts, which is about 15% of the power of the conventional freon unit.

3.11 ACKNOWLEDGEMENTS

The authors, Mr. E. Lee Huston, Project Manager and Mr. P. Mark Golben, Senior Design Engineer, are indebted to the helpful expertise and advice provided by Mr. Bob Rhodes, Technical Project Officer for Fort Belvoir for this project. We would also like to thank Ergenics technicians Mr. David J. Hanley and Mr. Stephen Simon for their patient fabrication of the prototype. Special mention is also due to Judy Rosner for the typing of this report and Rose Maslak for editing.

The Dow Corning Corp., Midland MI donated the Syltherm 800® heat transfer fluid for this project. Product Manager Mr Gary McEntire and his staff deserve our special thanks for their interest in new product development and applications.

3.12 REFERENCES

3.1 Golben, P.M. Multi-Stage Hydride-Hydrogen Compressor. Proc. 18th Intersociety Energy Conversion Engineering Conference, Aug. 21-26, (1983) 1746-1753.

3.2 Golben, P.M. and Huston E.L. A Technique for Analyzing Reversible Metal Hydride Systems Performance. J. Less-Common Metals, 89 (1983) 333-340.

3.3 Golben, P.M. and Storms, W.F. Flexible Means for Storing and Recovering Hydrogen, U.S. Patent 4,396,114 issued Aug. 2, 1983.

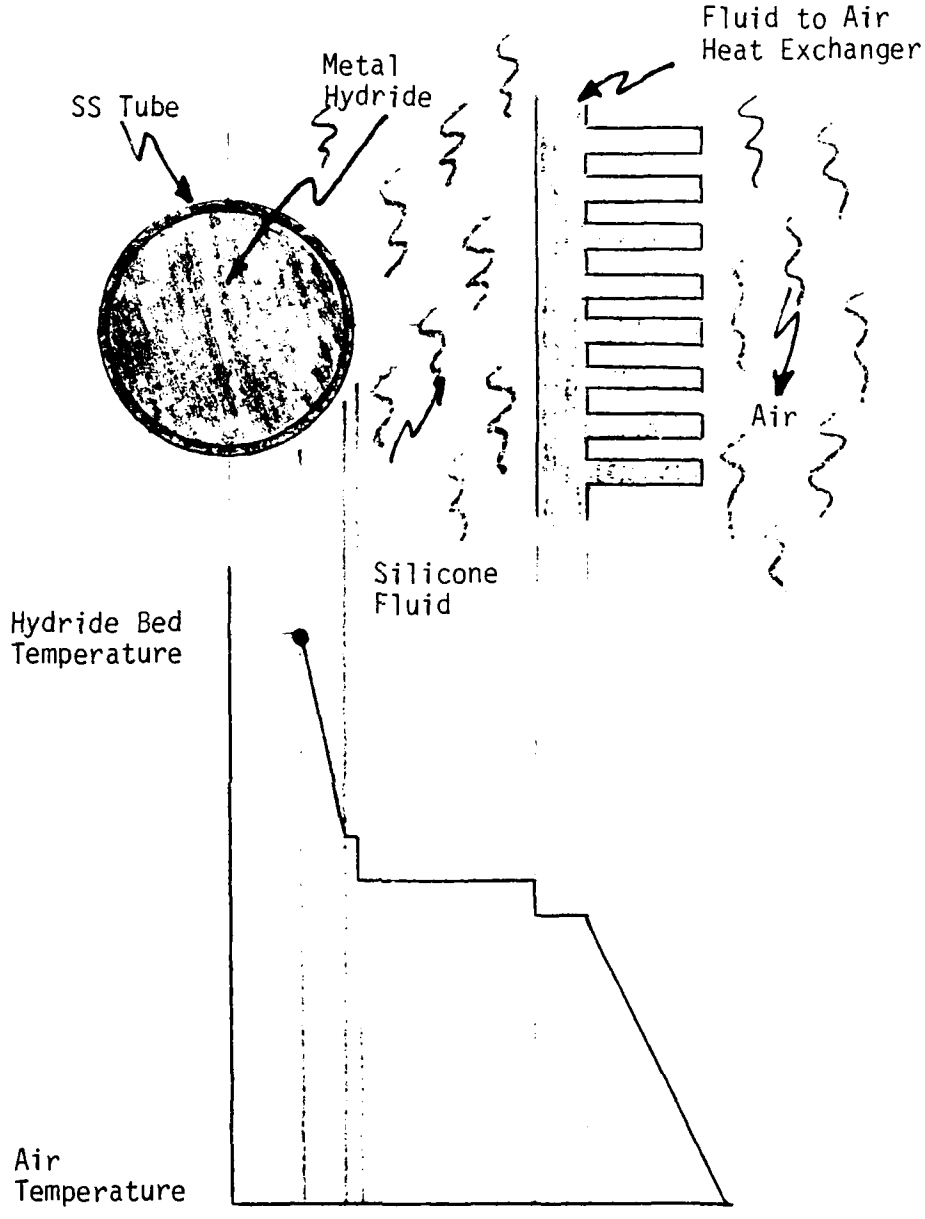

Figure 3.1 - Conceptual View of the Heat Transfer Processes Present in the "Liquid" System When Hydrogen is being Absorbed by the Metal Hydride

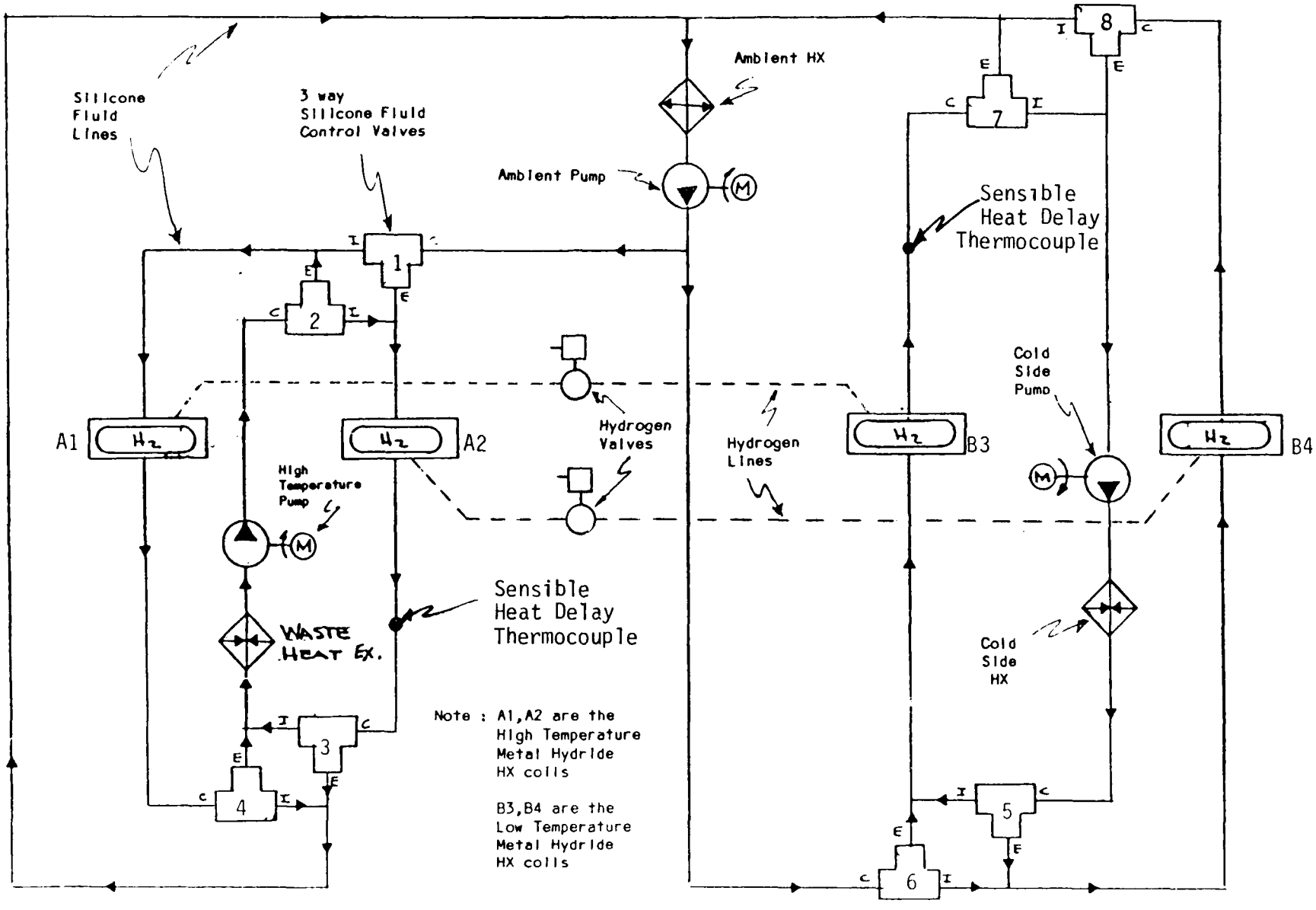

Figure 3.2 - WASTE HEAT METAL HYDRIDE AIR CONDITIONER OPERATION CONTROLS SCHEMATIC

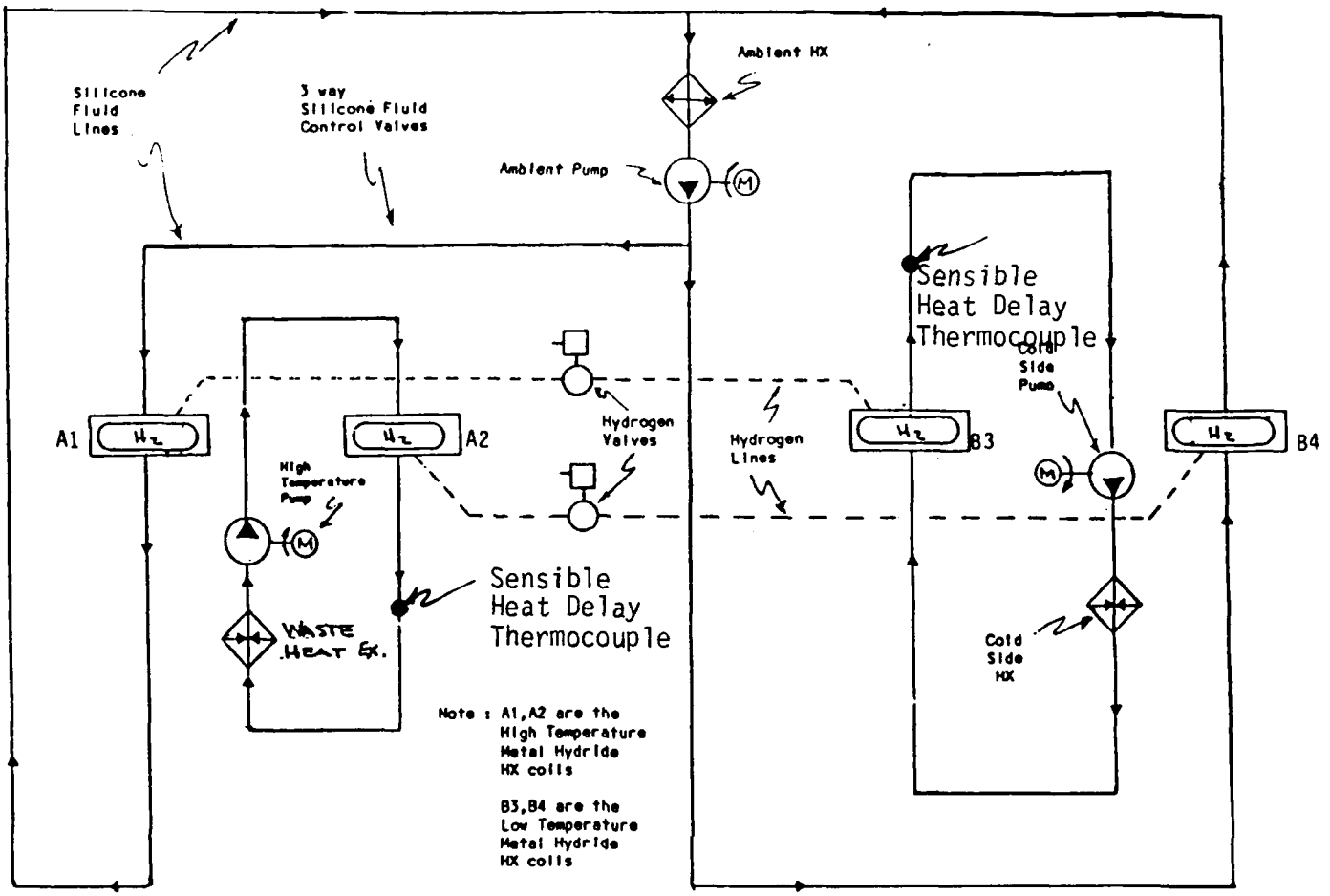

METAL HYDRIDE HEAT EXCHANGER CONDITIONS:

Bed A1 is rejecting heat to the ambient air
Bed A2 is receiving heat from the high temperature fluid
Bed B3 is producing "cooling" for the shelter
Bed B4 is rejecting heat to the ambient air

Figure 3.2A - Waste Heat Metal Hydride Air Conditioner Operation Controls Schematic

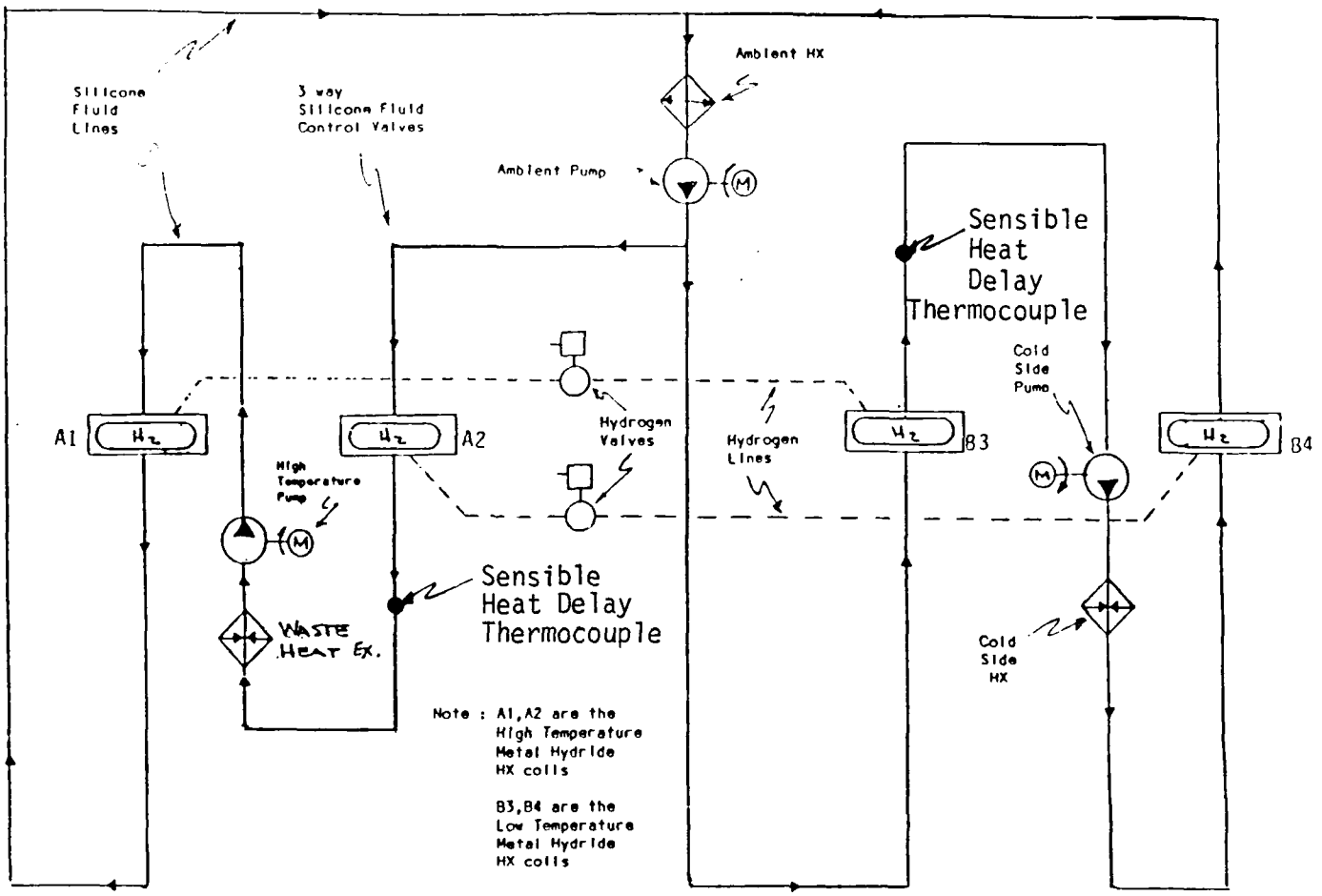

METAL HYDRIDE HEAT EXCHANGER CONDITIONS:
[TRANSIENT SWITCHOVER MODE]

Bed A1 is receiving fluid from the high temperature heater
Bed A2 is receiving fluid from the ambient heat exchanger
Bed B3 is receiving fluid from the ambient heat exchanger
Bed B4 is receiving fluid from the cold side heat exchanger

Figure 3.2B - Waste Heat Metal Hydride Air Conditioner Operation Controls Schematic

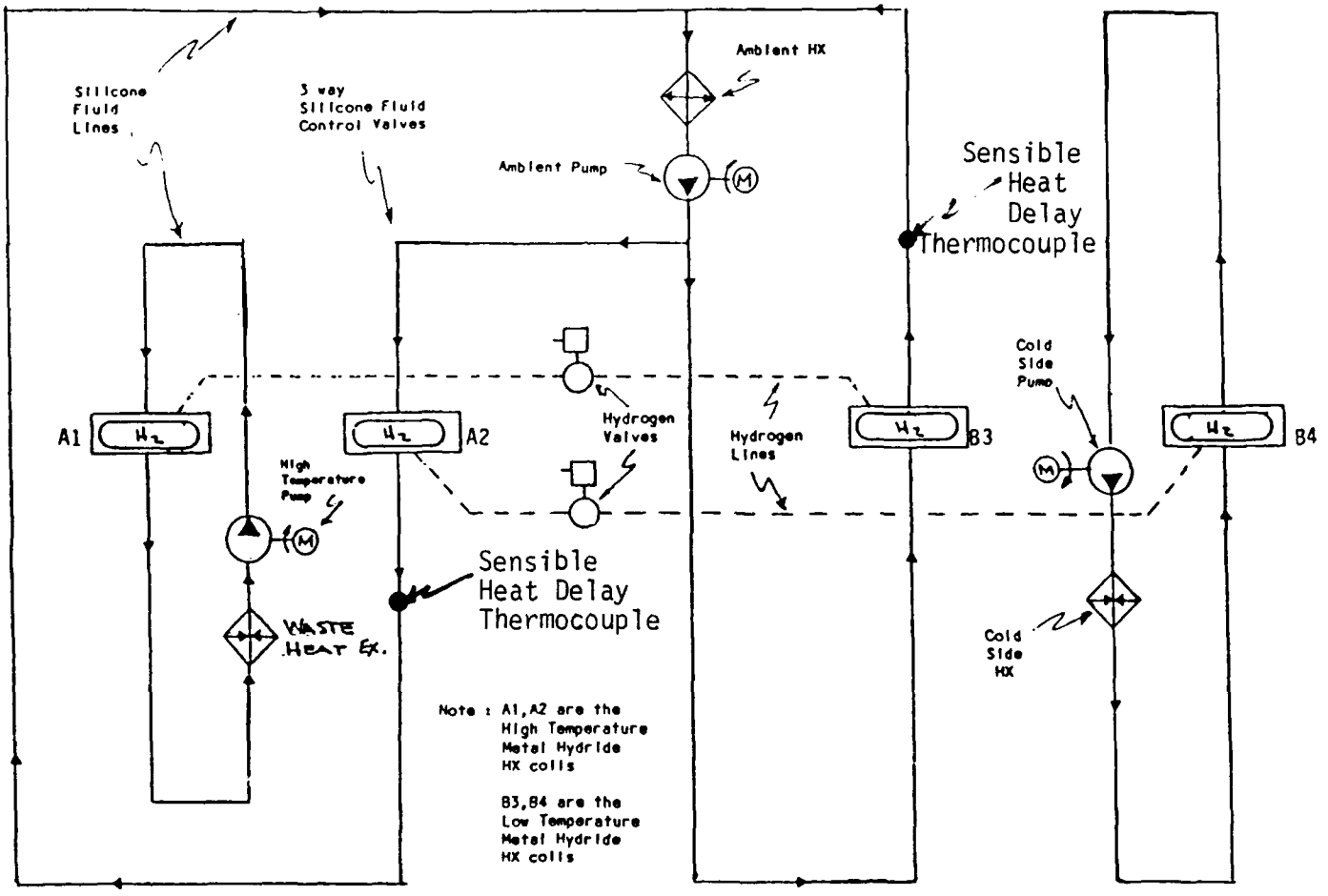

METAL HYDRIDE HEAT EXCHANGER CONDITIONS:

Bed A1 is receiving heat from the high temperature fluid
Bed A2 is rejecting heat to the ambient air
Bed B3 is rejecting heat to the ambient air
Bed B4 is producing "cooling" for the shelter

Figure 3.2C - Waste Heat Metal Hydride Air Conditioner Operation Controls Schematic

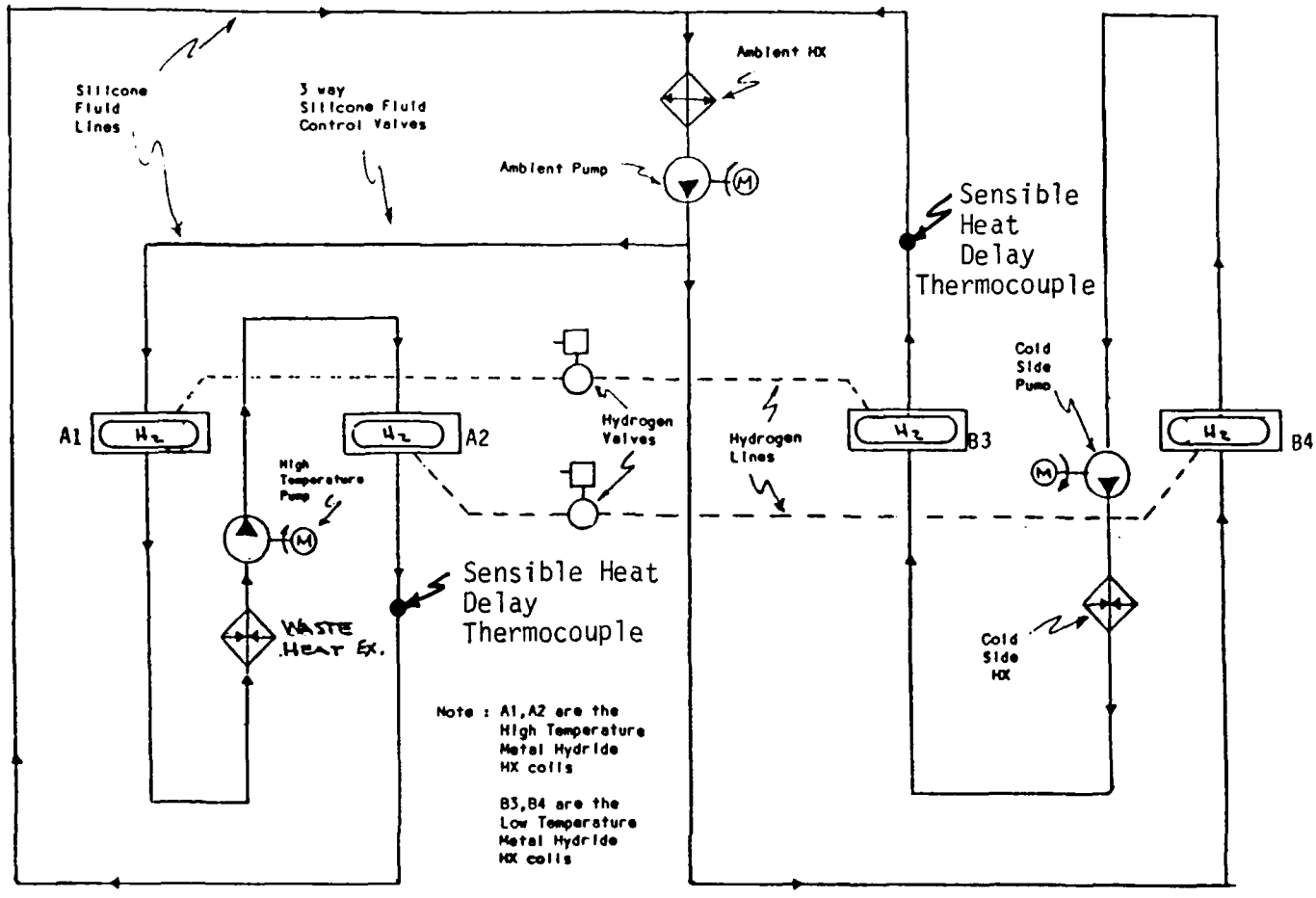

METAL HYDRIDE HEAT EXCHANGER CONDITIONS: (Transient Switchover Mode)

Bed A1 is receiving fluid from the Ambient Heat Exchanger
Bed A2 is receiving fluid from the high temperature heater
Bed B3 is receiving fluid from the cold side heat exchanger
Bed B4 is receiving fluid from the ambient heat exchanger

Figure 3.2D - Waste Heat Metal Hydride Air Conditioner Operation Controls Schematic

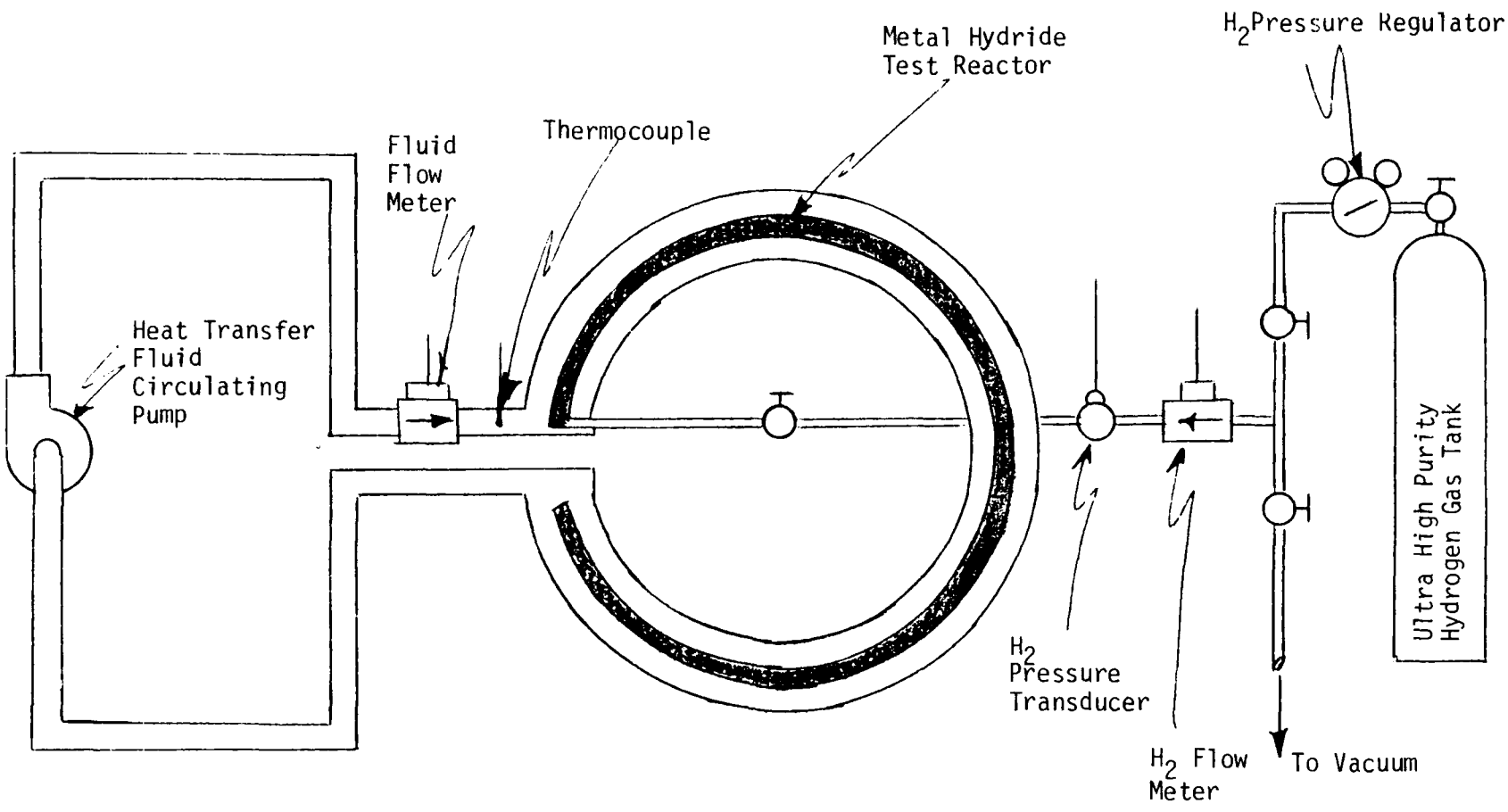

Figure 3.3 - Schematic of the Heat Transfer Test Setup

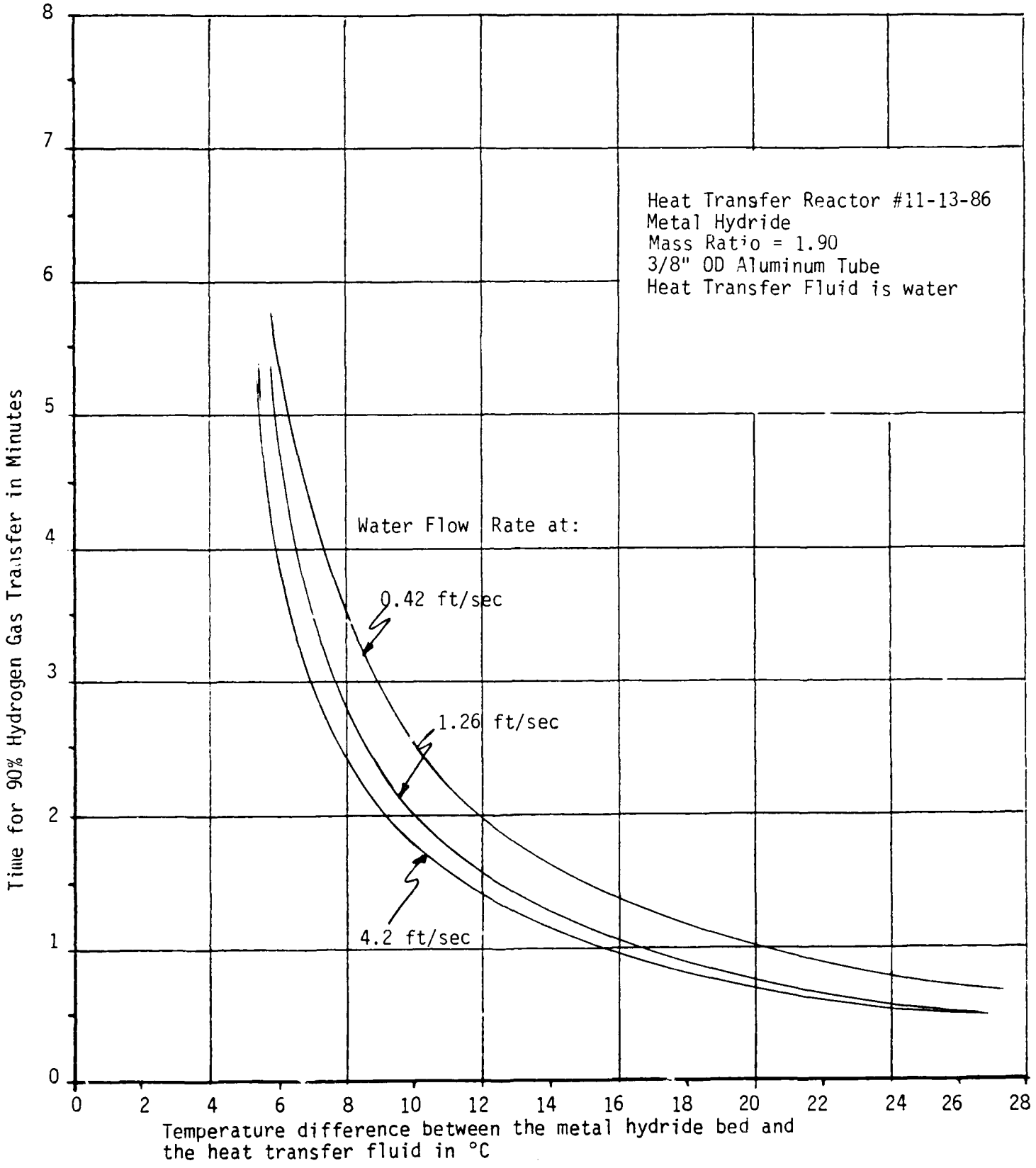

Figure 3.4 - Time for 90% Hydrogen Gas Transfer vs. Temperature for Test Reactor #11-13-86

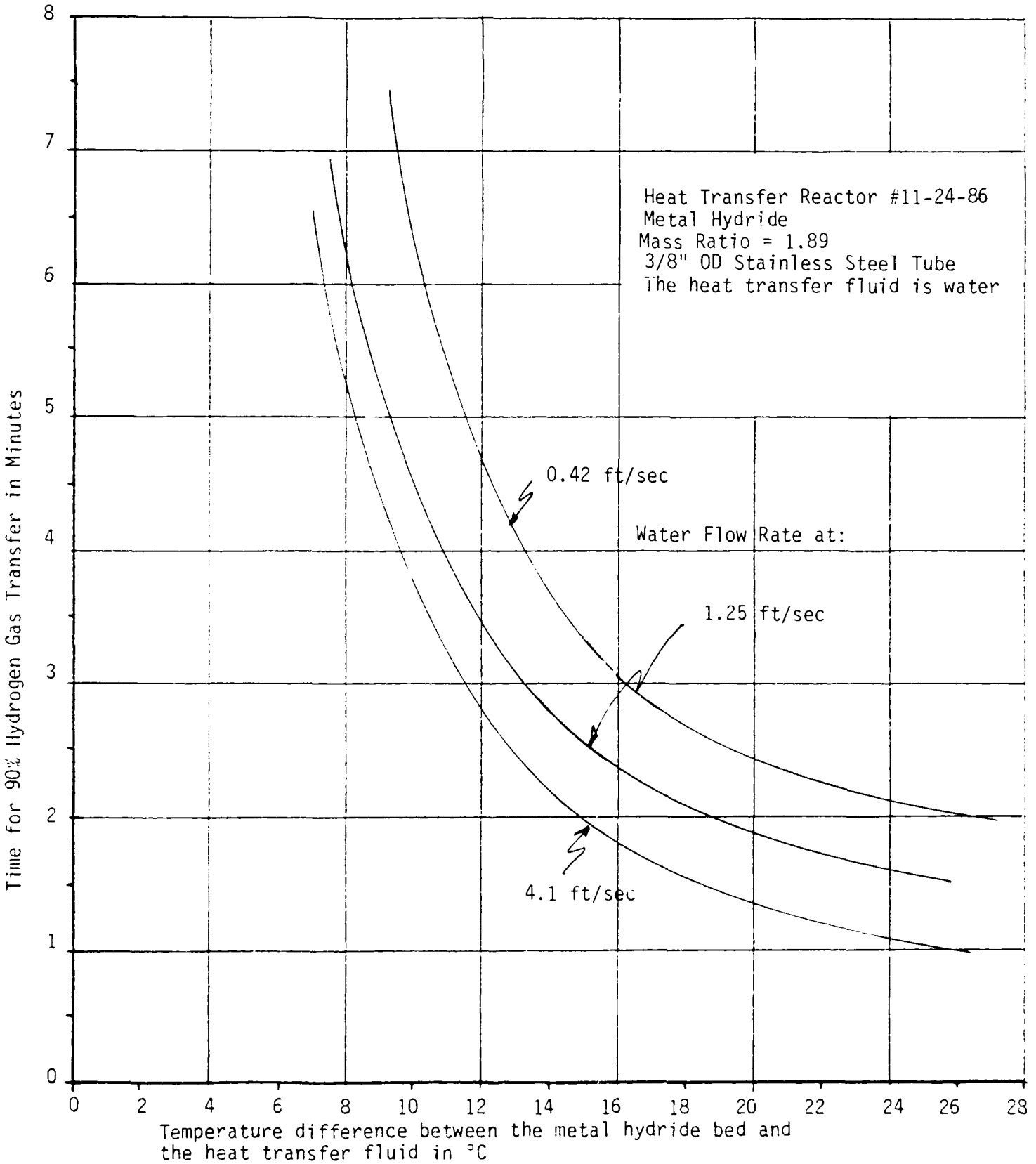

Figure 3.5 - Time for 90% Hydrogen Gas Transfer vs. Temperature for Test Reactor #11-24-86

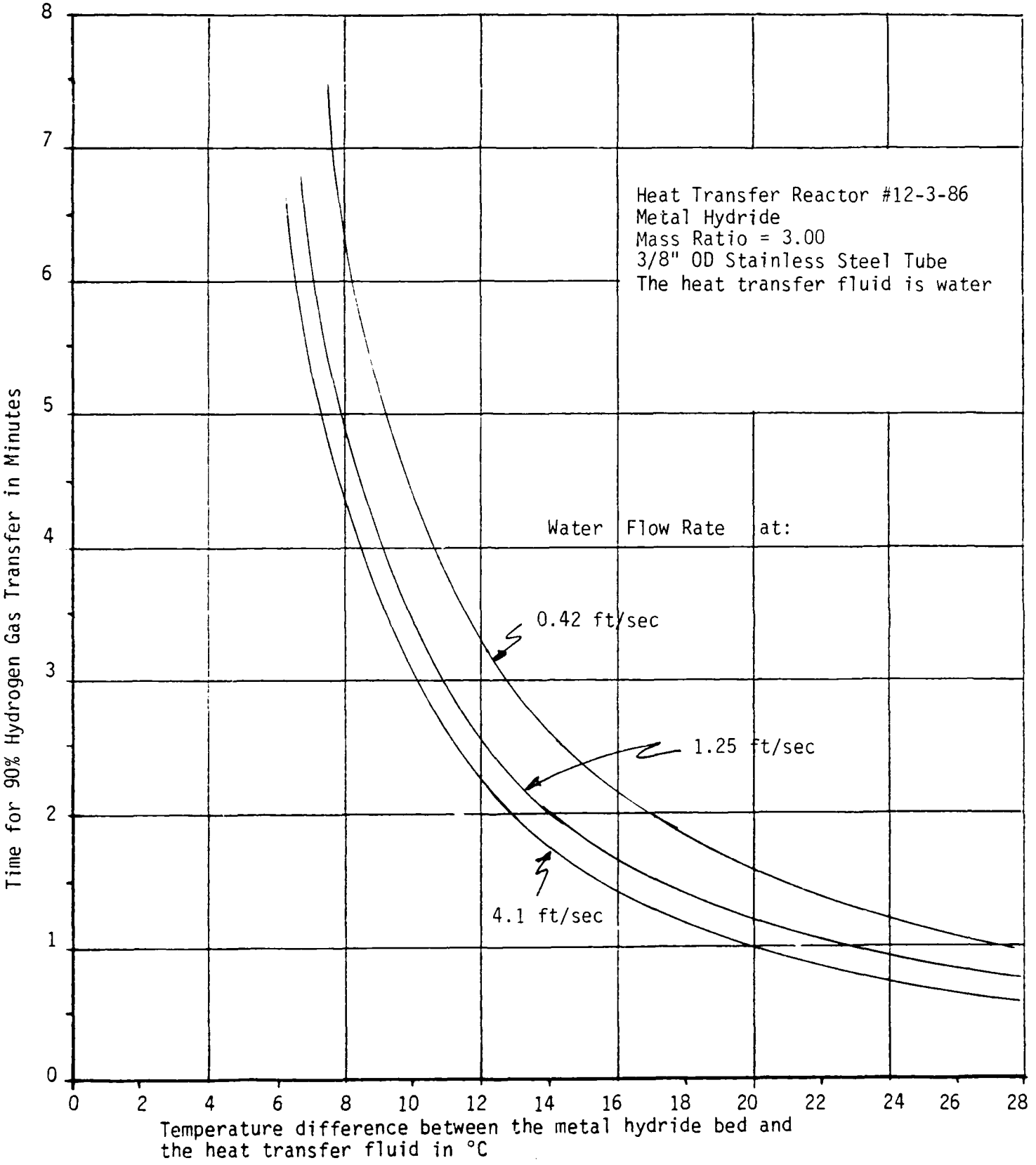

Figure 3.6 - Time for 90% Hydrogen Gas Transfer vs. Temperature for Test Reactor #12-3-86

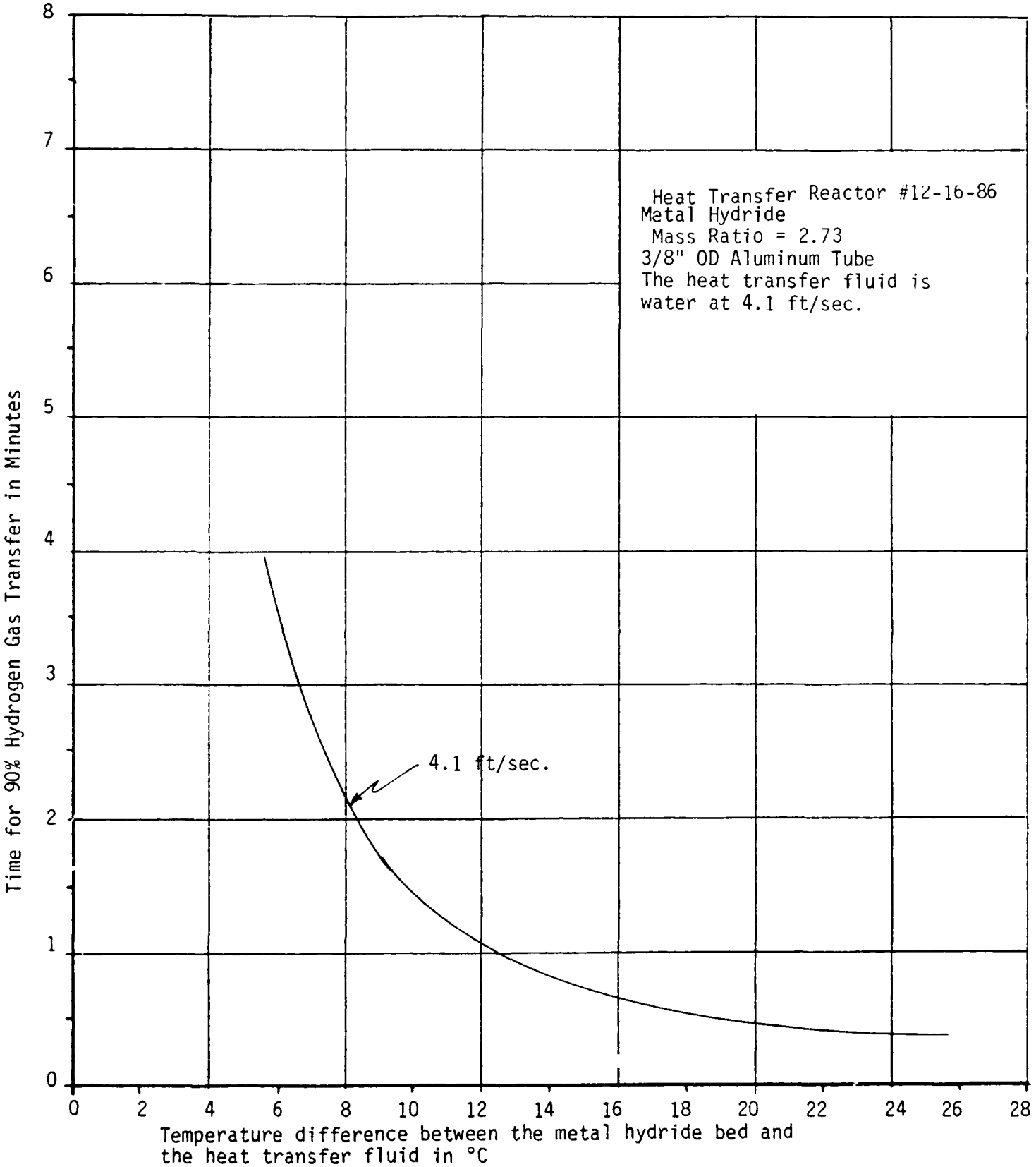

Figure 3.7 - Time for 90% Hydrogen Gas Transfer vs. Temperature for Test Reactor # 12-16-86

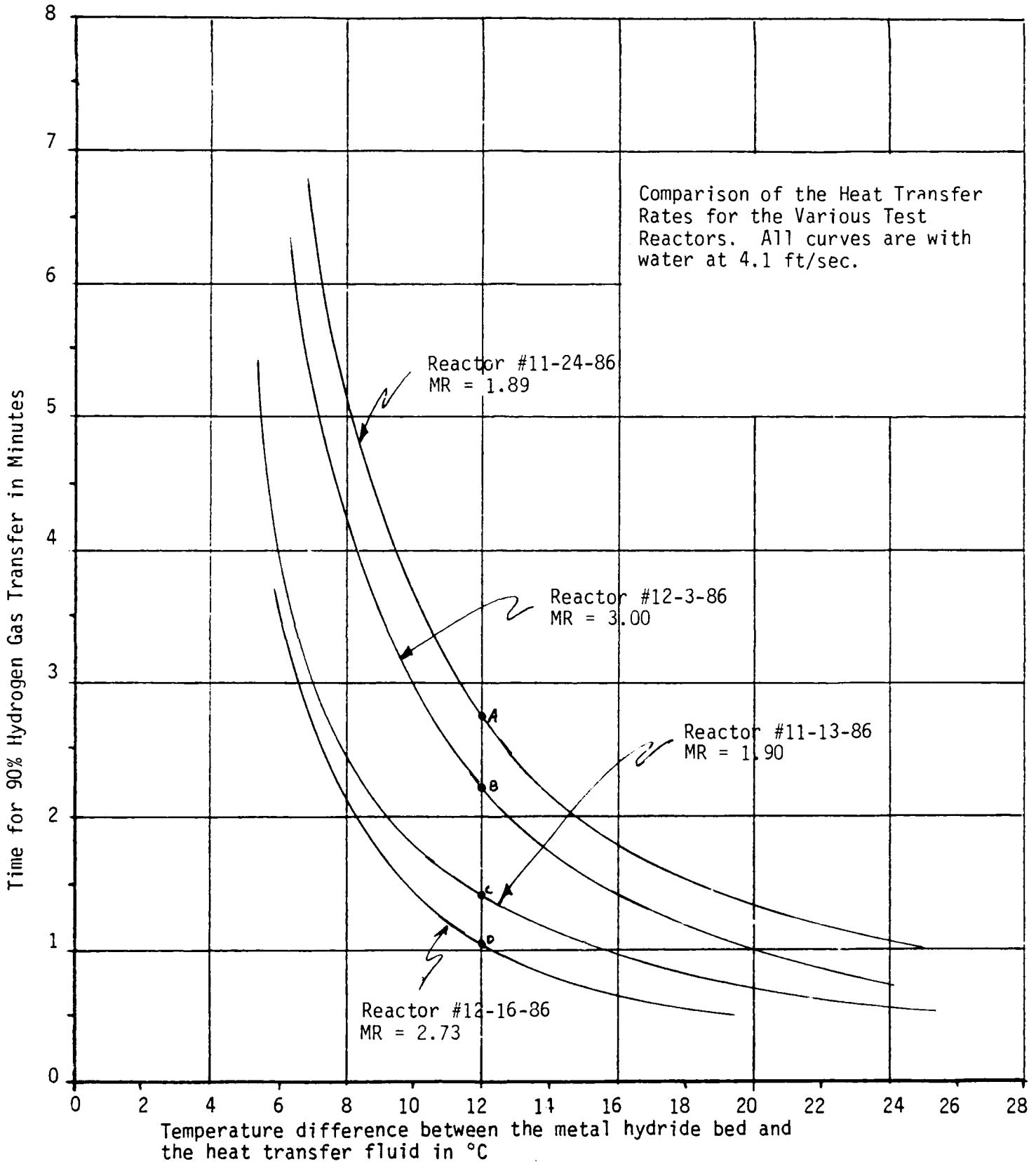

Figure 3.8 - Time for 90% Hydrogen Gas Transfer vs. Temperature for Test Reactors

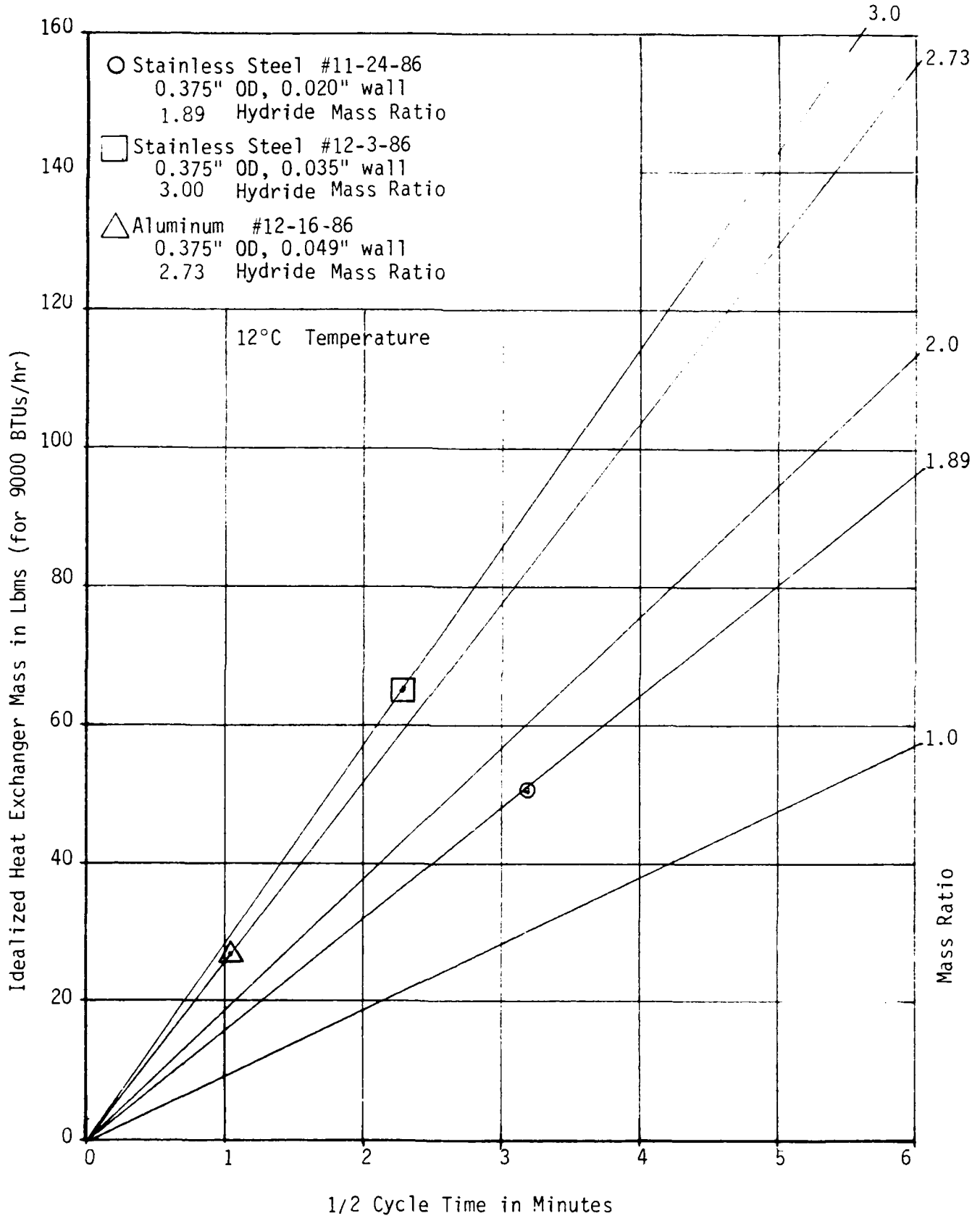

Figure 3.9 - Metal Hydride Heat Exchanger "Mass Map" for the Various Test Reactors Studied (at a 12°C Temperature)

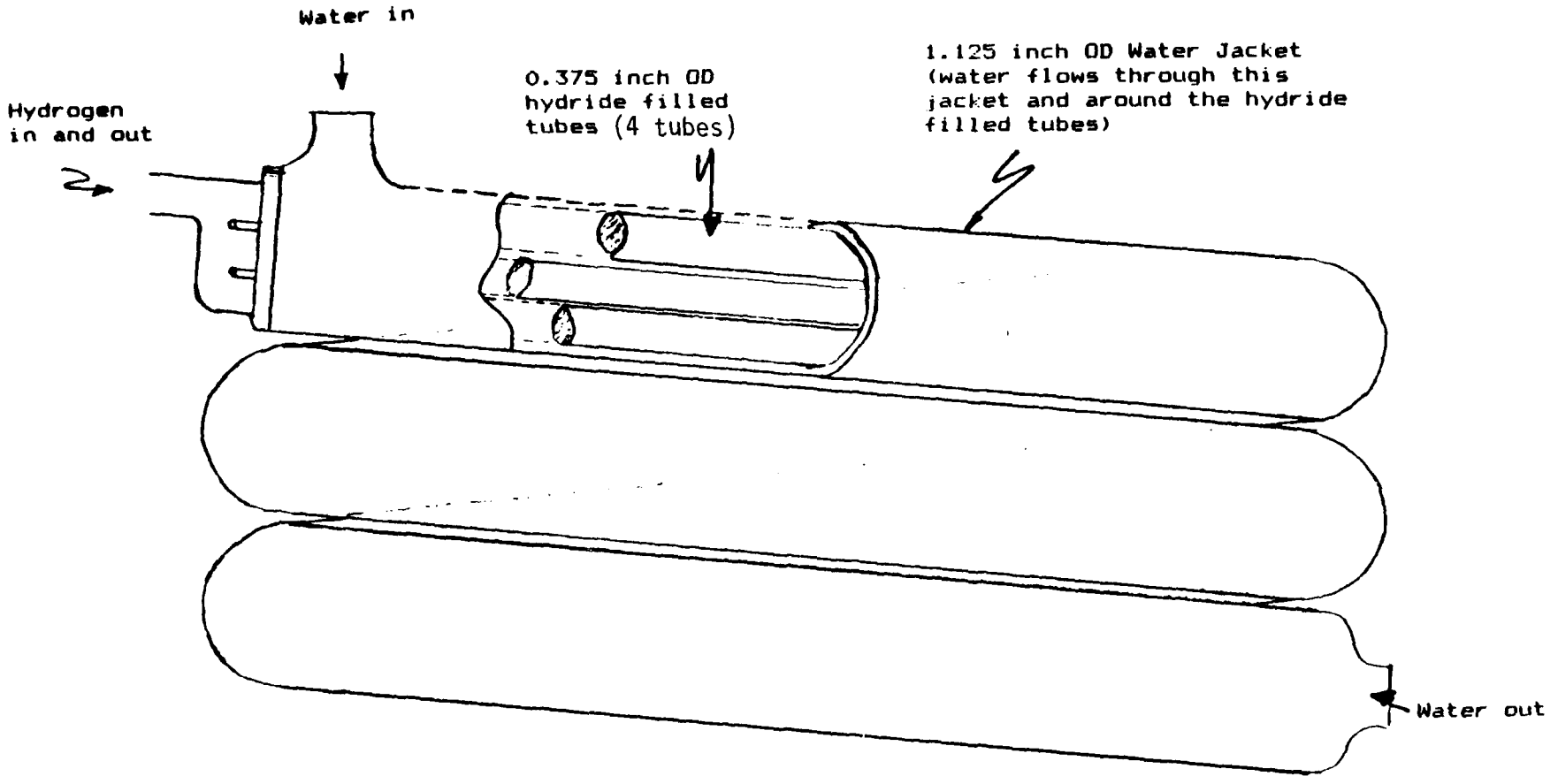

Figure 3.10 - Typical Ergenics Tubular Metal Hydride Heat Exchanger Configuration

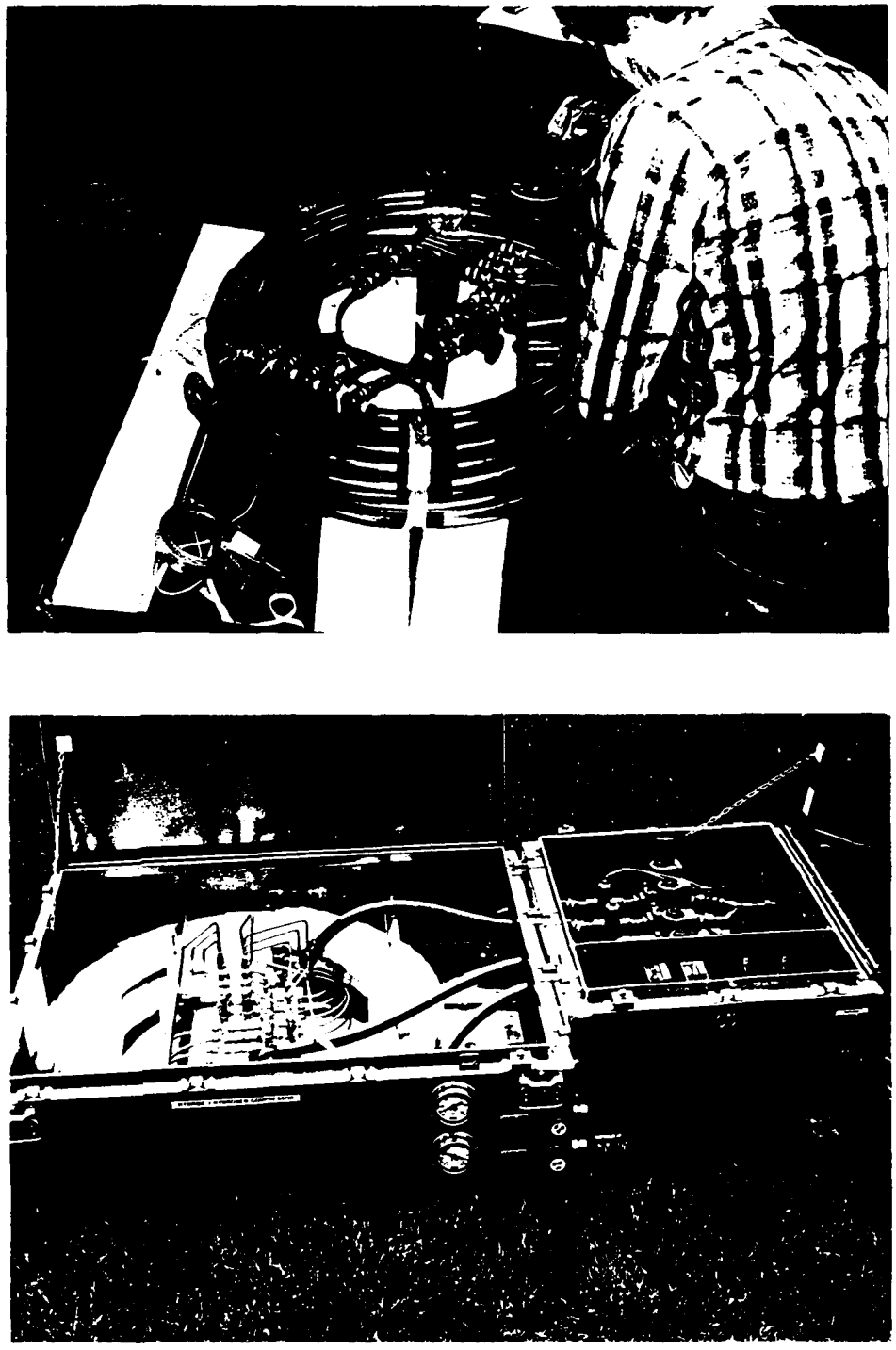

Figure 3.11 - Photograph of a Typical "Spirally Wrapped" Metal Hydride Heat Exchanger

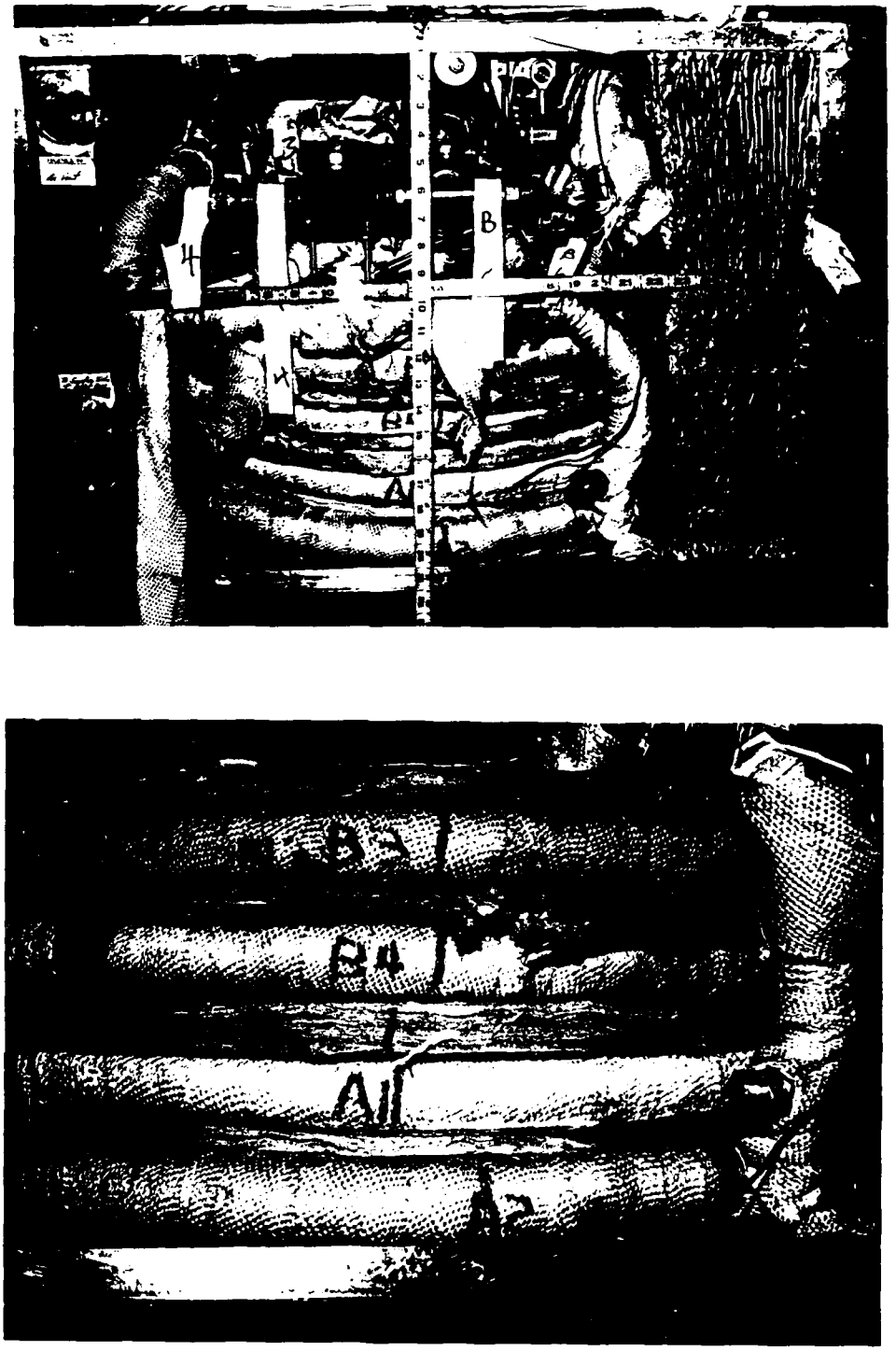

Figure 3.12 - Photograph of the Tightly Wrapped Metal Hydride Heat Exchangers used in this Project

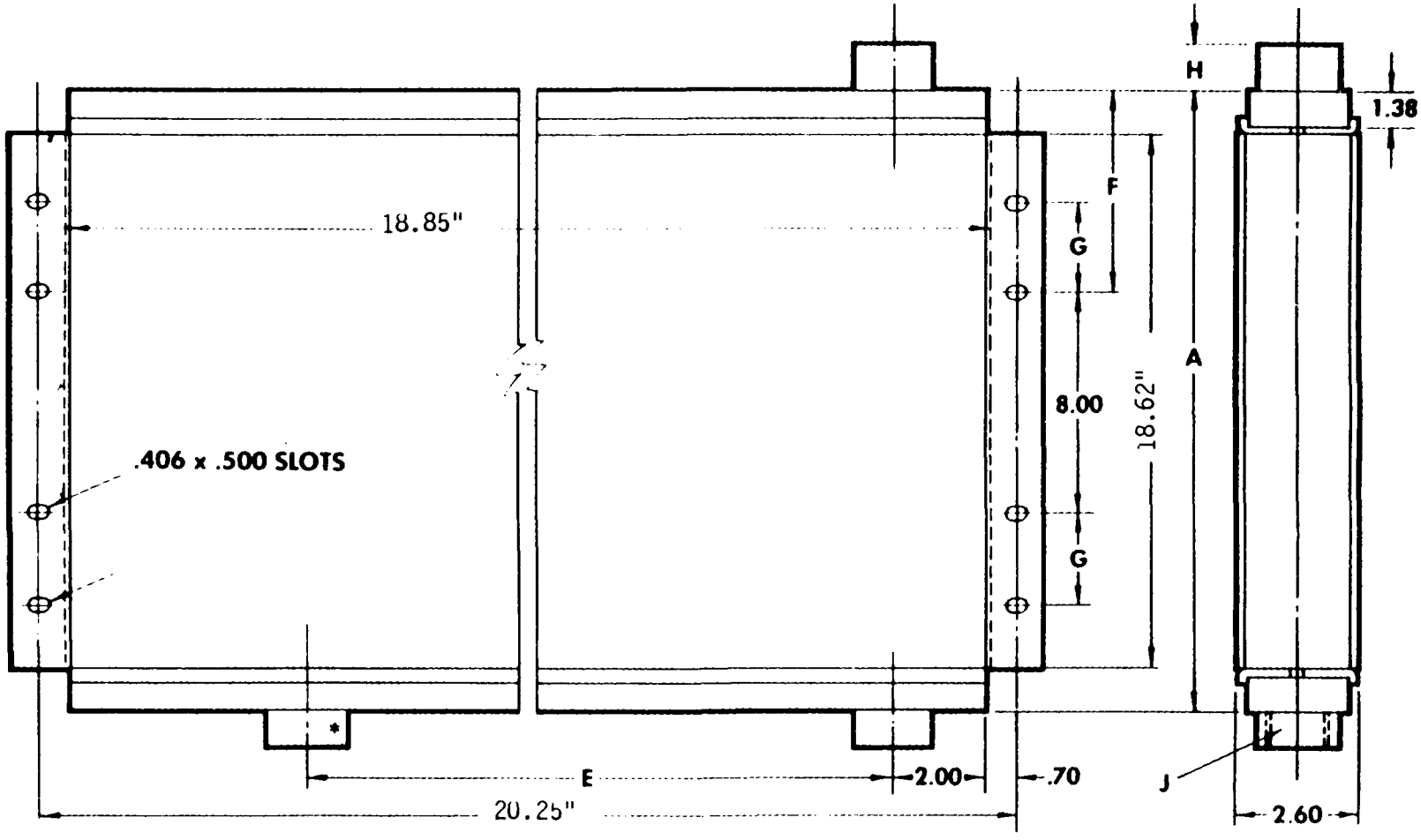

Figure 3.13 - Dimensional Drawing of the Modine 2930 Aluminum Oil Radiator

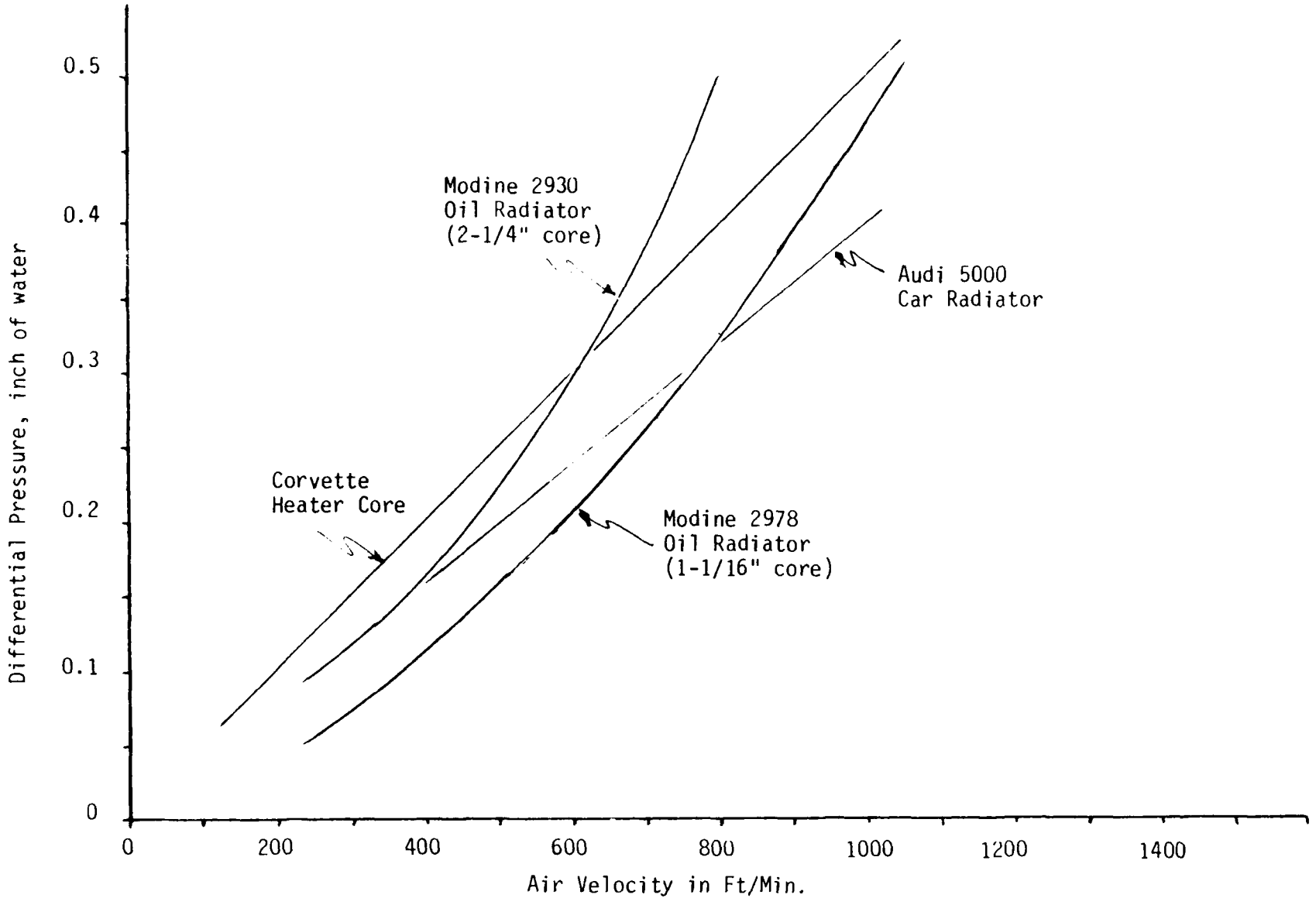

Figure 3.14 - Static Air Pressure vs. Air Flow Rate for the Various Fluid to Air Heat Exchangers

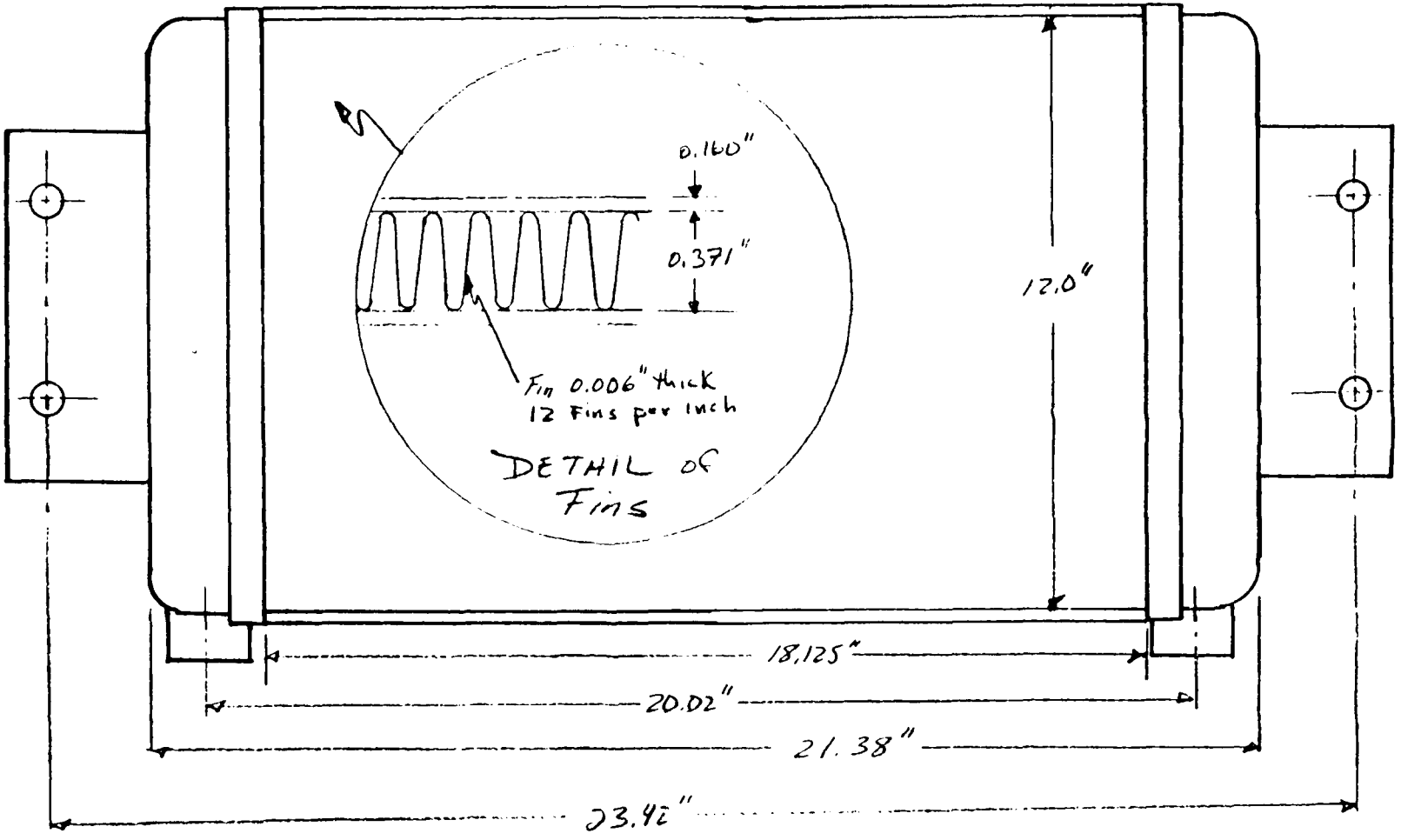

Figure 3.15 - Detailed Dimensional Drawing of the Modine #2978 Aluminum Radiator

Figure 3.16 - Test Setup Schematic for the Liquid to Air Heat Exchanger Testing

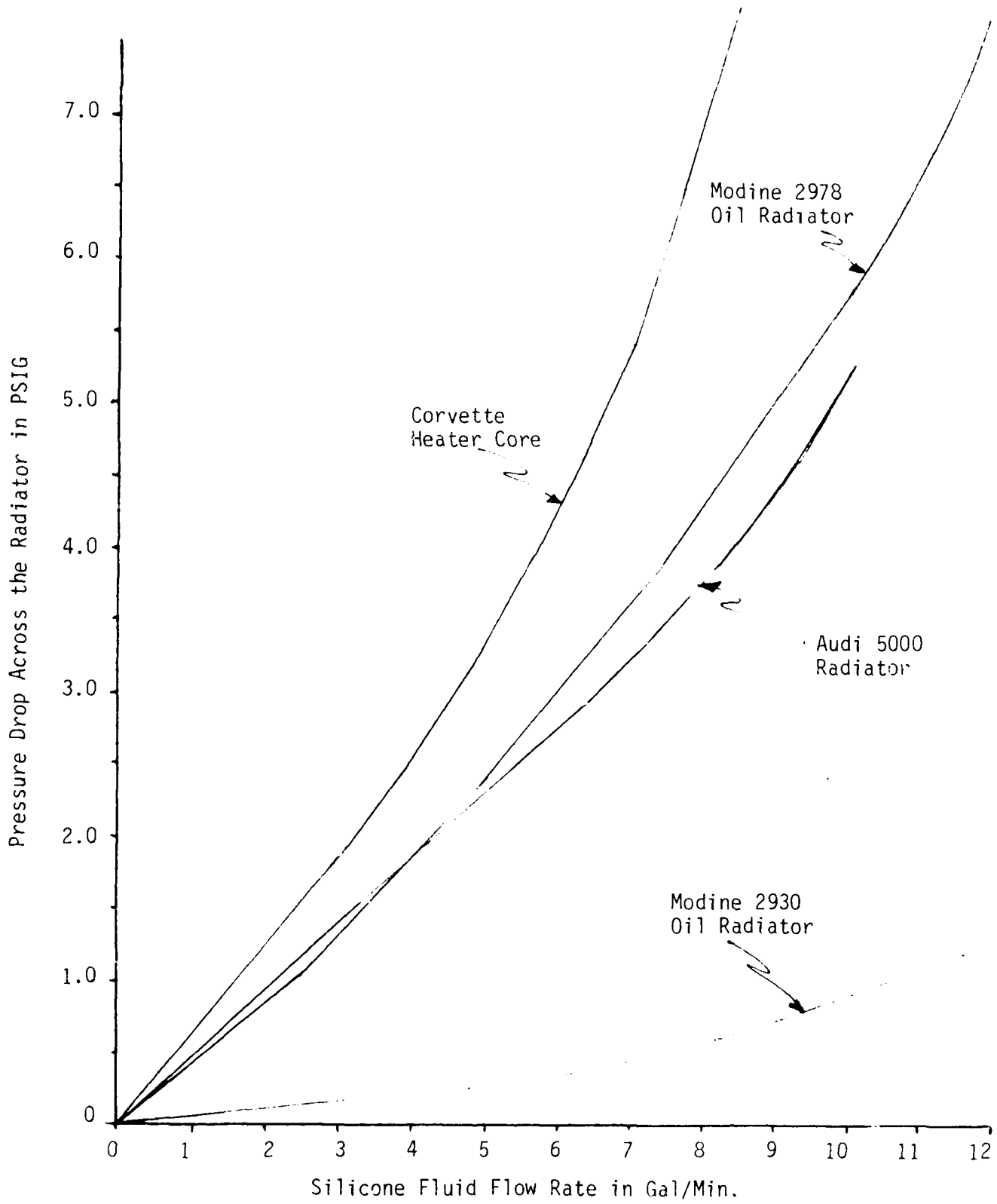

Figure 3.17 - Pressure Drop vs. Liquid Fluid Flow Rate for the Liquid to Air Heat Exchangers

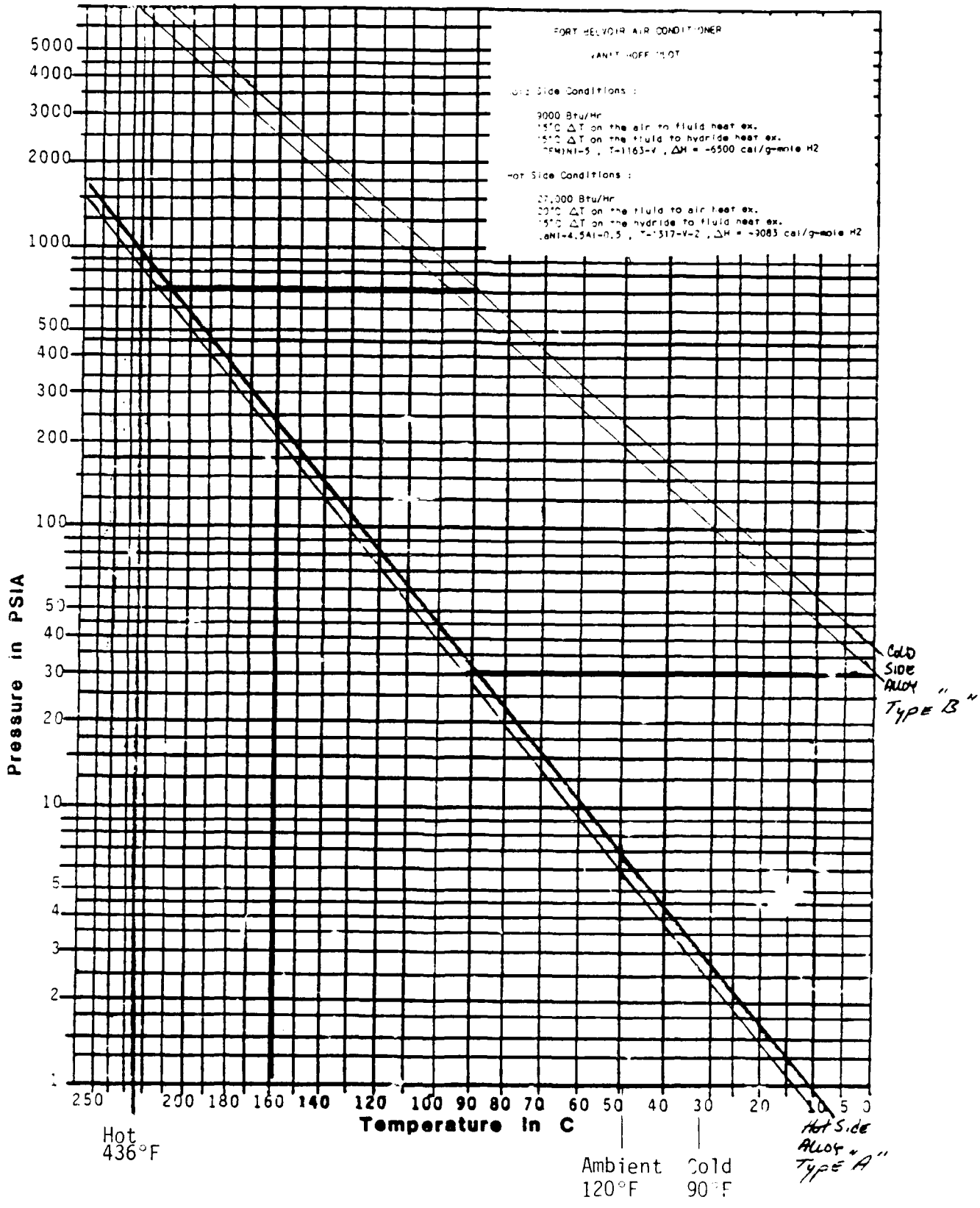

Figure 3.18 - Actual Metal Hydride van't Hoff Photo for the Metal Hydride Alloys used in the Liquid System, Metal Hydride, Waste Heat Driven Air Conditioner

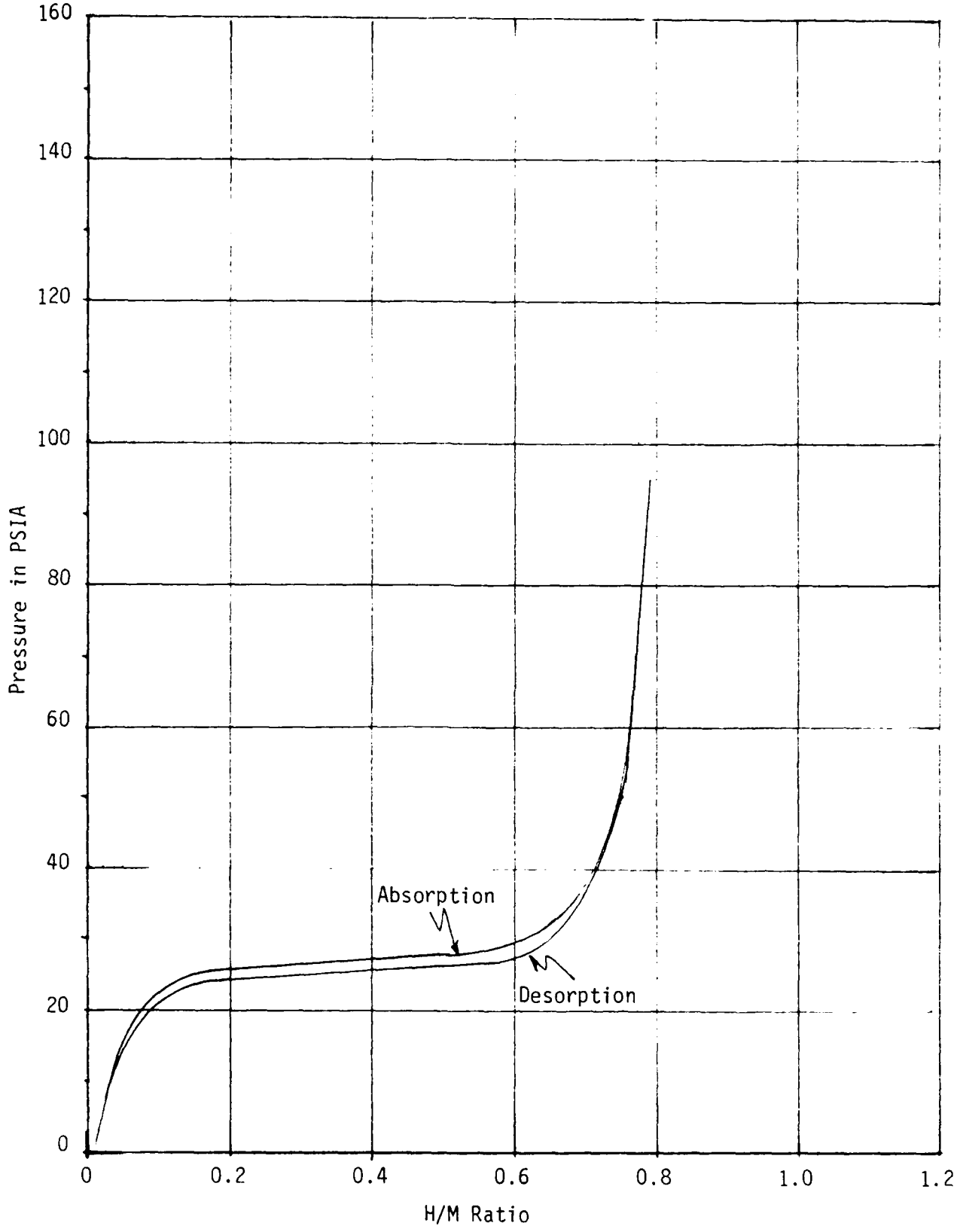

Figure 3.19 - Pressure/Composition-Isotherms for the Metal Hydride $LaNi_{4.5}Al_{0.5}$, T-1317-V-2, at 85°C (Hot Side Alloy)

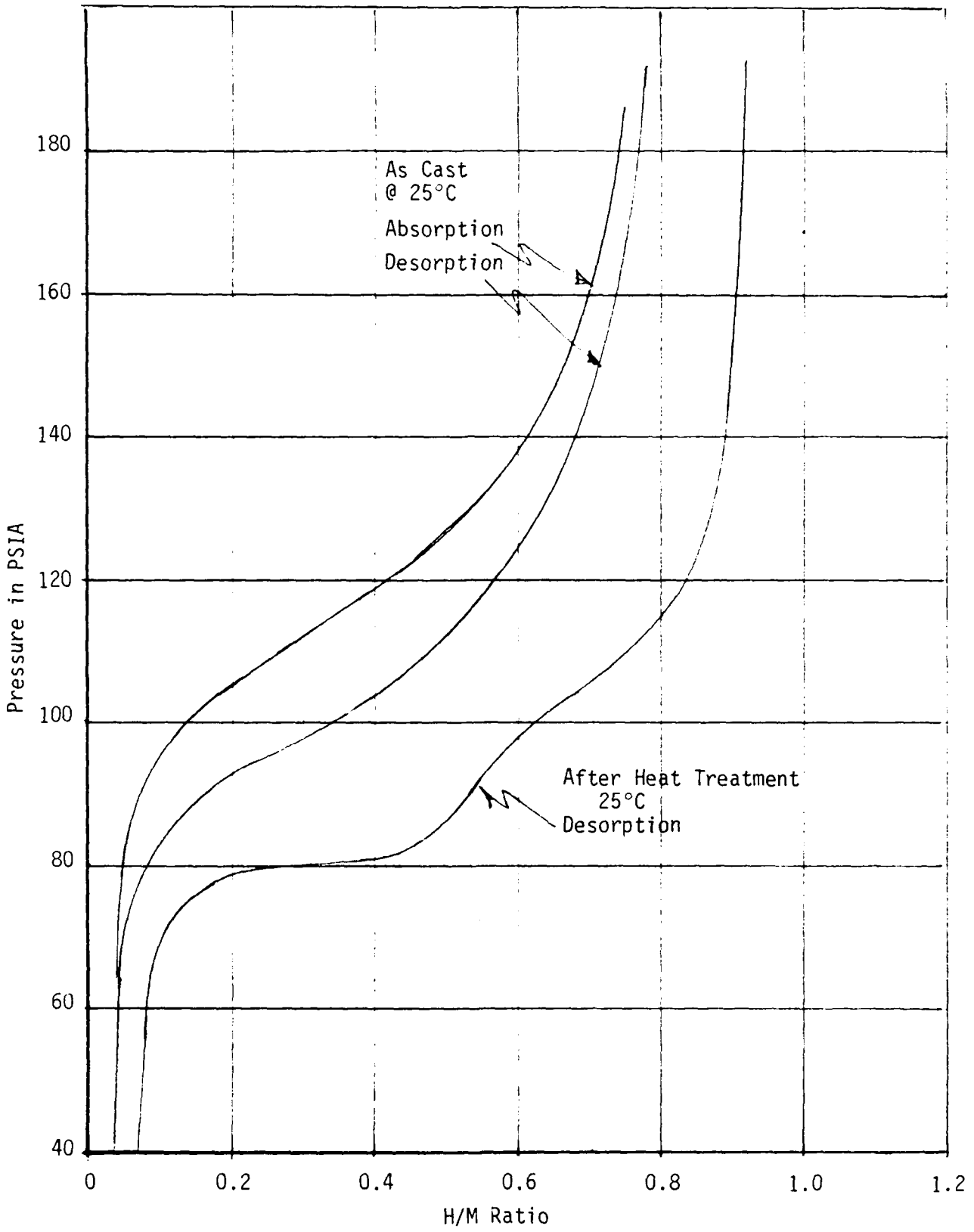

Figure 3.20 - Pressure/Composition - Isotherm for Metal Hydride Alloy (CFM) Ni_5, T-1163-V (Cold Side Alloy)

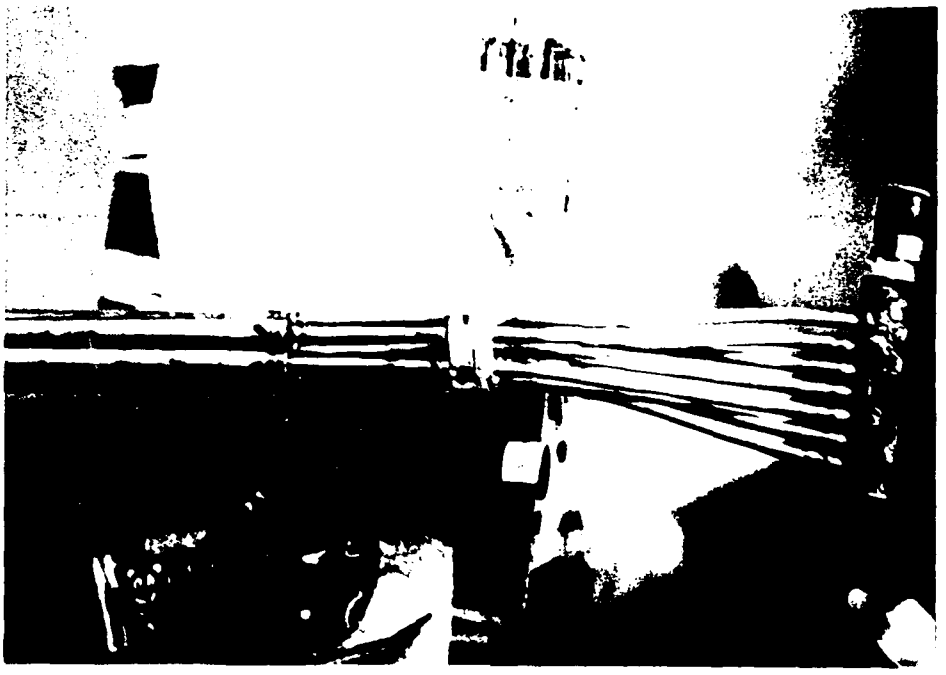

Figure 3.21 - Photograph of the Metal Hydride Heat Exchanger Construction

Figure 3.22 - Photograph of the Metal Hydride Heat Exchanger Construction

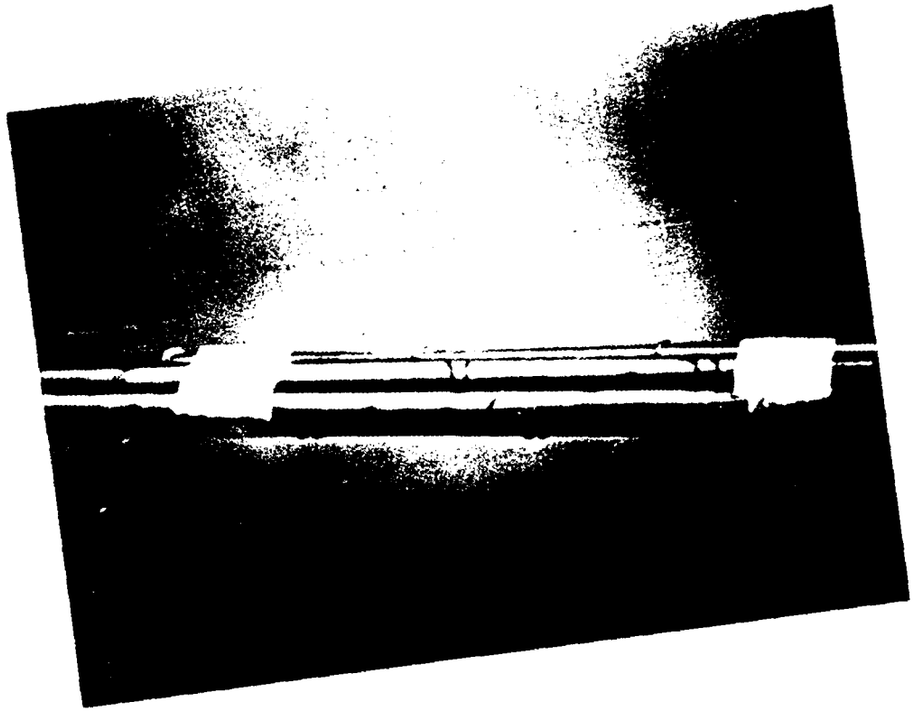

Figure 3.23 - Shows the Steel Wire Separator of the Metal Hydride Heat Exchanger Construction

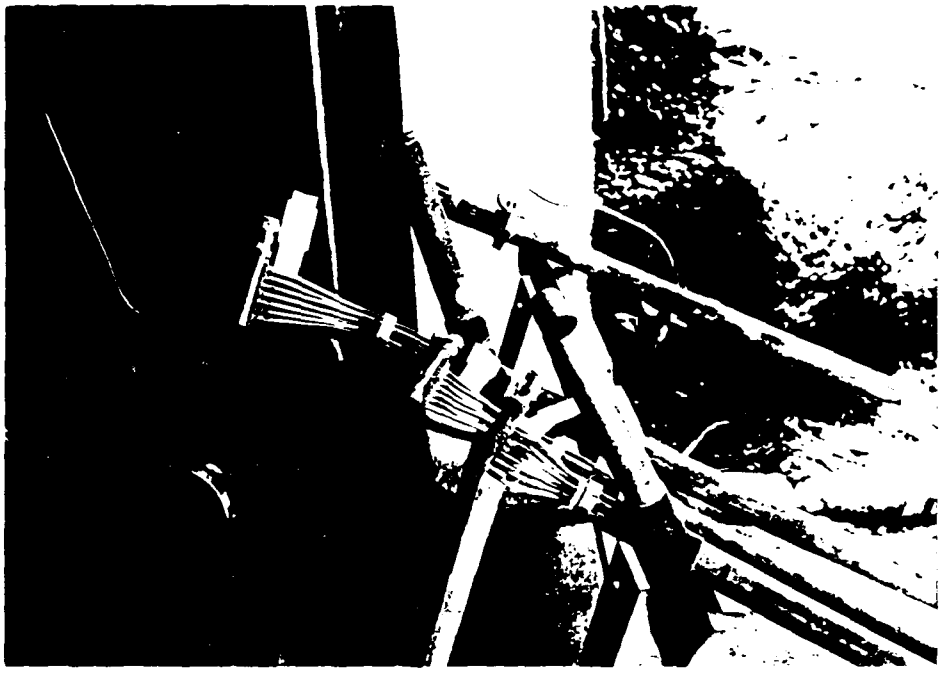

Figure 3.24 - Photograph of the Metal Hydride Heat Exchanger Construction

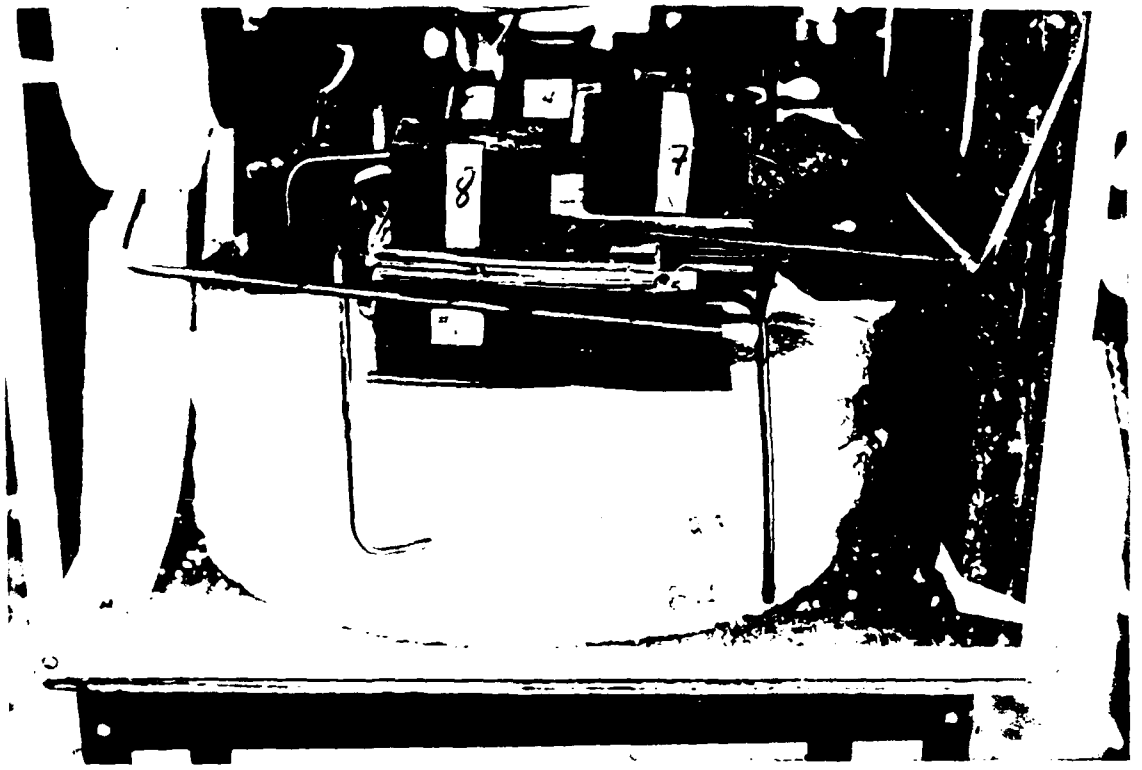

Figure 3.25 - Photograph of the Styrofoam Mockup

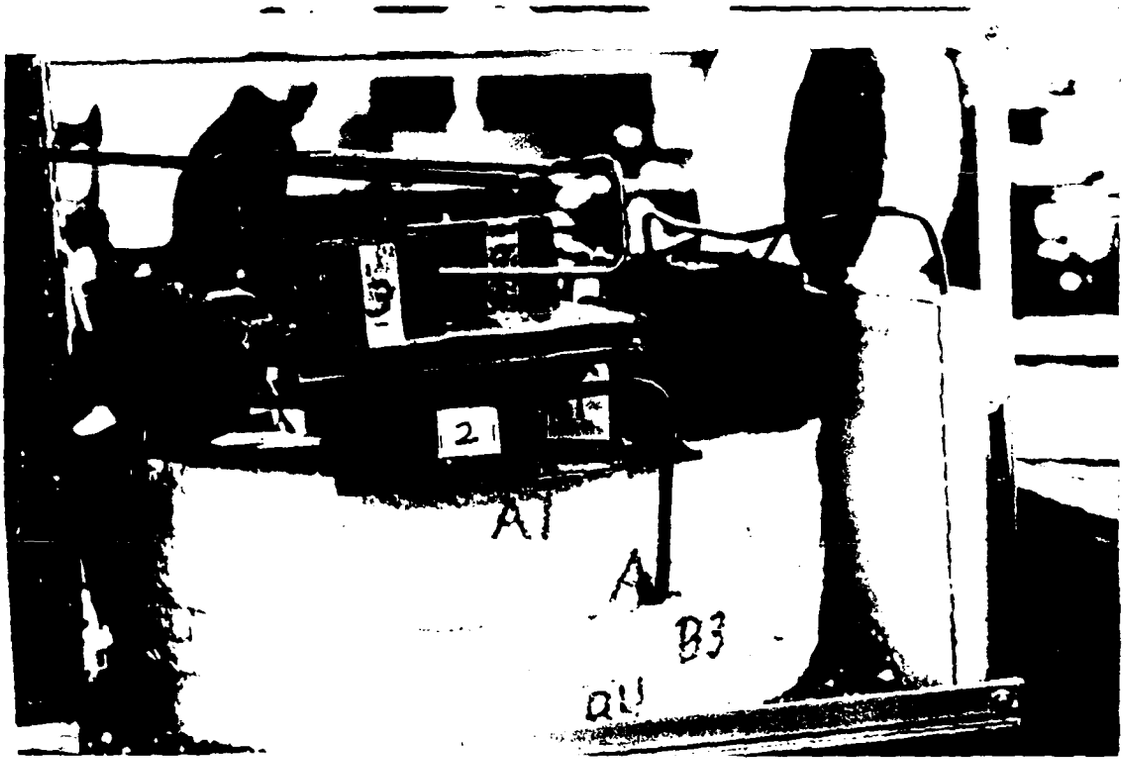

Figure 3.26 - Photograph of the Styrofoam Mockup

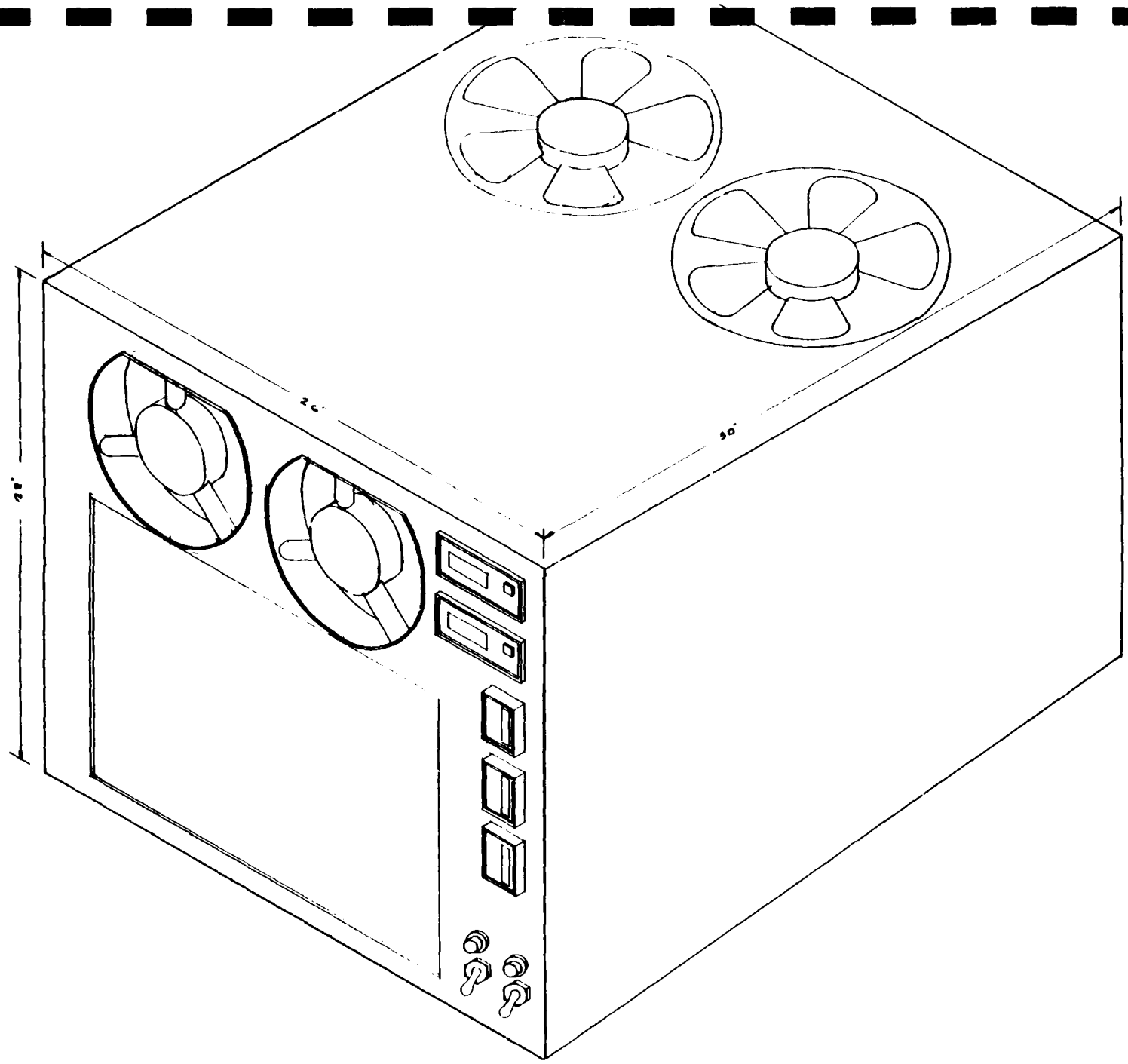

Figure 3.27A - Outside View of the "Liquid System" Metal Hydride, Waste Heat Driven Air Conditioner

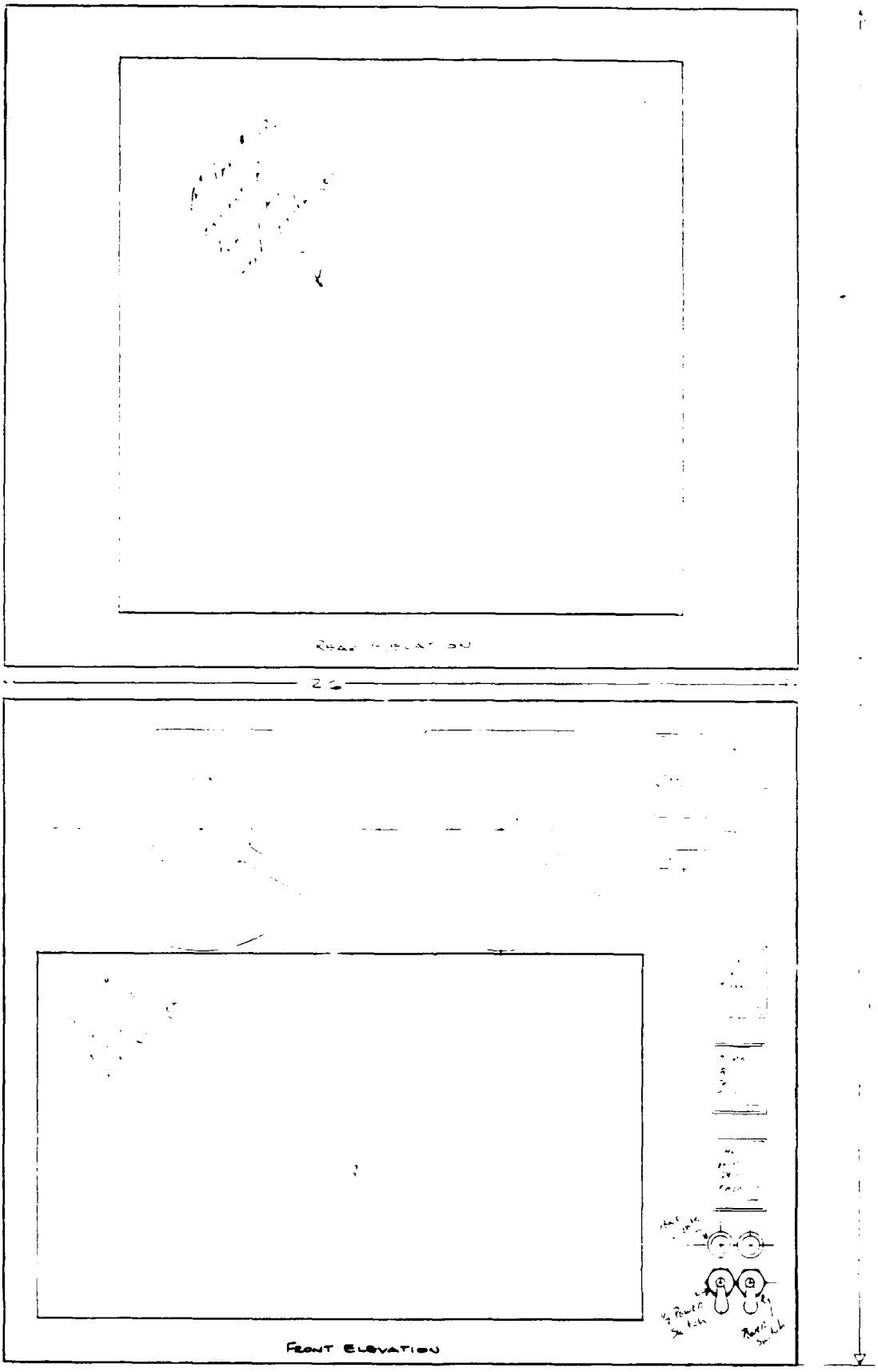

Figure 3.27B - Front and Rear View of the "Liquid System" Metal Hydride Air Conditioner

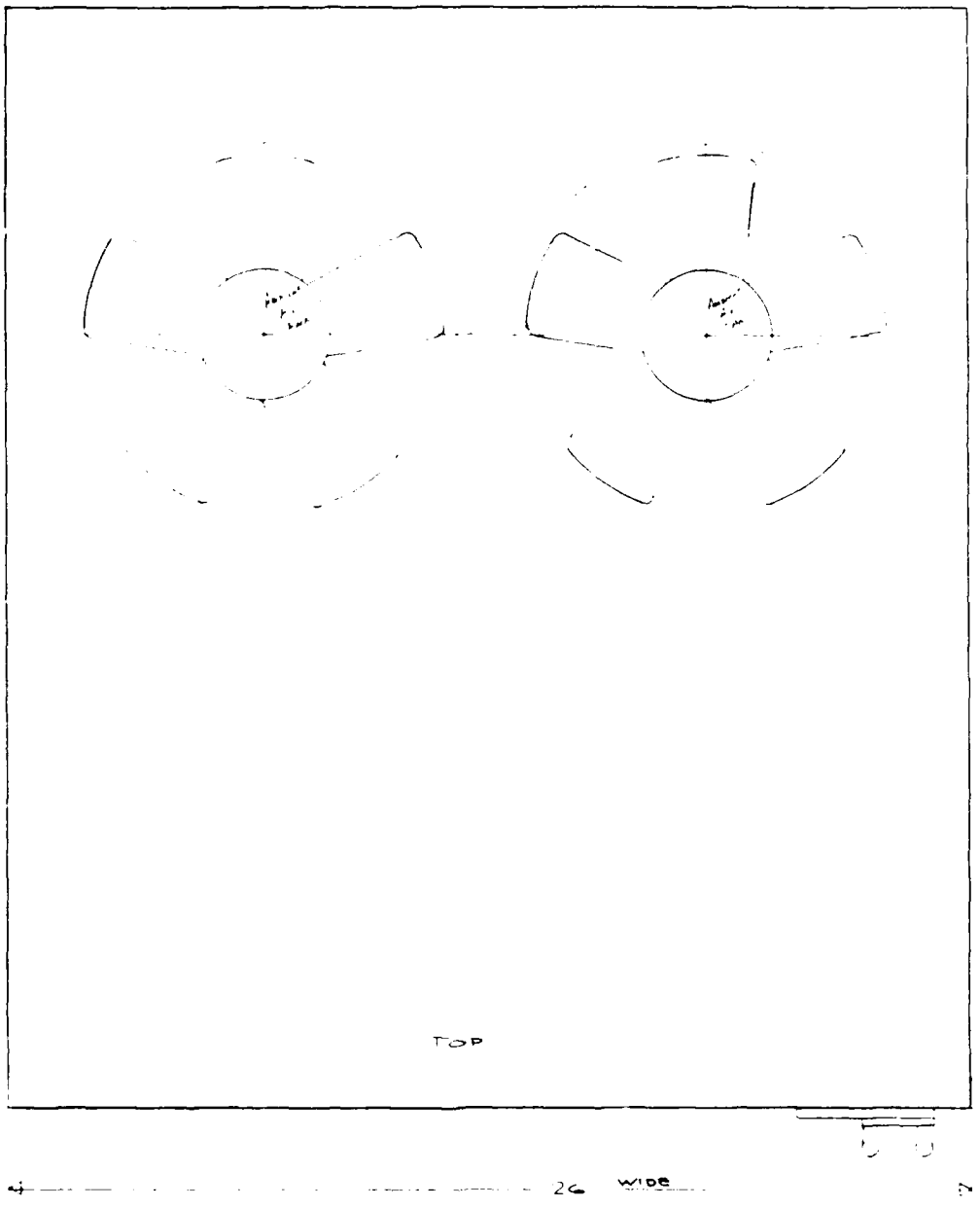

Figure 3.27C - Top View of the "Liquid System" Metal Hydride Air Conditioner

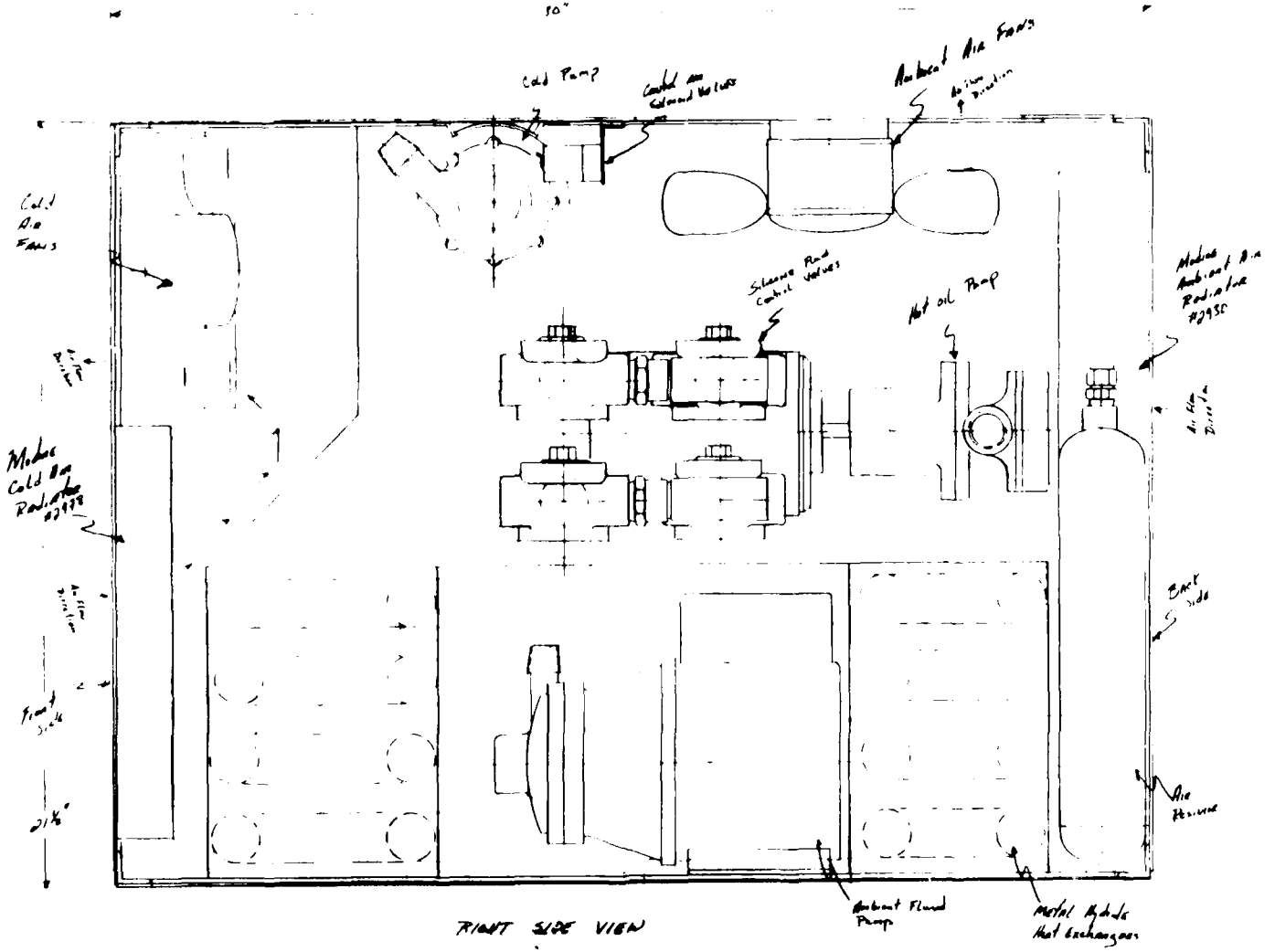

Figure 3.28A - Right Side Internal View of the "Liquid System" Metal Hydride Air Conditioner

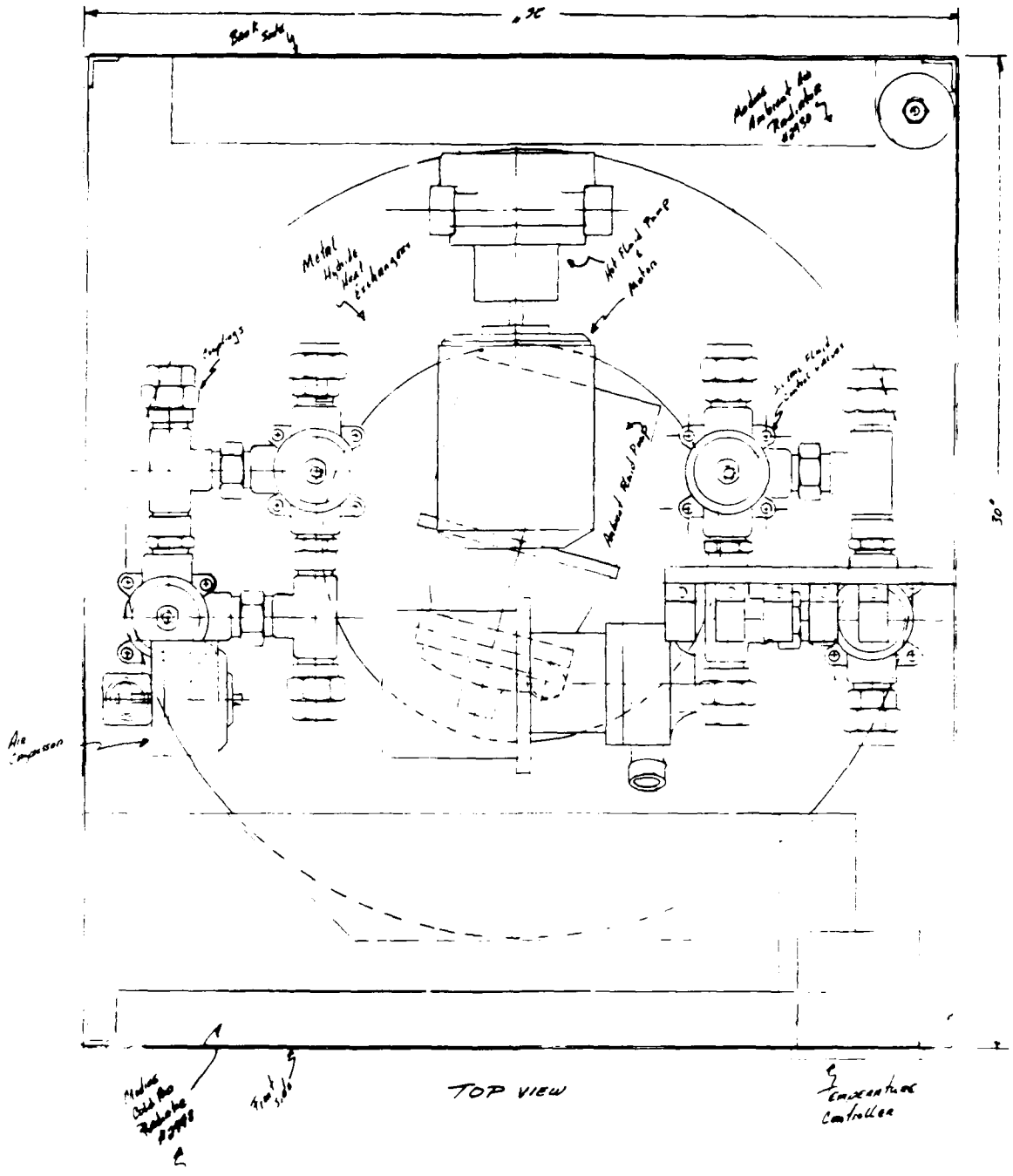

Figure 3.28B - Top Internal View of the "Liquid System" Metal Hydride Air Conditioner

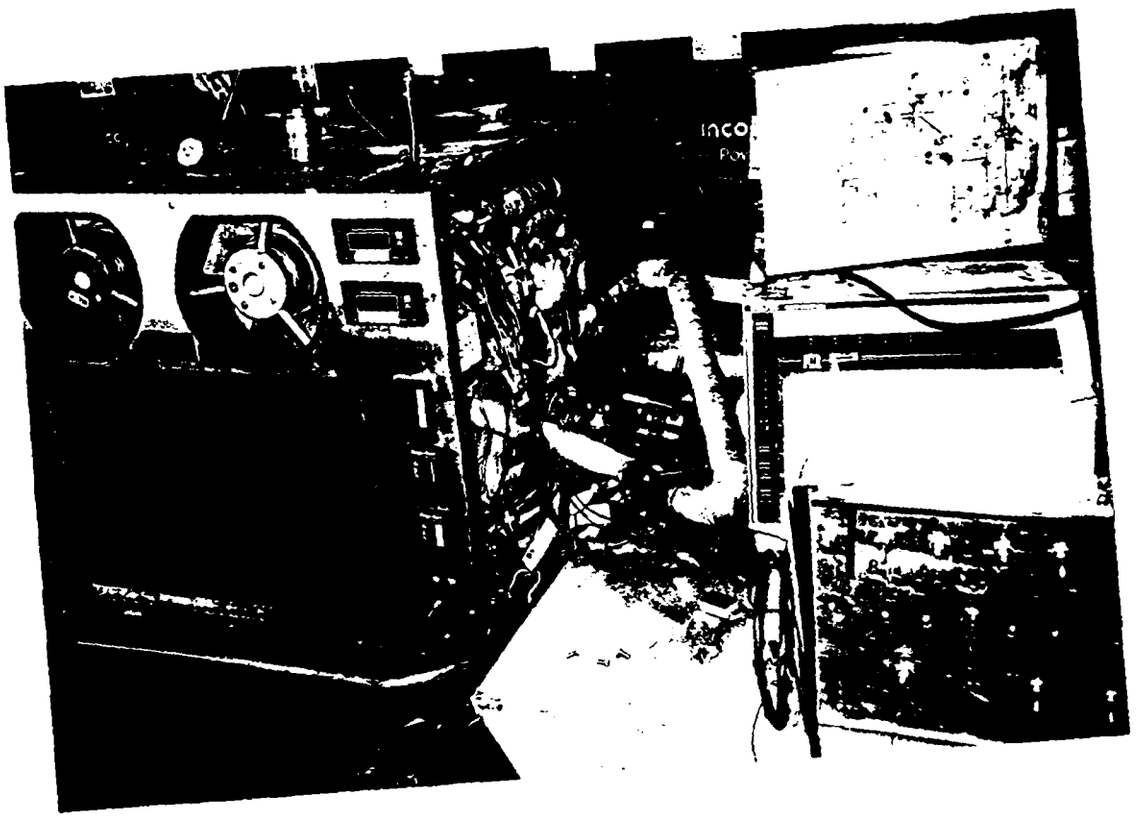

Figure 3.29 - Photograph of the Completed Metal Hydride Air Conditioner

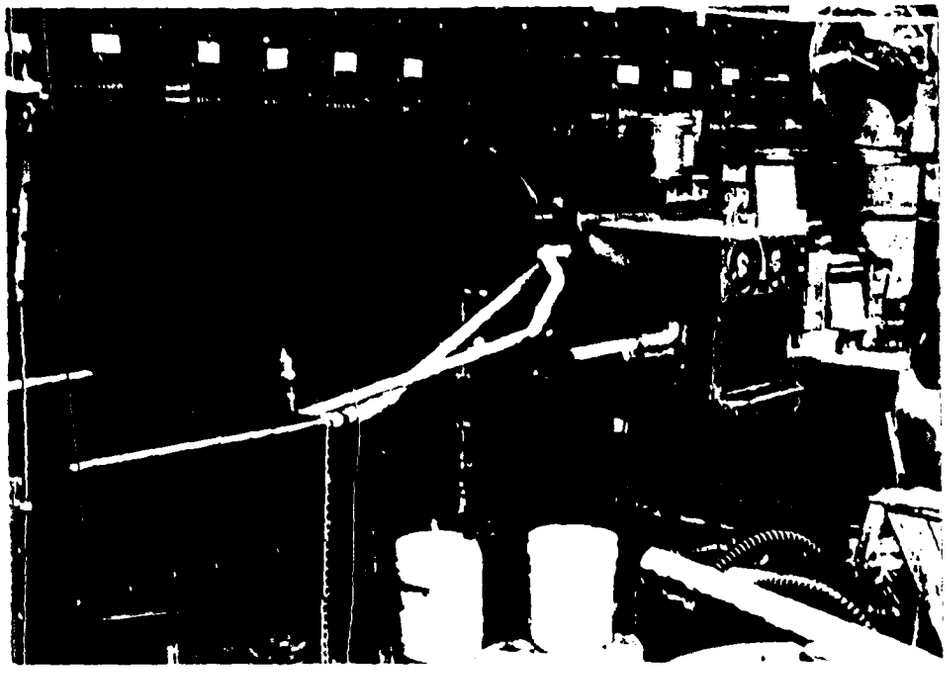

Figure 3.30 - Photograpn of the Completed Metal Hydride Air Conditioner

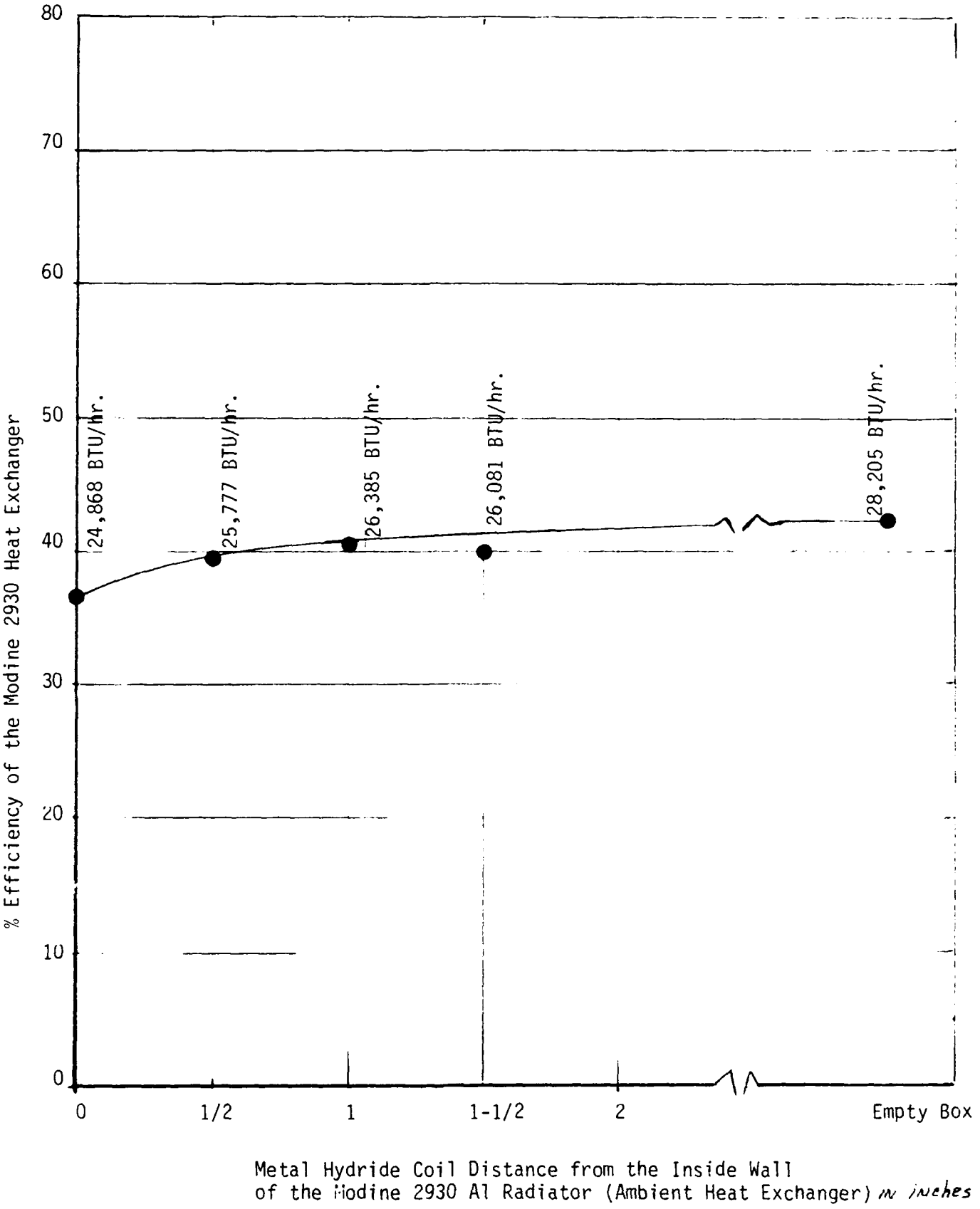

Figure 3.31 - Heat Rejection Efficiency of the Modine 2930 as a Function of its Distance from the Metal Hydride Heat Exchangers

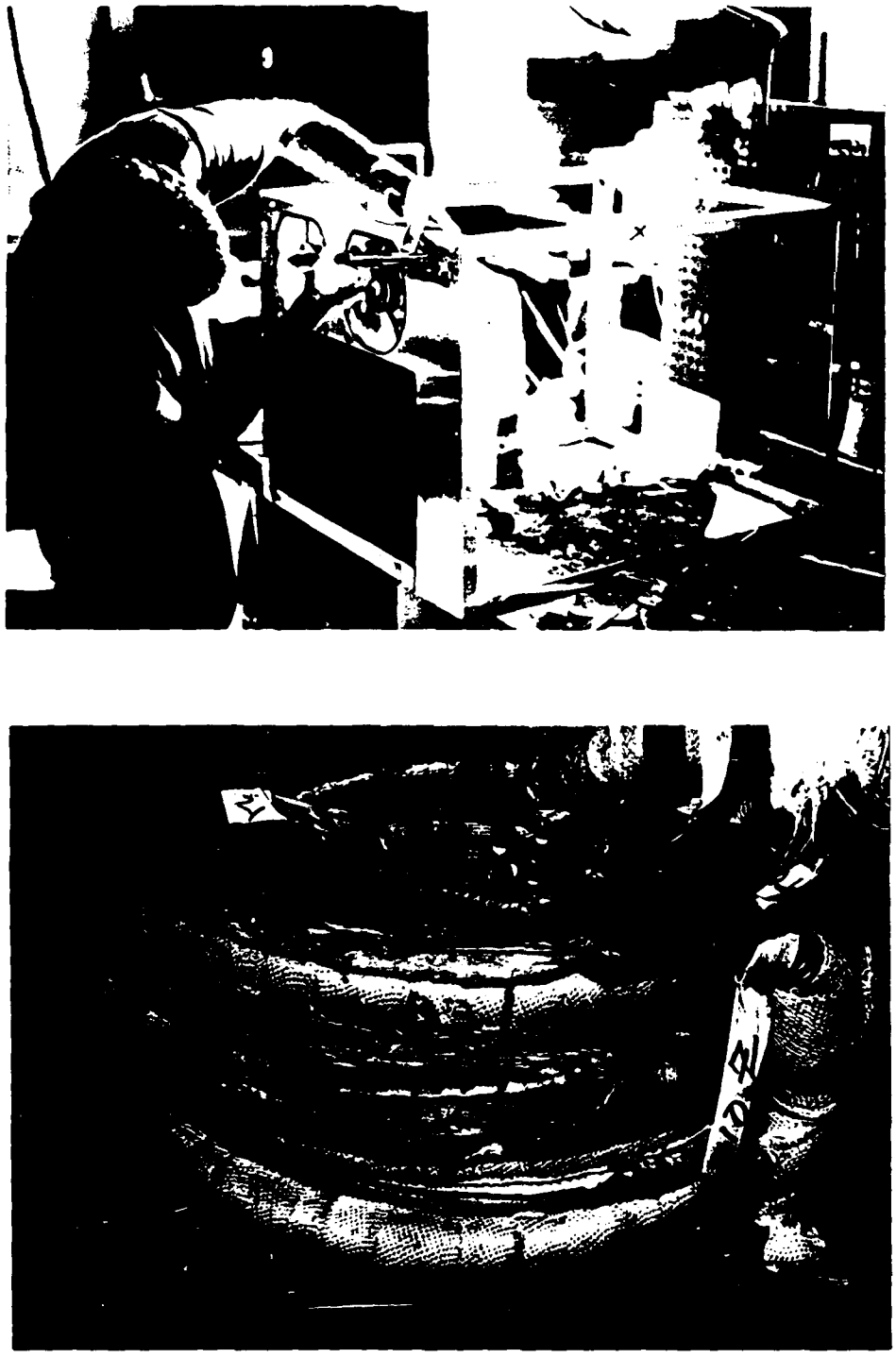

Figure 3.32 - Photograph of Prototype Metal Hydride Air Conditioner Construction

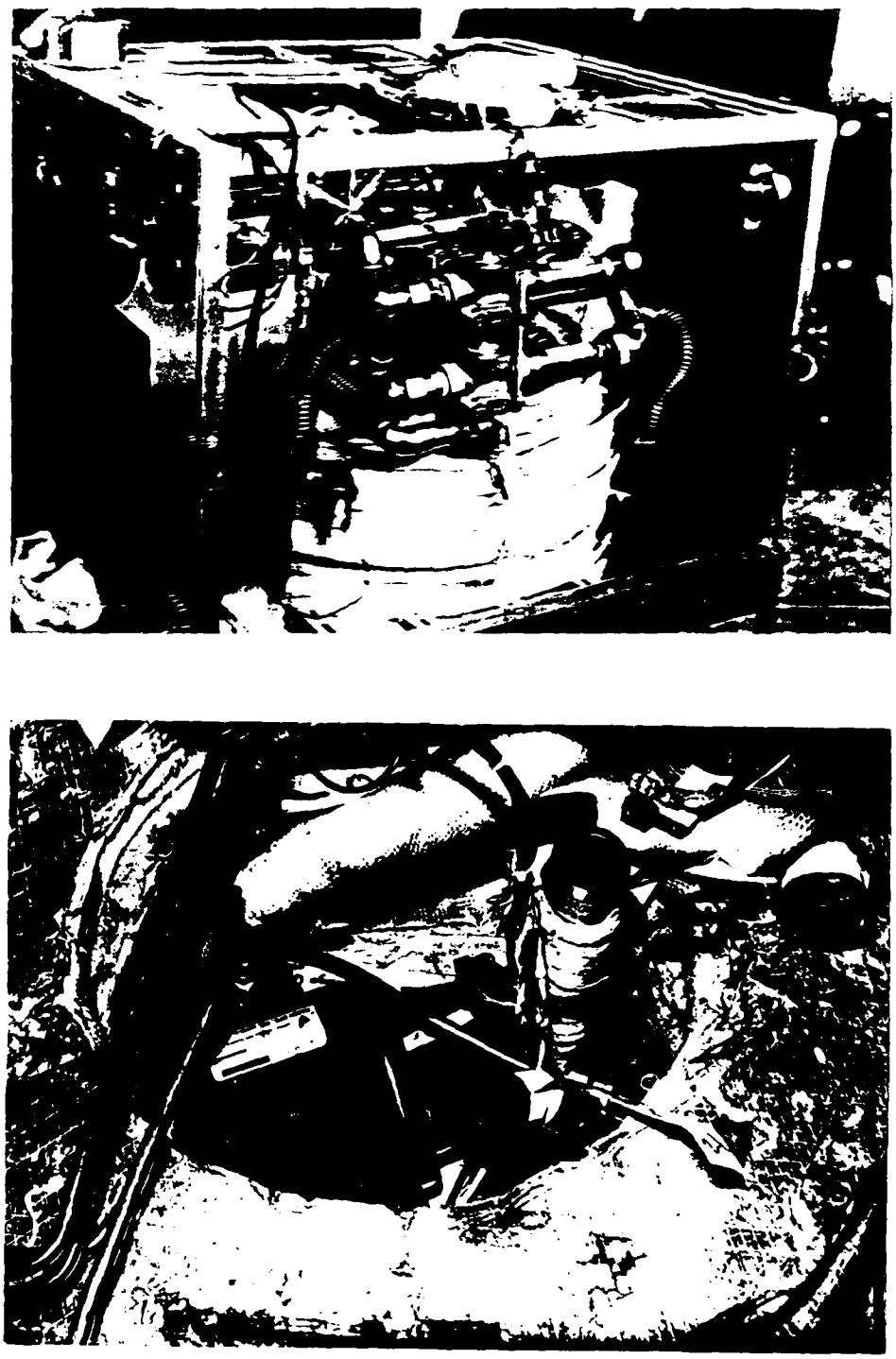

Figure 3.33 - Photograph of Prototype Metal Hydride Air Conditioner Construction

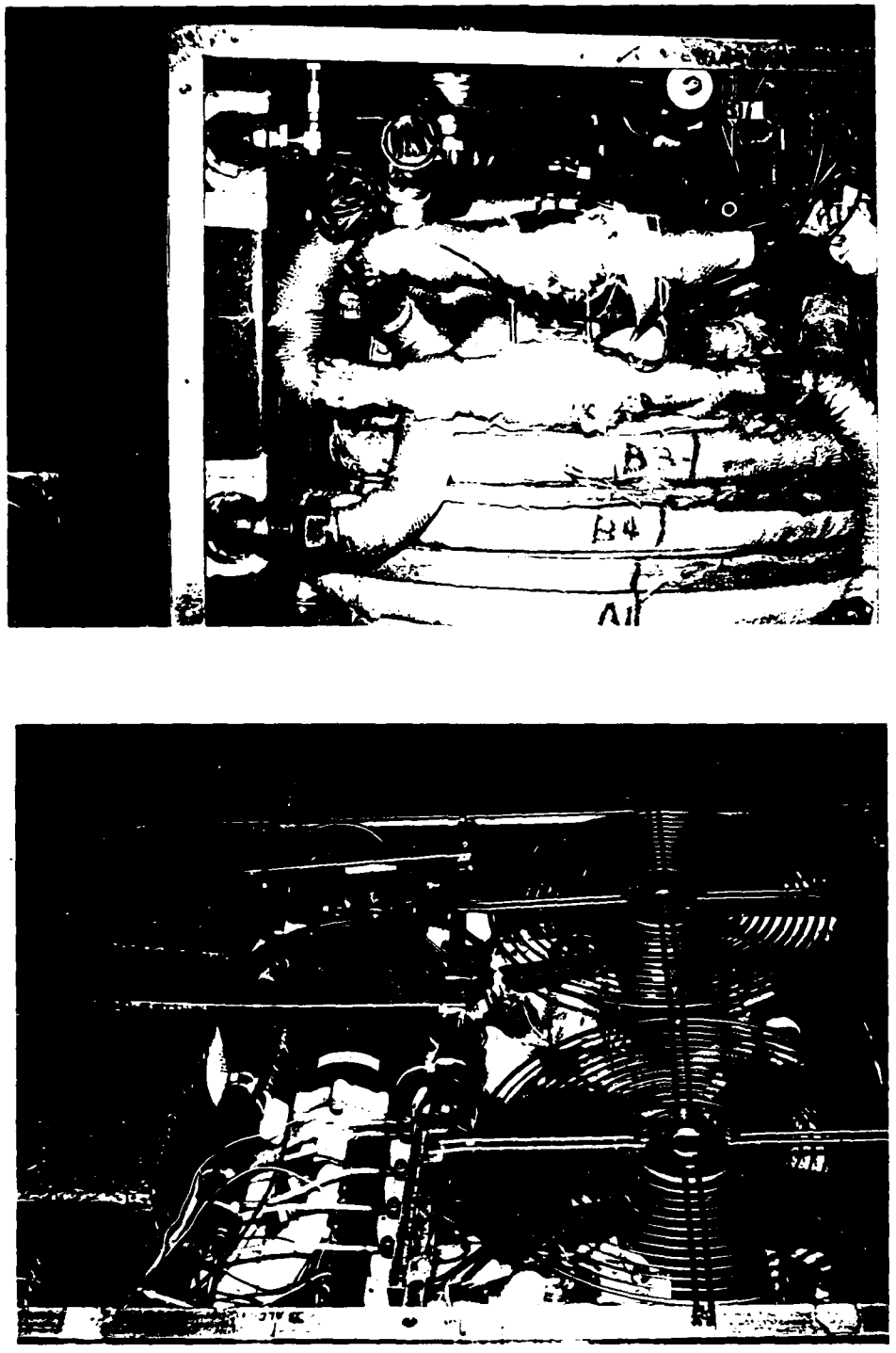

Figure 3.34 - Photograph of Prototype Metal Hydride Air Conditioner Construction

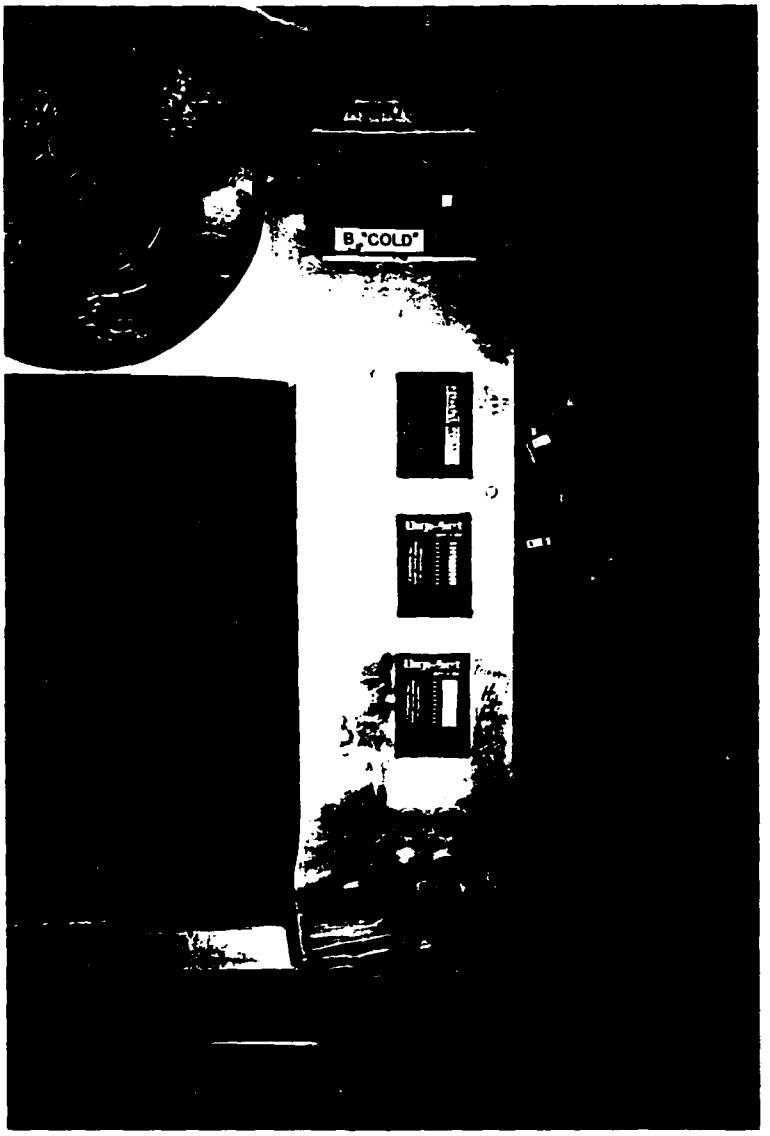

Figure 3.35 - Photograph of Prototype Metal Hydride Air Conditioner Construction

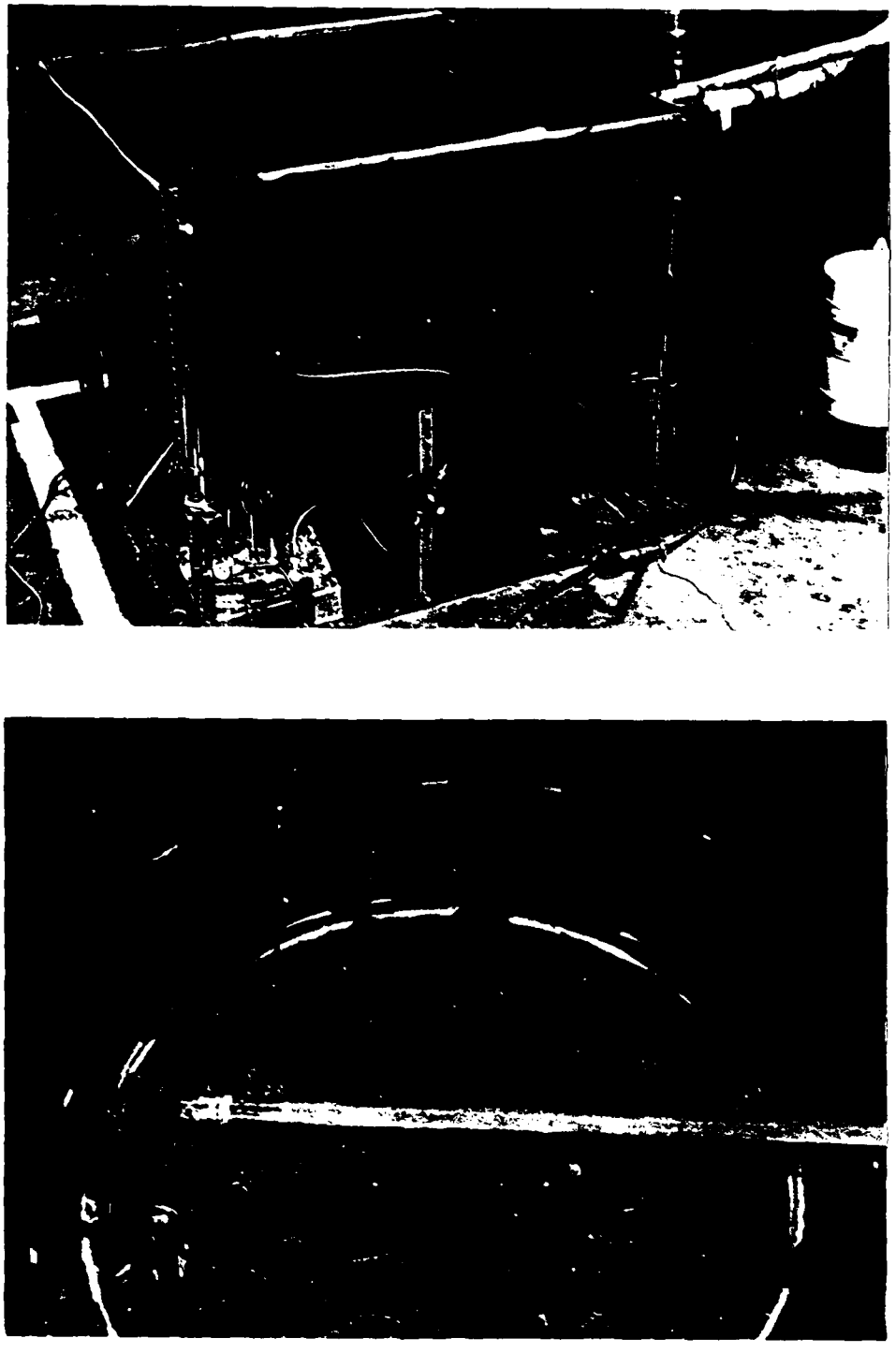

Figure 3.36 - Photograph of the 2nd Silicone Fluid High Temperature Heater

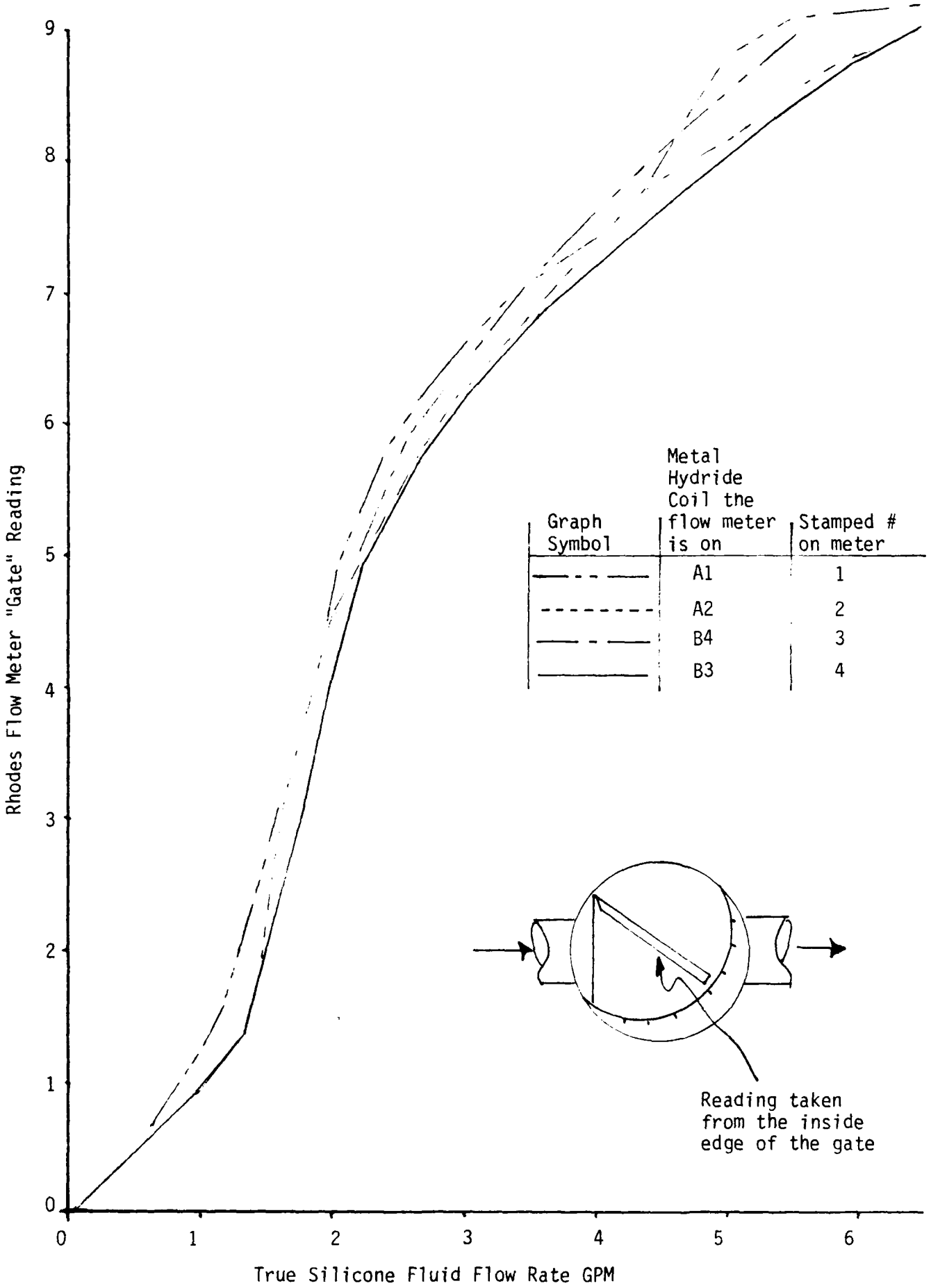

Figure 3.37 - Calibration Curve for the Sentinel/Rhodes Fluid Flow Indicator, Model #904

Figure 3.38 - Photograph of the Metal Hydride Air Conditioner with the Flow Indicator in Place

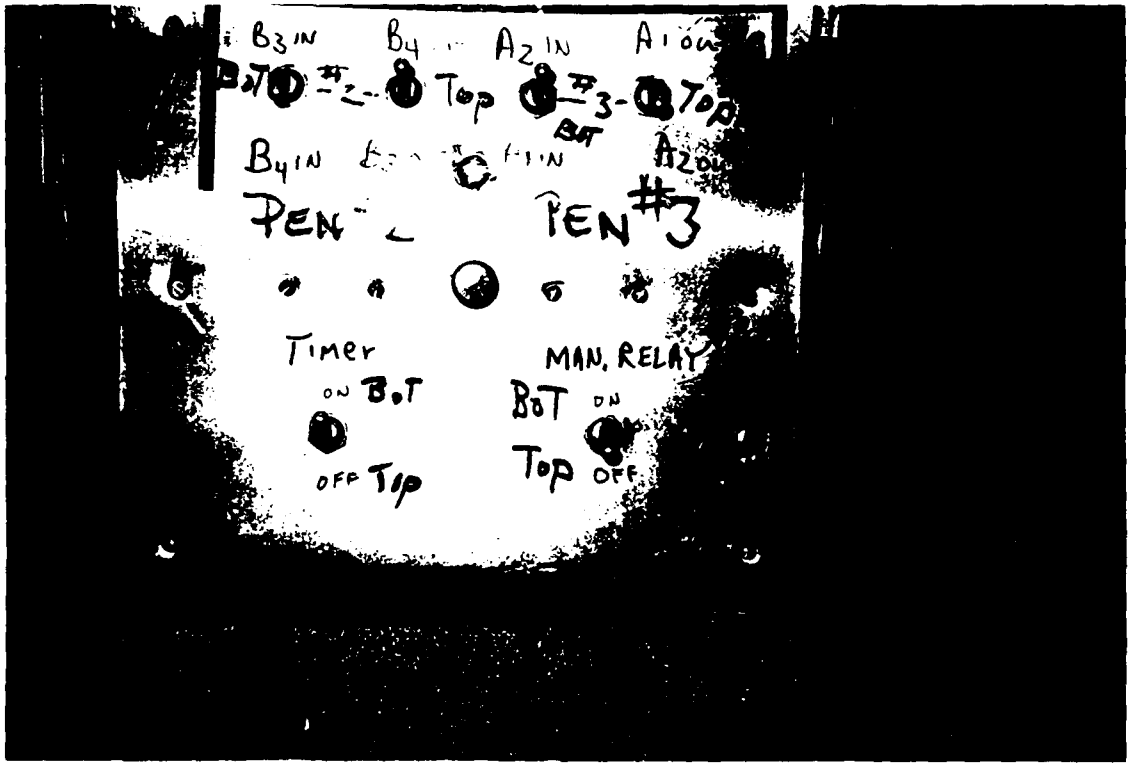

Figure 3.39 - Photograph of the Bread Board Switching Station for the Thermocouple

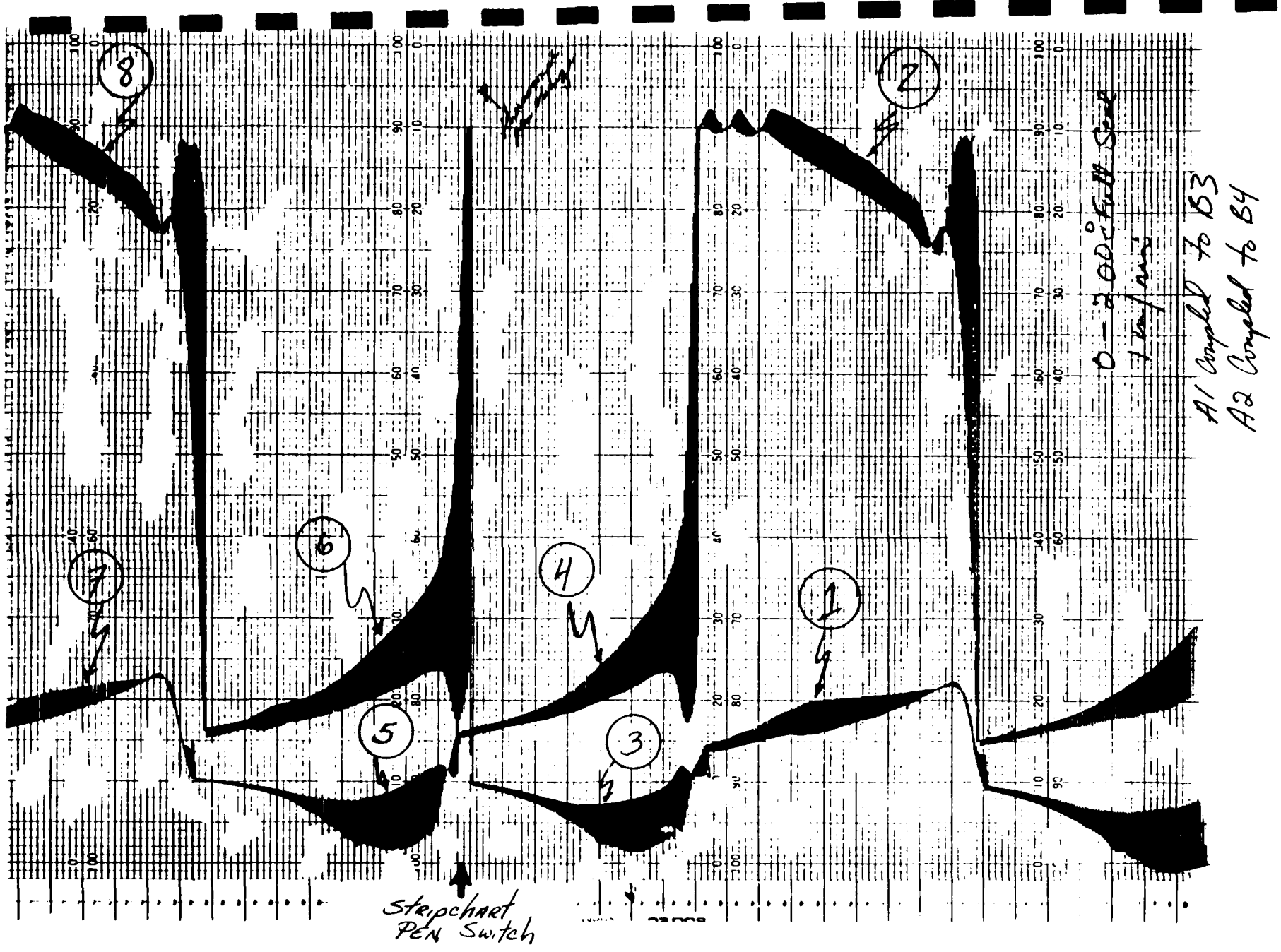

Figure 3.40A - Photograph of the "Shaded" Temperature Output Data Recorded on the Soltec Strip Chart Recorder

Event 1: Hydride coil B3 rejecting the hydrogen gas absorption heat to the ambient surroundings. Coil B3 is receiving hydrogen from coil A1 (event 2).

Event 2: Hydride coil A1 receiving heat from the high temperature heat exchanger, so that it can desorb its hydrogen into hydride coil B3 (event 7).

Event 3: Hydride coil B3 receiving heat from the shelter air (cooling mode) in order to release hydrogen so that it can be reabsorbed by hydride coil A1 (event 4).

Event 4: Hydride coil A1 rejecting ythe hydrogen gas absorption heat to the ambient surroundings. Coil A1 is receiving this hydrogen from hydride coil B3 (event 3).

----------STRIP CHART PEN SWITCH----------
(Strip chart now recording the thermocouples on hydride coils A2 and B4)

Event 5: Hydride coil B4 receiving heat from the shelter air (cooling mode). This heat releases hydrogen so that it can be reabsorbed by hydride coil A2 (event 6).

Event 6: Hydride coil A2 rejecting the hydrogen gas heat of absorption to the ambient surroundings. Coil A2 is receiving this hydrogen from hydride coil B4 (event 5).

Event 7: Hydride coil B4 rejecting the heat of hydrogen gas absorption to the ambient surroundings. This is the hydrogen that is being released by hydride coil A2 (event 8).

Event 8: Hydride coil A2 receiving heat from the high temperature heat exchanger, so that it can desorb its hydrogen into hydride coil B4 (event 7).

Figure 3.40B - Event Explanations

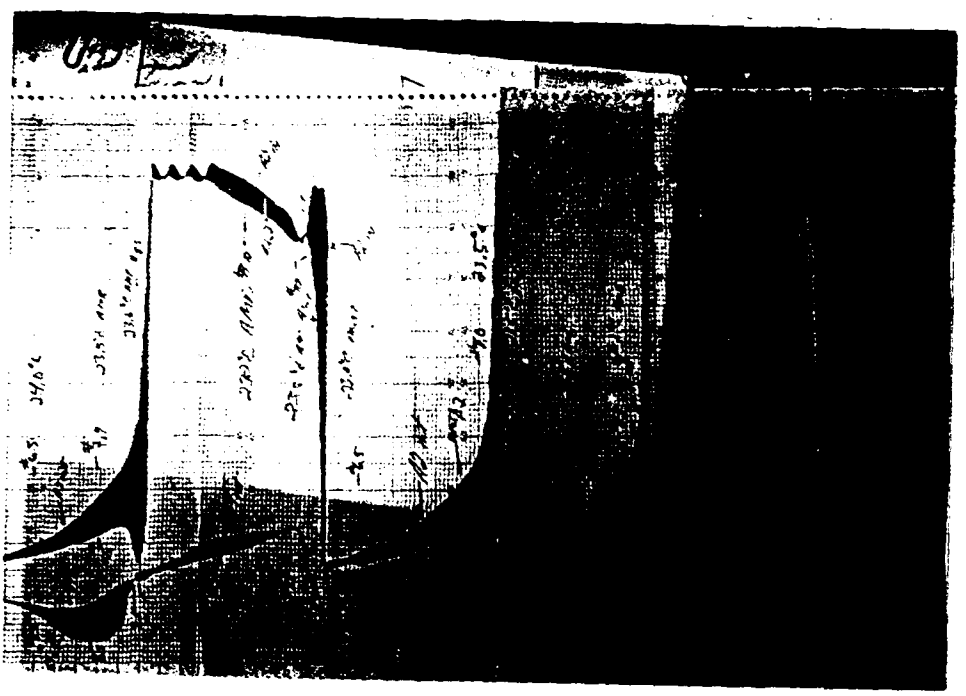

Figure 3.41 - Photograph of Example Raw Data from Air Conditioner Tests

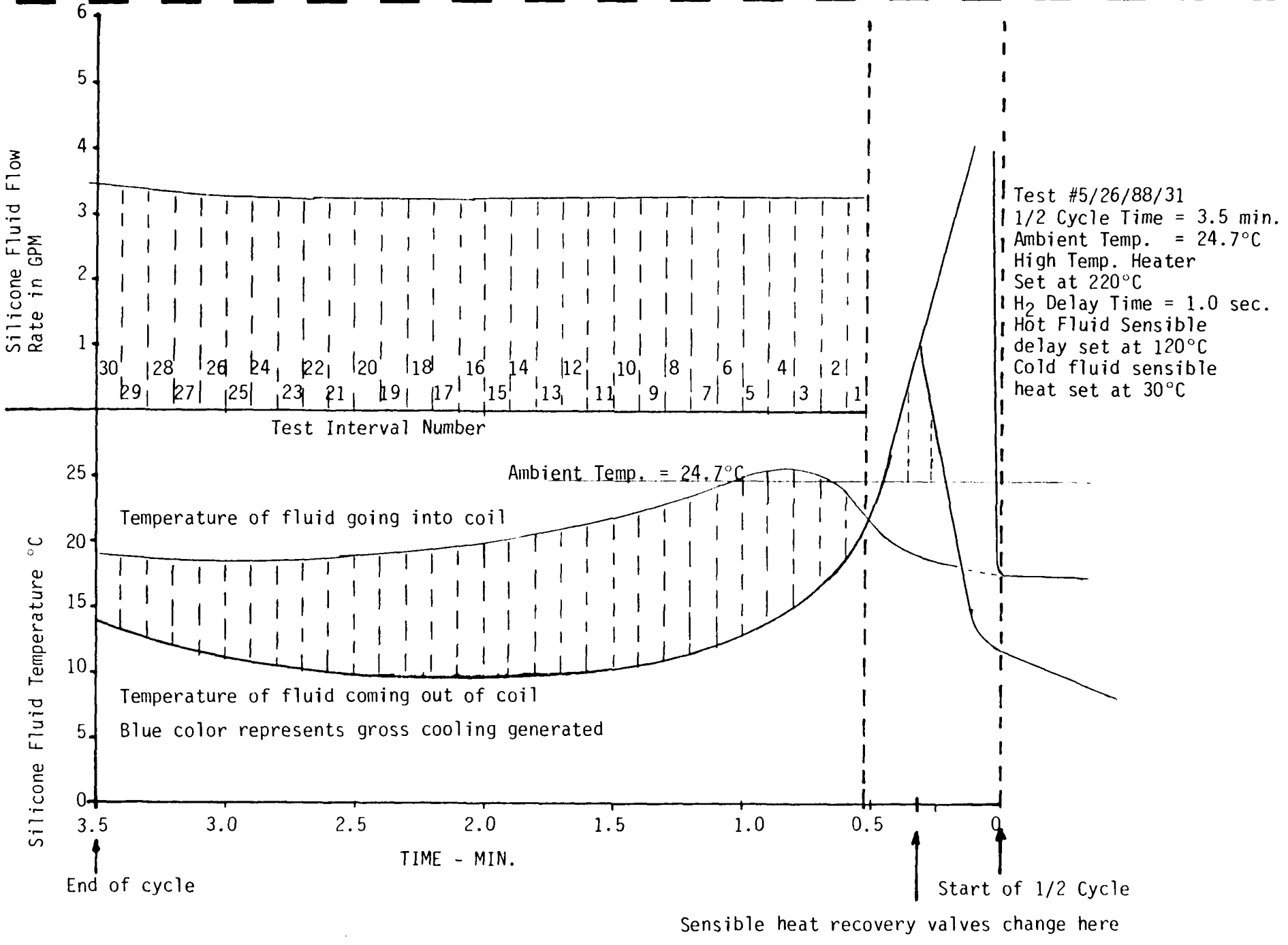

Figure 3.42A - Data from Test #5/26/88/31
Replotted on an Expanded Scale

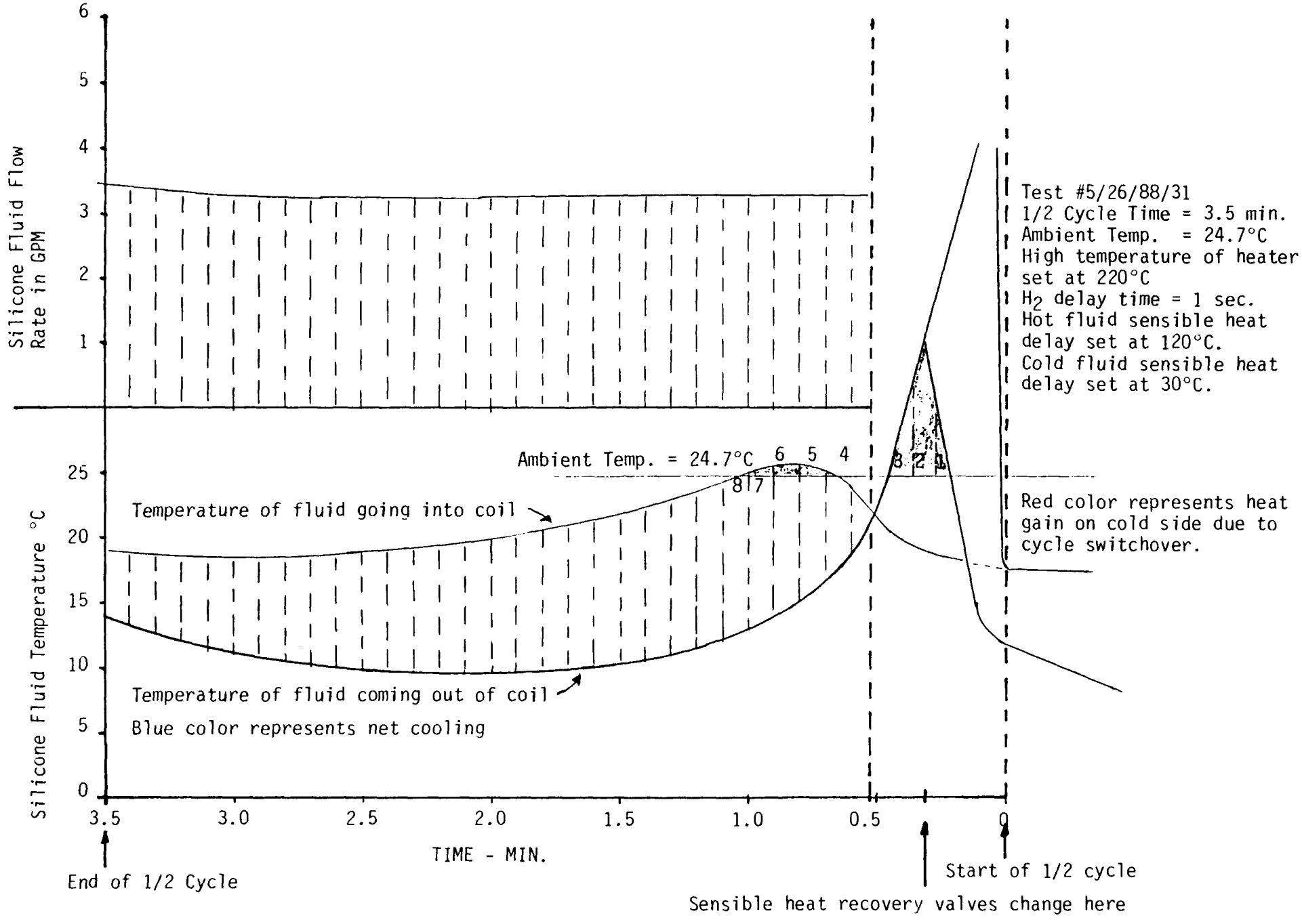

Figure 3.42B - continued

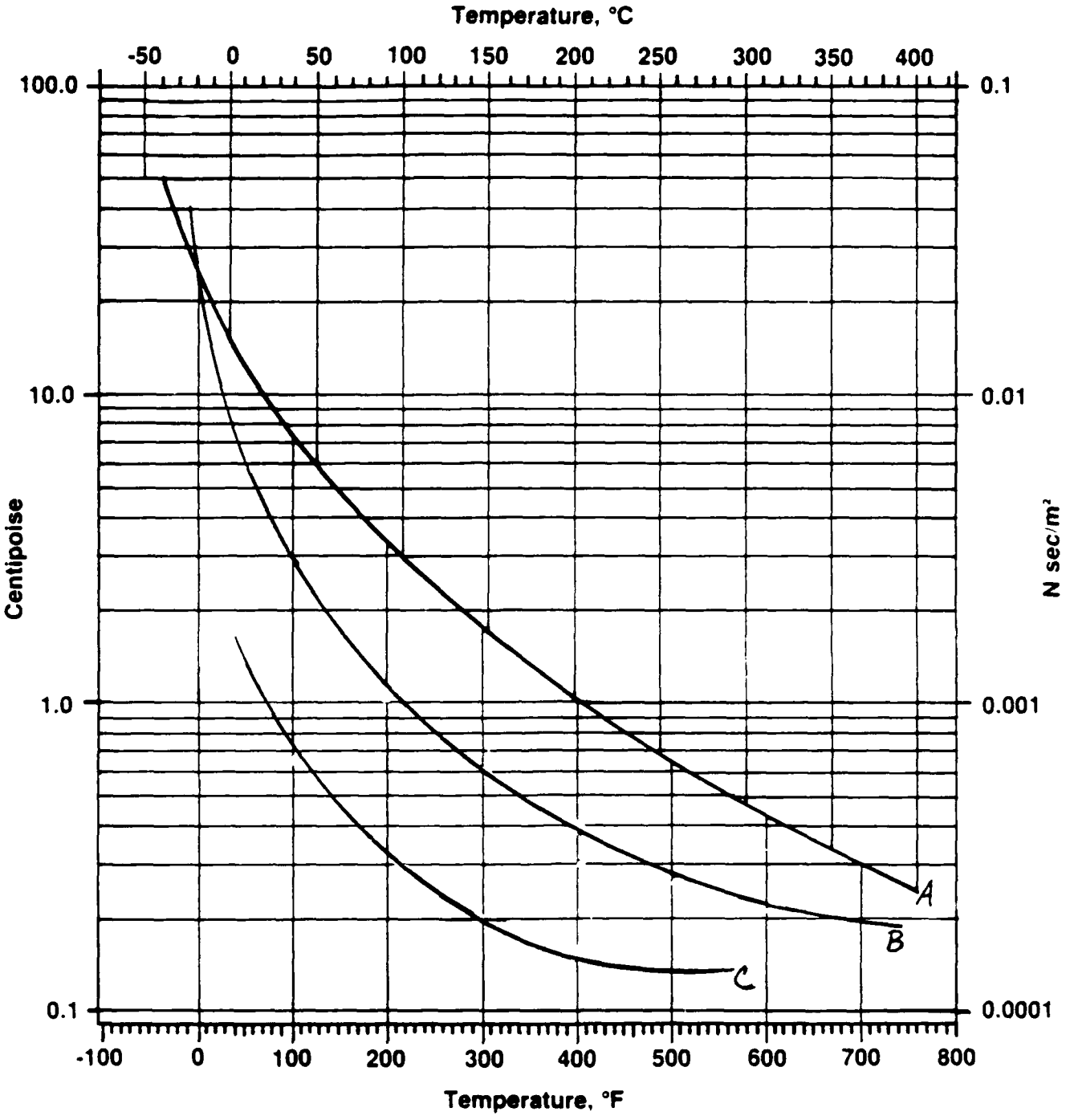

Figure 3.43 - Absolute Viscosity vs Temperature
For Various Heat Transfer Fluids

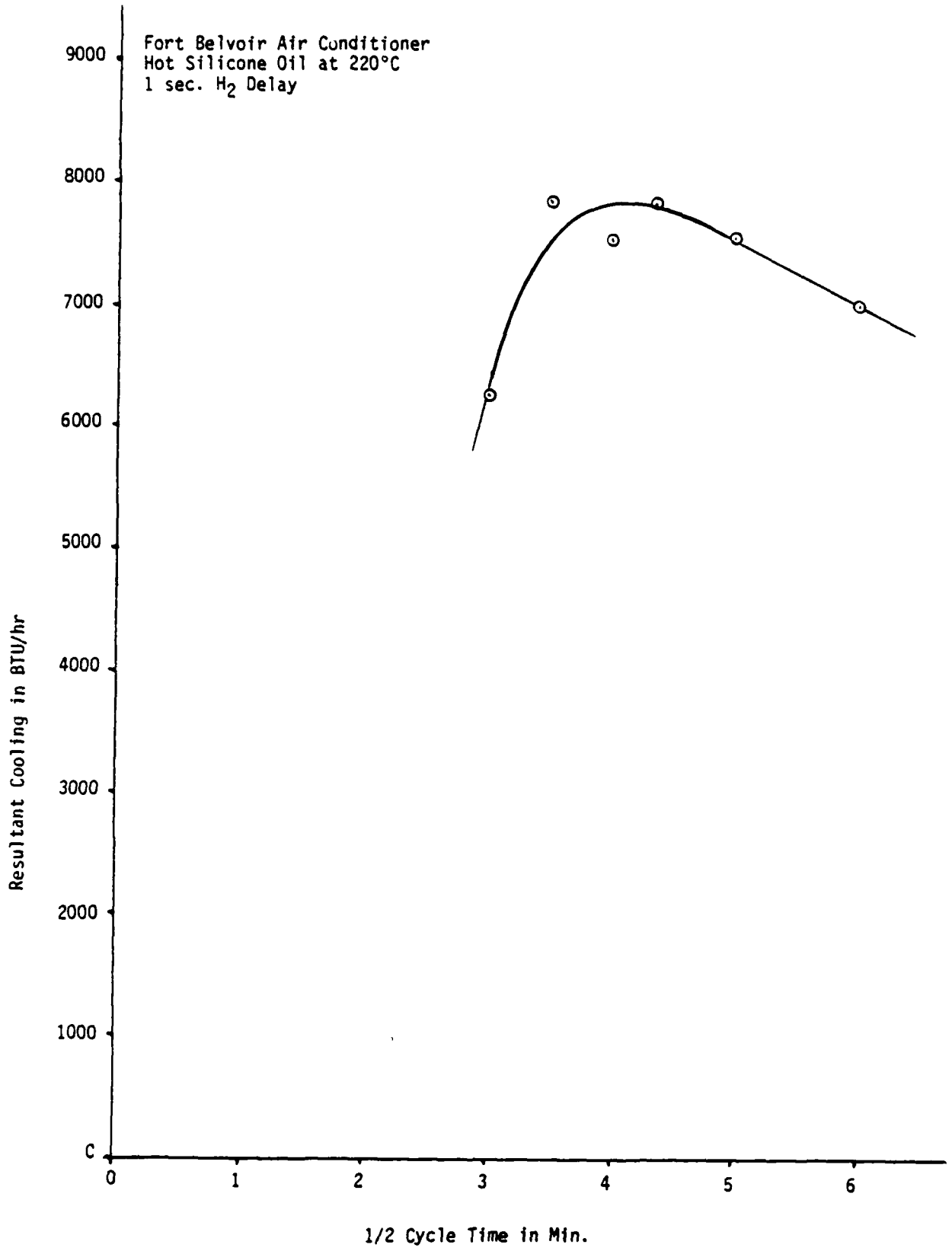

Figure 3.44 - Graph of the Net Cooling vs. the 1/2 Cycle Time for the Metal Hydride (Liquid Type) Air Conditioner Prototype

Heat Transfer Fluid	Manu-facturing	Density g/cc @25°C	Sensible Heat cal/g°C @25°C	Thermal Conduct-ivity cal/cm sec °C @25°C	Thermal Conduct-ivity BTU/h/Ft^2/ °Ft @25°C	Kinematic Viscosity Centi-stokes M^2/s CST	Flash Point °F
Water		1.0	1.0	0.00143	0.343	1 CST	---
Dow Corning 200 Fluid	Dow Corning	0.96	0.352	0.00037 @ 50°C	0.0887	50 CST	605°F
Dow Corning 550 Fluid	Dow Corning	1.07	0.350	0.0003	0.072	125 CST	575°F
UCON 500	Union Carbide	1.026	0.468	0.0004	0.097	100 CST	471°F
Slytherm 800	Dow Corning	0.938	0.383	0.00033	0.078	10 CST	320°F
LF Heat Transfer Fluid	Dow Chemical	1.03	0.39	0.00034	0.081	5 CST	520°F

Table 3.1 – Table of the Relevant and Important Fluid Characteristics of the Various Heat Transfer Fluids Examined

Heat Exchanger	Audi 5000	Audi 5000	Audi 5000	Audi 5000	Corvette	Corvette	Corvette
Fluid Type	Water	Water	Silicone Oil	Silicone Oil	Silicone Oil	Silicone Oil	Silicone Oil
Fluid Flow Rate in GPM	9.2	7.0	8.1	6.5	5.9	5.85	2.081
Air Static Pressure inches H_2O	0.38	0.38	0.39	0.35	0.56	0.21	0.46
Exposed Cou Area Ft^2	1.85	1.85	1.85	1.85	0.309	0.309	0.098
Air Velocity Ft/Min	800	800	800	800	800	420	992
Air Flow Rate SCFM	1480	1480	1480	1480	247	130	97
Temp. Fluid In °C	38.5	39.6	37.4	36.9	37.4	38.4	42.5
Temp. Fluid Out °C	35.9	35.5	33.2	31.9	36.2	37.6	40.4
Temp. Air In °C	24.5	22.4	24.0	21.3	25.1	24.7	21.2
Temp. Fluid Average °C	37.2	37.6	35.3	34.4	36.8	38.0	41.45

Table 3.2A - Results of the Heat Transfer Efficiency Tests Performed on the Various Liquid to Air Heat Exchangers

Heat Exchanger	Corvette Heater Core	Corvette Heater Core	Corvette Heater Core	Valley Plate	Valley Plate	Modine #2931 2¼" Core	Modine #2980 1-1/16" Core
Fluid Type	Silicone Oil	Silicone Oil	Silicone Oil	Silicone Oil	Silicone Oil	Motor Oil	Motor Oil
Fluid Flow Rate in GPM	2.081	0.285	5.9	5.8	5.8	12	10
Air Static Pressure in inches H_2O	0.32	0.32	0.31	0.55	0.25	0.25	0.35
Exposed Core Area Ft^2	0.309	0.309	0.309	0.3711	0.3711	3.54	3.81
Air Velocity Ft/Min	566	566	560	800	522	500	750
Air Flow Rate SCFM	175	175	173	287	193	1770	2858
Temp. Fluid In °C	38.3	43.7	38.4	36.9	36.9		
Temp. Fluid Out °C	34.6	27.0	37.3	35.9	36.4		
Temp. Air In °C	20.3	20.3	24.5	23.3	22.9		
Temp. Fluid Average °C	36.45	35.4	37.9	36.4	36.65		

TABLE 3.2B - Results of the Heat Transfer Efficiency Tests Performed on the Various Liquid to Air Heat Exchangers, cont.

Heat Exchanger	Modine #2931 2½"Core	Modine #2930 2½" Core	Vapor Mfg. Quote #860231	Vapor Mfg. Quote #860231			
Fluid Type	Motor Oil	Motor Oil	Silicon Oil	Silicon Oil			
Fluid Flow Rate In GPM	10	10	8.4	11			
Air Static Pressure in inches H_2O	0.24	0.47	0.33	0.32			
Exposed Core Area Ft^2	3.54	2.4	4.49	4.18			
Air Velocity Ft/Min	500	750	720	560			
Air Flow Rate SCFM	1770	1800	2933	2350			
Temp. Fluid In °C							
Temp. Fluid Out °C							
Temp. Air In °C							
Temp. Fluid Average °C							

TABLE 3.2C - Results of the Heat Transfer Efficiency Tests Performed on the Various Liquid to Air Heat Exchangers, cont.

Heat Exchanger	Audi 5000	Audi 5000	Audi 5000	Audi 5000	Corvette Heater Core	Corvette Heater Core	Corvette Heater Core
T Fluid Avg. -T Air in °C	12.7	15.2	11.3	13.1	11.7	13.3	20.25
Heat loss from fluid BTU/HR	21,522	25,824	10,977	10,488	2284	1510	1410
T air out -T air in °C	7.48	8.98	3.82	3.65	4.75	5.98	7.49
Fluid heat loss per °C BTU/HR/°C	16.95	1699	971	800	195	114	69.6
Efficiency %	58.9	59.1	33.8	27.9	40.6	45.0	37
Weight of unit with fluid - Lbms	18.75	18.75	18.75	18.75	4.0	4.0	4.0
Weight per 28,000 BTU/HR - Lbm	20.6	20.6	36.1	43.8	38.3	65.5	34
Q loss per °C per FT^2 $BTU/(HRx°CxFt^2)$	916	918	525	432	631	368	711
Ft^2 needed for 28,000 BTU/HR - Ft^2	2.04	2.03	3.56	4.32	2.96	5.06	2.62
$\frac{BTU}{HrxFt^2x15°Cx100\ ft/in\ Lbm}$	83.4	83.5	27.2	18.5	30.9	20.1	31.6

TABLE 3.2D Results of the Heat Transfer Efficiency Tests Performed on the Various Liquid to Air Heat Exchangers, cont.

Heat Exchanger	Corvette Heater Core	Corvette Heater Core	Corvette Heater Core	Valley Plate	Valley Plate	Modine #2931 2-1/4"cou	Modine #2980 1-1/16"cou
T Fluid Avg. -T Air in °C	16.15	15.05	13.35	13.1	13.75		
Heat Loss from Fluid BTU/HR	2,484	1,538	2,094	1,871	936		
T Air out -T Air in °C	7.3	4.52	6.22	3.24	2.5		
Fluid heat loss per °C BTU/HR/°C	122.4	102	157	142.9	68	1728	1755
Efficiency %	45.2	30.0	46.6	24.7	18.1		44
Weight of Unit with Fluid - Lbms	4.0	4.0	4.0	2.6	2.6	43.7	24.4
Weight per 28,000 BTU/HR, Lbm	61.0	73.2	47.6	34.0	71.0	47.2	26.0
Q loss per °C per ft^2 BTU/(Hr.x°Cxft^2)	396	331	508	385	183	488	461
Ft^2 needed for 28,000 BTU/Hr - FT^2	4.71	5.64	3.68	4.85	10.2	3.82	4.05
$\frac{BTU}{Hrxft^2x15°Cx100ft/min\ Lbm}$	17.2	12.0	28.6	21.2	7.4	31.0	35.4

TABLE 3.2E - Results of the Heat Transfer Efficiency Tests Performed on the Various Liquid to Air Heat Exchangers, cont.

Heat Exchanger	Modine #2931 2-1/4"Core	Modine #2930 2¼" Core	Vapor Manuf. Q#860231	Vapor Manuf. Q#860231			
T Fluid Avg. -T Air in °C							
Heat loss from fluid BTU/HR			30,000	30,000			
T Air out - T Air in °C							
Fluid heat loss per °C BTU/HR/°C	1620	1620	2000	2000			
Efficiency %							
Weight of unit with fluid - Lbms	44.4	31.2	28.6	35			
Weight per 28,000/BTU/HR - Lbm	51.2	36.0	26.7	32.7			
Q loss per °C per ft^2 BTU/(HRx°CxFT^2)	458	675	445	478			
FT^2 needed for 28,000/BTU/HR - FT^2	4.08	2.77	4.19	3.90			
$\frac{BTU}{HRxFT^2x15°Cx100\ ft/min\ Lbm}$	26.8	37.5	34.8	39.2			

TABLE 3.2F - Results of the Heat Transfer Efficiency Tests Performed on the Various Liquid to Air Heat Exchangers, cont.

Ambient Temperature = 24.7°C

Interval Number	Time of Interval Min.	Reading on the Rhodes Flow Meter	Actual Silicone Fluid Flow Rate GPM	Temperature of the Fluid going into Coil B4 - °C	Temperature of the fluid coming out of Coil B4 - °C	Difference Between the inlet and outlet fluid temperatures - °C	Cooling produced by the hydride coil during this interval - BTU	Accumulated cooling produced by the hydride coil - BTU
1	0.075	6.8	3.25	23.25	20.0	3.25	4.28	4.28
2	0.10	6.8	3.25	24.25	17.7	6.55	11.50	15.78
3	0.10	6.8	3.25	25.15	15.8	9.7	17.02	32.8
4	0.10	6.8	3.25	25.5	14.5	11.0	19.31	52.11
5	0.10	6.8	3.25	25.25	13.4	11.85	20.80	72.91
6	0.10	6.8	3.25	24.5	12.5	12.0	21.06	93.97
7	0.10	6.8	3.25	23.9	11.8	12.1	21.24	115.21
8	0.10	5.8	3.25	23.25	11.2	12.5	21.94	137.15
9	0.10	6.8	3.24	22.65	10.75	11.9	20.82	158
10	0.10	6.8	3.23	22.1	10.4	11.7	20.41	178
11	0.10	6.7	3.21	21.6	10.2	11.4	19.76	198
12	0.10	6.7	3.21	21.15	10.0	11.15	19.32	217
13	0.10	6.7	3.21	20.75	9.95	10.8	18.72	236
14	0.10	6.7	3.21	20.4	9.9	10.5	18.20	254
15	0.10	6.7	3.21	20.0	9.8	10.2	17.68	272
16	0.10	6.7	3.21	19.75	9.75	10.0	17.33	289
17	0.10	6.7	3.21	19.5	9.75	9.75	16.90	306
18	0.10	6.7	3.21	19.25	9.75	9.5	16.47	323
19	0.10	6.7	3.21	19.1	9.8	9.3	16.12	339
20	0.10	6.7	3.21	19.0	9.95	9.05	15.69	355
21	0.10	6.7	3.21	18.8	10.0	8.8	15.25	370
22	0.10	6.7	3.21	18.6	10.2	8.4	14.56	384

Table 3.3A - Head Load Integration of the Data Generated in Test #5/26/88/31

Ambient Temperature = 24.7°C

Interval Number	Time of Interval Min.	Reading on the Rhodes Flow Meter	Actual Silicone Fluid Flow Rate GPM	Temperature of the fluid going into Coil B4 - °C	Temperature of the fluid coming out of Coil B4 - °C	Difference between the inlet and outlet fluid temperatures - °C	Cooling produced by the hydride coil during this interval - BTU	Accumulated cooling produced by the hydride coil - BTU
23	0.10	6.7	3.21	18.5	10.4	8.1	14.04	398
24	0.10	6.7	3.22	18.5	10.6	7.9	13.74	412
25	0.10	6.7	3.24	18.5	10.9	7.6	13.30	425
26	0.10	6.7	3.28	18.4	11.3	7.1	12.58	438
27	0.10	6.7	3.30	18.5	11.75	6.75	12.03	450
28	0.10	6.7	3.32	18.5	12.25	6.25	11.21	461
29	0.10	6.7	3.38	18.7	12.80	5.90	10.76	472
30	0.10	6.7	3.40	18.9	13.0	5.90	10.83	483

TABLE 3.3B Heat Load Integration of the Data Generated in Test #5/26/88/31 cont.

(See figure 64B)

Interval Number	Time of Interval Min.	Reading on the Rhodes Flow Meter	Actual Silicone Fluid Flow Rate GPM	Ambient Temperature °C	Temperature of the fluid going in or out of Coil B4 - °C	Absolute difference in temperature °C	Heating produced by hydride coil switch-over - BTU	Accumulation heating produced by coil switchover - BTU
1	0.10	6.8	3.50	26.5	24.7	1.8	3.4	3.40
2	0.10	6.7	3.29	33.5	24.7	8.8	13.41	16.8
3	0.10	6.7	3.27	27.0	24.7	2.3	4.06	20.9
4	0.10	6.7	3.25	24.8	24.7	0.1	0.10	21.0
5	0.10	6.7	3.25	25.0	24.7	0.3	0.53	21.5
6	0.10	6.8	3.25	25.3	24.7	0.6	1.03	22.5
7	0.10	6.7	3.25	25.0	24.7	0.3	0.53	23.1
8	0.10	6.7	3.25	24.75	24.2	0.05	0.14	23.9

Test Conclusion:

Total cooling produced by hydride coil during its 3.5 min., 1/2 cycle = 483 BTU

Heating produced on the "cold" side by the hydride coil switchover = 23.9 BTU

Therefore, net cooling produced by the hydride coil during its 3-1/2 min., 1/2 cycle = 459.1 BTU

= 7868 BTU/HR

TABLE 3.3C Heat Load Integration of the Data Generated in Test #5/26/88/31 cont.

Test Number	1/2 Cycle Time Min.	H_2 Valve Delay Time Sec.	Ambient Temperature °C	Hot Fluid Temperature Set Point - °C	Hot Side, Sensible Heat Temperature Set Point °C	Cold Side, Sensible Heat, Temperature Set Point °C	Cooling generated by the hydride coil during this cycle - BTU	Reactant net cooling generated BTU/HR
5/26/88 -41	3.0	1 sec.	23.7	220°C	120°C	30°C	314	6283
-31	3.5	1 sec.	24.7	220°C	120°C	30°C	459	7868
-21	4.0	1 sec.	24.6	220°C	120°C	30°C	504	7555
-49	4.33	1 sec.	23.2	220°C	120°C	30°C	566	7843
-45	4.0	1 sec.	23.5	220°C	120°C	30°C	631.5	7578
-29	3.5	33 sec.	24.5	220°C	120°C	30°C	441.6	7571

Table 3.4 - Data Reduction Results on the Cooling Capacity Tests Conducted on the Metal Hydride Air Conditioner

APPENDIX 3.1

A TECHNIQUE FOR ANALYZING REVERSIBLE METAL HYDRIDE SYSTEM PERFORMANCE*

P. M. GOLBEN and E. LEE HUSTON

Ergenics Division, MPD Technology Corporation, 681 Lawlins Road, Wyckoff, NJ 07481 (U.S.A.)

Journal of the Less-Common Metals, 89 (1983) 333 - 340

A TECHNIQUE FOR ANALYZING REVERSIBLE METAL HYDRIDE SYSTEM PERFORMANCE*

P. M. GOLBEN and E. LEE HUSTON

Ergenics Division, MPD Technology Corporation, 681 Lawlins Road, Wyckoff, NJ 07481 (U.S.A.)

(Received May 31, 1982)

Summary

An experimental method is described which permits rapid characterization of hydride modules without requiring internal measurement of the bed temperature. The time to charge or discharge is measured as a function of the hydrogen pressure. A pressure-to-temperature transformation which relies on reversible metal hydride thermodynamics is applied to determine the bed temperature. This transformation facilitates conventional heat transfer analysis on hydride modules.

Results are presented for the charging of a 0.375 in (0.95 cm) tubular hydride module. The time to 90% charge is less than 5 min when the temperature difference between the $LaNi_5$ bed and the external cooling water exceeds 14 °C. This result compares very favorably with laboratory reactors designed for rapid heat transfer.

1. Introduction

Prototypes of a variety of thermochemical equipment and storage devices utilizing reversible metal hydrides have been developed. They include heat pumps [1], refrigerators [1, 2], hydrogen compressors [3], water pumps [4], hydrogen purifiers [5], hydrogen separators [6] and stationary and mobile hydrogen storage systems [7]. A common feature of all these systems is their reliance on low grade heat as the energy input. This implies that only small temperature differences are available to charge or discharge the hydride beds and to obtain the energy conversion. Much emphasis has been placed on improving the efficiency of the heat exchangers [8] and the thermal conductivity of the hydride beds themselves [9, 10] in an effort to reduce the hydride inventory (and hence the system cost) for a given level of system performance.

*Paper presented at the International Symposium on the Properties and Applications of Metal Hydrides, Toba, Japan, May 30 - June 4, 1982.

0022-5088/83/0000-0000/$02.75

The experimental verification of heat transfer improvements is time consuming and until now has been difficult to generalize because of the many system variables. A simplified technique that enables the heat transfer characteristics of a reversible metal hydride module to be determined quickly and compared with other designs is described in this paper.

2. Experimental apparatus and procedure

A schematic diagram of the test apparatus used to evaluate the charge–discharge characteristics of hydride storage modules is shown in Fig. 1.

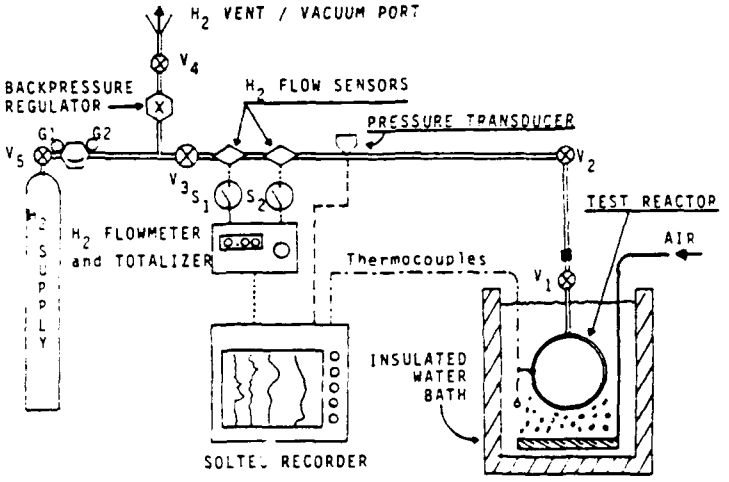

Fig. 1. Schematic diagram of test apparatus used to evaluate the charge–discharge characteristics of hydride storage modules.

It consists of a hydrogen tank and regulator for the supply of UHP grade (purity, 99.999%) hydrogen. Two hydrogen flowmeters (Mathesen model 8160) are used to measure the hydrogen flow at either 0 - 2 or 0 - 100 standard l min^{-1}. A Dynisco (model APT 380-5C) pressure transducer is used to measure the system pressure. A TESCOM 1700 series back pressure regulator is used to control the system pressure. The hydride storage module under test is immersed in a large (about 50 l) air-agitated water tank to maintain near-isothermal conditions on the surface of the module. (A second tank is utilized for forced air heat transfer tests.) One thermocouple is attached to the surface of the module and is covered with a small bead of silicone rubber. A second thermocouple is used to measure the water (or air) temperature. No internal temperature measurements are made. Outputs from the flowmeter, pressure transducer and thermocouples are recorded continuously using a Soltec six-pen strip chart recorder.

To initiate testing a hydride module is connected to the apparatus and all hydrogen lines are evacuated. Valve V_1 is opened and the module is

allowed to equilibrate in the constant temperature bath after which the system pressure and temperature are noted. For absorption tests V_1 is closed to adjust the hydrogen charging pressure and then reopened to start the test. It is often necessary to throttle the flow initially with V_3 to keep the flowmeter on scale. Testing can be discontinued at any time but normally proceeds until the flow falls to zero at which time the final system pressure and temperature are noted. For desorption the back pressure regulator is set to the desired level and testing is initiated by opening the desorption regulating valve V_4. A series of charging and discharging tests are normally run back to back to characterize a module completely.

The bulk of the experimental work reported here was performed on a coiled hydride module 10 ft long fabricated from copper tubing of outside diameter 0.375 in (0.95 cm) and inside diameter 0.32 in (0.8 cm).

The module, which has a capacity of approximately 73 l of hydrogen at 300 lbf in^{-2} (absolute) (2.04 MPa), is shown in Fig. 2. It was filled with

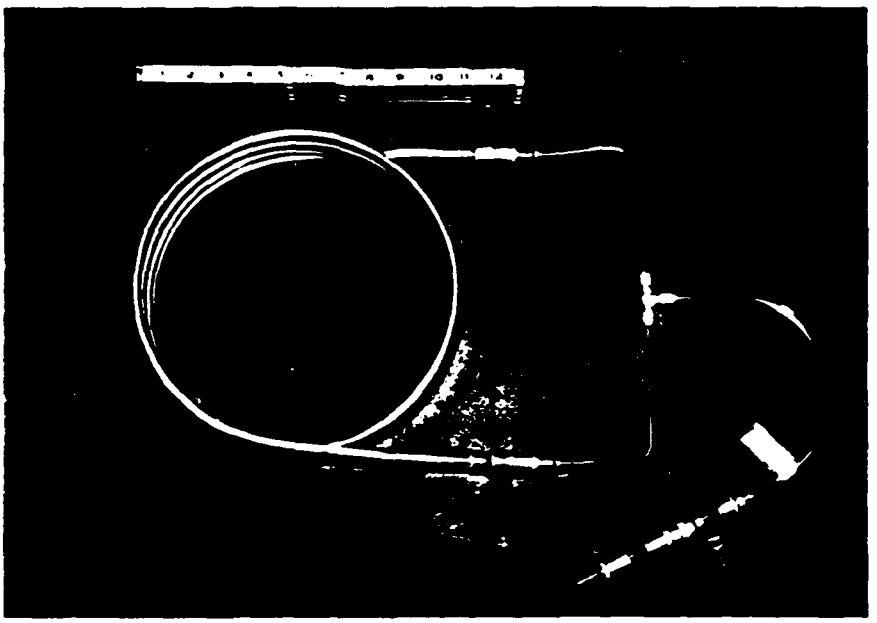

Fig. 2. Hydride storage module fabricated from 0.375 in (0.95 cm) copper tubing.

457 g of HY-STOR 205 ($LaNi_5$) (HY-STOR is the trademark of the Inco group of companies). Absorption and desorption isotherms were measured at 25 °C on a sample of this alloy. The isotherms are plotted in Fig. 3 as P (lbf in^{-2}) *versus* hydrogen-to-metal ratio to draw attention to the slope and hysteresis for subsequent discussion. The alloy is slightly nickel rich which accounts for the plateau pressure being rather higher than usual. Gas distribution along the entire length of the tube and the space for hydride expansion were provided by a proprietary internal design. A second module containing three capsules of diameter 0.5 in (1.27 cm) and length 3 in (7.62 cm) [11] was also evaluated.

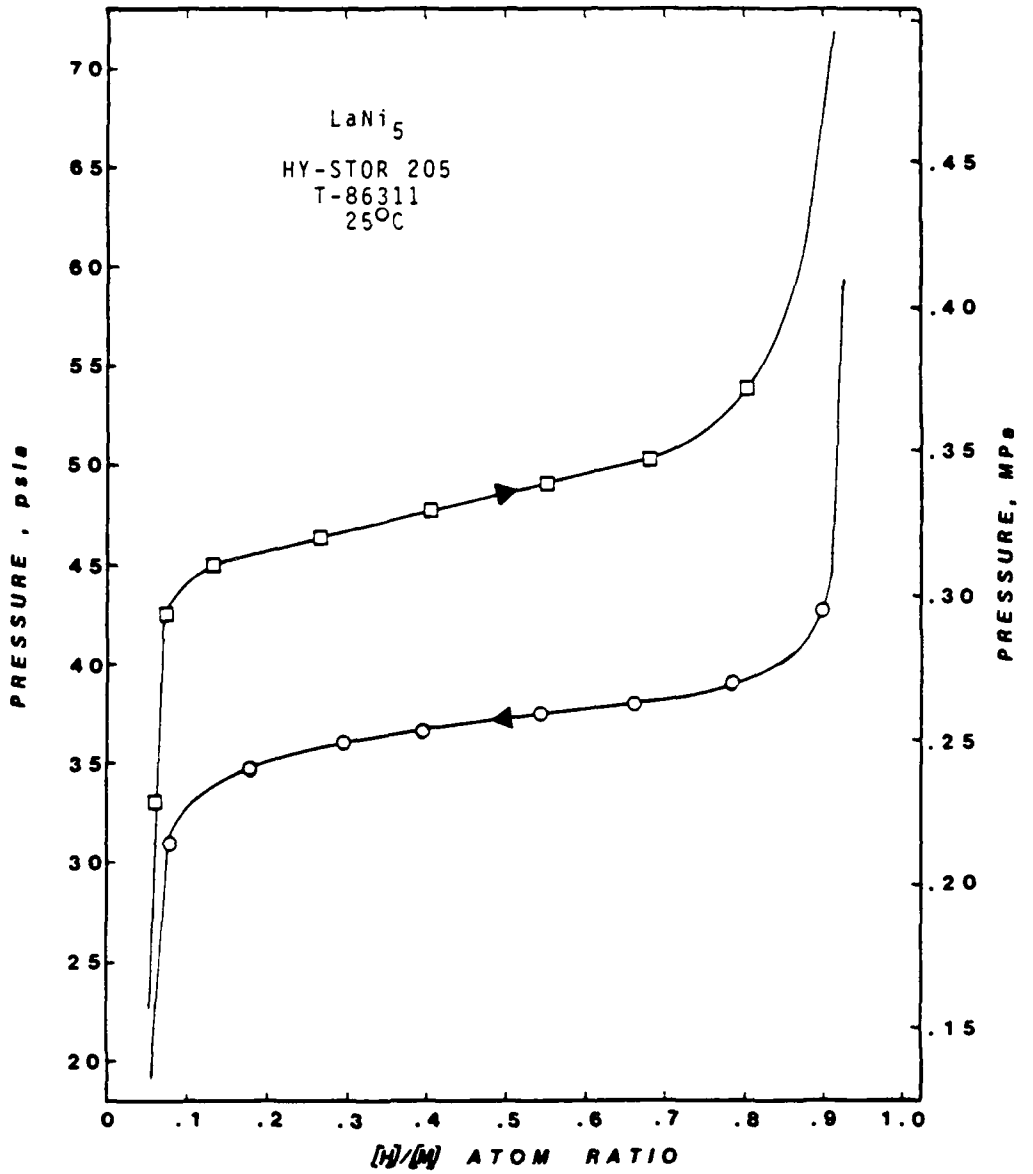

Fig. 3. Absorption and desorption isotherms obtained at 25 °C for the HY-STOR 205 alloy (analyzed composition $La_{0.89}Ni_{5.0}$) using the tubular module.

3. Experimental results and analysis

The results from a series of charging tests are shown in Fig. 4. The module charges to 90% of capacity in about 1.2 min at a hydrogen pressure of 155 lbf in^{-2}. The time for charging increases rapidly as the charging pressure approaches the absorption plateau pressure which, from the static isotherms of Fig. 3, is about 48.5 lbf in^{-2} (0.35 MPa) at [H]/[M] = 0.5. In addition, the quantity of hydrogen absorbed decreases with decreasing charging pressure. Two factors contribute to this effect: one is experimental and arises from cumulative errors in the flowmeters at low flow rates which

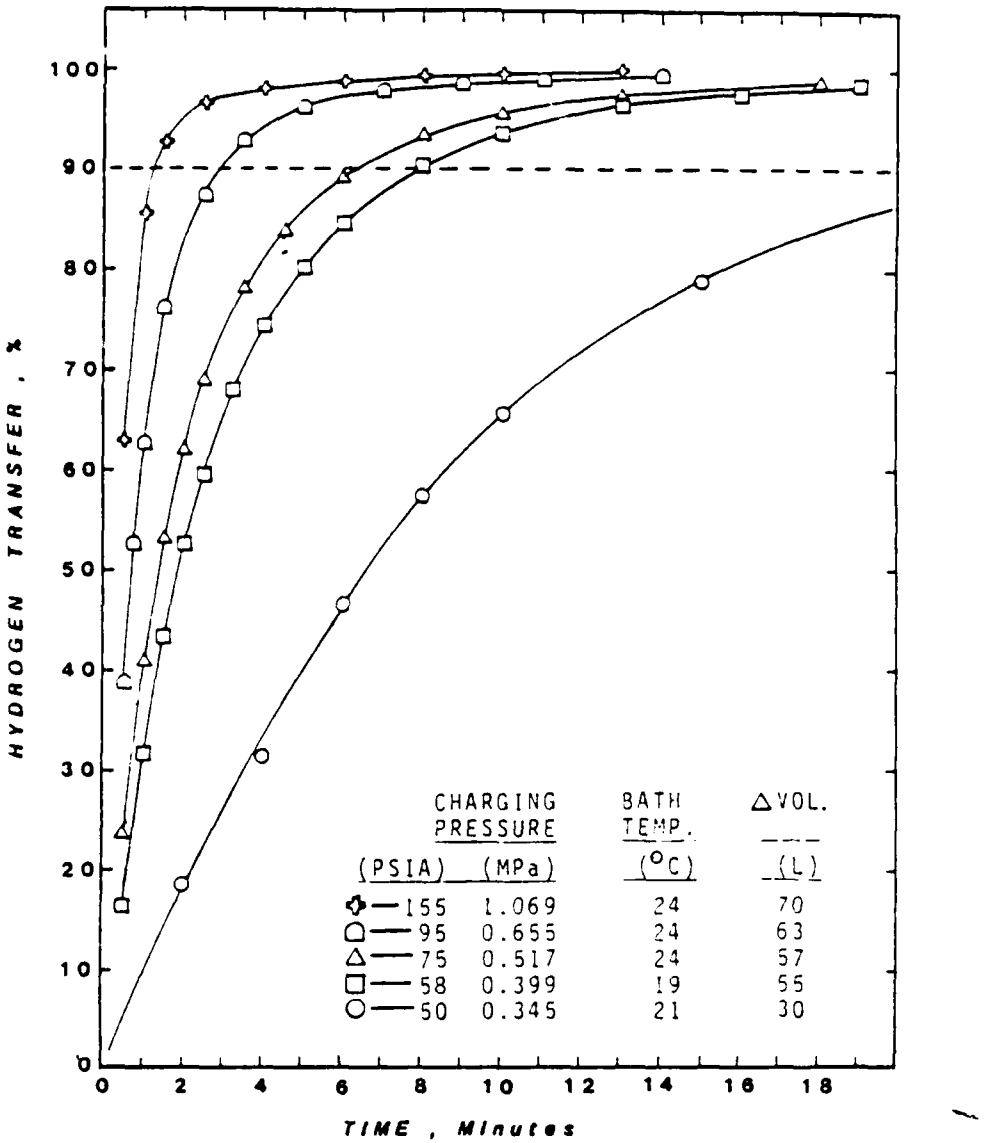

Fig. 4. Charging tests at various pressures using the tubular module.

are more prevalent at low charging pressures and the second is due to an increase in hysteresis for dynamic conditions. Goodell *et al.* [12] have reported a 15% increase (about 7.5 lbf in^{-2}) in the absorption plateau of $LaNi_5$ for a continuous charging rate of 0.02 hydrogen atoms per metal atom per minute. The average rate for the 58 lbf in^{-2} (0.40 MPa) test was about 0.1 hydrogen atoms per metal atom per minute. (1 hydrogen atom per metal atom per minute corresponds to 6.94 mol H_2 (kg $LaNi_5)^{-1}$ min^{-1}.)

The two thermocouples showed less than 1 °C difference between the water bath and the surface of the module during the charging tests. However, the temperature of the $LaNi_5H_x$ bed became much higher. This is the result of four factors. First the hydrogen absorption rate for $LaNi_5$ is exceedingly fast [13]. Second the heat of reaction (−7.4 kcal (mol $H_2)^{-1}$) is large relative to the heat capacity of the alloy (0.1 kcal kg^{-1} $°C^{-1}$). Thus

hydrogen absorption equivalent to only [H]/[M] = 0.097 (0.67 mol H_2 (kg $LaNi_5$)$^{-1}$) will produce an adiabatic temperature rise of 50 °C. Third our particular tubular design minimizes gas pressure drops along the length of the module. Finally the thermal conductivity of the $LaNi_5$ bed is exceedingly small (1.32 W m^{-1} K^{-1}) [14]. These factors imply that heat transfer limits the rate of charging and discharging of most systems and that the $LaNi_5H_x$ bed remains at an elevated temperature during charging.

When heat transfer limits the rate of charging, the bed temperature can be calculated directly from the hydrogen charging pressure [14 - 16]. This convenient relation has been overlooked in many earlier investigations. The equilibrium pressure (plateau pressure) for the hydride reaction is related to the absolute temperature T by the familiar van't Hoff equation

$$\ln P = \frac{\Delta H}{RT} + \frac{\Delta S}{R} \tag{1}$$

where ΔH and ΔS are the enthalpy and entropy changes for the reaction. The constants in eqn. (1) have been tabulated for many reversible metal hydrides [17]. They can be derived from absorption and desorption isotherms measured at several temperatures. The bed temperature T_A on charging is calculated from eqn. (1) by inserting the charging pressure and the appropriate ΔH and ΔS values. However, care should be taken when using this procedure. Most thermodynamic data are obtained from static desorption isotherms at [H]/[M] = 0.5. Pressure hysteresis implies that there must be small differences in the thermodynamic properties measured in absorption and desorption. Moreover differences between static and dynamic values have also been reported [12] and the pressure plateaux generally exhibit measurable slope. We have modified the static desorption values of $LaNi_5$ obtained from ref. 17 by assuming that the enthalpy is invariant at −7.4 kcal (mol H_2)$^{-1}$ and adjusting the entropy term to agree with the observed pressure hysteresis data of Fig. 3 at [H]/[M] = 0.5. Hence the bed temperature on charging was calculated from eqn. (1) by substituting the relation

$$T_A = \frac{3724}{13.691 - \ln P} \tag{2}$$

where P is in atmospheres. The temperature difference between the hydride bed and the water bath can then be computed. It is this difference that determines the heat transfer out of the module and hence the rate of system charging.

The time for 90% charge is plotted as a function of the temperature difference across the module in Fig. 5 (open circles). The 0.375 in (. 95 cm) module will charge in less than 5 min for ΔT values exceeding 14 °. The charging times are about a factor of 2 slower for the 0.5 in (1.27 cm) aluminum capsule configuration. Two additional curves are shown. Data for the 1 in (2.54 cm) capsules were derived from the charging curves reported by Lynch [15]. The "fast reactor" in Fig. 5 refers to the results of experiments by Goodell [14] using a thin (0.06 in (0.15 cm)) disk of $LaNi_5$

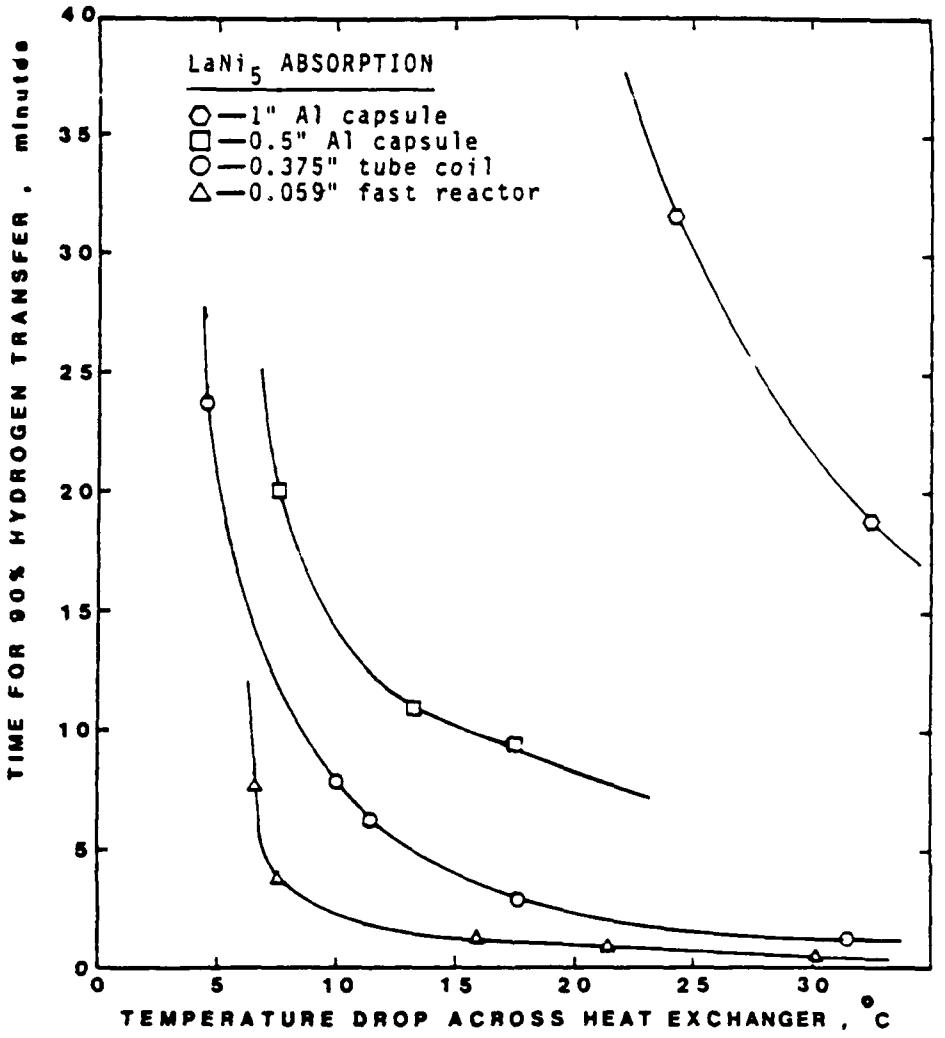

Fig. 5. Time for 90% charging of various hydride modules as a function of the temperature drop.

powder. One immediate conclusion from Fig. 5 is that the 0.375 in (0.95 cm) tubular module compares very favorably with the charging kinetics of laboratory equipment specially designed to optimize heat transfer.

Curves such as those in Fig. 5 allow the performance of a particular module to be predicted for virtually any set of charging pressures and bed temperatures. Moreover the pressure-to-temperature transformation of eqn. (2) permits analysis of the hydrogen absorption tests by conventional heat transfer methods. The heat generated is the product of the number of moles of hydrogen absorbed and ΔH. The average heat production rate is determined by the time for 90% charge. These rates, when correlated with ΔT and appropriate geometric factors, permit standard predictive equations to be established. Thus our method provides a very simple way of comparing many different hydride containment designs for both hydrogen absorption and desorption. This analytic technique in essence gives the "macro" heat transfer temperature difference driving the reaction as long as it is heat transfer limited. "Micro" heat transfer parameters such as the metal hydride

or metal powder thermal conductivities, the shape of the reaction front, the heat transfer boundary layers etc. need not be specifically analyzed.

The shape of the charging curves in Fig. 5 indicates an asymptote at about 5 °C. Such behavior is expected to occur at 0 °C. It is believed that this temperature shift reflects the difference between static and dynamic hysteresis for $LaNi_5$. The bed temperature was calculated on the basis of static van't Hoff data while the tests were run continuously.

Only charging data have been reported here. Similar tests have been performed for desorption to test the symmetry of the analysis. Tests with different alloys have also established the more general applicability of the analysis. This work will be reported elsewhere [18].

Acknowledgments

The authors wish to acknowledge the support and discussions provided by P. D. Goodell and L. E. Terry. Credit for experimental assistance with the 0.5 in capsules is also due to L. E. Terry.

References

1 D. M. Gruen, R. L. McBeth, M. Mendelsohn, J. M. Nixon, F. Schreiner and I. Sheft, HYCSOS: a solar heating, cooling and energy conversion system based on metal hydrides, *Proc. 11th Intersociety Energy Conversion Engineering Conf., State Line, NV, September 12 - 17, 1976*, Vol. 1, American Institute of Chemical Engineers, New York, 1976, p. 681.
2 L. E. Terry, personal communication, 1980.
3 F. E. Lynch, R. A. Nye and P. P. Turillon, *Phase I Final Rep. BNL 51369*, January 1981 (Brookhaven National Laboratories, Upton, NY).
4 A. A. Heckes, T. E. Hinkebein and G. J. M. Northrup, *Proc. 14th Intersociety Energy Conversion Engineering Conf., Boston, MA, July 1979*, Vol. 1, American Chemical Society, Washington, DC, August 1979, p. 743.
5 H. Wenzl and K. H. Klatt, in A. F. Andresen and A. J. Maeland (eds.), *Proc. Int. Symp. on Hydrides for Energy Storage*, Pergamon, Oxford, 1978, p. 323.
6 E. L. Huston and J. J. Sheridan, *Am. Chem. Soc. Symp. Ser. 164*, 1981, p. 223 (American Chemical Society, Washington, DC).
7 G. D. Sandrock, *Hydrogen Energy*, Royal Swedish Academy of Engineering Sciences, Stockholm, 1981.
8 G. Benson, *Brookhaven National Laboratories–U.S. Department of Energy Symp.–Workshop, Brookhaven, June 1978, Informal Rep.* (Brookhaven National Laboratories, Upton, NY).
9 E. E. Eaton, C. E. Olsen, H. Sheinberg and W. A. Steyert, *Int. J. Hydrogen Energy, 6* (6) (1981) 609 - 623.
10 M. Ron, D. M. Gruen, M. H. Mendelsohn and I. Sheft, *U.S. Patent 4,292,265*, September 29, 1981.
11 P. P. Turillon and G. D. Sandrock, *U.S. Patent 4,135,621*, January 23, 1979.
12 P. D. Goodell, G. D. Sandrock and E. L. Huston, *J. Less-Common Met., 73* (1980) 135 - 142.
13 P. D. Goodell and P. S. Rudman, *J. Less-Common Met., 89* (1983) 117 - 125.
14 P. D. Goodell, *J. Less-Common Met., 74* (1980) 175 - 184.
15 F. E. Lynch, *J. Less-Common Met., 74* (1980) 411 - 418.
16 P. S. Rudman, *J. Less-Common Met., 89* (1983) 93 - 110.
17 E. L. Huston and G. D. Sandrock, *J. Less-Common Met., 74* (1980) 435 - 443.
18 P. D. Goodell, unpublished data, 1981.

APPENDIX 3.2

MULTI-STAGE HYDRIDE-HYDROGEN COMPRESSOR

P. M. Golben

Ergenics Division, MPD Technology Corporation
681 Lawlins Road, Wyckoff, N.J. 07481

Reprinted from 18TH INTERSOCIETY ENERGY CONVERSION ENGINEERING CONFERENCE, August 21-26, 1983

APPENDIX 3.2

MULTI-STAGE HYDRIDE-HYDROGEN COMPRESSOR

F. M. Golben

Ergenics Division, MPD Technology Corporation
681 Lawlins Road, Wyckoff, N.J. 07481

ABSTRACT

A novel 4 stage metal hydride-hydrogen compressor that uses low temperature hot water (75°C) as its energy source has been built and tested. The compressor utilizes a new hydride heat exchanger technique that has achieved fast cycling time (with 20°C cooling water) on the order of 1 min. This refinement substantially decreases the size, weight and cost of the unit when compared to previous hydride compressors or even conventional mechanical diaphragm compressors.

INTRODUCTION

In recent years metal hydride technology has intrigued the scientific community by their unique ability to absorb and desorb large amounts of hydrogen gas. This hydrogen transfer phenomenon has been proposed as the "driving force" for many conventional utilities such as heat pumps (ref. 1), refrigerators (ref. 1, 2), power cycles (ref. 3) and hydrogen compressors (ref. 4). The energy source for these hydride devices is simply hot water which could be provided by waste heat or even solar energy. Previous prototypical hydride devices have been heavy and large (and therefore expensive) due to the difficulty in designing cost effective, fast heat transfer systems for use with such low grade heat sources. However, recent advancements in metal hydride heat transfer technology has produced systems that are competitively priced against conventional mechanical counterparts while yet in the pre-production stage. This paper discusses the design, fabrication and testing of one such hydride device, that being a four-stage hydrogen compressor that develops a 10 to 1 compression ratio with a flow rate of 40 SLPM (Standard Liters per Minute), and contains less than 5 Kgs of metal hydride alloy.

THEORY OF OPERATION

The following section assumes that the reader is generally familiar with the nature of metal hydrides and their reaction with hydrogen gas. If not, it may be helpful to refer to the appendix at the end of the paper for a short review on metal hydride technology.

The hydride compressor operates by successively absorbing and desorbing hydrogen into and out of several hydride beds. Hot water provides the energy needed to desorb the hydrogen from the hydride and cold water provides the heat sink needed to dissipate the heat generated when hydrogen is absorbed by the hydriding alloys.

In order to obtain high pressures, several hydriding alloys are 'staged' in series. This is achieved by selecting alloys with increasing desorption pressure in such a way that an upper stage hydride will absorb hydrogen (at the heat sink temperature), that is desorbed from the lower stage alloy (at the heat source temperature).

Figure 1 illustrates this staged compression by showing pressure vs composition curves for three different alloys. In each case, the absorption curve corresponds to the low temperature (typically 20°C), and the desorption curve corresponds to the higher temperature (75°C). The waved lines represent the flow of hydrogen from one alloy to the next. Figure 2 shows the same concept represented on a schematic pressure vs temperature diagram.

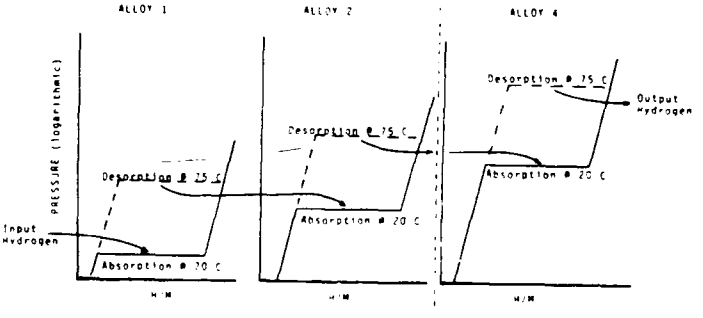

FIGURE 1 : Principle of Four Stage Hydride-Hydrogen Compressor

The transfer of hydrogen from one hydride bed to another is done automatically through the use of check valves which allow flow of hydrogen in one direction only.

The following description and figure 3 are useful in illustrating how hydrogen flows alternately from one hydride bed to the next in a four stage hydride compressor:

Process 1: While hydride bed A is being cooled by cold water and hydride bed B is being heated with hot water, hydrogen flows from the supply line to stage 1A, from stage 1B to stage 2A, from stage 2B to stage 3A, from stage 3B to stage 4A and from stage 4B to the outlet line.

Process 2: While hydride bed A is heated and bed B is cooled, hydrogen flows from the supply line to stage 1B, from stage 1A to stage 2B, from stage 2A to stage 3B, from stage 3A to stage 4B and from stage 4A to the outlet line.

Reprinted from 18TH INTERSOCIETY ENERGY CONVERSION ENGINEERING CONFERENCE, August 21-26, 1983

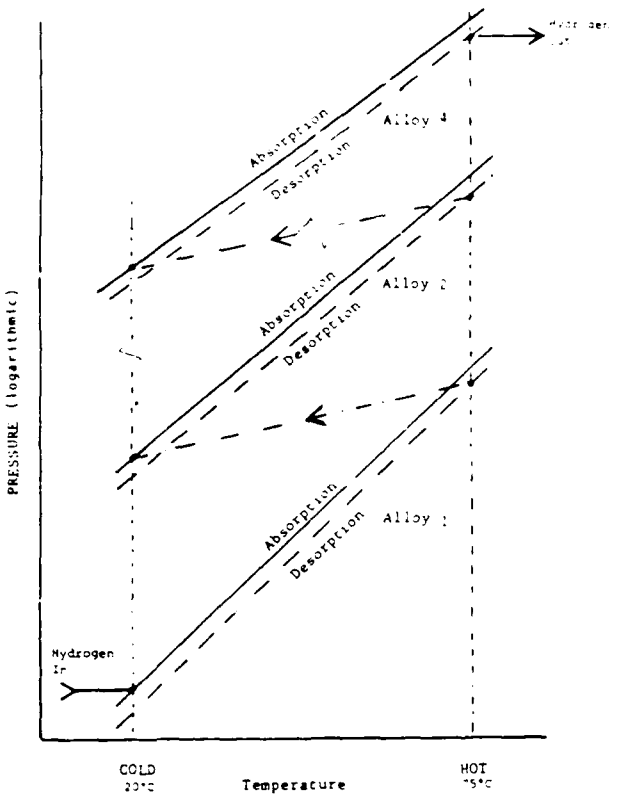

FIGURE 2 : Principle of Four Stage Hydride-Hydrogen Compressor

The use of check valves prevents a reverse flow of hydrogen from a high pressure stage to a lower pressure stage. The check valves get whenever there is a small pressure differential in the direction of hydrogen flow, and close tight" when the pressure differential reverses.

COMPONENT DESCRIPTION

The design of the hot water compressor consists of 4 major components: hydride heat exchangers, hydrogen flow control, water flow control and control timers. A photograph of these components are shown in figure 4 and can be referred to during the following component description. Table 1 lists the general reference and specification data on the compressor itself. U.S. Patent applications have been allowed and corresponding foreign applications filed.

Hydride Heat Exchangers

These exchangers are where the heat that is generated during hydrogen absorption by the metal hydride is dissipated (rejected) to the cooling fluid (cold tap water). They are also where the heat that is required to release the hydrogen out of the metal hydride is provided by the heating fluid (hot water). Since only one of these modes can occur at any one time, the hydride compressor incorporates two (2) separate "beds" so that when one bed is being cooled, the other one is being heated. This is the minimum number of beds possible if the compressor is to contain the multi-stages of hydride alloy needed for large compression ratios, since a higher pressure stage must be "charged' by the lower pressure stage.

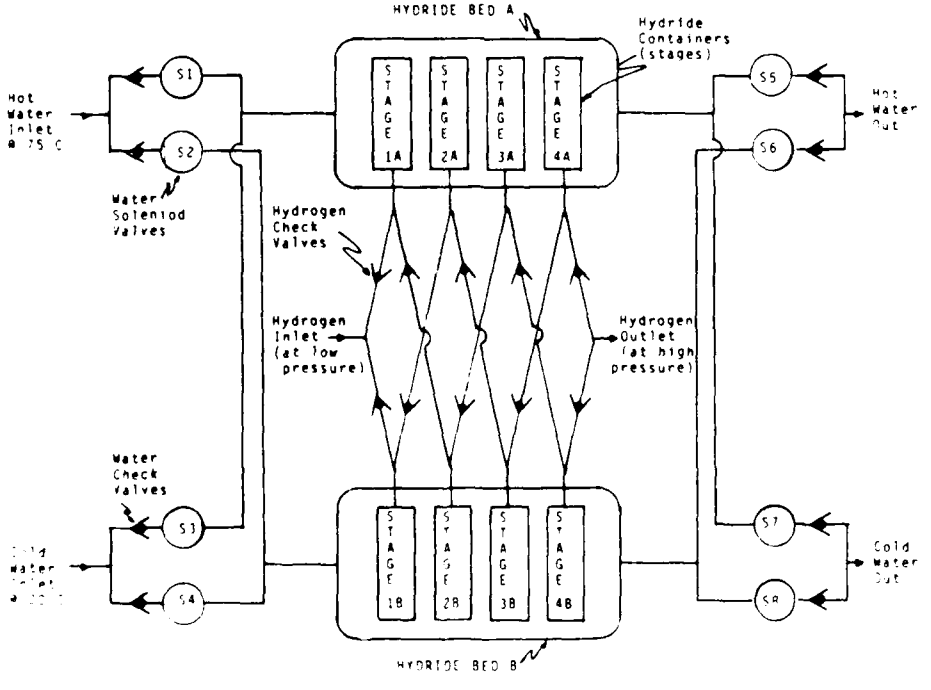

FIGURE 3 : Operational Schematic of Four Stage Hydride-Hydrogen Compressor

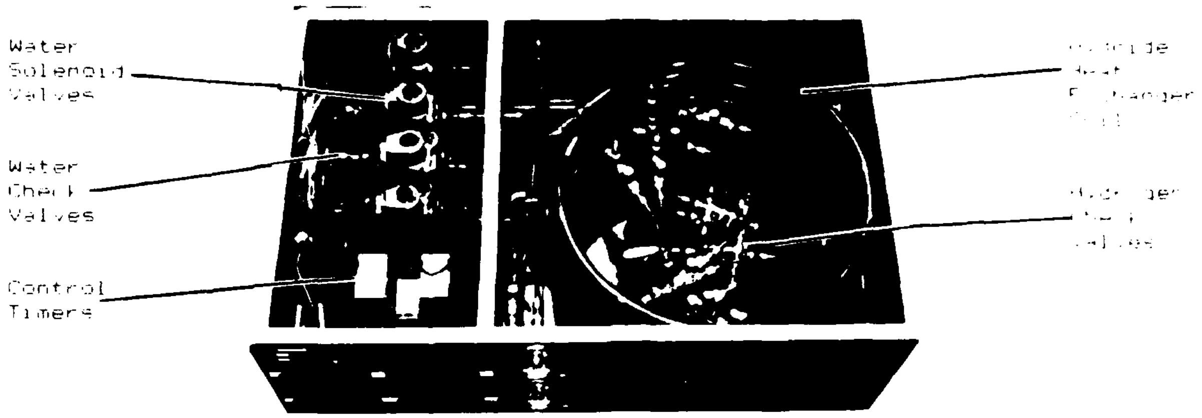

FIGURE 4 : Photograph of Four Stage Hydride-Hydrogen Compressor

Figure 5 is a sectional view showing the inside of the heat exchanger water jacket that houses four (4) hydride filled copper tubes*. Heat exchange occurs at the surface of these tubes with the heat exchange fluid flowing past the tubes which are contained in a larger copper water jacket**.

The design and therefore effectiveness of the heat exchanger tubes is the cornerstone to the successful operation of a rapid cycling hydride device such as this compressor. The external surface area per kilogram of hydride alloy stored is 353 sq. inches/Kg which results in heat transfer times (with the same [illegible] temperature) that are 5 to 10 times faster than the previous hydride containment technique of 1 2 inch Al capsules (ref. 6). It should be noted that all of the heat exchanger tubes used are of standard sizes and are easily obtainable from any plumbing or refrigerator supplier. This has resulted in a hydride heat exchanger that has a CF ratio *** of 3 to 1 (excluding the water jacket). No attempt as of yet has been made to optimize this ratio, but preliminary calculations suggest that CF ratios as low as 1.5 can be easily obtained by using slightly modified tubing.

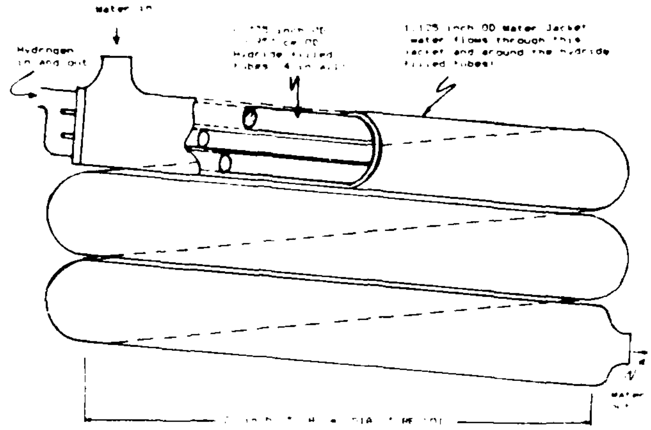

FIGURE 5 : Sectional View of Hydride Heat Exchangers

Hydrogen Flow Control

Hydrogen flow in a hydride compressor is controlled automatically through the use of one way valves (check valves). These valves open whenever the pressure on the input side is greater than the output side and close if the pressure is greater on the output side than on the input. Due to their simple operation, these valves are extremely reliable and maintenance free. It should be pointed out that what actually dictates the pressures generated in the hydride containers are the alloys themselves and the temperatures to which they are subjected.

Water Flow Control

[illegible] of the hot and cold water flow into the hydride heat exchangers [illegible] ... [illegible] figure 3 [illegible]

---

* Hydride tube dimensions are:
Outer Diameter = 0.375 inches (0.9525 cm)
Wall Thickness = 0.032 inches (0.0813 cm)

** Water Jacket dimensions are:
Outer Diameter = 1.125 inches (2.858 [illegible])
Wall Thickness = [illegible] inches ([illegible].127 cm)

*** The CF ratio is defined as:
CF ratio = ((mass of hydride x specific heat of hydride) + (mass of hardware x specific heat of hardware)) / (mass of hydride x specific heat of hydride).

valve provides a positive closing or opening of the fluid flow path. Also note in figure 2 the use of a one-way water check valve with each solenoid water valve to ensure that reverse water flow from either the cold to the hot or the reverse does not occur. This seemingly complex configuration has proven to be far more reliable and effective than 3 or 4 way type solenoid valves. The expected life of these valves is on the order of 5 million cycles.

Control Timers

The actual control of the water solenoid valves and hence of the compressor itself is obtained by the use of highly reliable electro-mechanical timers. Depending on the current being controlled, these timers can have an expected life of 5 million cycles. This corresponds to a compressor life of about 20 years assuming near continuous operation if the compressor is set at a 2 min cycle time.

An operational schematic of the timers and the water solenoid valves that they control is shown in figure 6. Here, three (3) control timers are actually used, that being a repeater, an "on" delay and "off" delay. The following is a brief description of each timer's function:

Repeat Timer: This timer controls the overall cycle time of the compressor which is directly related to the actual throughput of the device. Typical cycle times are on the order of one to two minutes, but can be varied from 30 sec. up to 10 min.

"On" Delay Timer: This timer controls the actual delay in the energizing of water solenoids 5 & 8 (See figure 3) for the conservation of thermal energy. The time delay that is used is dependent upon the water flow rates being used with the compressor.

"Off" Delay Timer: This timer is much like the "on" delay timer and controls the delay time in the energizing of solenoids 6 & 7 (see figure 3).

All of the timers are of a plug-in type and therefore are easily replaceable should one become faulty or a different timing range be desired.

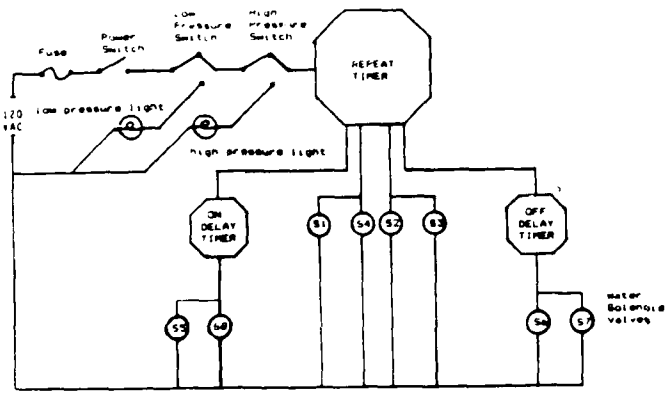

FIGURE 6 : Electrical Operational Schematic of Hydride-Hydrogen Compressor

Table 1: 4 Stage Hydride Compressor

Physical Dimensions:

Size: 100 cm W x 61 cm L x 31 cm H
(39 in W x 24 in L x 12 in H
Weight: 64 Kg (140 Lbms)

Electrical Requirements:

50 watts, 120 volts, 60 HzAC This power is used to operate the control timers and the solenoid water valves).

Hydrogen Requirements:

Designed Inlet Pressure: 81 psia
Designed Outlet Pressure: 800 psia
Average Hydrogen Throughput: 1 SCFM (28.3 SLPM) at the above conditions and a two minute cycle time.

Water Requirements:

Hot Water - 2 gal/min (7.57 L/Min) at 75°C
Cold Water - 2 gal/min (7.57 L/Min) at 20°C

SENSIBLE HEAT RECOVERY

The new hydride heat exchanger configuration along with the use of the delay timers possess some unique advantages over previous hydride heat transfer systems. The tubular nature of the device enables water that is present in the tube at the change of modes to be totally displaced by the incoming water flow and therefore not affect the overall heat capacity of the system. This water is returned to the appropriate fluid system (i.e. hot or cold return). In addition, fluid plug flow and the delay timers permit a sizeable degree of sensible heat recovery. The heat that is contained in the heat exchanger hardware is used to heat up the incoming cold water and return it to the hot water system. The actual switching of the delay solenoids are set to occur when the temperature of the heat transfer fluid leaving the "cold out" port and the temperature of the fluid leaving the "hot out" port are the same (see figure 3).

ALLOY SELECTION AND OPERATIONAL CONSIDERATIONS

Since the metal hydride compressor derives its energy from low-grade heat sources, (such as hot water at only 75°C), then the correct selection of the alloys used is critical to successful and optimal compressor operation. This selection procedure is complicated by the fact that many variables must be considered.

Some of the factors (variables) that can seriously affect a hydride compressor performance are:

Cycle Times...how fast is the hydrogen transfer expected to take?

Heat Transfer...how fast is the hydride's heat of formation energy being dissipated to absorbed by the heat exchanger fluid (ref. e.).

APPENDIX 3.2

Dynamic Hysteresis...the difference in a hydride alloy's plateau pressure in the absorption mode compared to the desorption mode at the same temperature.

Alloy Plateau Slope...not even classic hydride alloys such as $LaNi_5$ have a truly flat plateau.

Alloy Reaction Kinetics...how fast does the actual chemical reaction between hydrogen and the alloy take? This is important since even fast kinetic alloys such as a $LaNi_{4.7}Al_{0.3}$ show diminishing kinetic response at lower temperatures (ref. 8,9,10).

Hydrogen Pressure Drops...it should be remembered that even small hydrogen pressure drops will create a corresponding temperature loss in the hydride alloy itself (ref. 6). This variable can be especially aggravating in lower pressure alloys.

Disproportionation Resistance...or how long will the alloy last (ref. 10).

Heating and Cooling Water Temperatures... these temperatures actually set the limit on the maximum amount of energy available for compression.

CP Ratio...how much of the hydride heat exchanger's mass is due to non-hydrideable material such as the copper tubing and the water jacket?

Alloy Plateau Capacity...how much hydrogen can the alloy hold? This is important since the hydride alloy mass is parasitic and only increases the heat exchanger's CP ratio, and thus decreases the system's overall efficiency.

Hot and Cold Water Flow Rates...in the light of all of the above, is there enough hot and cold water to provide the energy needed for hydride compression.

It is beyond the scope of this paper to adequately address each of the variables listed above, but their correct assessment is critical to the successful performance of any hydride containing device. In other words..."the chain is only as strong as its weakest link". The alloys that were selected for the four stage compressor whose test results appear in the following section are listed in Table 2.

Table 2: Metal Hydride Alloy Data

Stage #	Alloy Used	Mass of alloy per bed (A,B)
1	$LaNi_{4.9}Al_{0.1}$	531 grams, 499 grams
2	$LaNi_5$	569 grams, 606 grams
3	$MNi_{4.5}Al_{0.5}$	664 grams, 628 grams
4	$MNi_{4.15}Fe_{0.85}$	620 grams, 603 grams

For this prototype compressor special consideration was given to alloy kinetics and heat transfer since it was desired to make a compressor that would have fast cycling rates and therefore a low initial cost. Pressure drops in the compressor were also considered important due to their direct influence on temperature drops (see Appendix). Therefore, care was taken to minimize these pressure drops by using sensitive hydrogen check valves that would open at pressure differentials as small as 1/2 psia. The total pressure drop at any time during the transfer of hydrogen from one stage to another is estimated at no more than 2 psi.

TESTING

The operational and testing setup for the compressor is shown in figure 7. In this case the hot water used by the hydride compressor is provided by an electric water heater. A circulating pump is included to circulate the hot water through the compressor and back to the heater, thus making the hot water supply side a "closed" system. Cooling water is also supplied to the compressor and thus provides the necessary heat sink needed to complete the thermodynamic compression cycle. This cold water is shown in figure 1 as flowing into a drain after it leaves the compressor, but it could also be passed through an external chiller system and thus be recycled making it too a "closed" system.

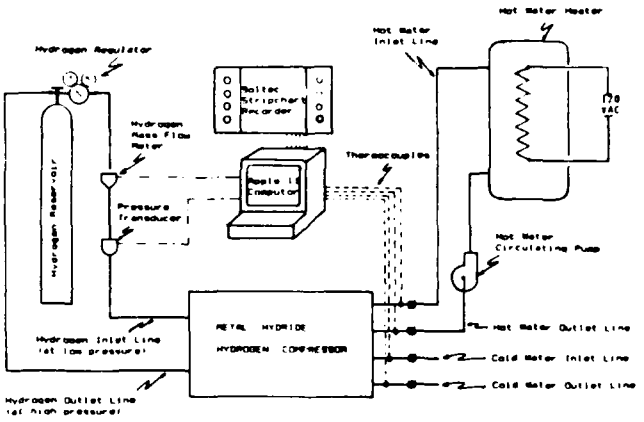

FIGURE 7 : Operational and Test Setup of the Hydride-Hydrogen Compressor

Ultra high purity hydrogen (99.999%) regulated down from 500 psia to about 50 psia flows into the compressor from the hydrogen accumulator (H_2"T" Tank). The high pressure hydrogen leaves the compressor and enters the accumulator at the required 500 psia discharge pressure. Thus the compressor performs a 10 to 1 compression ratio on the hydrogen gas without the need of a back pressure regulator.

Variables recorded during the testing program were as follows:

- Cold water input and output temperatures
- Hot water input and output temperatures
- Cold and hot water flow rates
- Hydrogen input and output pressures
- Hydrogen input flow rates

The data was recorded and stored by an Apple II computer and a Soltec 6 channel strip chart recorder. Due to the difficulty in ascertaining the influence that each variable contritutes to the

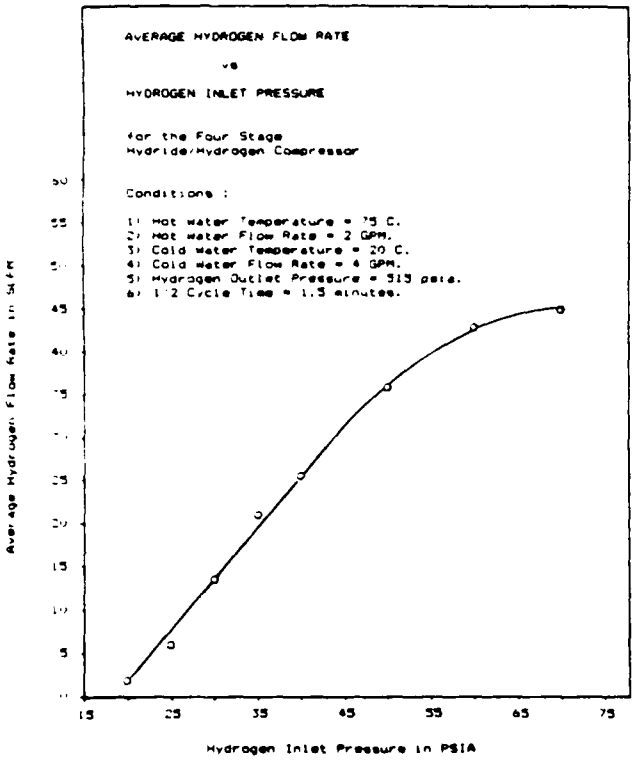

FIGURE 8 : Hydrogen Throughput vs Hydrogen Inlet Pressure for the Four Stage Hydride-Hydrogen Compressor

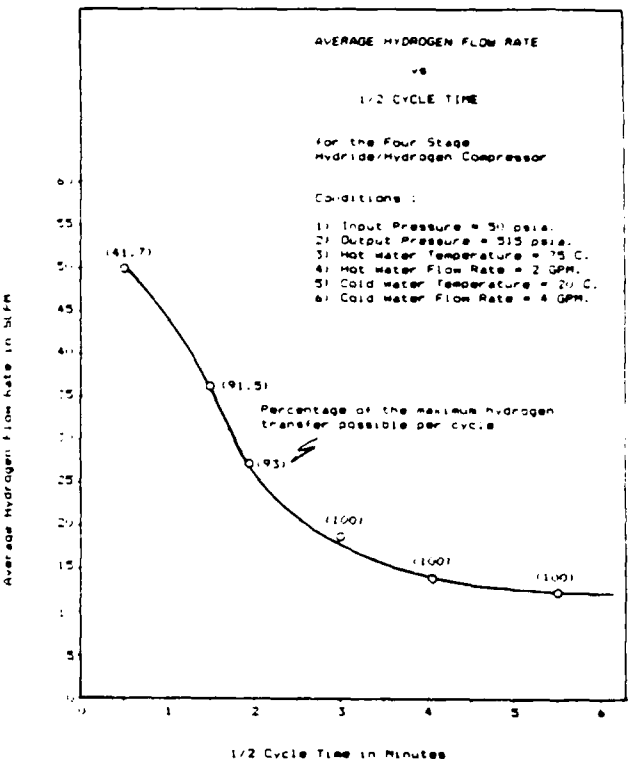

FIGURE 9 : Hydrogen Throughput vs ½ Cycle Time for the Four Stage Hydride-Hydrogen Compressor

overall compressor operation, it was decided to vary only two of the compressor variables, those being the cycle times and the input pressure, all other variables were monitored but kept constant.

Figure 8 is a plot of hydrogen throughput vs input pressure using a "1/2 cycle time" of 1.5 min.* This curve mainly reflects heat transfer effects on the first hydride stage since an increasing input pressure creates a higher hydride bed temperature and hence a larger Δ temperature for the first hydride alloy while in the absorption mode (ref. 6). For the conditions shown, the stages reach essentially full hydrogen capacity in 1.5 min for input pressures exceeding about 50 psia.

Figure 9 is a plot of hydrogen throughput vs the 1/2 cycle time for the compressor. It is interesting to note that even though full hydrogen transfer was not occurring at cycle times less than 1.5 min, the average hydrogen throughput was still increasing even at a 1/2 cycle time of 30 sec, though less than 1/2 of the hydrogen capacity of the alloy was being used. Throughput data at 1/2 cycle times less than 30 sec was not collected since this was the fastest setting possible for the repeat timer (see section on Component Description). However, from figure 9 it is clear that 1/2 cycle time rates less than 1.5 min there occurs a significant reduction in the amount of hydrogen that could be transferred. This indicates that heat transfer effects have begun to reduce the compressor's overall efficiency. This was confirmed. The first law efficiency at a 1/2 cycle time of 4.5 min was determined to be 5.5%, but at a 1/2 cycle time of 1 min it was found to be only 3%. It is believed that if care is taken to optimize hardware mass, (i.e.: Lower CP ratio), then first law efficiencies will approach 10%.

Long Term Testing

Since the initial testing, the compressor has been operated continuously over the past 8 months. The primary reason for this long term testing was to determine possible design flaws as well as alloy susceptibility to disproportionation (ref. 9). To date, the compressor has logged over 35,000 cycles with no detectable damage to either the hydride heat exchangers or the other components. Recent hydride capacity tests have suggested a loss of capacity on the order of 10-15%. More testing is being done to determine if this loss of capacity is due to disproportionation or possible oxygen poisoning from air leaks in the compressor.

*Due to the batch type process of a hydride compressor, the time it takes to complete one mode of operation (either absorption or desorption) is 1/2 of a full cycle, hence the term "1/2 cycle time".

Acknowledgment

The author wishes to acknowledge the support and discussions provided by M. Rosso, W. Storms and L.E. Terry. Special credit is also due to L.E. Terry for his help in the testing and evaluation of the compressor.

References

1. D.M. Gruen et al., Proc. 11th Intersociety Energy Conversion Engineering Conf., September 1976, Vol. 1, American Institute of Chemical Engineers, New York, 1976, p.681.

2. L.E. Terry, personal communication.

3. A.A. Heckes, T.E. Hinkebein and G.J.M. Northrup, Proc. 14th Intersociety Energy Conversion Engineering Conf., July 1979, Vol. 1, p. 743.

4. F.E. Lynch, R.A. Nye and P.P. Turillon, Phase 1 Final Rep. BNL 51369, January 1981 (Brookhaven National Laboratories, Upton, N.Y.).

5. G.D. Sandrock and E.L. Huston, "How Metals Store Hydrogen", CHEMTECH, 1981, 11, pp. 754-762.

6. P.M. Golben and E.L. Huston, "A Technique for Analyzing Reversible Metal Hydride System Performance", Journal of the Less-Common Metals, 89 (1983) pp. 333-340.

7. P.D. Goodell, G.D. Sandrock and E.L. Huston, "Kinetic and Dynamic Aspects of Rechargeable Metal Hydrides", Journal of the Less-Common Metals, 78 (1980) pp. 135-142.

8. P.S. Rudman, 'Hydriding and Dehydriding Kinetics", Journal of the Less-Common Metals, [illegible] (1983) pp.93-110.

9. P.D. Goodell and P.S. Rudman, "Hydriding and Dehydriding Rates of the $LaNi_5$-H System", Journal of the Less-Common Metal, 89 (1983) pp.117-125.

10. P.D. Goodell, personal communication.

APPENDIX

METAL HYDRIDE REVIEW

The hydride compressor operates by successively absorbing and desorbing hydrogen gas into and out of several metal hydride alloys. This process is a reversible reaction of a solid metal (Me) with gaseous hydrogen (H_2) to form a solid metal hydride MeH_x:

$$\frac{2}{x}\,Me + H_2 \underset{\text{desorption}}{\overset{\text{absorption}}{\rightleftharpoons}} \frac{2}{x}\,MeH_x + \text{heat of reaction}$$

This reaction is totally reversible which means that the same amount of heat that is generated by the reaction while in the absorption mode must be supplied to the reaction while in the desorption mode. Ideally the above reaction could be "cycled" indefinitely.

The amount of hydrogen a metal hydride can hold can vary widely for different types of hydrides. The hydride alloys used in this compressor are of the rare-earth penta nickel type*, which store about 1% of their weight in hydrogen. Volumetrically, this represents about 1000 cubic centimeters of stored hydrogen gas for every 1 cubic centimeter of hydride alloy. This type of alloy was chosen because of its ability to produce high hydrogen pressures at room temperatures.

The chemical equation that dictates exactly how much heat is generated by the metal hydride is called the Van't Hoff equation, and is shown below in one of its forms used to predict the hydrogen gas pressure (P) needed to generate a temperature (T) in the hydride alloy. The Van't Hoff equation is

$$P = \left\{ EXP\left[\frac{\Delta H}{1.987}\left(\frac{1}{T} - \frac{1}{T_{std}} \right) \right] \right\} \times P_{std} \qquad \text{Equation 1}$$

Where:

T = Temperature of the hydride, K.
P = Pressure of hydrogen gas in the hydride at hydride temperature T, psia.
T_{std} = Specified standard temperature, K.
P_{std} = Pressure of hydrogen gas in the hydride at hydride temperature T_{std}, psia.
ΔH = Heat of formation for the particular hydride used in calories per mole of hydrogen gas (H_2). If equation 1 is used then ΔH must be negative since it represents the amount of heat given off when one mole of hydrogen gas reacts with the metal hydride.

The Van't Hoff equation can therefore be used to predict hydrogen pressure and/or hydride temperatures (for both absorption and desorption) for the specific hydride alloy used if the other components of the equation have been determined. Values for T_{std} and P_{std} are often determined experimentally by taking a small sample of the hydride alloy and carefully measuring the hydrogen pressure as small amounts of hydrogen gas are exposed to the hydride sample (and thus are absorbed by the alloy) while it is kept at a constant temperature. These tests are called pressure-composition-temperature isotherms (PCT curves), and are vital in determining not only the pressure/temperature relationship for the alloy but also in determining the hydrogen holding capacity of the alloy. An example of one such PCT curve is shown in figure 10. Please note that when using a Van't Hoff equation such as equation 1, values for P and P_{std} are usually taken at a H/M ratio of 0.5 .

The H/M ratio is defined as:

$$\frac{H}{M} = \frac{\text{Number of Hydrogen atoms}}{\text{Number of Metal atoms}}$$

*Rare-earth elements refer to the Lathanide series of elements whose major constituents are cerium (Ce), lanthanum (La), praseodymium (Pr) and neodymium (Nd).

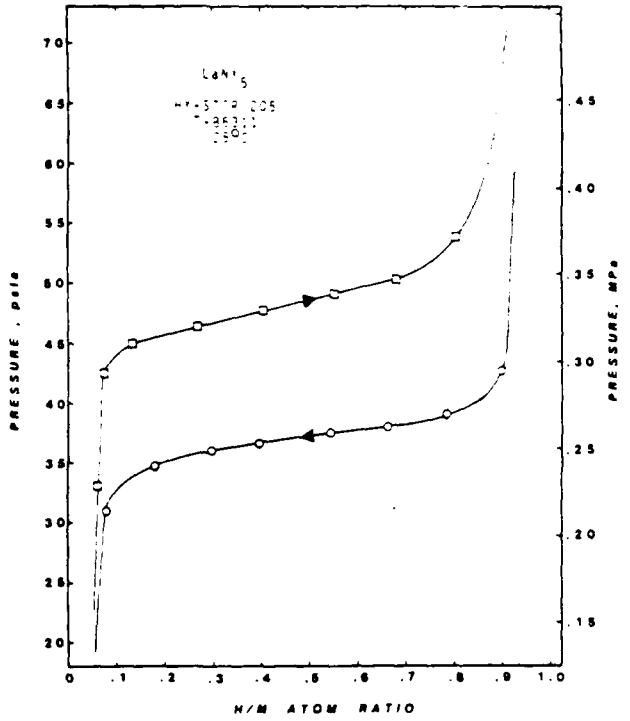

FIGURE 10 : Absorption and Desorption Pressure-Composition-Temperature Isotherms for $LaNi_5$

Since equation 1 is exponential in nature, one can see that even small increases in the temperature will result in very large pressure increases. This is illustrated in the following example:

Example: What is the pressure rise when a $LaNi_5$ hydride sample is heated from 25°C up to 75°C?. Assume that the $LaNi_5$ is in a closed container with negligible void volume.

Answer: From the PCT curves for $LaNi_5$ at 25°C, we find that the hydrogen desorption pressure is 37.5 psia. It is also known that the heat of formation (ΔH) for $LaNi_5$ is about -7400 cal per gram mole H_2. Therefore, by using equation 1 we can determine the hydrogen desorption pressure at 75°C to be 225 psia.

$$P = \left\{ EXP \left[\frac{-7400}{1.987} \left(\frac{1}{348.2} - \frac{1}{298.2} \right) \right] \right\} \times 37.5 = 225 \text{ psia}$$

Thus we see that even though the temperature changed only by 16.8%, the pressure changed by 500%.

Unfortunately, due to the non ideal conditions that exist in the operation of a hydride compressor (see section: Alloy Selection and Operational Considerations), not all of this large pressure change can presently be realized. The actual pressure change realized in the operational hydride compressor is more on the order of 100%-150% for the same conditions given in the example. This explains the need for multiple hydride stages to effect the large compression ratios needed to provide useful work. Each additional stage is a hydride alloy that has a higher plateau pressure at room temperature. Thus in actual operation, this higher pressure alloy is designed to absorb the hydrogen (at the cold water temperature) that is being desorbed by the preceding stage (at the hot water temperature).

APPENDIX 3.2

APPENDIX 3.3

METAL HYDRIDE AIR CONDITIONER OPERATING PROCEDURE

METAL HYDRIDE AIR CONDITIONER OPERATING PROCEDURE

SET-UP:

The following procedure assumes that the metal hydride air conditioner is set-up according to the schematic shown in figure 3.2A. Please refer to figures 3.2.7A, 3.2.7B and 3.35 for the location of the control components on the front panel of the air conditioner.

OPERATING PROCEDURE

1. Set the silicon fluids heat source temperature controller to 220°C, but do not start up the heater (keep the manual supply valve closed).
2. Set the digital repeat time to the desired 1/2 cycle time (this is normally set at around 4 minutes).
3. Set the hydrogen valve delay timer to the desired delay timer (1 sec. is fine).
4. Turn on the air conditioner (power switch to on) and ensure that silicone fluid is flowing through all of the heat exchangers (via the visual in line flow meters).
5. Double check the settings of the "hot" and "cold" sensible heat temperature controllers. These should be set at about 120°C for the "hot" and about 29°C (4°C above ambient for the "cold").
6. The unit is now ready to operate, light the propane pilot light and open the propane supply valve to the silicone fluid heater. This will ignite the propane gas and heating of the silicone fluid will begin. Please note that a propane pilot flame should always be maintained during the units operation.
7. Allow the air conditioner to run while this silicone fluid heats up. Cooling of the shelter air will begin when the temperature of the silicone fluid gets up to around 180°C.

8. After operating temperatures have been reached, changes in the operation variables such as the 1/2 cycle timer and the temperature control settings can easily be made while the unit is operating.

SHUT DOWN

After all of the desired data is acquired, unit shut down is very simple.

1. Close the propane supply valve to the silicone heater. Heating of the silicone will immediately stop.
2. Turn off the air conditioners power switch.

SUBSEQUENT START UPS

Once the temperature controllers have been set to the desired settings they will not charge even after the unit is shut off, therefore, subsequent start ups are also very easy.

1. Turn on the air conditioners power switch to on.
2. Light the propane pilot flame and open the propane supply valve. Heating of the silicone fluid will now begin and metal hydride produced cooling will start when the temperature of this fluid reacnes about 180°C, full cooling power is achieved at about 220°C.

CHAPTER 4

ACCELERATED HYDRIDE LIFE TESTING

TABLE OF CONTENTS

The continuous operation of a metal hydride air conditioning system results in the accumulation of many thousands of charge-discharge cycles on each of the hydride coils. These coils must operate throughout their design life with little change in either the physical or chemical properties of the contained hydride. Since several decay mechanisms have been identified in the hydride literature (1,2), this evaluation program was undertaken to evaluate the cyclic stability of the hydrides selected for the prototype.

4.1 INTRODUCTION

Reversible metal hydrides are known to be susceptible to two degradation mechanisms - alloy poisoning and disproportionation. Alloy poisoning refers to surface or bulk reactions with O_2, H_2O or CO which consume the alloy or block its surface and reduce hydriding capacity. For closed, leak-free systems such as the hydride heat pump, this mechanism is inoperable. Disproportionation, on the other hand, refers to the gradual formation of thermodynamically more stable hydrides within the reactor beds. For $LaNi_5$, this reaction can be written as:

$$LaNi_5H_6 \rightleftharpoons LaH_2 + 5Ni + 2H_2 \quad . \qquad \text{EQ. (4.1)}$$

The compound LaH_2 is the thermodynamic end point for a series of hydrides based on known stoichiometric compounds (La_2Ni_7, $LaNi_3$, $LaNi_2$, LaNi, La_2Ni and La_5Ni) and possibly non-stoichiometric compounds as well with increasing La content. The disproportionation reaction can be written in more general terms as:

$$LaNi_5H_6 \rightleftharpoons LaNi_xH_n + (5-x)Ni + (3-n/2)H_2 \quad . \qquad \text{EQ.(4.2)}$$

The $LaNi_xH_n$ hydrides, once formed, have a lower equilibrium hydrogen pressure (i.e., they are more stable) than $LaNi_5H_6$. The hydrides are not reversible under the same pressure-temperature conditions as $LaNi_5H_6$. Their presence has two pronounced effects on hydride bed performance. First, the reversible hydrogen capacity is decreased resulting, for heat pumps, in less thermal

output per cycle. Secondly, the plateau on the hydrogen pressure-composition isotherm becomes more sloping. This also results in a loss of thermal output per cycle.

Disproportionation requires only short range diffusion of the metallic species. Consequently, it can occur at low to moderate temperatures with the rate accelerating on increasing temperature. The rate varies from compound to compound and is also dependent on the pressure-temperature-composition path of the hydride-dehydride cycle (3). For example, Sandrock etal (3) obtained a 50% loss of capacity by exposing $LaNi_5$ at 180°C and 136 atma for 260 hrs. On the other hand, Dantzer (4) reported no capacity loss for $LaNi_5$ temperature cycled between 25 and 80°C in a heat pump for approximately 600 hrs.

Alloy disproportionation has traditionally been quantified by measuring the hydrogen pressure composition isotherm at a given temperature before and after a prescribed static or cyclic exposure. Accelerated tests are possible by raising the exposure temperature (but consequently the hydrogen pressure).

4.2 EXPERIMENTAL PROCEDURE

4.2.1 Pressure-Composition-Isotherms

The equilibrium hydrogen desorption isotherms presented in this report were determined in a high pressure (68 atma capacity) Sieverts apparatus of carefully calibrated volumes. Samples for hydriding were crushed in air to -12 +35 mesh (US Standard Sieve) size. The 8 gram sample was placed in a 0.75" OD tubular stainless steel reactor. Ultra-high purity hydrogen (UHP, >99.999%) was used and the reactor temperature is controlled to within 0.1°C with a circulating water bath or an electric furnace. Gas pressures are measured by either a Dynisco transducer (1000 psi, 5 volt) or Heise gauge (0-1000mm).

The reactor is capable of operating pressures and temperatures of 3500 psi and 350°C respectively. A schematic drawing is shown in Fig. 4-1. The reactor contains an internal thermocouple well to monitor the specimen temperature.

The desorption isotherm is obtained by removing small aliquots of hydrogen gas and waiting for the pressure to stabilize (usually 15 to 20 minutes). A period of 6-8 hours is required to obtain a complete isotherm and assure thermal equilibrium at each point. The raw data is computer reduced by Ergenics' program HPTC to obtain hydrogen gas pressure and hydride composition. The computer program automatically compensates for non-ideal gas law behavior by applying a reduced version of the NBS equation of state for hydrogen. Hydride composition is expressed as the ratio of hydrogen atoms to metal atoms in the sample, H/M. A second Ergenics' program, DESPLOT, produces a graphical representation of the data as lnP vs. H/M. Absorption isotherms are obtained in a similar manner by adding small aliquots of hydrogen gas to the specimen reactor.

4.2.2 Test Alloy

The hot side hydride of the metal hydride air conditioner has the higher service temperature and hence is more prone to disproportionation. The alloy selected for the hot side was heat 1317-V-2. This alloy was vacuum induction melted to the nominal composition $LaNi_{4.5}Al_{0.5}$. A 22.7 kg (50 lb) heat was prepared. The ingots were solution annealed for 16 hours at 1115°C under an argon atmosphere prior to crushing. This anneal reduces chemical heterogeneities resulting from ingot solidification.

Two hydrogen desorption isotherms were obtained on heat 1317-V-2. Test temperatures were 85°C and 175°C. These temperatures were selected to give plateau pressures of approximately 1 and 10 atma respectively. Two pressure values ab mid-plateau are required to evaluate the constants in the van't Hoff equation. An absorption isotherm was also run at 85°C. These isotherms are shown as Fig. 4-2. At H/M=0.40 the desorption plateau pressure increases from 1.70 atma at 85°C to 22.05 atma at 175°C. The pressure-temperature relationship (van't Hoff) for this alloy is :

$$\ln P = (-4571.2/T) + 13.294 \qquad \text{EQ. (4.3)}$$

where P is the plateau pressure in absolute atmospheres and T is the specimen temperature in degrees Kelvin. The absorption plateau at H/M=0.40 and 85°C is 1.84 atma and pressure hysteresis (1.84/1.70=1.08) is very low for this alloy. The van't Hoff curve constructed from EQ. 4.3 and the hysteresis ratio is shown in Fig. 4.3.

4.2.3 Exposure Conditions

The projected operating temperature for the hot side hydride is approximately 200°C. This corresponds to a hydrogen pressure during desorption of 34 atma (500 psia), see Fig. 4.3. Higher exposure temperatures, and consequently higher pressures, are required to accelerate disproportionation. Exposure conditions are ultimately limited by a 3500 psia/350°C restriction on the test reactors.

At 285°C, the hydrogen absorption plateau pressure is 178 atma (2617 psia). An overpressure is required to assure that the alloy remains fully hydrided at the exposure condition. The maximum allowable hydrogen gas pressure, 3500 psia, permits an overpressure ratio of 3500/2617=1.34. This is an acceptable value for an alloy with the flat plateaus shown in Fig. 4.2.

Two exposure conditions were selected; 285°C/3500 psia and 245°C/3500 psia. They are shown on Figure 4.3. Disproportionation should proceed more rapidly at the higher temperature. However, two sets of data should permits more meaningful extrapolation of the results to service conditions.

4.2.4 Test Apparatus

The exposure test apparatus is shown schematically in Fig. 4.1. It consists of an Ergenics standard, 0.75" diameter hydride reactor. The reactor has a thermocouple well in the bottom to monitor specimen temperature. A fiberglass insulated electric heating tape (Briskheat, 96 watt) is the heat source. In service the heating tape is wrapped with additional layers of fiberglass insulation. The specimen temperature is maintained at the desired valve (285 or 245°C) by an Omega (Model CN310-K-C) temperature controller.

The specimen reactor and valve are attached via a VC-O fitting (1/4" tube size) to a tee arrangement containing a 0-10,000 psi ABM pressure gauge, a 5800 psi pressure relief valve (Circle Seal, 5332-B-2PP-5800) and a second valve. The assembly is attached to a mechanical vacuum pump to evacuate the sample or a hydrogen source to charge and/or pressurize the specimen reactor. Three systems were assembled and mounted on a separate bench. A 0.75" thick plexiglass sheet was placed in front of the reactors as a safety shield.

An exposure test consisted of the following steps:

1. Evacuate activated sample to <50u at room temperature with mechanical pump.
2. Charge to 1000 psia with UHP tank hydrogen.
3. Switch hydrogen source to high pressure hydride coil.

4. Heat hydride coil to pressurize system to 3500 psia.
5. Heat specimen to desired test temperature (285 or 245°C).
6. Close access valve to lock up system.
7. Cool hydride coil.
8. Monitor hydrogen pressure and specimen temperature as exposure test progresses.

4.3 EXPOSURE TEST RESULTS

Two 8-gram samples of 1317-V-2 ($LaNi_{4.5}Al_{0.5}$) were placed in specimen reactors, activated at 68 atma and room temperature and cycled (dehydrided/hydrided) three times to stabilize particle size. A base line isotherm was obtained for each sample prior to exposure at elevated temperature and pressure.

4.3.1 Disproportionation at 285°C/3500 psia

Figure 4.4 shows 100°C hydrogen desorption isotherms after three exposures totalling 388 hours. The hydrogen capacity offset for each isotherm was determined by desorbing to <2 torr hydrogen pressure (.0026 atma) at 100°C. The sample was not baked-out in the dehydrided state between exposures. Reversible hydrogen capacity (H/M ratio) decreases with exposure time. If the H/M ratio at 10 atma is taken as the measure, reversible hydrogen capacity decreases from 0.775 to 0.545 (almost 30%) in 388 hours. In addition as disproportionation progresses, the midpoint pressure on the plateau decreases and the plateau slope increases.

4.3.2 Disproportionation at 285°C/1200 psia

Following the 3500 psia exposures discussed above, the exposure pressure was reduced to 1200 psia (81.7 atma). This value is below the plateau pressure for the virgin alloy at 285°C. Nevertheless, a gradual decrease of hydrogen

capacity can be seen in Fig. 4.5 for this exposure condition. Disproportionation continues, possibly, because a portion of the sloping isotherm dips below 1200 psia (81.7 atma) at this temperature.

4.3.3 Reproportionation at 285°C/100 psia

The hydrogen pressure was subsequently reduced to 100 psia, a value well below the plateau pressure, and the exposure continued. Isotherms after 512 and 4616 hrs. are compared with the virgin curve in Figure 4.6. A gradual capacity improvement is noted. However, even after 4616 hours, only 55% of the capacity has been restored.

4.3.4 Reproportionation at 285°C/Vacuum

The sample was returned to the exposure apparatus, heated to 285°C and evacuated with a mechanical vacuum pump for 1 hour. The resulting isotherm is shown in Fig. 4.7. Hydrogen capacity has been restored to H/M = 0.745 which is 96% of the virgin value. The plateau pressure and slope also approach their initial values.

In the foregoing, a single sample of alloy was exposed to a series of hydrogen gas pressures at 285°C. The accumulated time during the exposure was 5433 hours. Hydrogen capacity fell from H/M = 0.775 to a low of 0.475. At the end, a majority of this capacity loss was restored by simply pumping on the heated (285°C) sample with a mechanical vacuum pump for one hour.

4.3.5 Disproportionation at 245°C/3500 psia

Hydrogen isotherms for the sample aged at 245°C are shown in Fig. 4.8. The effects of disproportionation are qualitatively the same as at the higher

temperature; i.e., capacity and plateau pressure decrease and slope increases. However, the rate of decrease is only about 20% as fast. The H/M ratio at 10 atma after 1203 hours at 245°C is 0.615. A similar decrease at 285°C was obtained in less than 223 hours.

4.3.6 Reproportionation at 245°C/Vacuum

Only vacuum reproportionation treatments were attempted on this specimen. Results are shown in Fig. 4.9. After 24 hours, 72% of the hydrogen capacity loss is recovered. Prolonged pumping (215 hours) produces little additional improvement. Comparison of the vacuum reproportionated curves in Figures 4.7 and 4.9 show that the initial conditions are more nearly recovered at the higher treatment temperature.

4.4 LIFE ESTIMATES

The hydrogen capacity, measured at 10 atma, is shown as a function of exposure time for both exposure temperatures in Fig. 4.10. Hydrogen capacity decreases with increasing exposure time. The rate of decrease is non-linear gradually decreasing with time. These data can be used to estimate service life under operating conditions.

Disproportionation models (1) are based on the short-range diffusion of La and Ni in the presence of H to form more stable hydride clusters. This solid-state diffusion is thermally activated and obeys Ahrenius type kinetics (i.e., atmomic diffusion is proportional to exp (- H/RT), where H is an appropriate activation energy). Ahrenius plots (ln D vs. 1/T, where D is some rate dependent parameter) permit the extrapolation of accelerated test data to service conditions.

The time for the hydrogen capacity to fall to 0.7 (10%) and 0.65 (16%) were

obtained from Fig. 4.10 and used to construct the Ahrenius plot shown as Fig. 4.11. Estimated life for two service temperatures (200 and 220°C) are shown below:

% Loss of Capacity	Service Life (Hours/Days) 220°C	200°C
10	1636/68	5166/215
16	2697/112	8519/355

Based on these results, the hydride air conditioning system will require a reproportionation treatment after periods of 2 to 12 months of service. The exact operating period will depend upon the designed overcapacity (eg 15%) and the design service temperature of the hot coil (eg 210°C). Service life under these operating conditions would be approximately 6 months. Reproportionation can be done on-site as a simple vacuum bake-out. Alternatively, the thermal cycle of the hydride air conditioning system can be altered to include a high temperature, low pressure exposure for the hot coil during each cycle.

4.5 REFERENCES

1. Goodell, P.D., J. Less-Common Metals, 99, (1984) 1.

2. Sandrock, G.D. and Suda, S., Hydrogen in Intermetallic Compounds II, Topics in Appl. Phys. 64, (1989), in press.

3. Sandrock, G.D., etal, Proceedings of the International Symposium on METAL-HYDROGEN SYSTEMS, to be published in Zeitschrift fur Physikalische Chemie Neue Folge.

4. Dantzer, P., J. Less-Common Metals, 131 (1987) 349-363.

FIG 4.1

DISPROPORTIONATION APPARATUS

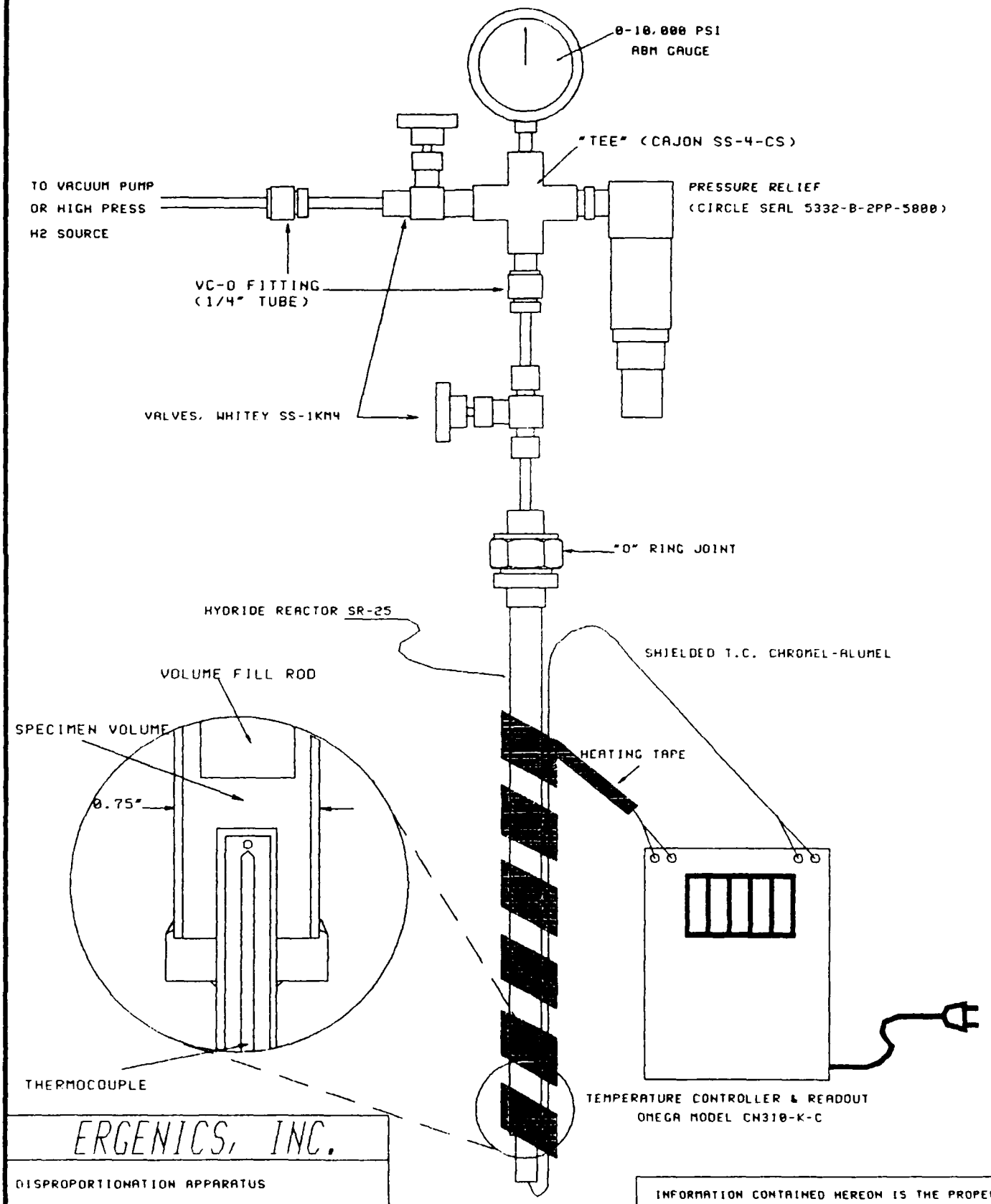

ERGENICS, INC.

DISPROPORTIONATION APPARATUS

DATE: 10/3/88 DRAWN BY: S. SIMON

FIG 4.2 $LANI_{4.5}AL_{.5}$ ISOTHERMS

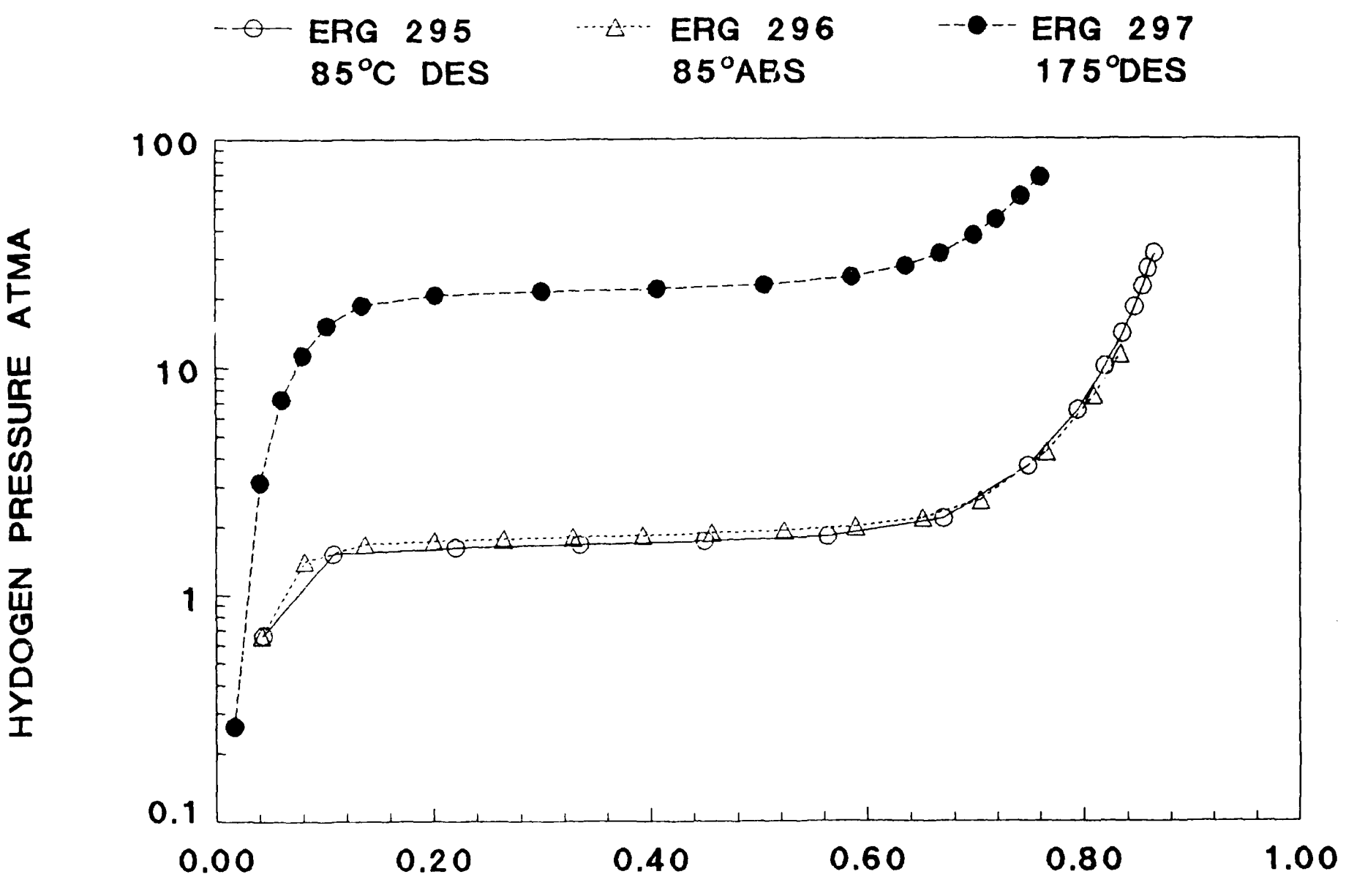

FIG 4.3 VAN'T HOFF RELATION

$LANI_{4.5}AL_{.5}$

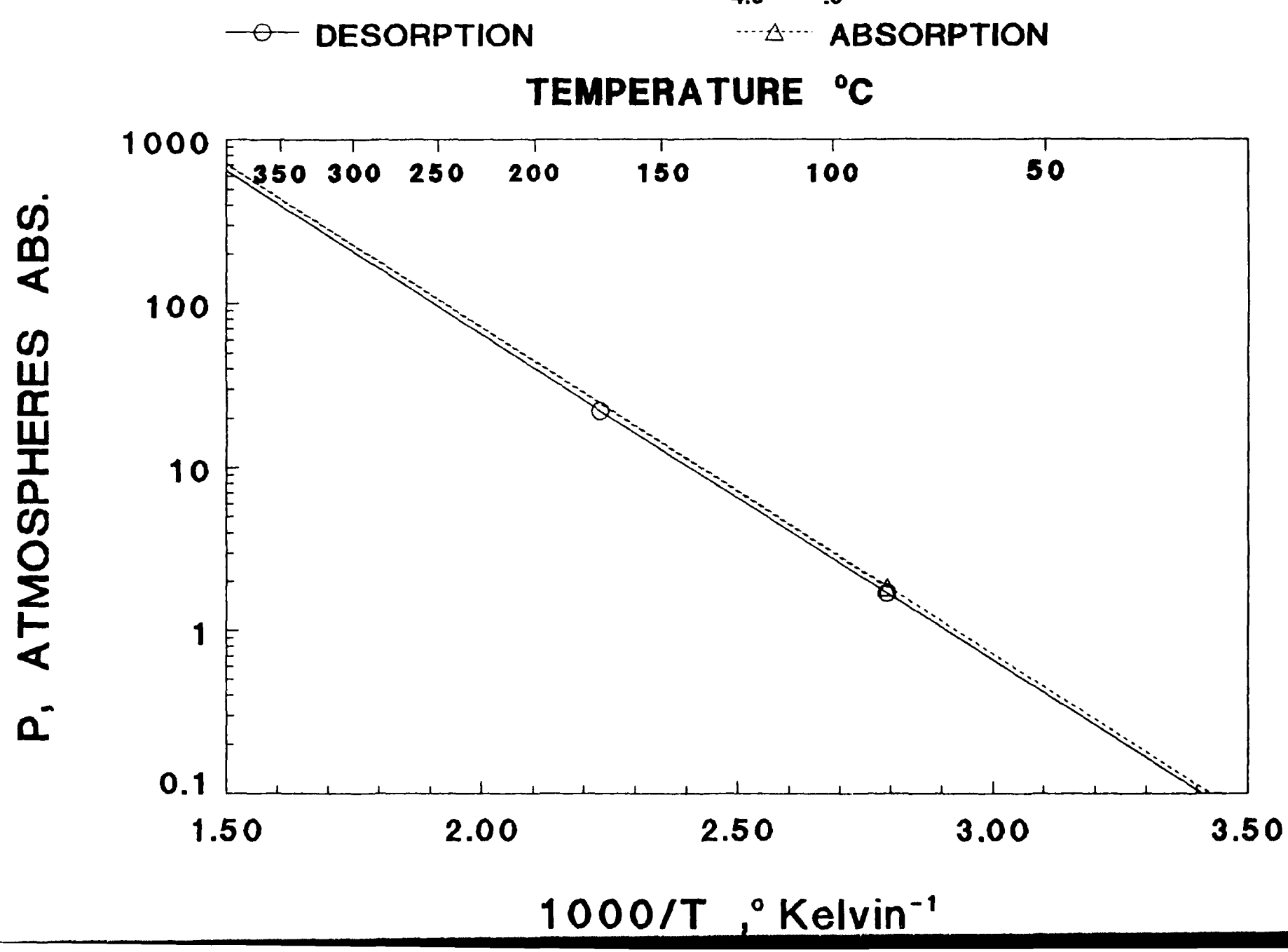

FIG 4.4 DISPROPORTIONATION

$LANI_{4.5}AL_{.5}$ 285°C, 3500 PSIG

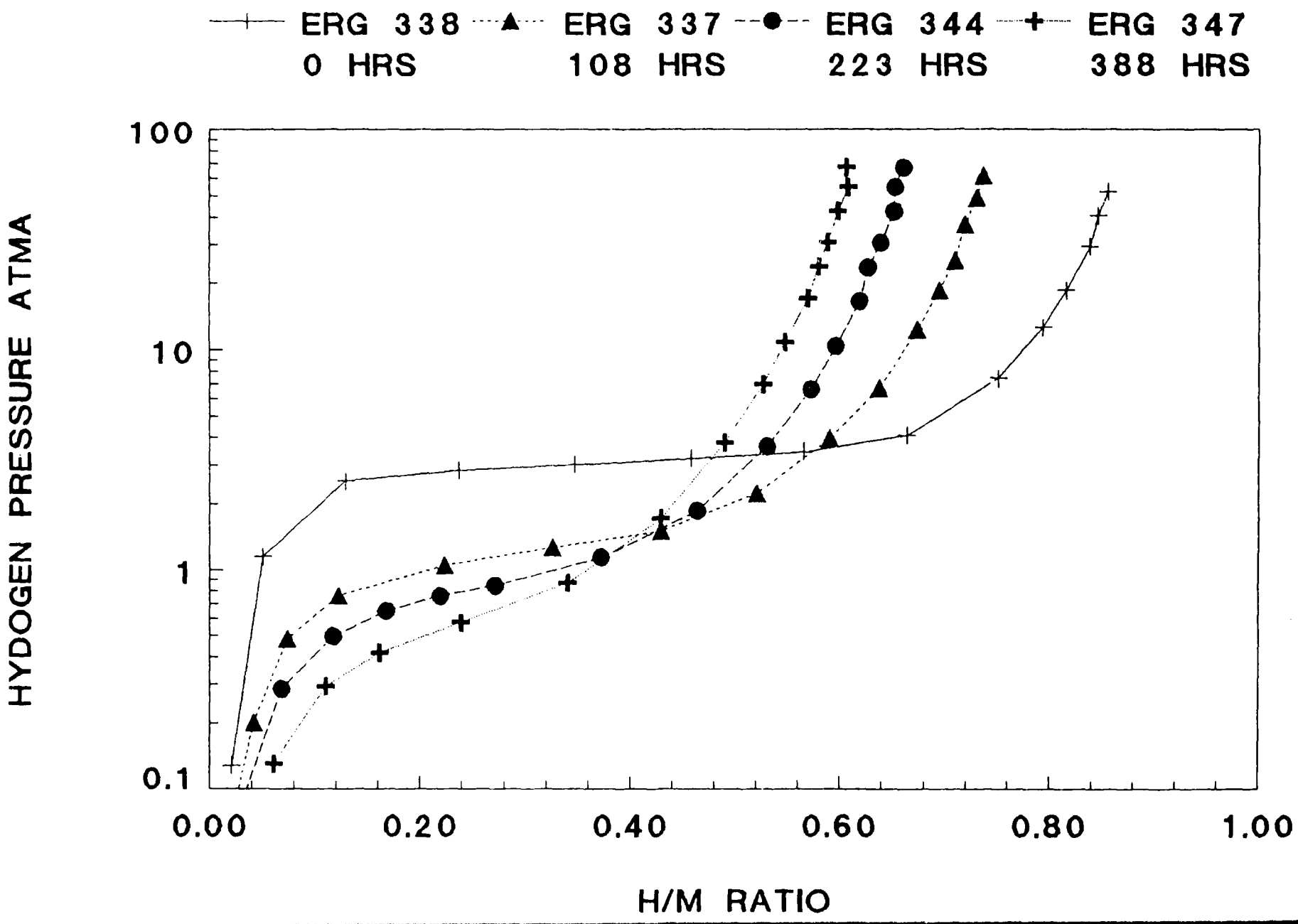

FIG 4.5 DISPROPORTIONATION

$LANI_{4.5}AL_{.5}$ 285°C, 1200 PSIG

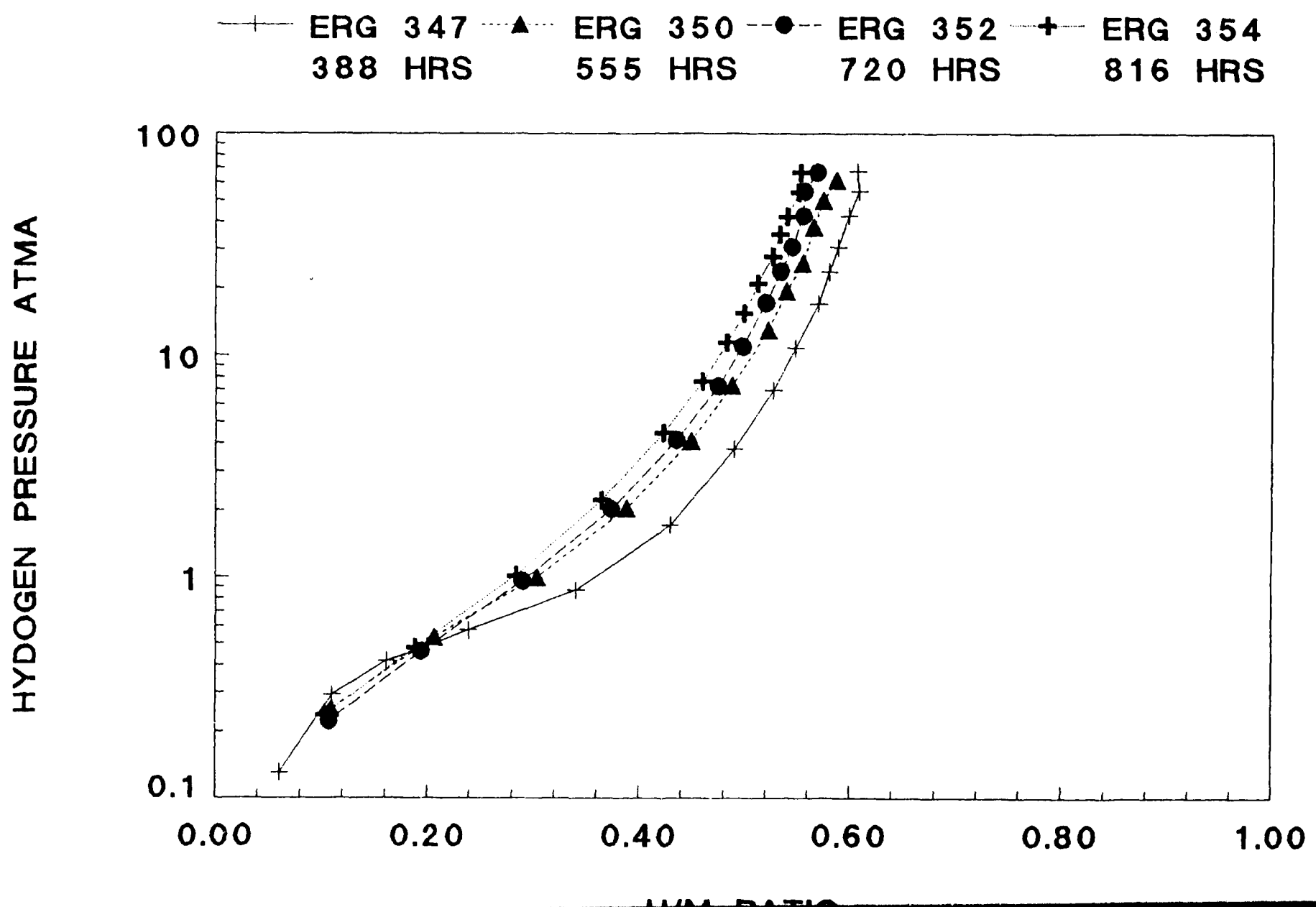

FIG 4.6 REPROPORTIONATION

$LANI_{4.5}AL_{.5}$ 285°C, 100 PSIG

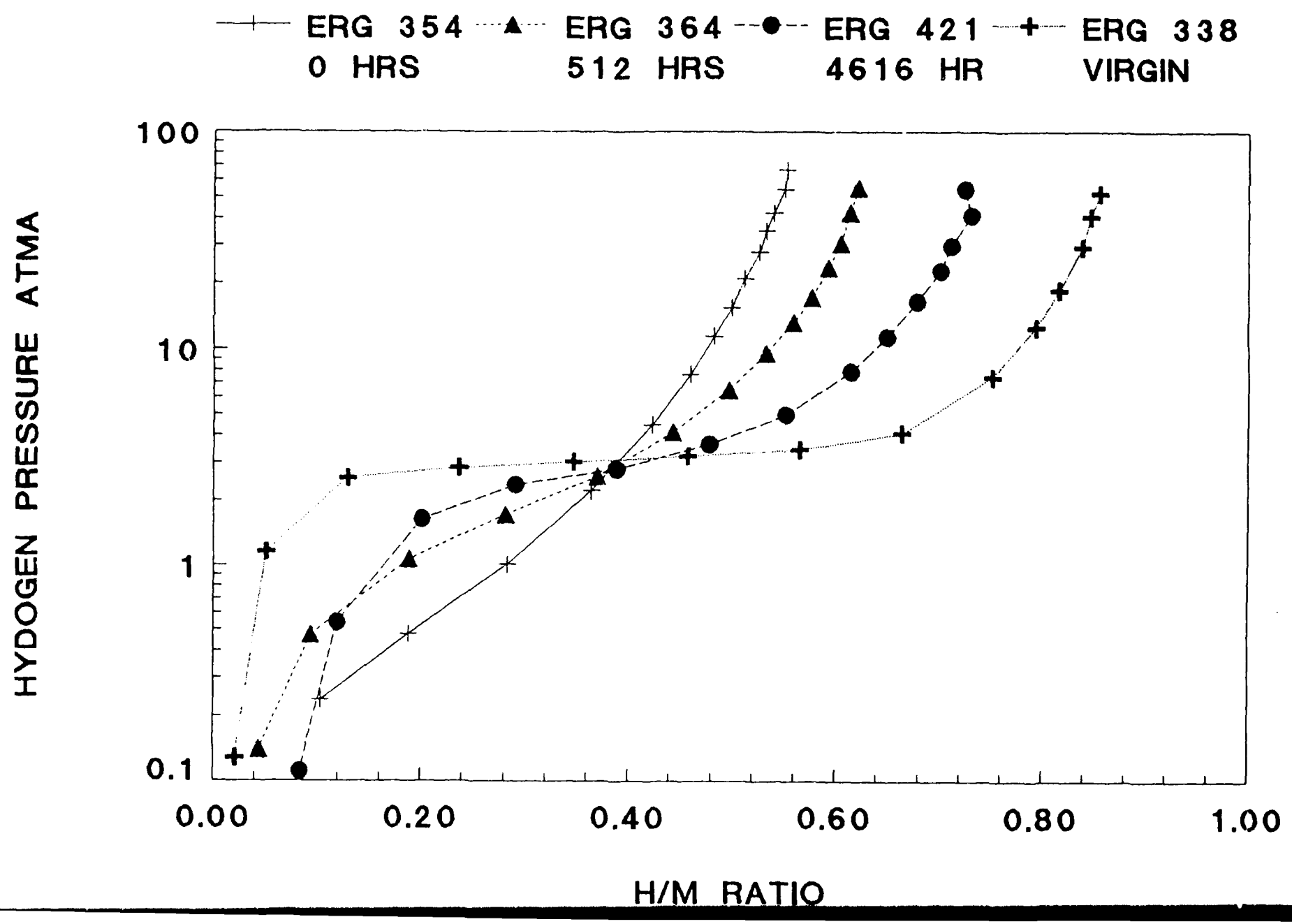

FIG 4.7 REPROPORTIONATION

$LANI_{4.5}AL_{.5}$, 285°C, VACUUM

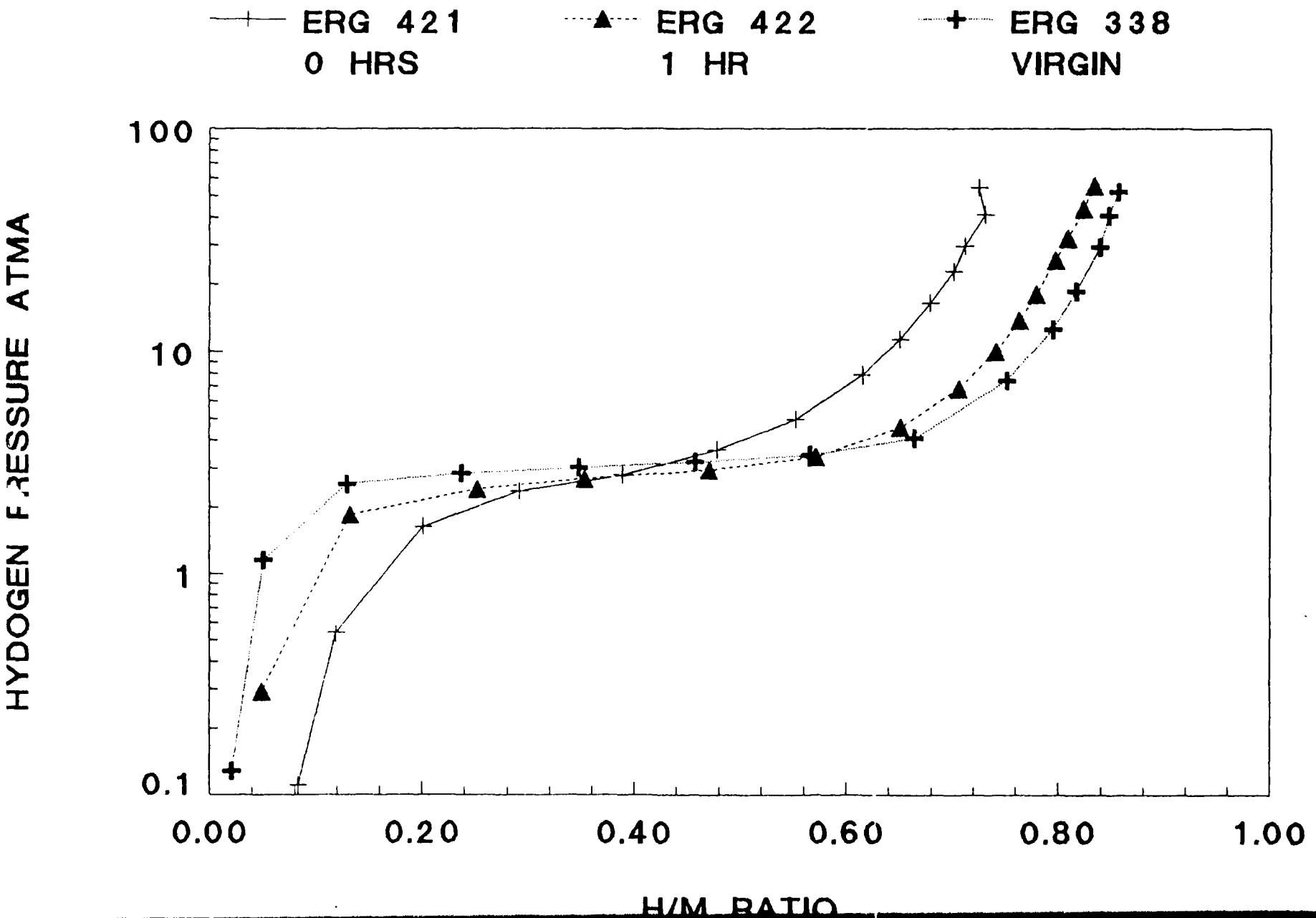

FIG 4.8 DISPROPORTIONATION

$LANI_{4.5}AL_{.5}$ 245°C, 3500 PSIG

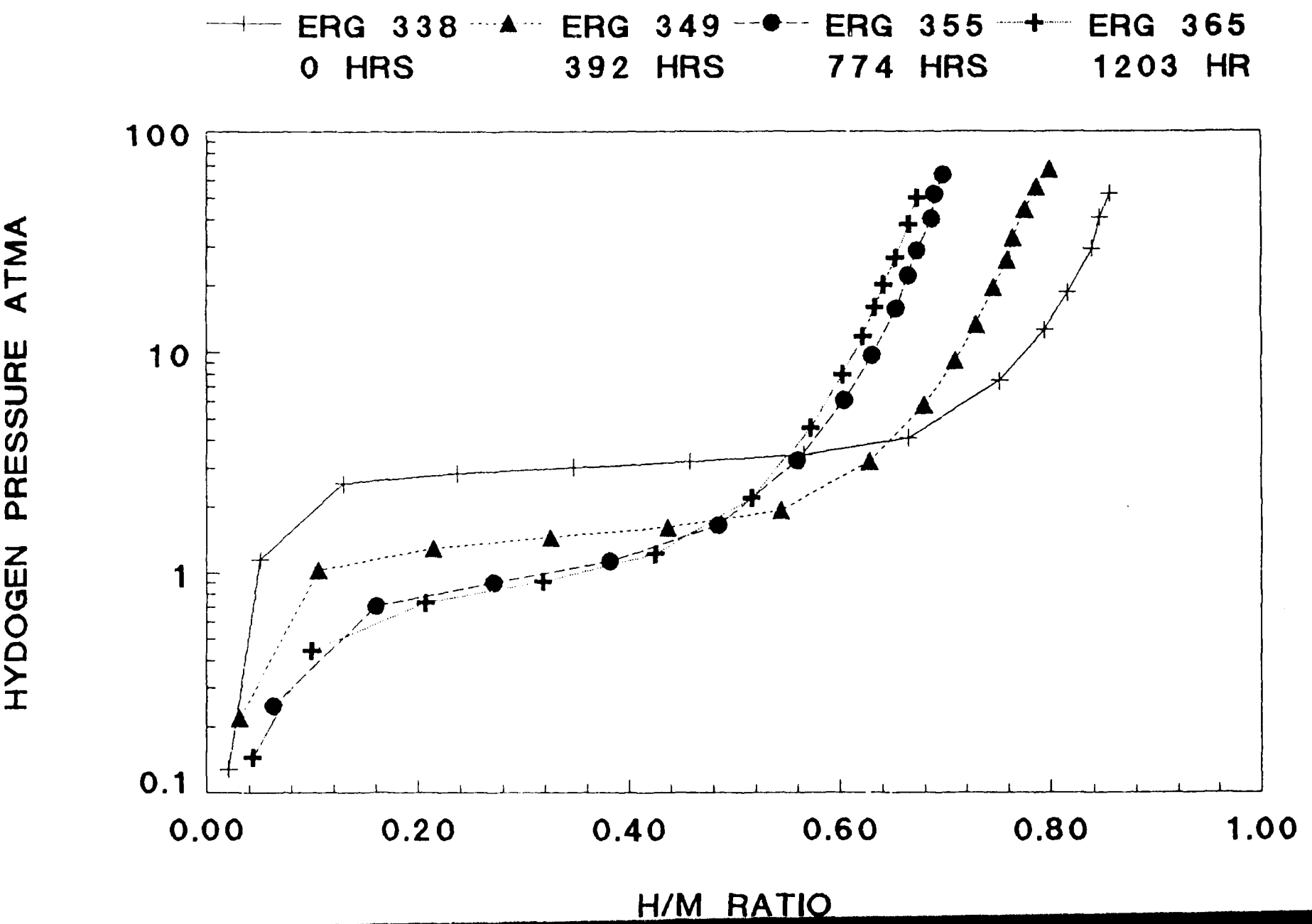

FIG 4.9 REPROPORTIONATION

$LANI_{4.5}AL_{.5}$ 245°C, VACUUM

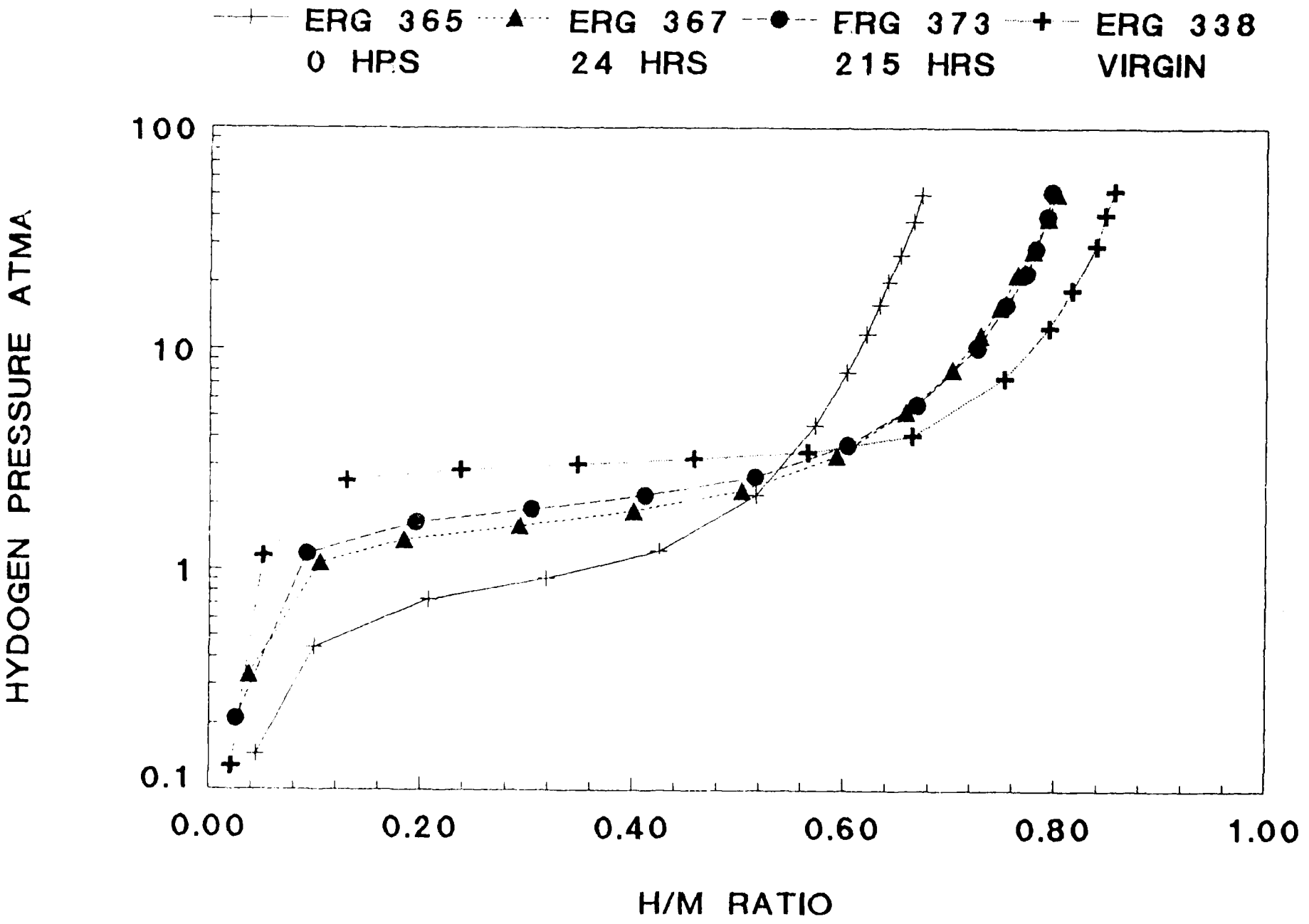

FIG 4.10 SUMMARY OF RESULTS

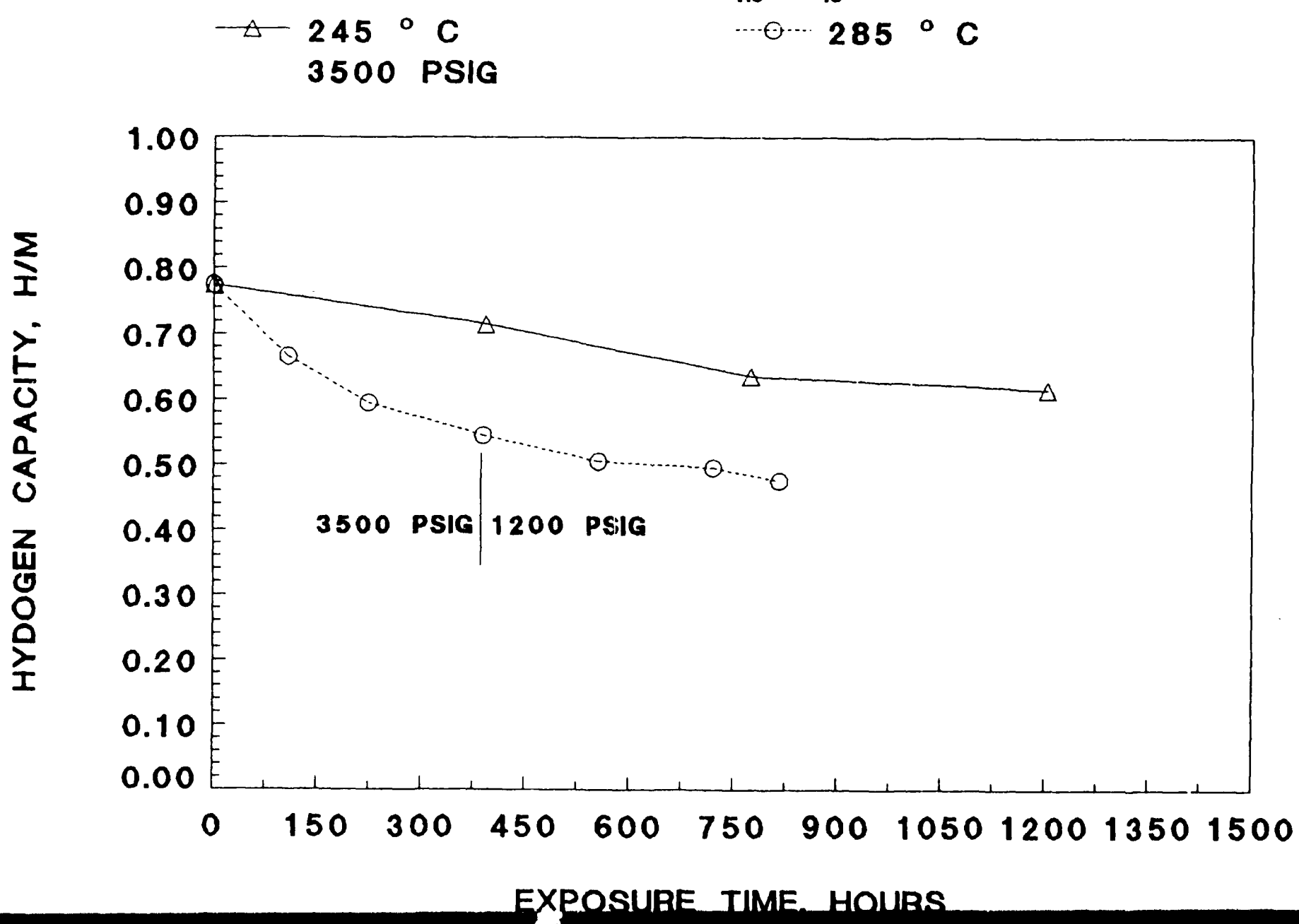

FIG 4.11 LIFE ESTIMATES

AHRENIUS EXTRAPOLATION

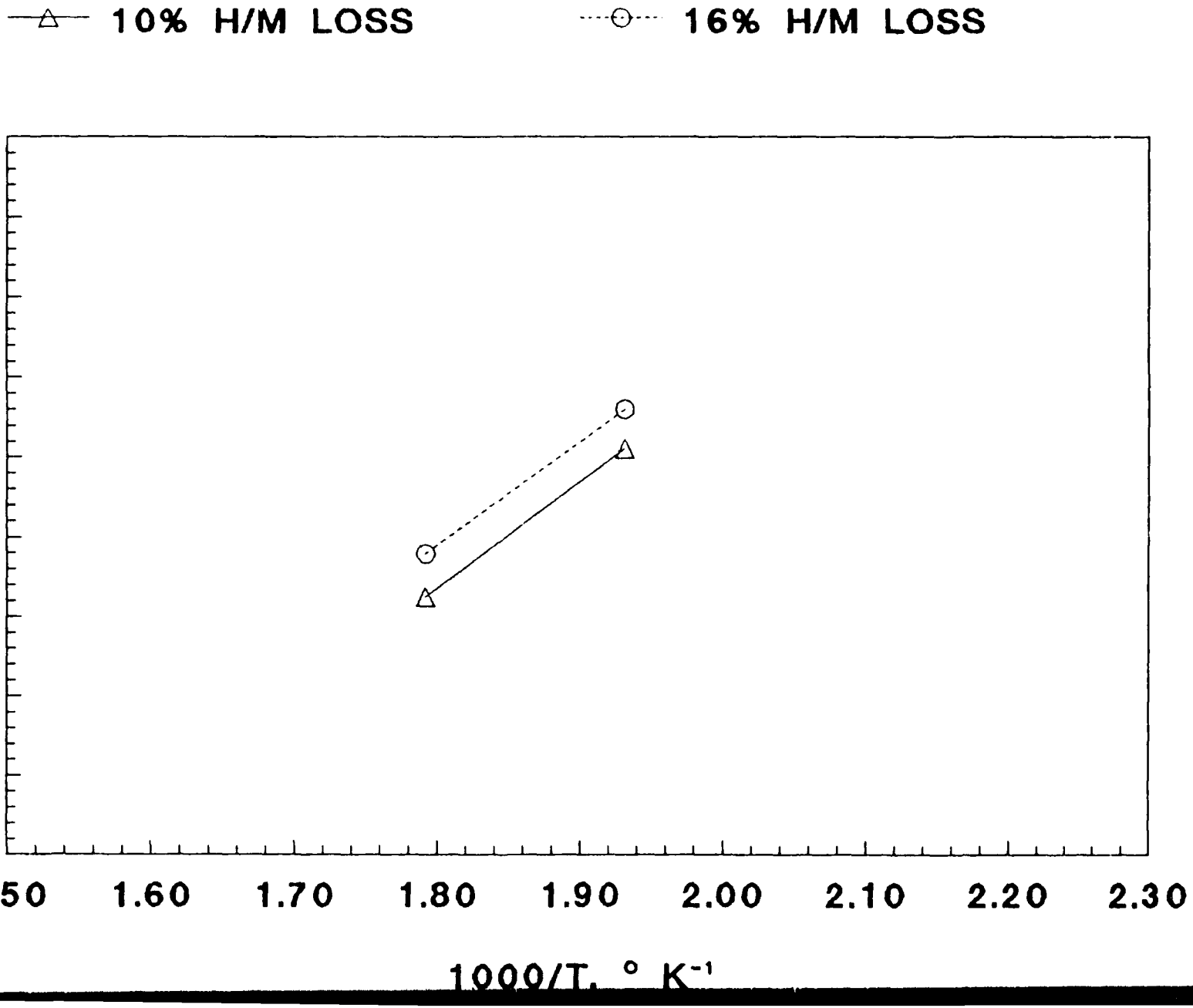

CHAPTER 5

METAL HYDRIDE AIR CONDITIONER

HYDRIDE TO AIR DESIGN STUDY

TABLE OF CONTENTS

5.11 LIST OF TABLES

5.1 SUMMARY

A comprehensive design of an air-to-air metal hydride air conditioner has been performed. Hot engine exhaust gas is used as the primary energy source. This new air conditioner design is unique since it will achieve heat absorption and heat rejection from the metal hydride containers directly to the air streams, and does not require a liquid heat transfer fluid. This design has resulted in a waste heat air conditioner that weighs 17% less (165 lbm compared to 200 lbm) and uses 8 times less electricity (385 watts compared to 3000 watts) than the current conventional freon based air conditioners. This novel metal hydride to air system design uses conventional Ergenics hydride heat transfer design concepts. The design of this new air conditioner is shown in Figures 5.13 A&B and 5.14.

5.1 BACKGROUND AND OBJECTIVE

The prototype hydride air conditioner incorporating Slytherm 800® heat transfer fluid has proven the feasibility of using metal hydrides as an air conditioner or heat pump device. The question that arises is ... can a hydride air conditioner be made that does not require the liquid heat transfer fluid interface, but transfers heat from the metal hydride tube directly to the air, and thus be lighter, less complex and consume less power? The theoretical answer to this question is an immediate "yes" when it is realized that the "liquid" design is in actuality already an "air" design, since the heat that is generated by the metal hydride is eventually dissipated to an air stream.

This conclusion is shown graphically in Figure 5.1. The various heat transfer interfaces along with the relative temperature drops associated with each interface are shown for both the "liquid" and "air" systems. In the "liquid" system it is seen that the heat conduction path is one of ..

- metal hydride to hydride containment tube
- hydride containment tube to silicone liquid
- silicone liquid to Modine aluminum heat exchanger
- aluminum heat exchanger to the air stream

thus the heat from the metal hydride ends up being dissipated to the air. This is exactly the same result that would be accomplished with an air system--heat is transfered directly from the metal hydride to the hydride tube then to the air stream. In other words, the silicon fluid is acting only as a heat transfer media that takes heat from the low surface area hydride tubes and transfers it to the high surface area Modine radiators. The liquid system was selected to increase the heat transfer rate from the hydride tubes and thereby minimize the quantity of metal hydride required.

Table 5.1 is a list of the power, weight and in a sense, the complexity, that would be eliminated by a successful air design. From this table one can see that almost 200 lbm and 900 watts of electric power consumption can be eliminated by a good air design. The question now has become ... how do you design and make a high surface area metal hydride reactor? A successful engineering answer to this question will be very important, since it would result in the elimination of much of the weight and power consumption of the hydride air conditioner.

5.3 DESIGN ASSUMPTIONS

From the previous discussion it was shown that a direct hydride to air system should be possible since the present proven "liquid" system is, in fact, already an "air" system. What then must be done to eliminate the liquid interface? The answer is seen by analyzing the critical element in each system -- the metal to air heat transfer interface. In the liquid system this interface was the Modine aluminum radiators. The hydride reactors must be redesigned to meet the same heat transfer requirements.

The governing heat transfer relationship (Reference 5.1) for any metal to air heat transfer situation is

$$Q = h*A*(T_s - T_a),$$

where:

Q = heat transferred from metal surface to surrounding air, BTU/hr.

A = area of metal surface, Ft^2.

T_s = temperature of metal surface, °F.

T_a = temperature of the ambient air that is unaffected by the heat transfer process, °F.

h = convective heat transfer coefficient, BTU/Hr.Ft^2.°F

In the design of our metal hydride to air heat exchanger, the amount of heat transferred from the metal hydride to the air stream will be exactly the same as that transferred by the Modine heat exchanger. The amount of heat transferred, therefore, becomes Q(Modine) = Q(hydride) = $h*A*(T_s - T_a)$. The driving temperature difference $(T_s - T_a)$, will be by definition, the same as that required by the Modine radiators. In addition, since the heat transfer media (ie: air) is the same for both heat exchangers, then the convective heat transfer coefficient, h, will be almost totally dependent on the velocity of the air as it travels <u>through</u> the heat exchangers. This means that if we design the hydride heat exchanger to have the same air velocity as the Modine, then the heat transfer coefficient, h, will also be very much the same. This leaves the last design variable A, as the critical variable, which means that if unity conditions are to exist (ie: Q(Modine) = Q(hydride)), then the external surface area of the hydride heat exchanger must be equal to the external surface area of the Modine radiator.

At first glance, it would seem that there are many possible hydride containment designs that would satisfy this high surface area requirement. But there are also some other basic design constraints that must also be fulfilled. These are ...

a) the new hydride to air heat exchanger must be designed to withstand a 1000 psig working hydrogen gas pressure.

b) the new design should be of such a nature that questions of its ability to withstand thousands of hydriding/dehydriding cycles are minimized.

c) the new design should lend itself to mass production techniques.

Due to the "B" constraint listed above, the proposed design of this new hydride to air heat exchanger quickly narrows down to variations of ERGENICS hydride coil technology (Reference 5.6) since this storage technology has been proven to successfully withstand hundreds of thousands of hydriding and dehydriding cycles. In addition, due to the tubular nature of ERGENICS coil technology, very high internal pressures can be contained with very thin walled tubing, thus satisfying constraints A and C. The question that now remains is whether the hydride tubes need to be externally fined in order to achieve the required surface area. If a hydride tube design can be found that achieves the required external surface area without the need of external finning, then we have found not only the easiest, but also the lowest "cost to produce" design.

Table 5.2 illustrates the driving rational for an unfined tubular aprroach for the metal hydride to air heat exchanger. Table 5.2 shows that as the outer diameter of a tube decreases, the corresponding amount of internal volume also decreases, but at a faster rate. This means that smaller tube diameters provide greater external surface areas for a given stored volume. In fact, it is this very engineering fact that is used extensively in the design of commercial heat exchangers -- the surface-to-volume ratio (S/V) increases linearily with decreasing tube diameter. However, in a conventional heat exchanger, another limit is reached at an outer diameter of about 1/2" to 3/8", for it is at this point that the energy required to pump liquid through these small diameter tubes becomes excessive. The engineering reponse to this condition has been to externally fin the tube, an initially costly procedure. In the hydride tube system, however, excessive fluid pumping power losses are not reached until a smaller tube diameter (about 1/8") is reached. This is due to the fact that hydrogen gas is the fluid that is being "pumped" through the tubing, and tremendous quantities of hydrogen can be passed through a very

small tube diameter, with very little pressure drop. Therefore, the approach will be to assume a small diameter, finless tube design, and attempt to minimize its size and mass.

5.4 GENERAL DESIGN PROCEEDURES

The process of designing a hydride tube for large surface area and minimum mass involves many steps, some of which are iterative. The general procedure is as follows:

1) Determine what is the desired external surface area of the tube. This is actually the external surface area of the Modine radiator, with a special check done to ensure that the fins used in the Modine design are operating at a high enough efficiency as to be acceptable as true "base" material surface area.

2) Compare the driving heat transfer temperature gradients present and recalculate the required hydride external surface area.

3) For a given tube diameter, determine the length of tubing required to produce the amount of external surface area determined in step 1 above.

4) For the tube diameter in question, determine the tube wall thickness needed for a working pressure of 1000 psig. In all cases, it is assumed that the tube material is 304 stainless steel.

5) For a given 1/2 cycle time, determine the amount of mass of metal hydride needed to produce the required 9000 BTUs per hour.

6) From steps 4 and 5, a total mass for the hydride heat exchanger can now be determined.

7) Determine an acceptable switchover delay time, which involves an analysis of transient heat flow.

8) Incorporating this transient heat switchover delay time, recalculate

the variables in steps 5, 6 and 7.

9) Allow for a temperature loss of 25°C due to the sensible heat of the hydride heat exchanger at switchover. Recalculate the variables in steps 5 and 6.

10) With the new required tube length, and assuming that the hydride heat exchanger will consist as a large torous shape (e.g. ID = 4", OD = 18") with each layer being a spiral wrap of a single tube (see Fig. 5.2A&B); determine the pressure drop for air flowing through the coils. This will assume different tube spacings.

11) Repeat steps 10 until a desired balance between fan power and heat exchanger volume is achieved.

12) Recalculate steps 5 thru 10 and 11 for new 1/2 cycle times.

13) Recalculate step 11 for all of the 1/2 cycle times desired.

14) Select a new tube diameter and repeat steps 3 thru 13.

15) Repeat step 12 for all the tube diameters desired (see Table 5.2).

16) Select the optimum tube diameter and desired 1/2 cycle time. T' is will be the design that will have the lowest mass and the longest 1/2 cycle time before the H_2 pressure drops become excess (>3 psig).

Calculations of the above steps were accomplished by computer programs. The computer program call "Coil-7" is primarily involved with the coil spacing and air flow power requirements, and is listed in Appendix 5.1.

5.5 DETAILED DESIGN PROCEDURES

The following section is a detailed explanation of the equations and assumptions used in each of the design procedure steps listed above and subsequently used in the computer programs. The step by step walk through presented in this section will familiarize the reader with these procedures.

Design Procedure Step 1: Determine the desired external surface area of the tubing. This is actually the external surface area of the Modine #2978 radiator modified by the thermal inefficiency of the fins.

Figure 5.3 is a detailed dimensional drawing of the Modine #2978 aluminum radiator. This radiator contains 22.6 tube rows, with each row consisting of a tube core and connecting fins. The length of each row is 18.125 inches. Therefore, the total external surface will be the surface area of the tube cores plus the surface area of the external fins (with a correction factor for the efficiency of the fins factored in later).

Tube core external area = (tube perimeter)*(tube length)*(number of tubes).

Surface area = [(0.160+1.0625+0.160+1.0625) * (18.125)] * (22.6)

= 1001.5 in^2

= 6.96 Ft^2

Fin surface area = Surface area of one fin * number of fins (before fin efficiency factor)

= ((1.0625+1.0625) * 0.371) in^2/fin * 4916 fins

= 3875.4 in^2

= 26.91 Ft^2

Calculation of the fin efficiency factor η_f:

From Reference 5.1, we find the fin efficiency factor graphed as a function of the quantity...

$$(L_c)^{3/2}(h /(k * A_m))^{1/2} = 0.273$$

where:

$L_c = L * t/2 = 0.01596$ Ft

$A_m = t * L_c = 0.00000798$ Ft^2

h = 20 BTU / (Hr . Ft^2 . °F)

k = 137 BTU / (Hr . Ft . °F), (for aluminum)

From Figure 10-4 (reproduced here as Figure 5.4), we find that the fin efficiency of the Modine 2978 is about 90% ($\eta_f = 0.90$).

This means that the Modine fins are operating as if 90% of the fin material is at the base temperature, which is the condition that will be present in the hydride to air system. Therefore, the true effective fin surface area is now...

Fin surface area = η_f * 26.91 Ft^2
(after fin efficiency factor)

= 0.90 * 26.91 Ft^2

= 24.22 Ft^2

Therefore, the total amount of external surface area of the Modine 2978 unit is...

External Surface area total = tube core area + fin area
(of Modine 2978)

= 6.96 Ft^2 + 24.22 Ft^2

= 31.18 Ft^2.

Design Procedure Step 2: As was pointed out in the section "5.2 DESIGN ASSUMPTIONS", the new proposed hydride to air design will operate without the temperature loss that is encountered when heat is transferred from the hydride tube to the silicone fluid and from the silicone fluid to the Modine aluminum radiator. Adding these temperature gradients together will yield about 4°C of temperature potential that can be added to the hydride to air temperature gradient of 15°C. The summation yields a new hydride to air temperature gradient of 19°C, which is about 25% larger than was designed into the liquid silicone fluid system (at 15°C). But instead of compensating for this greater temperature gradient in the hydride to air design by lowering the design temperature gradient on the hydride to air side by 15/1.25 = 12°C, we will keep

this temperature gradient at 15°C, and lower the required external surface area by 25%. This means that the surface area of 31.18 Ft^2 calculated for the Modine 2978 radiator in step 1 can be changed to 31.18/1.25 = 25 Ft^2.

Design Procedure Step 3: Now that we know the amount of external surface area needed for the hydride heat exchanger (25 Ft^2), we now must calculate the corresponding tube length. This is the surface area divided by the tube's circumference. For example, in the 1/4"Φ case...

Length of 1/4"Φ tubing needed = area/circumference

$$= \frac{25\ Ft^2 * 12\ in.}{* (0.25)\ in.Ft.}$$

$$= 382\ Ft.$$

Design Procedure Step 4: For the tube diameter in question, determine the tube wall thickness needed to provide a working pressure of 1000 psig. Assuming that the tube material is 304 stainless steel, the tube wall thickness equation from Reference 5.2 is...

$$t_m = \frac{P * D}{2(SE + (P*y))}$$

where:

t_m = tube wall thickness in inches

P = maximum working pressure in psig

D = outer diameter of tube in inches

SE = maximum allowable stress in psi, for 304 SS SE = 18,750 psi, this provides a stress safety factor of 4 to 1.

y = joint efficiency factor = 0.4 for welded butt joints

Therefore, for the case of the 1/4"Φ, SS tube designed to operate at hydrogen pressures under 1000 psi, the tube wall thickness is...

$$t_m = \frac{(1000)(0.25)}{2(18{,}750 + (1000)(0.4))} = 0.0065"$$ say 0.007".

Design Procedure Step 5: For a given 1/2 cycle time, determine the amount of mass of hydride alloy needed to produce the required 9000 BTU per hour of cooling.

If we are generating 9000 BTU/Hr, then the cooling rate needed per minute is 9000/60 = 150 BTU/min. Now, assuming that one mole of hydrogen gas (reacting with the metal hydride) will produce 27 BTU (6,800 cal/mole H_2) of cooling, and that the metal hydride will store at least 1% by weight hydrogen gas, means that each kilogram of metal hydride alloy will produce 134 BTU of cooling. Therefore, the equation that determines the amount of hydride alloy needed is...

Mass of hydride alloy in kilograms needed to produce 9000 BTU/hr of cooling equals:

$$= \frac{(1/2 \text{ cycle time in minutes}) * (150 \text{ BTU/min.})}{134 \text{ BTU/kg of hydride}}$$

For example, a 1/4"Φ tube design utilizing a 5 minute 1/2 cycle time will require...

$$\text{Mass of hydride} = \frac{5 * 150}{134}$$

$$= 5.60 \text{ kg of hydride alloy (12.3 lbm)}$$

Please note, this step ignores the sensible heat of the hydride and the hydride heat exchanger. These important effects will be delt with subsequently.

Design Procedure Step 6: In "Design Procedure Step 5", we found the amount of metal hydride alloy needed to produce 9,000 BTU/Hr of cooling. In the case of the 1/4"Φ, 0.007" walled, stainless steel hydride tube the hydride mass ratio is 1.91. Thus the total mass for the hydride heat exchanger is 23.90 lbms.

Design Procedure Step 7: What is an acceptable switch over delay time? The switchover time delay is the time interval between the changing of the modes between the two hydride coils (i.e.,going from absorption to desorption) and the point in time when cooling of the hydride bed takes place. The hydride bed coil that is really governing this time delay is the "A" type hydride bed coil that has just switched from being heated with hot exhaust gas (@220°C) to being cooled by the ambient outside air (@49°C). This "A" type hydride bed must cool down to a point where its temperature (and thus its internal hydrogen pressure), is low enough such that hydrogen stored in the paired "B" type hydride bed will start flowing into this "A" bed.

The hydride system is designed so that this "hydrogen transfer point" occurs when the "A" coil in question has reached about 85°C. Therefore, all of the sensible heat (between the temperatures of 220°C and 85°C) that is stored in the "A" bed must be rejected to the ambient air.

The heat transfer equations that govern this type of situation are called transient equations and take on the form (Reference 5.1):

$$e^{-(hA/MC)\tau} = (T - T_\infty)/(T_o - T_\infty)$$

where:

τ = time into transient mode in seconds

T = the temperature of the heat exchanger at time τ, in °C

T_o = the initial temperature of the heat exchanger at time t=o

T_∞ = the bulk temperature of the ambient fluid, in °C

h = the convection heat transfer coefficient, BTU/Sec.Ft^2.°F.

A = the surface area for heat transfer in Ft^2

C = the specific heat of the heat exchanger, BTU/Lbm.°F

M = the total mass of the heat exchanger, in Lbms

Rearranging this equation to determine the required switchover transient time yields...

$$\tau = - [M*C*\ln (T - T_\infty)/(T_o - T_\infty)] / (h * A).$$

Inputing the values (on a per Ft basis)

M = 28.44 g/ft = 0.06257 lbm/Ft

C = the specific heat of the hydride heat exchanger

= [(8.24)(1.2)+(14.66)(1.0)+(5.539)(0.22)]/28.44 g/ft

= 0.12916 cal/g°C = 0.12916 BTU/lbm°F

h = 20 BTU/Hr. Ft^2.°F = 0.00556 BTU/sec.Ft^2 °F

A = $\pi * D * l$ = π (0.25)(12) = 9.42 in^2/Ft = 0.06545 Ft^2/Ft

T = 85°C

T_∞ = 49°C

T_o = 220°C

then,

$$\tau = - \frac{[(0.06257)(0.12916) \ln ((85 -49)/(220 -49))]}{(0.00556)(0.06545)}$$

$$\tau = - (22.208) \ln [(85 -49)/171]$$

$$\tau = 34.6 \text{ sec}$$

We will proceed with the conservative assumption that the switchover time will take 60 seconds, or really twice the calculated value of 34.6 seconds.

Design Procedure Step 8: The step 7 determination of a transient switchover delay time of 1 minute means that we must now add additional metal hydride heat exchanger capacity. This is because the switchdown time is additional time that has been added to the 1/2 cycle time, and thus the hydride heat exchanger cooling capacity must increase in order to accommodate this new additional load.

For instance, if our 1/2 cycle time is 5 minutes long and we add an additional 1 minute for the switchover (a 20% increase) then the hydride tube length must also be increased by an additional 20%. This yields the following results:

The new metal hydride heat exchanger tube length	=	382 Ft. x 1.20
	=	458.4 Ft.
And the new total mass of the hydride heat exchanger	=	23.90 Lbms x 1.20
	=	28.68 Lbms (13.04 kg)
new mass of metal hydride alloy	=	14.81 lbms.
new mass of tubing	=	13.87 lbms.

Design Procedure Step 9: Step 9 is an additional design refinement that takes into account the loss of sensible heat in the "B" type cooling coil during the switchover mode. The amount of sensible heat temperature loss is about 25°C (this is the temperature difference between the ambient temperature and the cooling shelter temperature), and represents the amount of additional cooling that must be provided (via metal hydrides) to the heat exchanger. However, since this cooling loss involves only the sensible heat of the heat exchanger, the metal hydride is added directly to the metal hydride already in storage, and therefore, does not require an increase of tube length (which would result in additional external surface area). This is because this additional cooling capacity cools down the heat exchanger prior to the transfer of cooling to the air stream.

The additional metal hydride mass required to provide this sensible heat cooling is calculated by first determining the drop in temperature of the hydride heat exchanger if all of the cooling potential of the metal hydride were used to provide sensible heat cooling. Then the fraction of this total temperature drop that the 25°C sensible heat temperature loss results in, will

be the fractional increase required of the metal hydride mass.

Therefore,

Mass of metal hydride (including the mass of the metal hydride alloy) heat exchanger coil = 28.68 lbms = 13.036 kgs.

The number of moles of H_2 gas stored = 6,720 grams / 201.6 g/mole H_2 = 33.3 gram moles of hydrogen.

Cooling potential of metal hydride heat exchanger =

(33.3 moles of H_2) * (6,800 cal/gram mole of H_2) = 226,666 cal

Heat capacity of the hydride heat exchanger = 1,684 cal/°C

Therefore, the total temperature potential of tube =

[(226,666 cal) / (1,684 cal/°C)] = 134.6°C

The fraction of this total temperature potential that the 25°C sensible heat loss during switchover represents = 25°C/134.6°C = 0.1857.
Therefore, the amount of metal hydride put inside the tube per foot must increase by 18.57%.

The new mass of metal hydride alloy in the heat exchanger =

6,720 grams * 1.1857 = 7,968 grams

The new total mass of the hydride heat exchanger = 31.02 lbms (14.1 kg)

Design Procedure Step 10: This step will determine the lengths of the individual hydride tubes used to fabricate the torous shaped hydride heat exchanger shown in Figure 5.5. Knowing the lengths of the individual tubes that make up the heat exchanger is important since this will determine the pressure drop of the air passing (perpendicularly to) the outside of the tube.

Air Flow Pressure Drop:

Figure 5.6 is an enlarged detailed look at the staggered tube arrangement present in the proposed hydride to air heat exchanger design.

The pressure drop equation governing air flow through this type of heat exchanger (from reference 5.4) is

$$\Delta P = N * f ((\rho * U_{av}^2) / 2g),$$

where:

ΔP = the pressure drop across the heat exchanger in Lbf/Ft^2

N = the number of tube rows in the flow direction

f = a friction factor coefficient that is determined by the heat exchanger's tube and tube spacing dimensions

ρ = the density of the air flowing across the tubes evaluated at the inlet temperature

U_{av} = the average velocity of the air flowing through the area between the tubes in Ft/sec.

g = the gravitational constant, 32.17 $Lbm.Sec^2/Lbf.Ft$

The friction factor coefficient, f, is determined by the equation.....

$$f = \left\{ 0.044 + \left[\frac{(0.08) * (S_L / D)}{((S_t - D)/D)^{[0.43 + ((1.13 * D)/S_L)]}} \right] \right\} * R_e^{(-0.15)}$$

where:

D = the outer diameter of the tube in inches

S_T = D + the space between each tube in inches

S_L = D + the space between each tube <u>row</u> in inches

R_e = the Reynolds number, calculated at the point of highest air velocity

$$R_e = (\rho * U * D) / \mu$$

μ = the dynmic viscosity, Lbm.Sec/Ft

Before we can solve these equations for our test case of the 1/4"Φ, 458.4 ft. long hydride tube, we must first derive the value for the air velocity . This is done by analyzing the heat transfer of our model, the Modine 2978 radiator. Figure 5.7 is a graph of the heat transferred vs. the nominal air speed for the Modine 2978 radiator. The most efficient point (for fan power) of heat transfer on this curve occurs at the lower air speed of 500 Ft. per min. and it is at this point that we have designed our system. The 500 Ft/min. nominal air speed value is the velocity of the air speed as measured outside of the radiator core. The true value of the air speed is its velocity inside the core, where the heat transfer is taking place. The true air velocity is easily found by assuming that the full air flow volume must pass through the free space core area (i.e., subtract the cross-sectional area of the metal heat transfer surface from the full core area).

When this is done, we find that the true "free space" core area is about 1.0 Ft^2, and therefore the true core air velocity is about 755 Ft/min (12.58 Ft/sec) when the nominal air speed reads 500 Ft/min (8.33 Ft/sec). In addition, the volumetric air flow rate at this point is 13 Ft^3/sec.

This true core air velocity is the air velocity value that will be used to

dimentions, the maximum Reynolds number value, and the hydride tube spacing diameters, needed to produce this maximum air velocity. It should again be noted here that since the fluid media and construction dimensions have nearly the same values for both the Modine radiators and the hydride heat exchangers, then the convective heat transfer coefficient, h, will be a direct function of the velocity of the air passing through the exchangers. What must be done now is to construct the hydride heat exchanger so that it will possess the same core air velocity (12.58 Ft/sec) at the same volumetric flow rate (of 13 Ft^3/sec).

This is done by varying the space between the coiled hydride tube in the tube row until the free air area is of the size that will generate a U_{max} of 12.58 Ft/sec. at an air flow of 13 Ft^3/sec. Therefore, the required free area = (13 Ft^3/sec)/(12.58 Ft/sec) = 1.04 Ft^2. This occurs when the tube space distance is about 0.29 inches.

Now all of the relevant data needed to determine the Reynolds number the friction factor, and thus the air pumping power are known. These values are...

U_{max} = maximum air velocity = 12.58 Ft/sec

D = outer diameter of tube = 0.25 inches = 0.0208 Ft

ρ = air density = 0.07519 Lbm/ft^3

μ = dynamic viscosity of air = 1.241×10^{-5} Lbm.sec/Ft

Tube spacing = 0.29 inches

Row spacing = 0.29 inches

S_t = D + tube spacing = 0.25 + 0.29 = 0.54 inches

S_L = D + row spacing = 0.25 + 0.29 = 0.54 inches

g = gravitational constant = 32.17 Lbm.sec^2 / Lbf.Ft

Therefore the Reynolds number is...

$$Re = [(0.07519)*(12.58)*(0.0208)]/(1.241*10^{-5})$$

$$Re = 1585$$

And therefore, the friction factor f is,

$$f = \left\{0.044 + \left[\frac{(0.08)*(0.54)/(0.025)}{((0.54-0.25)/(0.25))^{[0.43+(1.13)*(0.25)/(0.54)]}}\right]\right\} + 1585^{(-0.15)}$$

$$f = (0.044 + 0.15) * (0.3311) = 0.0642$$

And lastly, the pressure drop per row of tubing is

$$\Delta P = [(1)*(0.0642)*(0.07519)*(12.58_2)]/[(2)*(32.17)]$$

$$\Delta P = 0.01187 \text{ lbf/Ft}_2 = 0.00217 \text{ inches of water}$$

The equation used to calculate theoretical power needed to move a given air flow with a given pressure drop is...

Power watts = (Volumetric Air flow rate Ft^3/sec)(Pressure Drop Lbf/Ft^2)(1.356)

Letting the volumetric air flow rate equal 13 Ft^3/sec, and the pressure drop equal 0.01187 lbf/Ft^2, yields a power of 0.2093 watts/row. Therefore, the total power required to overcome the frictional losses of air passing through the heat exchanger (for the above conditions) will be 0.2093 watts/row * the number of tube rows. Since we already know the full and free air areas for this torous shaped heat exchanger, the length of hydride tubing per row is easily calculated to be 42 ft. for this example. Therefore, if the total tube

length is 458.4 then we will need about 11 rows of tubes. This means that the total power to drive air through this heat exchanger will be 11 * 0.209 = 2.3w.

Design Procedure Step 11: We have now found that for the same heat transfer conditions present in the Modine 2978 radiator, a comparable compact hydride heat exchanger can be built. In Step 10, we found that this hydride heat exchanger would consist of 11 rows of the spirally wrapped 1/4" Φ tubing, with a distance between the tubing of 0.29". We also found that the power needed to pull the air through this heat exchanger is still quite low being only 2.3 watts. Step 11, therefore, repeats Step 10 in order to reduce the size of the heat exchanger. This involves decreasing the tube spacing dimensions (and thus increasing the air power requirements) until an optimum condition is found, that being a smaller size with an air pumping power of 12 watts or less.

When this is done, it is found that if the tube spacing is decreased to 0.1 inches, the length of a single tube now becomes 63 ft. Therefore, 8 tube rows will be needed, with the corresponding air pumping power requirement of 11.6 watts.

The new size for this optimum condition will be; hydride coil ID = 4 inches, hydride coil OD = 18 inches and the hydride coil bed thickness of 2.70 inches, or more than twice the thickness of the 1-1/16" thick Modine 2978. The new hydride air coil will have better heat transfer capabilities since the maximum air velocity going through the tube spaces is now 24.5 Ft/sec, or about double what it was when the tube spacing was 0.29 inches. From Reference 5.5, we see that the Reynolds number, R_e, is directly proportional to the air velocity. However the effect on the heat transfer is much less pronounced since the Prandtl number remains unchanged

$$P_r = (C_p * \quad * 3600) / k$$

$$= (0.24 * 1.241*10^{-5} * 3600)/0.01516$$

$$= 0.7073$$

and the entrance factor **X*** (a dimensionless coordinate) will change from...

$$X^*_{(@\ R_e = 1588)} = \frac{X}{(r_w) * (R_e) * (P_r)}$$

$$= \frac{(5.65/12)}{(0.145/12) * (1588) * (0.7073)}$$

$$= 0.0347$$

to,

$$X^*_{(@\ R_e = 3090)} = \frac{(2.7/12)}{(0.05/12) * (3090) * (0.7073)}$$

$$= 0.0247$$

And thus from Table 8-1 in Reference 5.5, the corresponding averaged Nusselt number will change from 5.442 at X* = 0.0347 to 5.917 at X* = 0.0247. And since Nu avg = h*d/k, then the real increase in the convective heat transfer coefficient is only about 8.76% (i.e., 100*(5.917)/5.442).

5.6 DESIGN RESULTS

Results from the computer programs were compiled and are presented as graphs shown on Figures 5.8 through 5.11. Figure 5.8 shows the relationship between the total mass of a single hydride heat exchanger and the 1/2 cycle time for three progressive design conditions involving a 1/4"Φ tube. The basic design

conditions are:

- The 1/4"Φ tube length is sized to provide the required external surface area of 25 Ft_2., which is the external surface area of the Modine #2978 aluminum radiator.
- The 1/4"Φ tube is assumed to be made out of stainless steel and is designed to provide a working pressure of 1000 psig.

Curve A in Figure 5.8 shows that the total mass of a single hydride heat exchanger varies linearily as the 1/2 cycle time of the hydride heat exchanger increases. The curve slope is related to the tube mass ratio. No allowances for any time delays or sensible heat loss at switchover are given in this curve.

Curve B in Figure 5.8 shows how the total mass of a single hydride heat exchanger varies with 1/2 cycle time when a 1 minute switchover delay time is incorporated into the 1/2 cycle time. This means that extra hydride tubing must be added to the system mass shown in curve A in order to maintain the average cooling load of 9000 BTU/hr. The effect of the one minute switchdown delay time is very pronounced at short 1/2 cycle times since the 1 minute delay has now become a very sizable portion of the cooling load.

Curve C in Figure 5.8 shows the final effect of adding a 25°C sensible heat loss to the mass of the hydride heat exchanger. This is the heat (i.e., cooling) that is lost when the cooling hydride coil drops from the outside ambient temperature to the inside shelter cold air temperature at switchover. This heat is not transferred to the air stream, but only drops the temperature of the hydride coil itself in preparation for heat transfer to the air stream. Therefore, additional hydride tubing is not required to provide increased surface area,but only additional metal hydride alloy is added to the tube.

The absolute minimum hydride heat exchanger mass is found at the point on curve C where the tangent is horizontal. This point, however, is not the best point for system design, (even though it has the lowest mass). This is because as one increases the 1/2 cycle time past the critical minimal mass point, the possibility of producing greater cooling rates exixts. For instance, if a design is picked that produces 9000 BTU/hr at a 1/2 cycle time of 5 minutes and we were able to operate the unit at a 1/2 cycle time of 2-1/2 minutes, then we would be producing 18,000 BTU/hr of cooling since these coils actually contain twice the amount of hydriding alloy as a 2-1/2 minute design point.

Heat Exchanger mass vs 1/2 cycle time curves for the different tube diameters 3/8", 5/16", 3/16" are shown respectively in Figures 5.9, 5.10 and 5.11. Since it is curve C in these figures that provides the most relevant information on the hydride tube mass, these curves have been reproduced together for comparison in Figure 5.12. In addition, the 3 psig pressure drop point for these tubes is also shown on curve C. The best pick is the hydride tube design that contains the lowest mass, at the highest 1/2 cycle time, with a H_2 pressure drop under 3 psig. From Figure 5.12 it is seen that the 1/4"Φ tube design is the best pick that satisfies the above criteria. The relevant dimensions and information on this "best pick" design are shown below.

BEST PICK DESIGN RESULTS

Tube outer diameter = 0.25 inches

Tube material = 304 stainless steel

Tube wall thickness = 0.007 inches (for 1000 psig service)

Tube inner diameter = 0.236 inches

The 1/2 cycle time is = 5 minutes

Total length of 1/4"Φ tubing = 458.4 ft.

Mass of hydride = 7.967 kg

Total mass of hydride heat exchanger = 31.02 Lbms

The mass ratio = 1.77

The hydride heat exchanger will, therefore, consist of 8 rows of 1/4"Φ tubing spaced 0.1 inches apart. Each row of tubing will be 57.3 ft. long with a 0.1 inch space between each spiral wrap. The heat exchanger will be torus shaped with the dimensions of 4" ID, 18" OD and 2.70" thick (see Figure 5.2A and 5.2B).

5.7 FAN REQUIREMENTS

As shown in the detailed design Step 12 in section 5.5 , the setting of the tube spacing at 0.1 inch was the result of calculating the pressure drops and power consumption for air flow through the hydride heat exchanger for many different design conditions. An air power level of 12 watts was selected as the design point since this resulted in an acceptable hydride tube bed thickness (2.70 inches), and yet did not require an excessive amount of power to push the air through the heat exchanger. This 12 watt air power requirement, however, is not the "real" amount of power that will be needed due to the large inefficiences present in fan technology.

Figure 5.13A and 5.13B shows the air system layout for the proposed prototype. Notice that the typical air flow pattern is one that will draw air into a 4 inch plenum space, the air direction then changes by 90° and passes through the hydride heat exchanger and into another 4 inch plenum space. In this second plenum space, the air direction changes again (90°) and is directed out of the

prototype. Each 90° change of the air direction will result in a 30% increase in the power needed to move the air. In other words, the real power now needed to move the air through the hydride heat exchanger in the prototype will be = 12 watts x 1.3 x 1.3 = 20.28 watts, therefore, a fan should be selected that can produce 20.28 watts of friction power at the 13 ft^3/sec (780 Ft^3/min.) required air flow rate.

Figure 5.15 shows the power curve for one such fan that will be able to supply these power needs. This fan is the EBM Industries, Inc. #4E300 which has a total electrical power consumption of 115 watts. The power difference between the 115 watts electrical and the 20.28 watts air friction is, of course, due to the inefficiencies of electric to mechanical (air motion) conversion. The EBM #4E315, (135 watts electrical) fan is similarly sized to provide the 13 Ft^3/sec air flow needed for the ambient cooling of the hydride heat exchangers with outside air during their H_2 reabsorption mode.

Since only one of the EBM #4E300 fans on the cold side will be on at any given time, then the total power (electrical) consumption of the prototype will be the two ambient air fans and one of the cooling air fans. Therefore, total electrical power required for prototype's operation is 2 * 135 + 115w = 385 watts. This is about 4 times smaller than the power that was used in the liquid hydride prototype and about 8 times less power than the power requirements of the freon air conditioners currently used.

5.8 AIR PROTOTYPE CONFIGURATION

Figures 5.13A, 5.13B and 5.14 show the proposed layout for the air system prototype. Dimensions for this new system are 36 inches long, 32 inches wide

and 25 inches high or 14.5 Ft^3. The total weight of the unit is estimated at 165 Lbms. Electric power consumption (as shown in section 5.7) is 387 watts. Table 5.3 is a list of the components and their respective weights and electrical power requirements.

As can be seen in the drawings, the air system prototype promises to be much simpler and easier to build than the previous liquid unit. This is due to the absence of the liquid pumps and diaphram control valves that pumped and controlled the flow of the silicon fluid. Air flow control in the new air system will be accomplished through the use of air louvers that will quickly close and open the air flow passages. These air louvers will be operated by compressed air (provided by a small air compressor) in much the same way that compressed air controlled the operation of the diaphragm control valves in the liquid system. Since this small air compressor is on for only a very short length of time, its average power consumption is less than 2 watts.

The air system as shown in Figures 5.13 A&B and 5.14 is thought to be presented in a larger volume than necessary (the conventional unit is 5.8 Ft^3). This is due to the desire to maintain large plenum air spaces for unrestricted air flow. Once testing of this new prototype has confirmed its predicted performance, then attempts will be made to decrease its dimentional profile.

5.9 LIST OF REFERENCES

5.1 Engineering Heat Transfer" by, B.V. Karlekar and R.M. Desmond.

5.2 pg. 8-149 of "Mark's Standard Handbook for Mechanical Engineers". Eighth Edition by, Baumeister, Avallone, Baumeister.

5.3 pg. 107 of "Engineering Heat Transfer" by B.V. Karlekar and R.M. Desmond.

5.4 "Heat Transfer and Flow Resistance in Cross flow of gases over Tube Banks", by M. Jakob. Trans. ASME. Vol 60 pg. 384.

5.5 pg. 347 of "Engineering Heat Transfer" by, B.V. Karlekar and R.M. Desmond.

5.6 Golben, P.M. and Storms, W.F., Flexible Means for Storing and Recovering Hydrogen, U.S. Patent 4,396,114 issued Aug. 2, 1983.

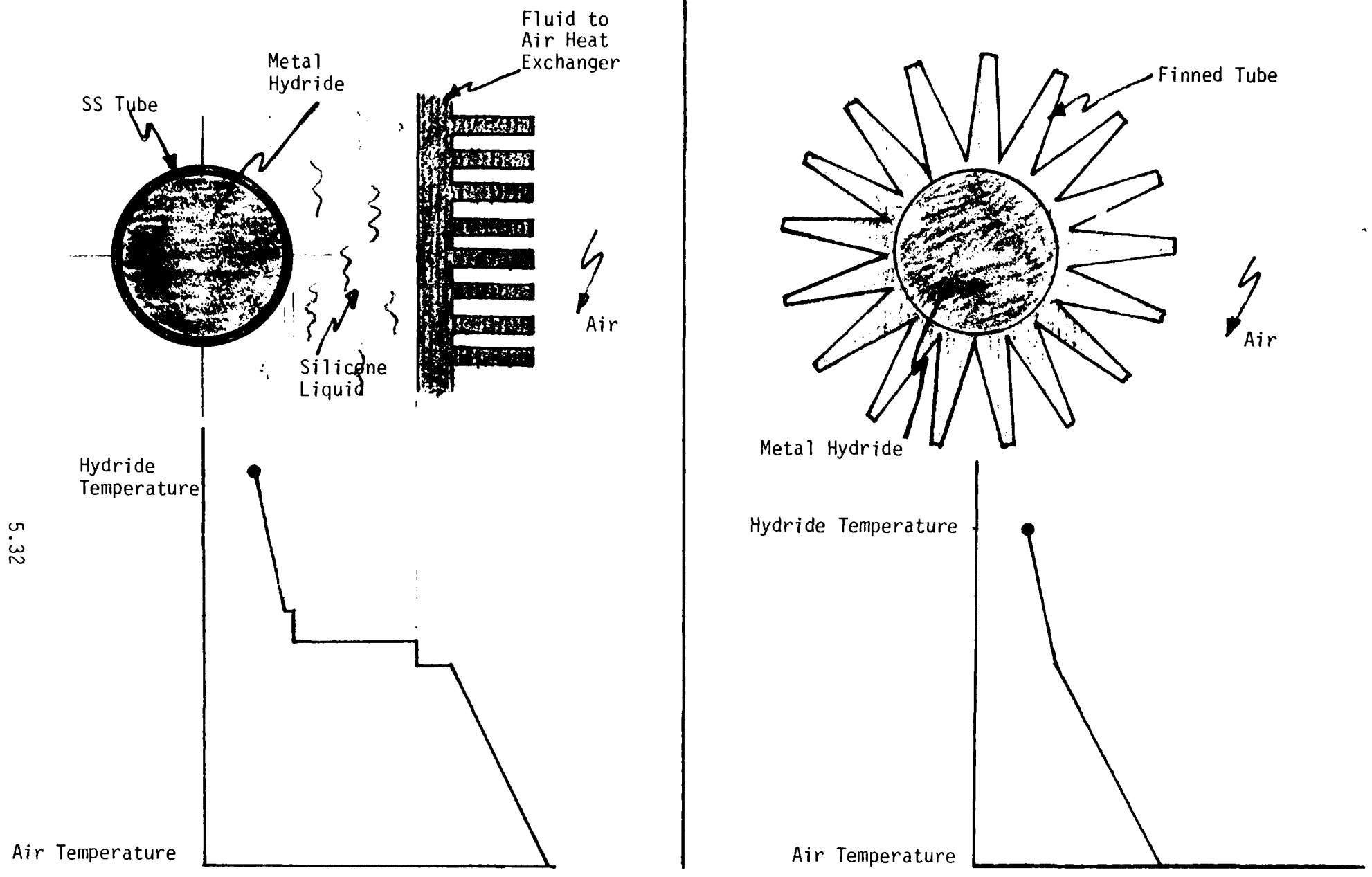

Figure 5.1 - Graphical Representation of Temperature Drops Present in Both the Liquid and Air System

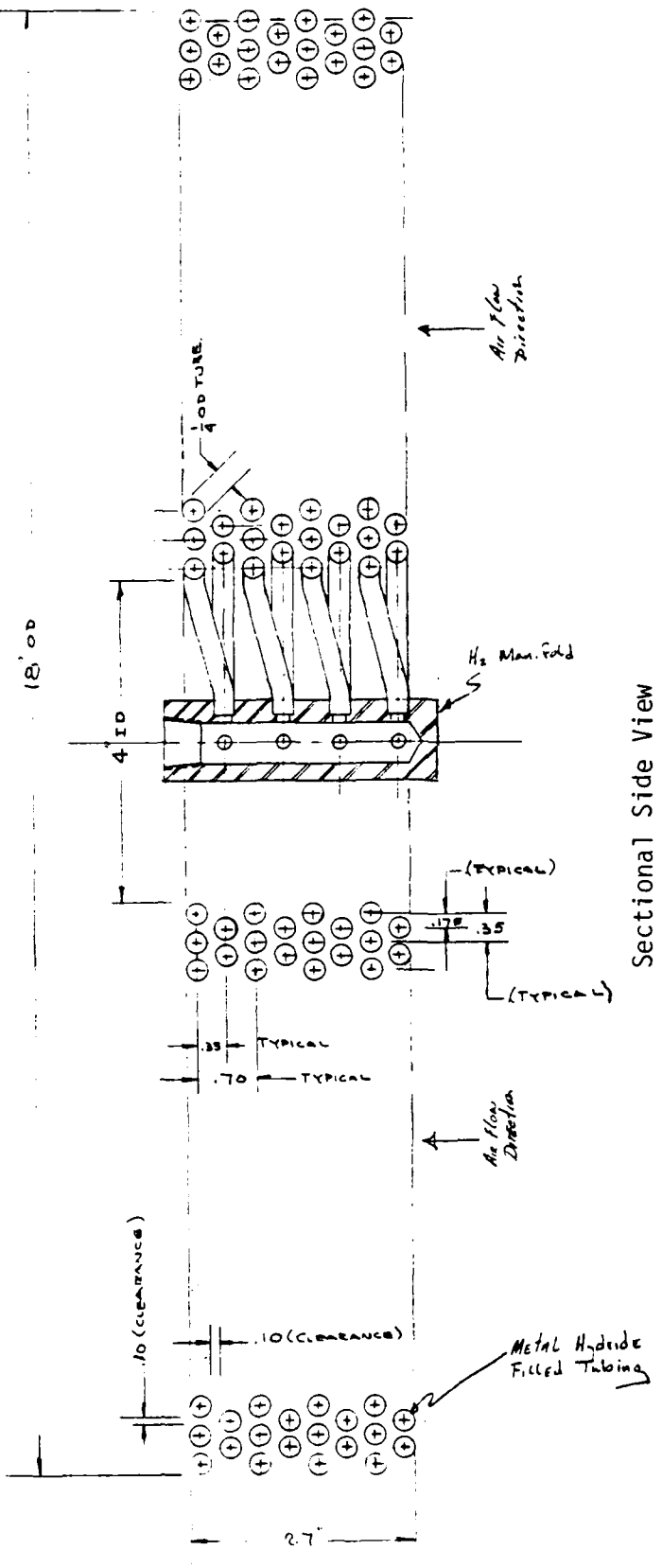

Sectional Side View

Figure 5.2A - Proposed Spiral Tube, Torous Shaped Metal Hydride to Air Stream Heat Exchanger

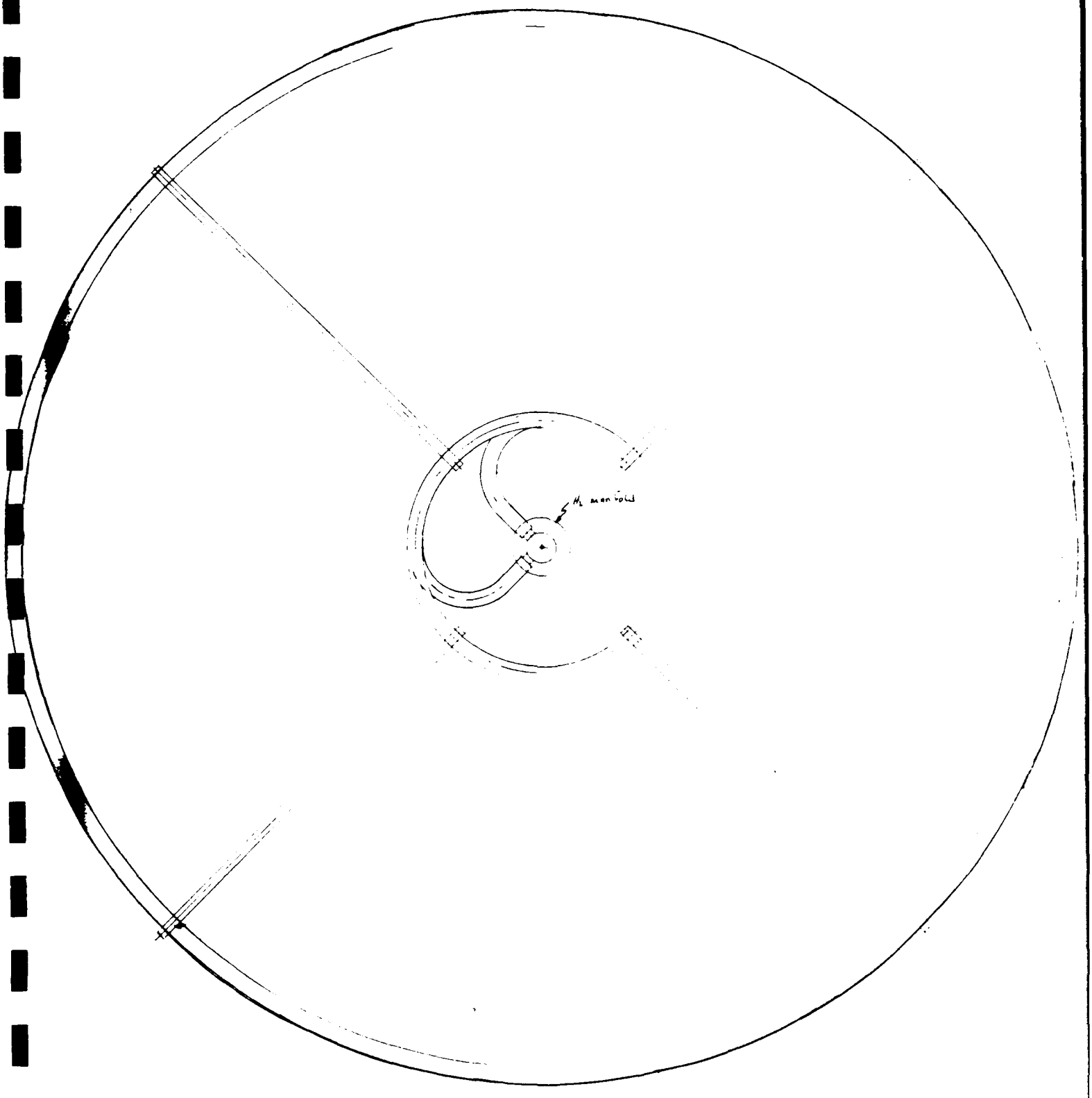

TOP VIEW

Figure 5.2B - Proposed Spiral Tube, Torous Shaped Metal Hydride to Air Heat Exchanger

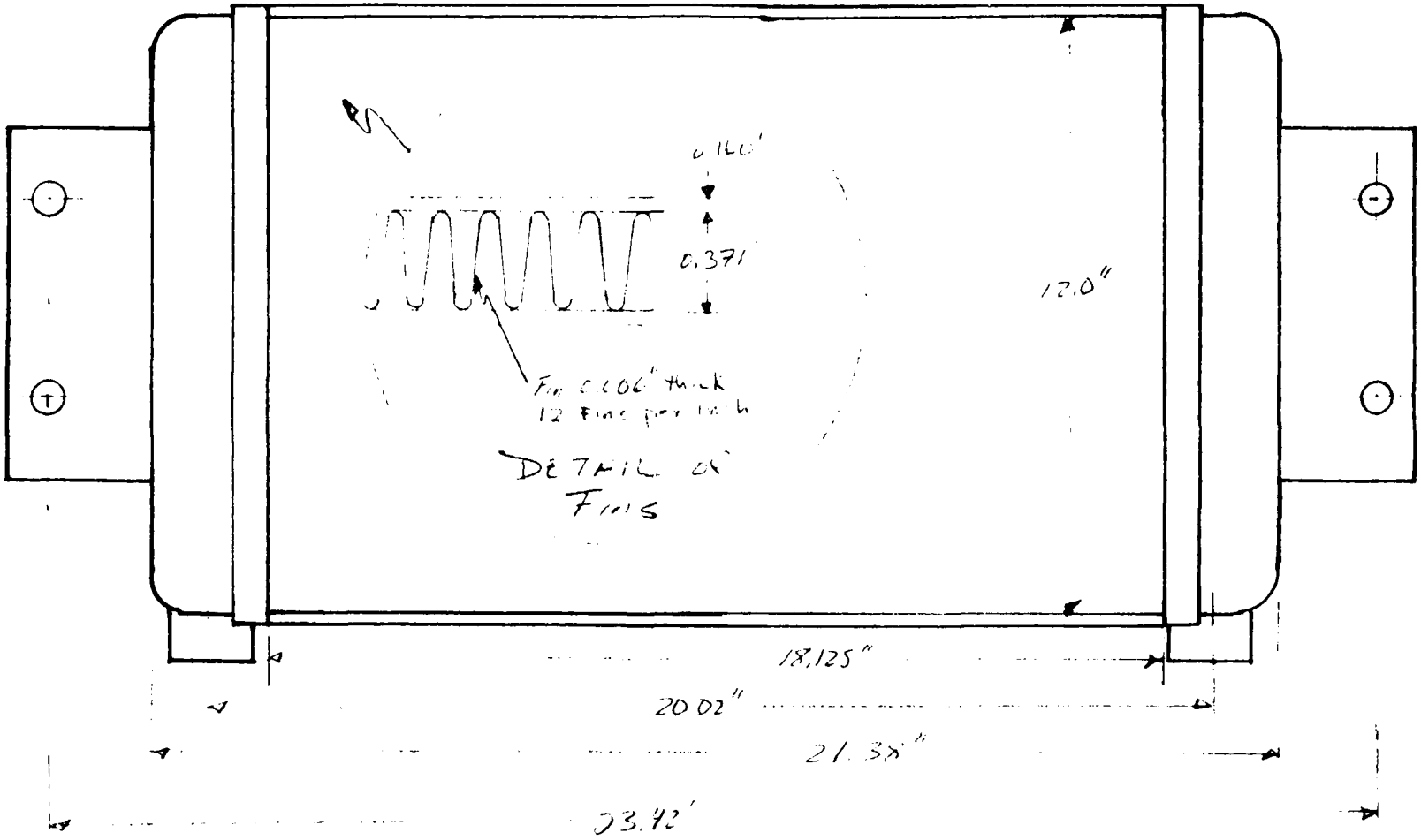

Figure 5.3 - Detailed Dimensional Drawing of the Modine #2978 Aluminum Radiator

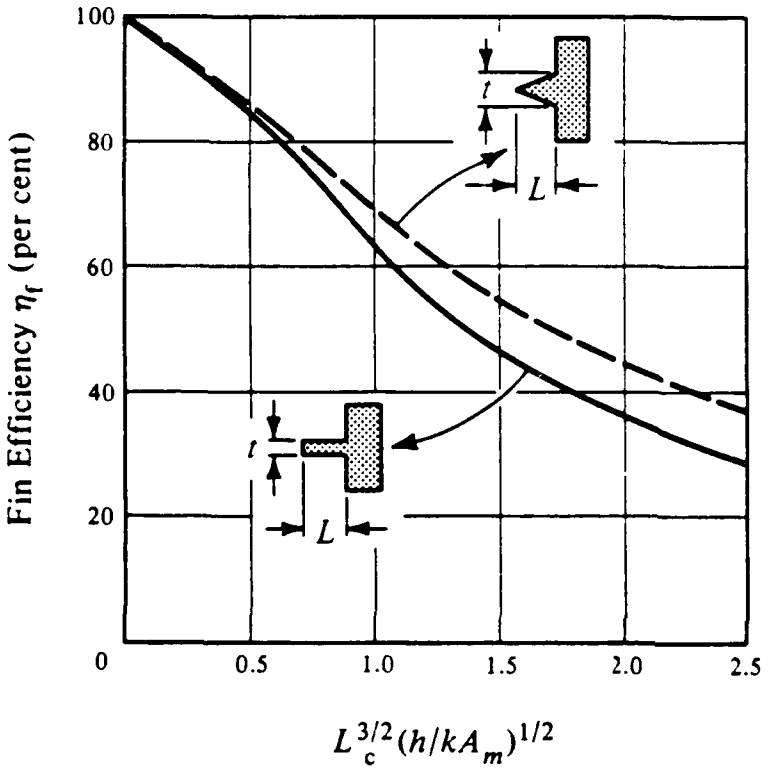

$$L_c = \begin{cases} L + t/2 & \text{rectangular fin} \\ L & \text{triangular fin} \end{cases}$$

$$A_m = \begin{cases} tL_c & \text{rectangular fin} \\ (t/2)L_c & \text{triangular fin} \end{cases}$$

Figure 5.4 - Basic Fin Reference Diagram and Fin Efficiency Diagram (from Reference 1)

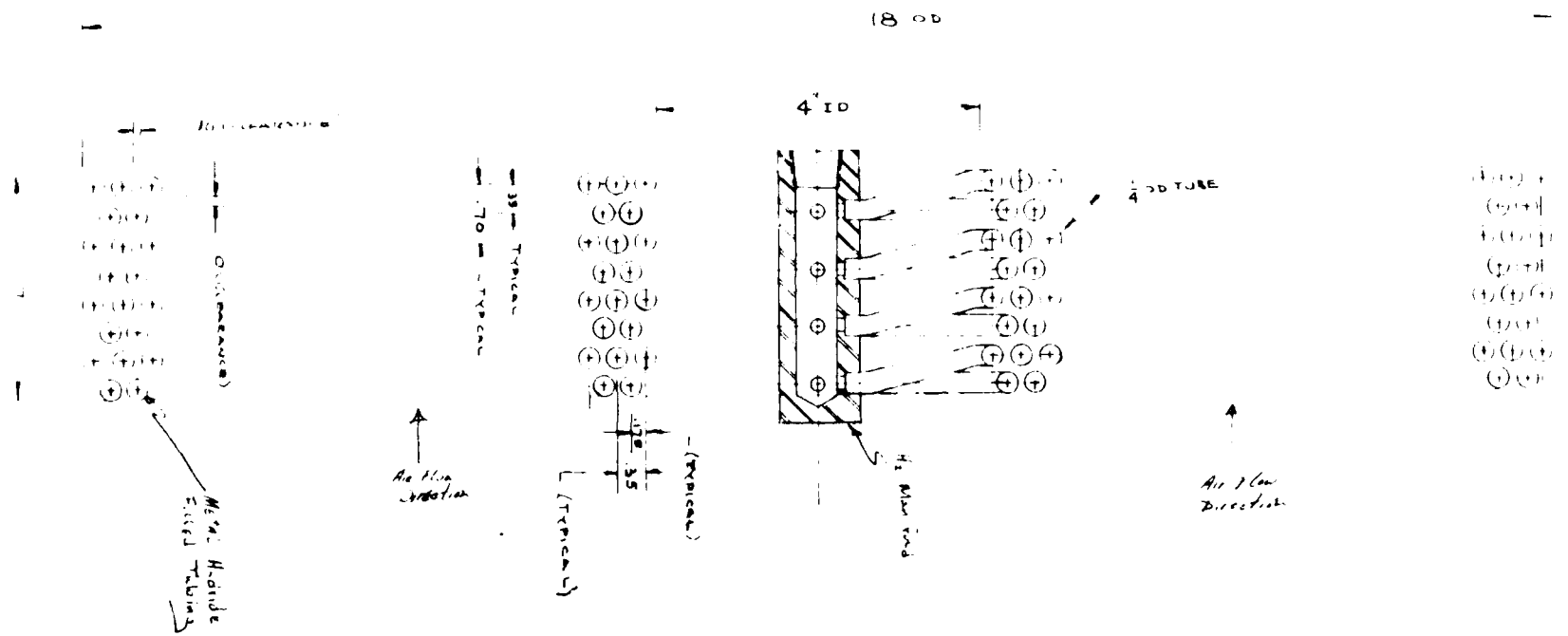

Figure 5.5 - Design Drawing of the Proposed Torous Shaped Metal Hydride to Air Heat Exchanger

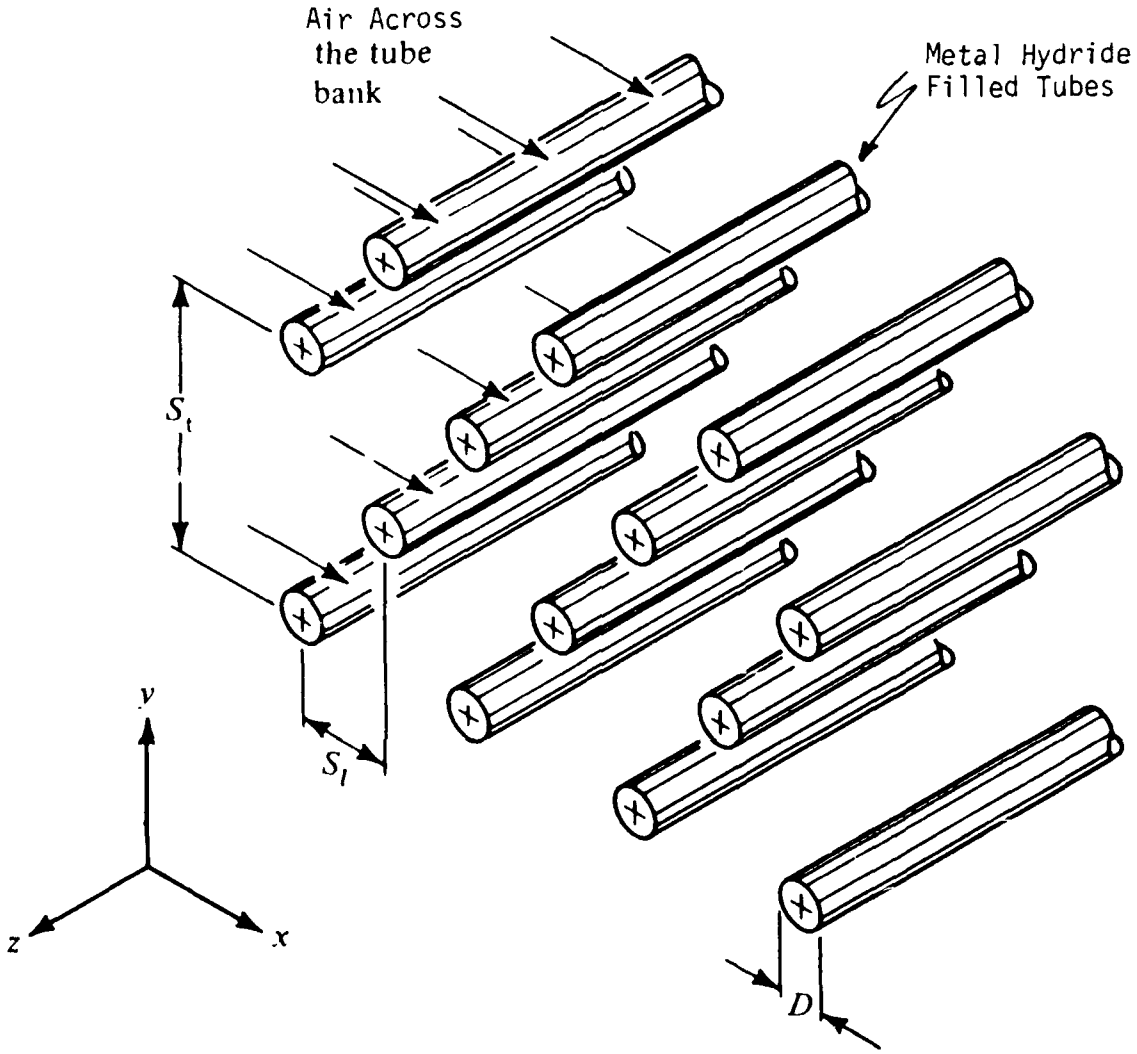

Staggered Arrangement

Figure 5.6 - Detailed View of the Staggered Tube Arrangement in the Torous Shaped Metal Hydride to Air Heat Exchanger

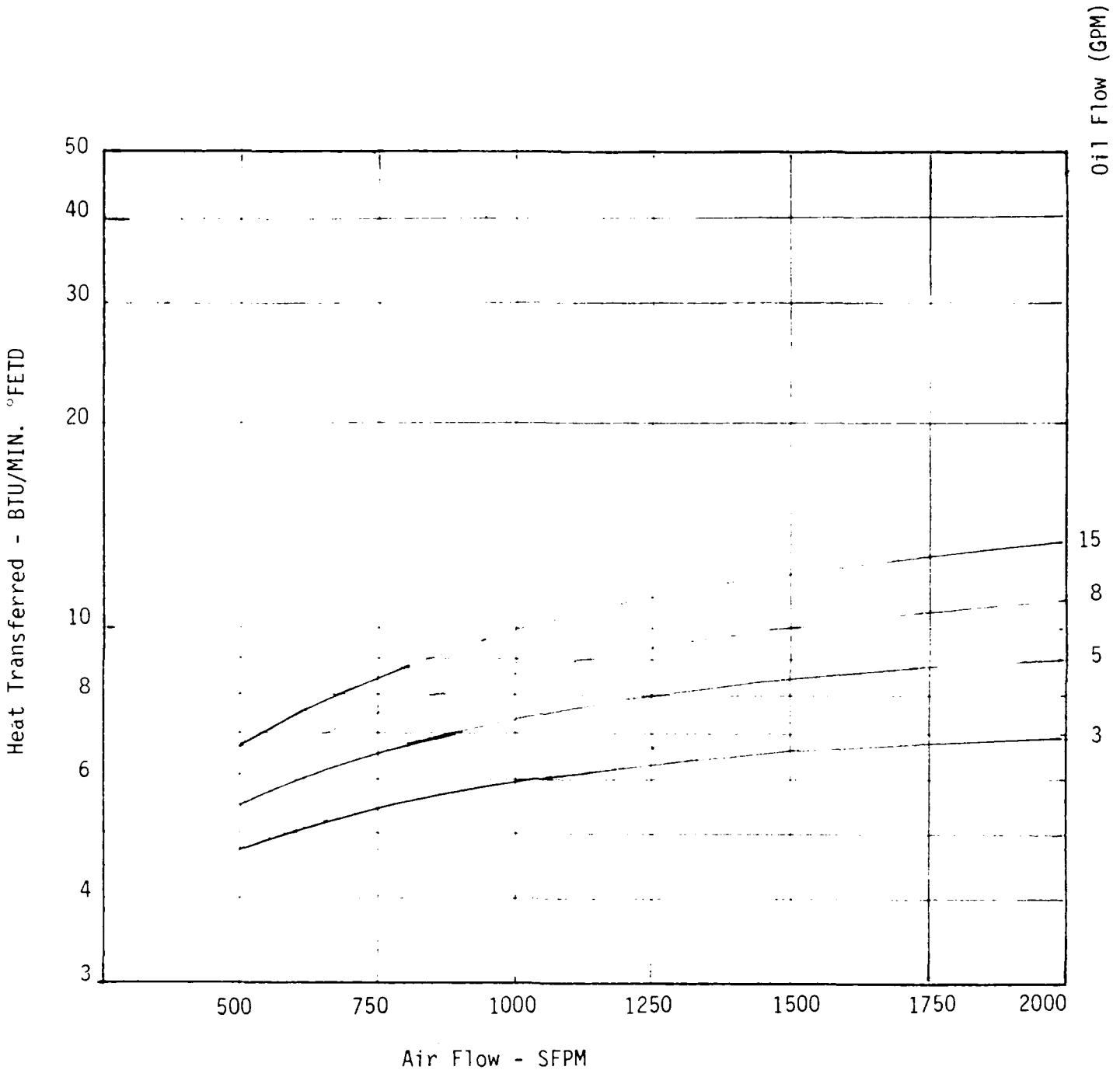

Figure 5.7 - Heat Transfer vs. Nominal Air Speed for the Modine 2978 Aluminum Radiator

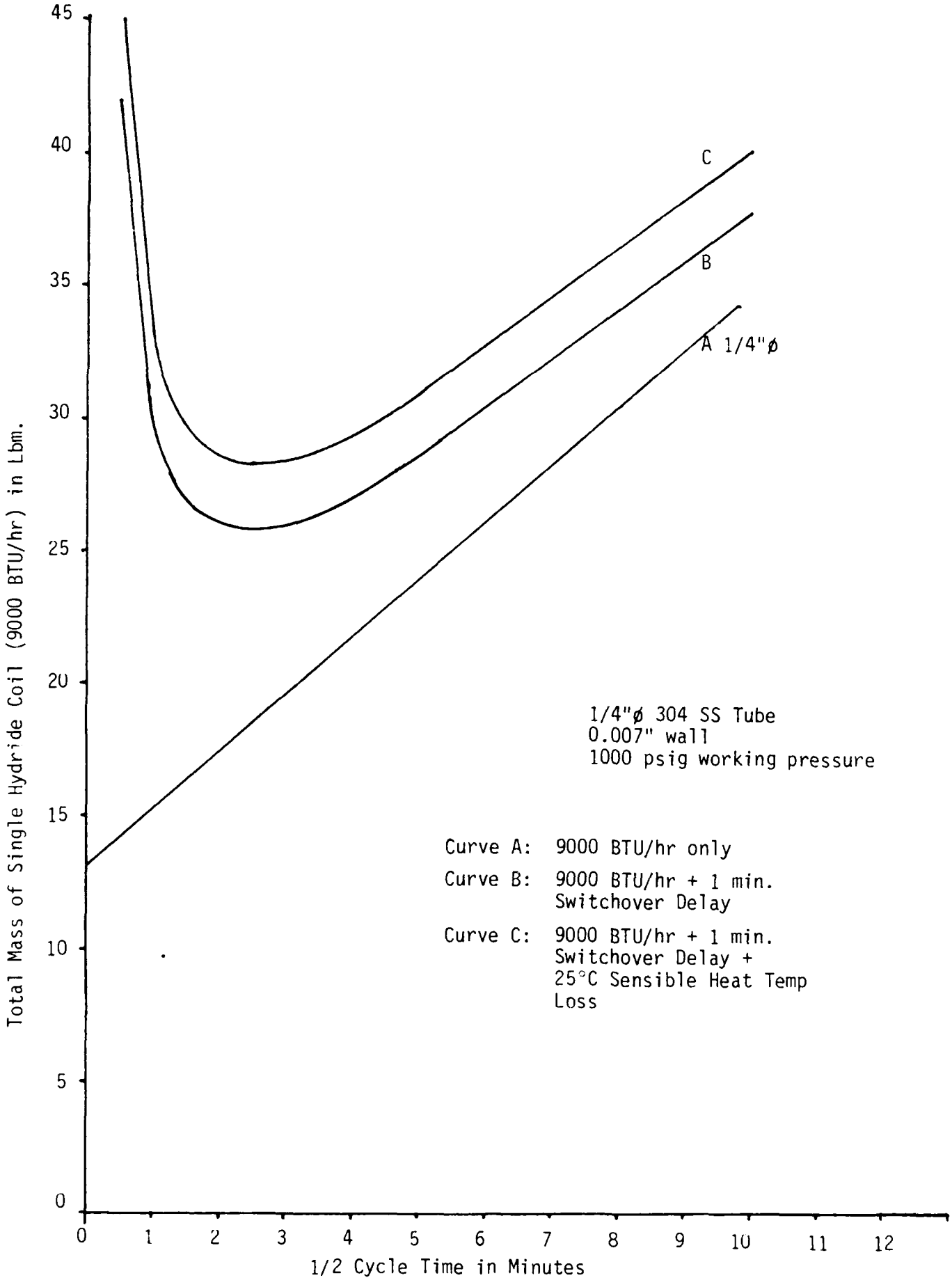

Figure 5.8 - Metal Hydride Heat Exchanger Mass vs. 1/2 Cycle Time, Generated for the 1/4"ø Hydride Tube

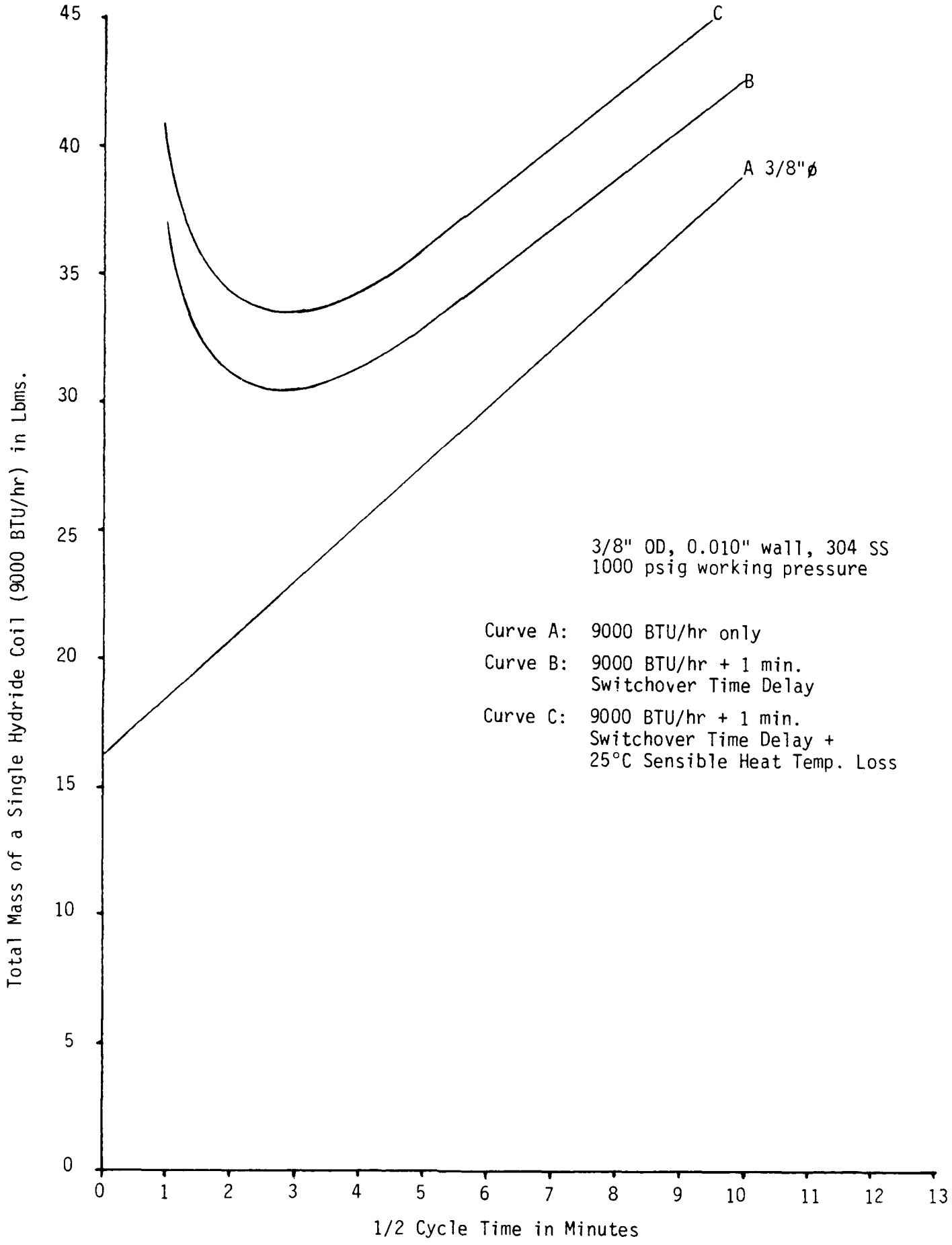

Figure 5.9 - Metal Hydride Heat Exchanger Mass vs. 1/2 Cycle Time, Generated for the 3/8"ø Hydride Tube

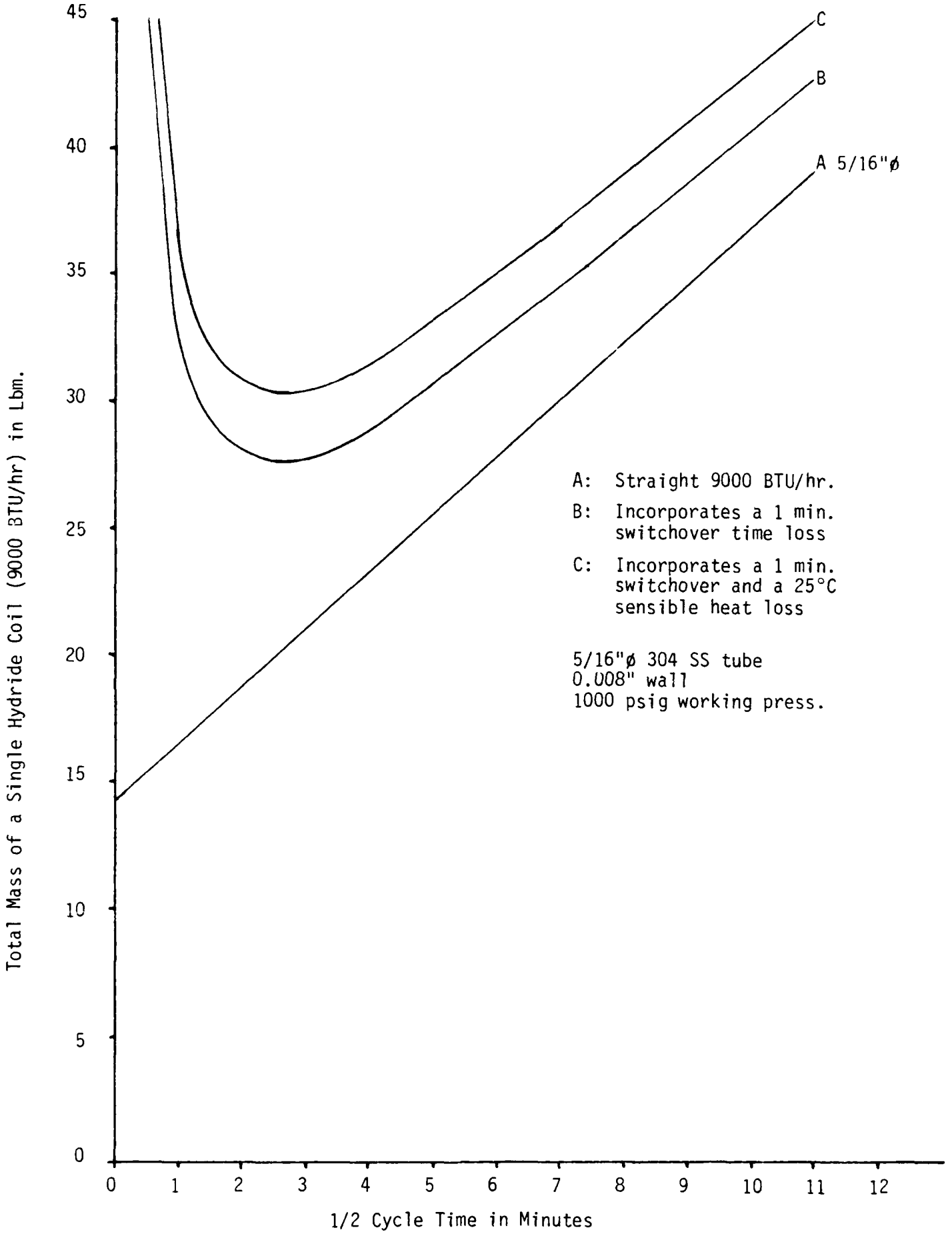

Figure 5.10 - Metal Hydride Heat Exchanger Mass vs. 1/2 Cycle Time, Generated for the 5/16"ø Hydride Tube

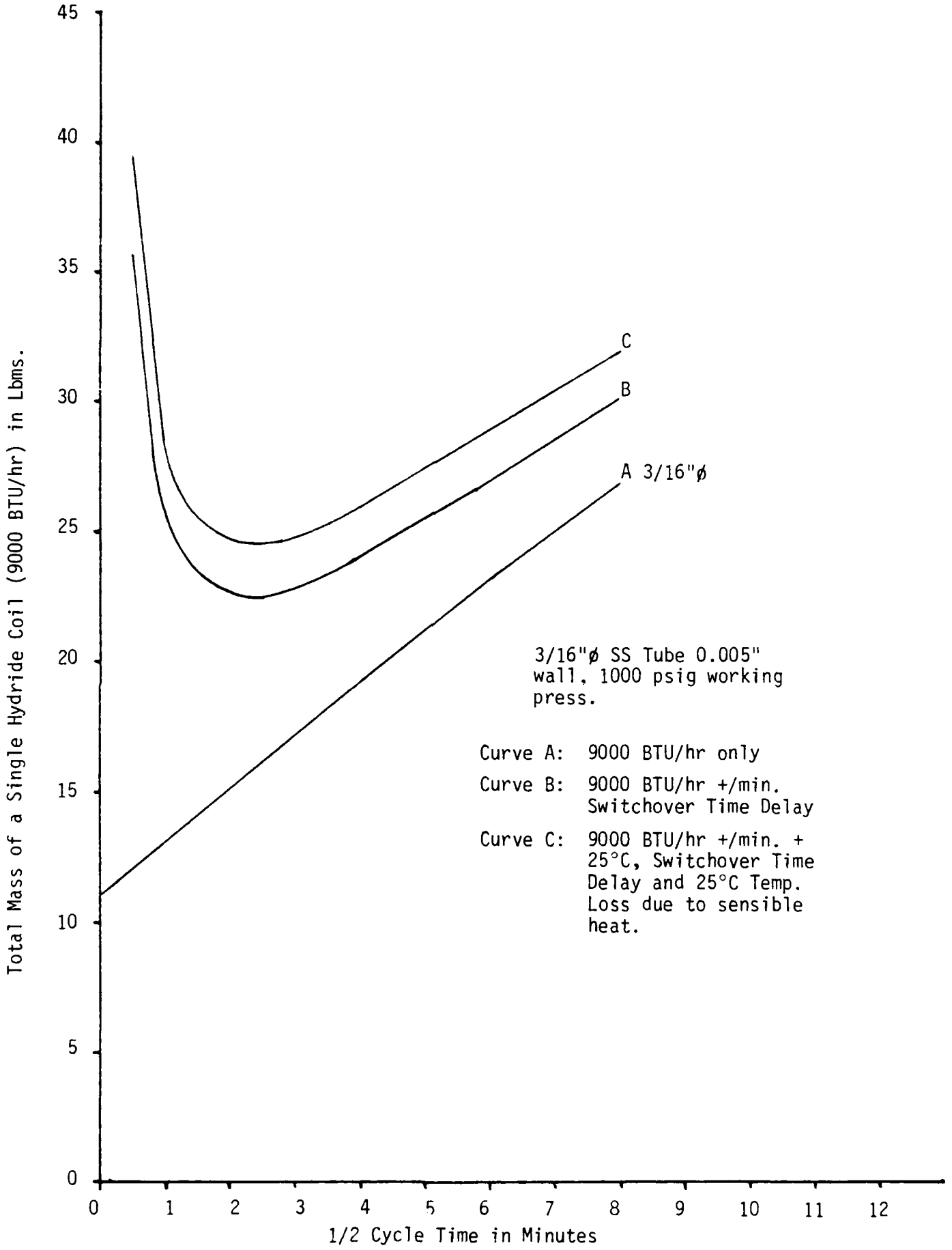

Figure 5.11 - Metal Hydride Heat Exchanger Mass vs. 1/2 Cycle Time, Generated for the 3/16"ø Hydride Tube

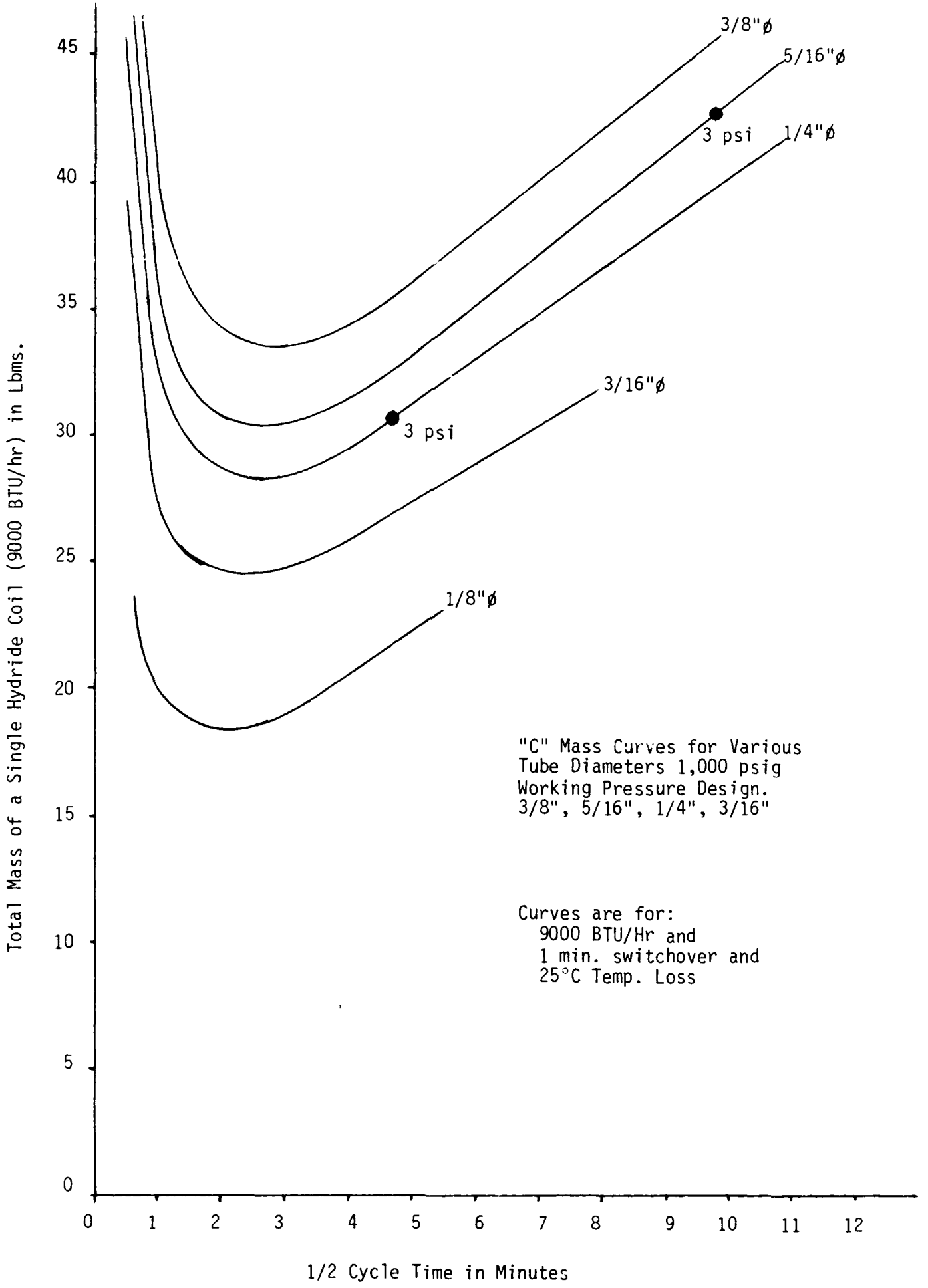

Figure 5.12 - Metal Hydride Heat Exchanger, Mass vs. 1/2 Cycle Time
Optimum Curve C for the 3/16"ø, 1/4"ø, 5/16"ø and
3/8"ø Hydride Tubes

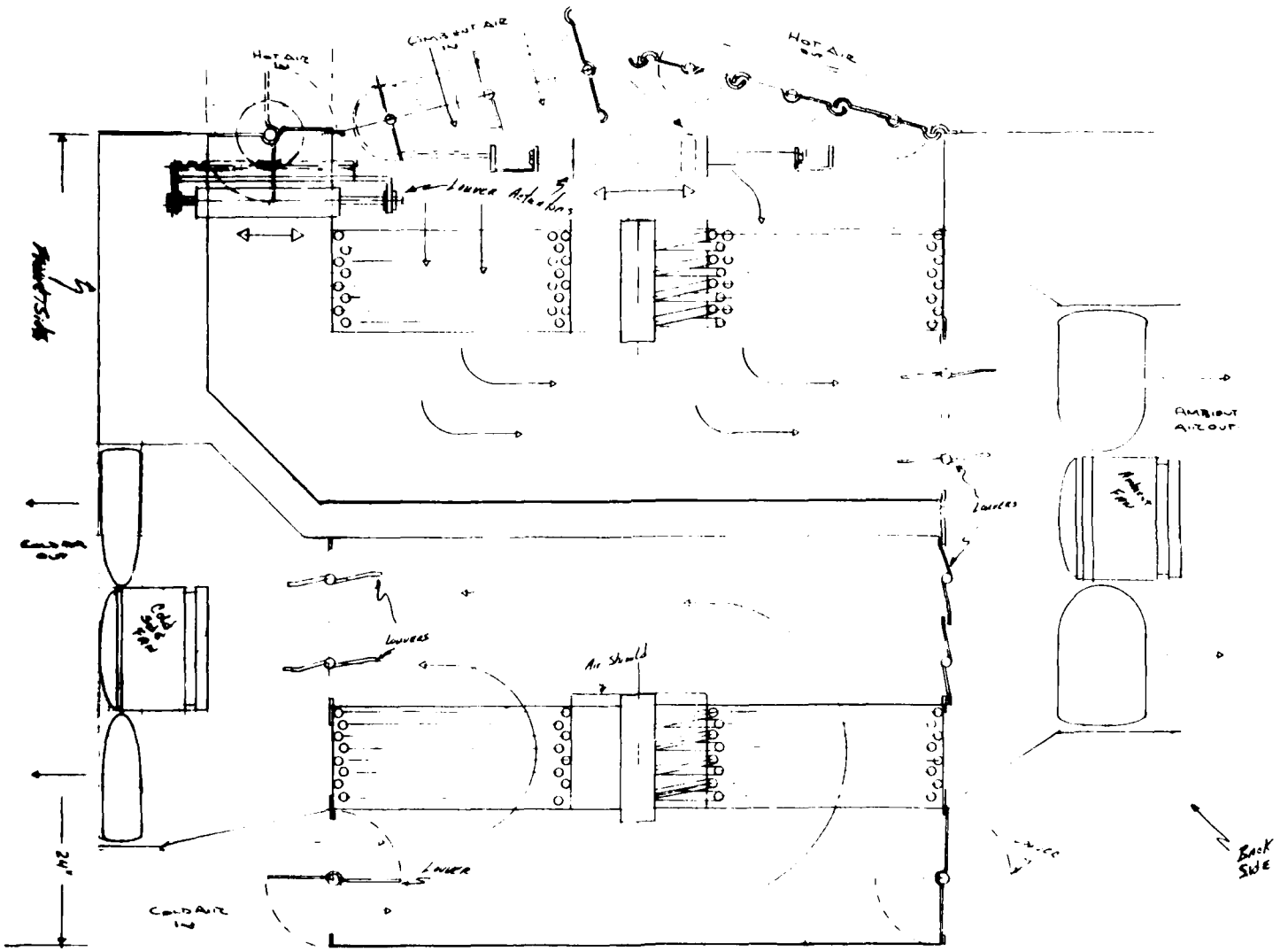

Sectional Side View

Figure 5.13A - Proposed Layout for the "Air System" Metal Hydride Air Conditioner

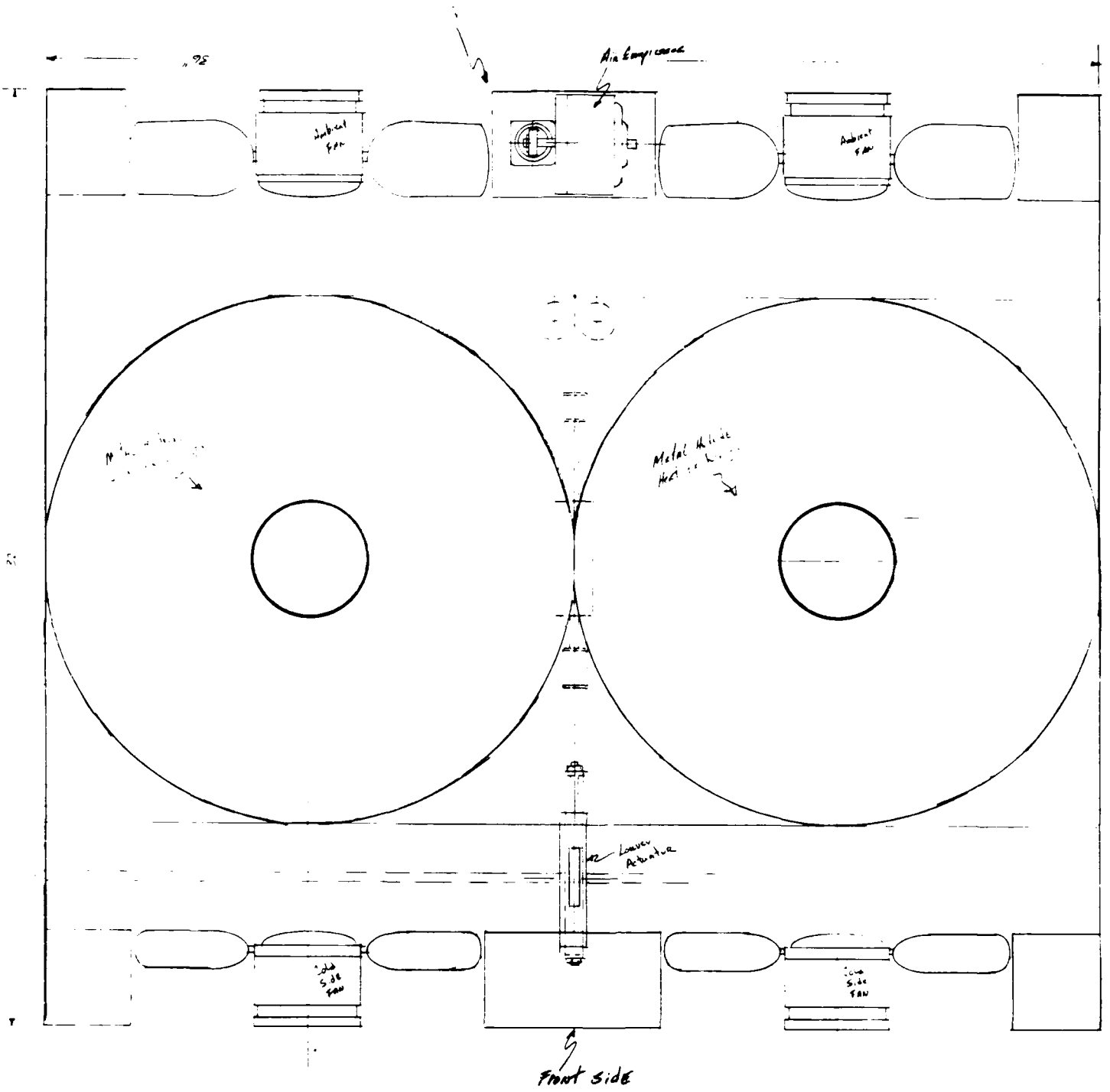

TOP VIEW

Figure 5.13B - Proposed Layout for the "Air System" Metal Hydride Air Conditioner

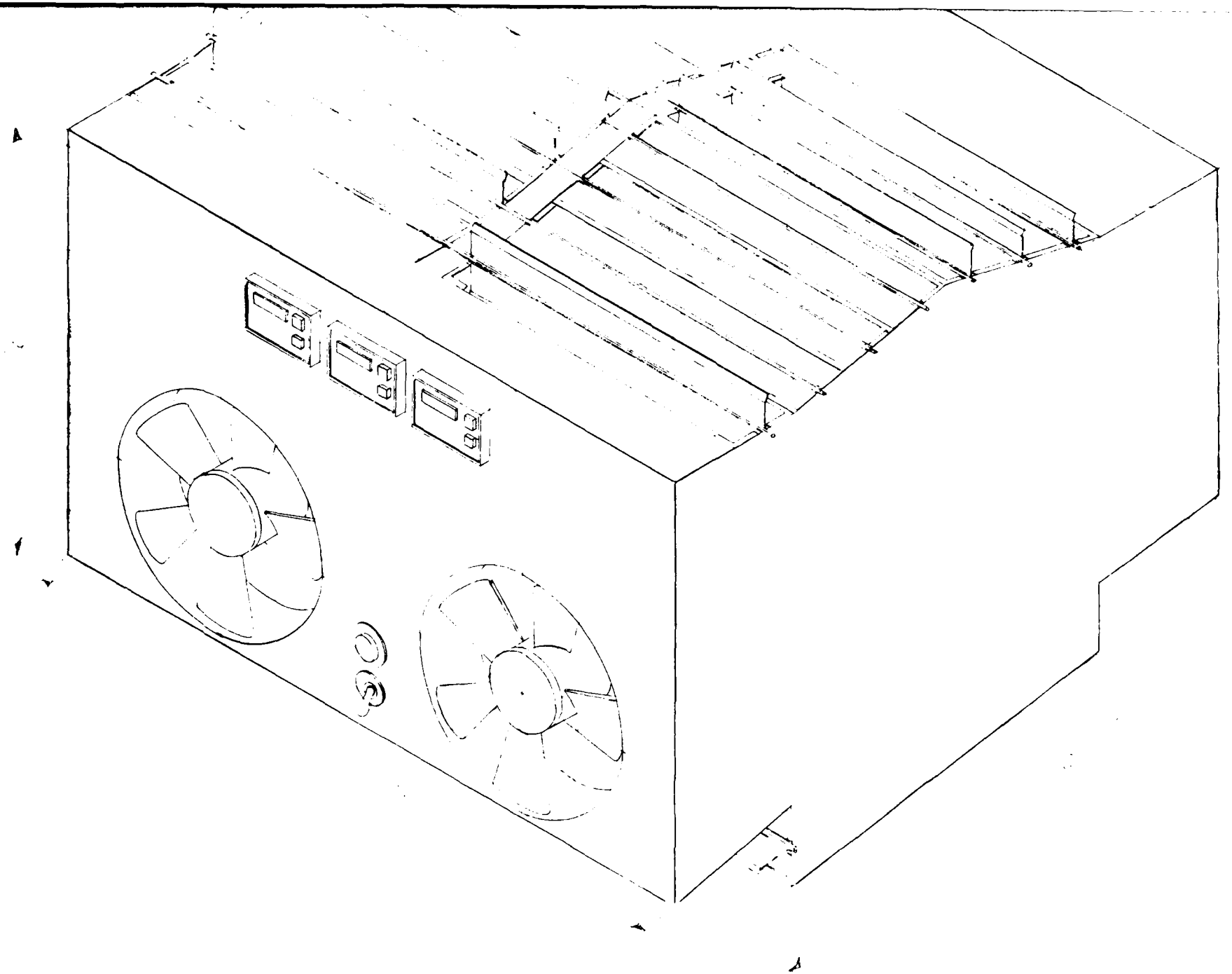

Figure 5.14 - Outside View of the "Air System" Metal Hydride Air Conditioner

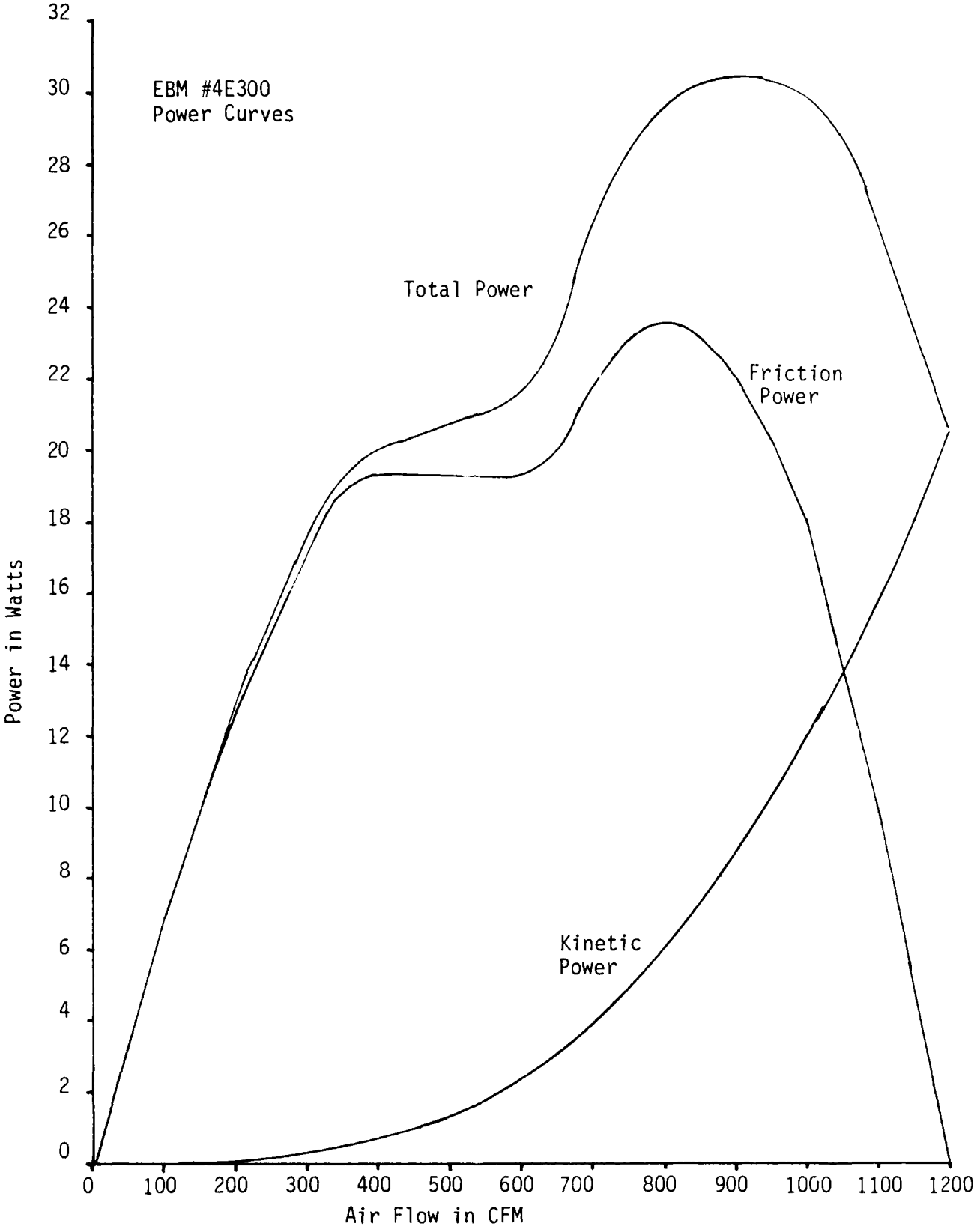

Figure 5.15 - Power Curve for the EBM #4E300 Fan

COMPONENT	WEIGHT LBM	POWER WATTS	WILL BE ELIMINATED IN THE AIR DESIGN
Metal Hydride Heat Exchanger (4 req)	126 Total	---	---
Component Box	29.6	---	---
Air Compressor and Associated Fittings	7.3	20 watts	---
Modine #2978 Cold Side Fluid/Air Radiator	9.0	---	Yes
Modine #2930 Ambient Side Fluid/Air Radiator	25.0	---	Yes
8"ø EBM #S2E200 Cold Side Fans	8.0 total	164 total	
12"ø EBM #S2E300 Ambient Side Fans	13.0 total	460 total	
March #AC-5C-MD Cold Side Fluid Pump	9.5	227	Yes
March #AC-5.5C-MD Ambient Side Fluid Pump	15.5	290	Yes
Hypro #505C Hot Side Fluid Pump	19.0	375	Yes
Humphrey #590A Fluid Control Valves	12.0	---	Yes
Nupro #SS-HBVDC04-0 H_2 Valves	3.0	---	Yes
Slytherm 800 Silicone Fluid	42.0	---	Yes
Assorted Fluid Unions	20.0	---	Yes
Copper Piping for the Silicone Fluid	26.0	---	Yes
Sum of what will be eliminated in air design	181 Lbm	892 watts	

Table 5.1 - Table of the Components and their Weight and Electrical Power Consumption that would be Eliminated in an "Air" System Design

Tube's outer diameter in inches	Tube's External Surface Area per foot of length in ft^2/ft	Tube's Internal Volume per foot of length in $(ft^3/ft) \times 10^{-3}$	Tube's External Surface Area per cubic foot of Internal Volume ft^2/ft^3
1"	0.262	5.45	48.0
3/4"	0.196	3.07	63.8
5/8"	0.164	2.13	77.0
1/2"	0.131	1.36	96.3
3/8"	0.098	0.767	127.8
5/16"	0.082	0.533	153.8
1/4"	0.065	0.341	190.6
3/16"	0.049	0.192	255.2
1/8"	0.033	0.085	388.2

Table 5.2 - Table of the Outer Diameter of a Tube Compared to the Inner Contained Volume of this Tube

Component	Weight Lbms	Average Power Requirement Watts
Aluminum Enclosure	10.5	
Metal Hydride Heat Exchangers, 4 @ 31 Lbms each	124	
12"ø EBM #4E300 Cold Side Fans, 2 @ 4.9 Lbm each, 115 watts each	9.8	115
12-1/2"ø EBM #4E315 Ambient Side Fans, 2 @ 5.5 Lbms each, 135 watts each	11	270
Thomas #004CA-33 Air Compressor	3.5	2
Humphrey Minimizer Air Valve, 5 @ 0.15 Lbms each	0.8	
Vane Actuators, 6 @ 0.2 Lbms each	1.2	
Miscellaneous Wiring, Timer, and Insulation	4.5	
TOTAL	165.3 Lbm	387 watts

Table 5.3 - List of Components; Their Weights, and Average Power Requirements in the Air System Design

APPENDIX 5.1

Listing and Example Run
of the Computer Program

"Coil-7: Hydride Heat Exchanger Tube Spacing Program"

```
10 LPRINT"Hydride tube coil program 5-12-88, M. Golben"
20 LPRINT
30 LPRINT"This program calculates the length of tubing needed to occupy"
40 LPRINT"a given horizontal coiling constrant."
50 LPRINT"Variables needed to run this program are the..."
60 LPRINT"Coil ID (CID), Coil OD (COD), Tube OD (TOD), Tube Spacing (TS)."
70 LPRINT"Volumetric air flow (VAF) in qubic feet per sec"
80 LPRINT"This program will also calculate the air pumping"
90 LPRINT"power needed to move the stated volumetric air"
100 LPRINT"flow rate through the hydride heat exchanger (line 290)."
110 LPRINT"The friction factor equation wsed to compute this is..."
120 LPRINT"F=(RE^(-0.15))*(0.044+(0.08*SL/D)/((ST-D/D)^(0.43+(1.13D/SL))))"
130 LPRINT
140 LET SLT =0
150 LET CID=0
160 LET COD=0
170 LET TOD=0
180 LET TS=0
190 LET SD=0
200 LET SL1=0
210 LET SL2=0
220 LET SL3=0
230 LET SL4=0
240 LET A1=0
250 LET A2=0
260 LET A3=0
270 LET AT=0
280 LET ATF=0
290 LET VAF=0
300 LET DEN=.07519
310 LET VIS=1.241E-05
320 LET RE=0
330 LET ST=0
340 LET SL=0
350 LET C1=0
360 LET C2=0
370 LET C3=0
380 LET C4=0
390 LET C5=0
400 LET F=0
410 LET GC=32.17
420 LET N1=0
430 LET PD=0
440 LET PDT=0
450 LET PW=0
460 LET PWW=0
470 LPRINT"What is the volumetric air flow rate in FT^3/SEC ?"
480 INPUT VAF
490 LPRINT"What is the coil ID in inches ?"
500 INPUT CID
510 LPRINT"What is the coil OD in inches ?"
520 INPUT COD
530 LPRINT"What is the hydride tube OD in inches ?"
540 INPUT TOD
550 LPRINT"What is the hydride tube spacing in inches ?"
560 INPUT TS
570 LPRINT"what is the hydride row spacing in inches ?"
580 INPUT TRS
590 LPRINT"How many tube rows are there ?"
600 INPUT N1
610 LET ST=TOD+TS
620 LET SL=TOD+TRS
630 LET SD=CID+TOD+TOD
640 LET SL1=3.1416*SD
```

Written in BASIC VERSION 2®
To be used on IBM compatable
personal computer
(See the reference - "Basic Version 2
Reference Guide" Compaq Computer Corp.
Copyright 1983, 84)

continued

Appendix 5.1 - Listing of the Computer Program "Coil-7" that computes the Hydride Heat Exchanger's Configuration

```
650 LET A1=3.1416/4*(((SD+2*TS)^2)-(SD^2))
660 LET SD=SD+TOD+TOD+TS+TS
670 LET SL2=3.1416*SD
680 LET A2=3.1416/4*(((SD+2*TS)^2)-(SD^2))
690 LET SL3=SL1+SL2
700 LET SD=SD+TOD+TOD+TS+TS
710 LET SL4=3.1416*SD
720 LET A3=3.1416/4*(((SD+2*TS)^2)-(SD^2))
730 LET AT=AT+A1+A2+A3
740 LET A1=0
750 LET A2=0
760 LET SLT=SLT+SL4+SL3
770 LET SLTF=SLT/12
780 LET SL3=0
790 IF SD>=COD GOTO 810
800 GOTO 700
810 LPRINT
820 LET ATF=AT/144
830 LET U=VAF/ATF
840 LET RE=DEN*U*TOD/(VIS*12)
850 LET C1=(.43+(1.13*TOD/SL))
860 LET C2=(ST-TOD)/TOD
870 LET C3=.08*(SL/TOD)
880 LET C4=RE^(-.15)
890 LET C5=.044+C3/(C2^C1)
900 LET F=C5*C4
910 LET PD=((F*DEN)*(U^2))/(2*GC)
920 LET PDT=N1*PD
930 LET PD2=(PD/144)*27
940 LET PD3=N1*PD2
950 LET PW=VAF*PDT
960 LET PWW=PW*1.356
970 LET PW2=PWW/N1
980 LPRINT"When the coil ID = ";CID
990 LPRINT"and the coil OD = ";COD
1000 LPRINT"and the tube diameter =";TOD
1010 LPRINT"and the tube spacing =";TS
1020 LPRINT "and the tube row spacing = ";TRS
1030 LPRINT "The number of tube rows = ";N1
1040 LPRINT"the total length of the tube in feet = ";SLTF
1050 LPRINT"The free air flow surface area in square feet is = ";ATF
1060 LPRINT"The volumetric air flow in qubic feet per sec is = "VAF
1070 LPRINT"The average air velocity in feet per sec = ";U
1080 LPRINT"The renolds number is = ";RE
1090 LPRINT"The friction factor = ";F
1100 LPRINT"The pressure drop per row in LBF/FT^2 = ";PD
1110 LPRINT"The pressure drop per row in inches of water = ";PD2
1120 LPRINT"The total pressure drop through the rows in inches of water = ";PD3
1130 LPRINT"The total pressure drop through the bed = ";PDT
1140 LPRINT"The air pumping power per row in watts = ";PW2
1150 LPRINT"The total air pumping power in watts = ";PWW
1160 LPRINT
1170 IF TS<=0 GOTO 1450
1180 LET TS=TS-.005
1190 LET TRS=TRS-.005
1200 LET SD=0
1210 LET SL1=0
1220 LET SL2=0
1230 LET SL3=0
1240 LET SL4=0
1250 LET SLT=0
1260 LET A1=0
1270 LET A2=0
1280 LET A3=0
```

Appendix 5.1 - continued:

Continued Listing of the Computer Program "Coil-7"

```
1290 LET AT=0
1300 LET ATF=0
1310 LET RE=0
1320 LET ST=0
1330 LET SL=0
1340 LET C1=0
1350 LET C2=0
1360 C3=0
1370 C4=0
1380 C5=0
1390 F=0
1400 PD=0
1410 PDT=0
1420 PW=0
1430 PWW=0
1440 GOTO 610
1450 END
Hydride tube coil program 5-12-88, M. Golben
```

Appendix 5.1 - continued:

Continued Listing of the Computer Program "Coil-7"

```
Hydride tube coil program 5-12-88, M. Golben

This program calculates the length of tubing needed to occupy
a given horizontal coiling constrant.
Variables needed to run this program are the...
Coil ID (CID), Coil OD (COD), Tube OD (TOD), Tube Spacing (TS).
Volumetric air flow (VAF) in qubic feet per sec
This program will also calculate the air pumping
power needed to move the stated volumetric air
flow rate through the hydride heat exchanger (line 290).
The friction factor equation wsed to compute this is...
F=(RE^(-0.15))*(0.044+(0.08*SL/D)/((ST-D/D)^(0.43+(1.13D/SL))))

What is the volumetric air flow rate in FT^3/SEC ?
What is the coil ID in inches ?
What is the coil OD in inches ?
What is the hydride tube OD in inches ?
What is the hydride tube spacing in inches ?
what is the hydride row spacing in inches ?
How many tube rows are there ?



When the coil ID =  4
and the coil OD =  18
and the tube diameter = .25
and the tube spacing = .1000002
and the tube row spacing =  .1000002
The number of tube rows =  8
the total length of the tube in feet =  63.22474
The free air flow surface area in square feet is =  .5314565
The volumetric air flow in qubic feet per sec is =  13
The average air velocity in feet per sec =  24.46109
The renolds number is =  3087.612
The friction factor =  .1174343
The pressure drop per row in LBF/FT^2 =  8.211557E-02
The pressure drop per row in inches of water =  1.539667E-02
The total pressure drop through the rows in inches of water =  .1231734
The total pressure drop through the bed =  .6569246
The air pumping power per row in watts =  1.447533
The total air pumping power in watts =  11.58027
```

Appendix 5.1 - continued:

Example Run of the Computer Program "Coil-7"